NOVEMBER, 1953
IN TWO SECTIONS—SECTION I

Journal of METALS

November JOURNAL OF METALS Highlights:

"Metallurgical Aspects of the Development of Small Gas Turbines" - p. 1419

"Ultra-Pure Metals Produced By Zone-Melting Technique" - p. 1428

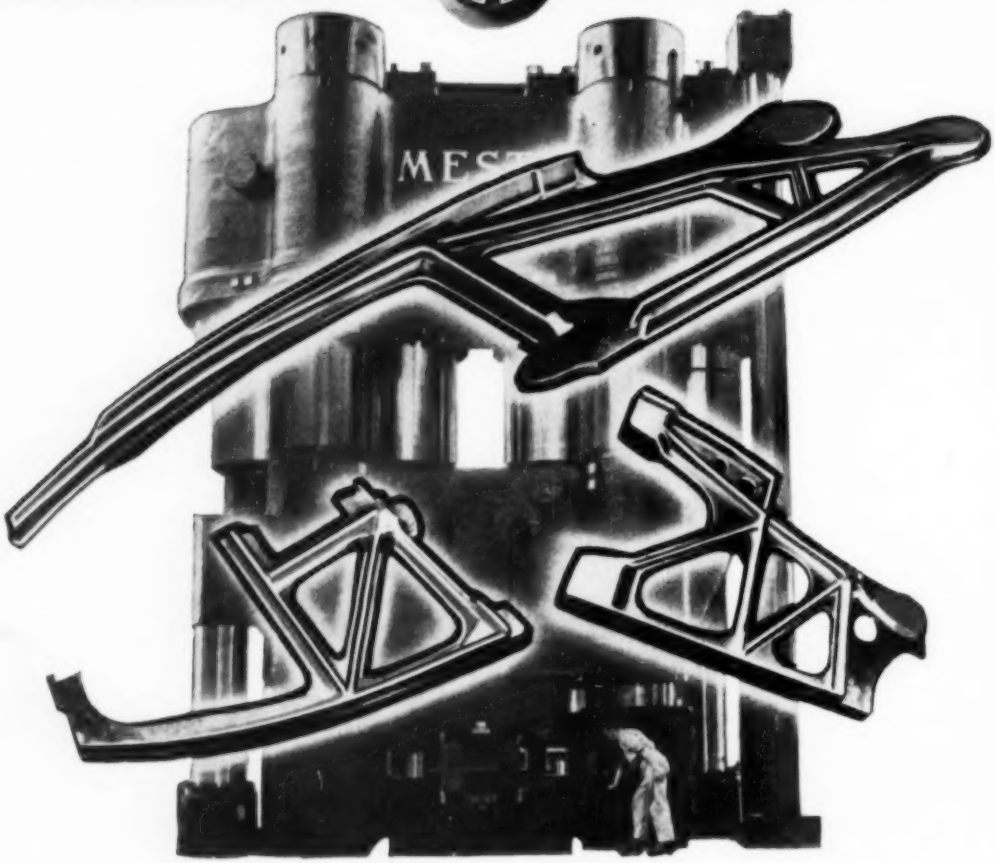

Greater Size and Speed in Aircraft have created engineering problems, the solution of which has required larger and larger forgings of high-strength aluminum alloy. *Examples* shown above are forged structural members used in a modern military bomber, the largest more than seven feet over all. These are forged on an 18,000-ton press, the biggest ever built in this country.

Wyman-Gordon Experience—the most extensive in the industry—is keeping abreast of new forging demands involving the use of Steel, Aluminum, Magnesium, High Density Alloys and Titanium.

• • •

Standard of the Industry for More than Sixty-five Years

WYMAN-GORDON

FORGINGS OF ALUMINUM • MAGNESIUM • STEEL

WORCESTER, MASSACHUSETTS

HARVEY, ILLINOIS — DETROIT, MICHIGAN

Journal of METALS

VOL. 5, NO. 11 NOVEMBER, 1953

IN TWO SECTIONS — SECTION 1

Published to provide a continuing, authoritative, and up-to-date record of technological, engineering, and economic progress in all branches of the metals industry by the
Metals Branch
American Institute of Mining and Metallurgical Engineers, Inc.
29 West 39th Street, New York 18

ALVIN S. COHAN
Manager of Publications

Editor, JOURNAL OF METALS

D. G. GARRETT M. A. MATZKIN
E. M. WEISS G. M. ZILL
Assistant Editors

GRACE PUGSLEY Production Manager

W. J. SEWING Asst. Prod. Mgr.

METALS BRANCH COUNCIL
K. C. McCutcheon Chairman
E. O. Kirkendall Secretary
M. Cohen IMD Chairman
T. J. McLoughlin ISD Chairman
R. R. McNaughton EMD Chairman
W. A. Dean R. D. Parks
T. D. Jones D. S. Eppelsheimer

EDITORIAL ADVISORY COMMITTEE
J. S. Smart, Jr. Chairman
W. A. Dean Evan Just
J. C. Kinnear, Jr. John Marsh
T. D. Jones M. Tenenbaum

TECHNICAL PUBLICATIONS COMMITTEES
Robert Aborn AIME Chairman
Otto Zmeskal ISD Chairman
S. J. Dickinson EMD Chairman
W. R. Hibbard, Jr. IMD Chairman
E. J. Kennedy, Jr. Secretary

JAMES A. STANGARONE
Advertising Manager
FRED STANLEY
Eastern Representative

The AIME Publishes:
Journal of Metals
Mining Engineering
Journal of Petroleum Technology

COVER

No. 3 blast furnace at Youngstown Sheet and Tube Co.'s Indiana Harbor works, this month's cover, has a rated capacity of 1500 tons of iron every 24 hr. Its hearth diameter is 28 ft and it is Youngstown's largest blast furnace.

NEWS

Meet the Authors	1402	Drift of Things	1415
Employment Service	1404	Journal of Metals Reporter	1417
New Products	1407	Electric Furnace Program	1483
Industrial Notes	1410	AIME News	1484
Trends	1412	Personals	1485
Books for Engineers	1414	Coming Events	1486

TECHNICAL FEATURES

Metallurgical Aspects of the Development of Small Gas Turbines — W. L. Slosson — 1419

CF&I Opens Streamlined Tube Mill at Pueblo, Colo. — 1427

Ultra-Pure Metals Produced by Zone Melting Technique — Earle E. Schumacher — 1428

Composition Control of Steel Castings Improved by New Furnace Sampling Methods — Vincent E. Beluska — 1430

Programs Underway to Increase U. S. Production of Strategic Beryllium — B. H. Clemmons, J. S. Browning — 1433

TRANSACTIONS

Hurley Furnace and Boiler Description and Design — E. A. Slover — 1435

Preparation of Metallic Iron of High Purity — G. A. Moore — 1443

Manganese as an Indicator of Blast Furnace Slag Oxidation and Desulphurizing Power — N. J. Grant, J. W. Dowding, Jr., R. J. Murphy — 1451

Diffusion of Calcium Ion in Liquid Slag — H. Towers, M. Paris, J. Chipman — 1455

Neptunium-Aluminum Intermetallic Compounds — O. J. C. Runnalls — 1460

Diffusion and Solubility of Boron in Iron and Steel — P. E. Busby, M. E. Warga, C. Wells — 1463

Effects of Temperature on the Flow and Fracture Characteristics of Molybdenum — J. H. Bechtold — 1469

Bending of Molybdenum Single Crystals — K. T. Aust, R. Maddin, N. K. Chen — 1477

TECHNICAL NOTES

Change in Ingot Shape During Zone Melting — W. G. Pfann — 1441

The Habit Plane of Beta in Alpha Titanium — P. A. Albert — 1449

The Silver-Cadmium Beta and Zeta Phases — L. Muldawer, M. Amsterdam, F. Rothwarf — 1458

Formation of Sigma Phase in the Mn-Mo System — B. F. Decker, R. M. Waterstrat, J. S. Kasper — 1476

Published the first day of each month by the American Institute of Mining and Metallurgical Engineers, Inc., 29 West 39th Street, New York 18, N. Y. Telephone: PEnnsylvania 6-9220. Subscription $8 per year for non-AIME members in United States and North, South and Central America; $10, foreign; $6 for AIME members, or $4 additional in combination with a subscription to "Mining Engineering" or "Journal of Petroleum Technology". Single copies, 75 cents; single copies foreign, $1.00; special issues, $1.50 . . . The AIME is not responsible for any statement made or opinion expressed in its publications. . . . Copyright 1953 by the American Institute of Mining and Metallurgical Engineers, Inc. . . . Registered cable address, AIME New York . . . Indexed in Engineering Index, Industrial Arts Index and Chemical Abstracts . . . Reentered as second-class matter Sept. 21, 1949, at the post office at New York, N. Y. under the Act of March 3, 1879. Additional entry established at Manchester, N. H.

Aluminum is *Why*

4 men can erect 1500 sq. feet of wall per day

In Davenport, Iowa, there is a structure that building men from all over the country come to see and study. It is Alcoa's sheet and plate mill—the world's largest—covering 55 acres.

Most of the building is aluminum. Aluminum covers the steel framework and forms the walls. Modular panels of aluminum building sheet, enclosing glass wool insulation, were bolted to the lightweight steel framing. A minimum of scaffolding was needed to erect the 2 x 10-foot sections into place. The building was quickly enclosed.

Aluminum was used for all practical applications, especially to effect economy in maintenance.

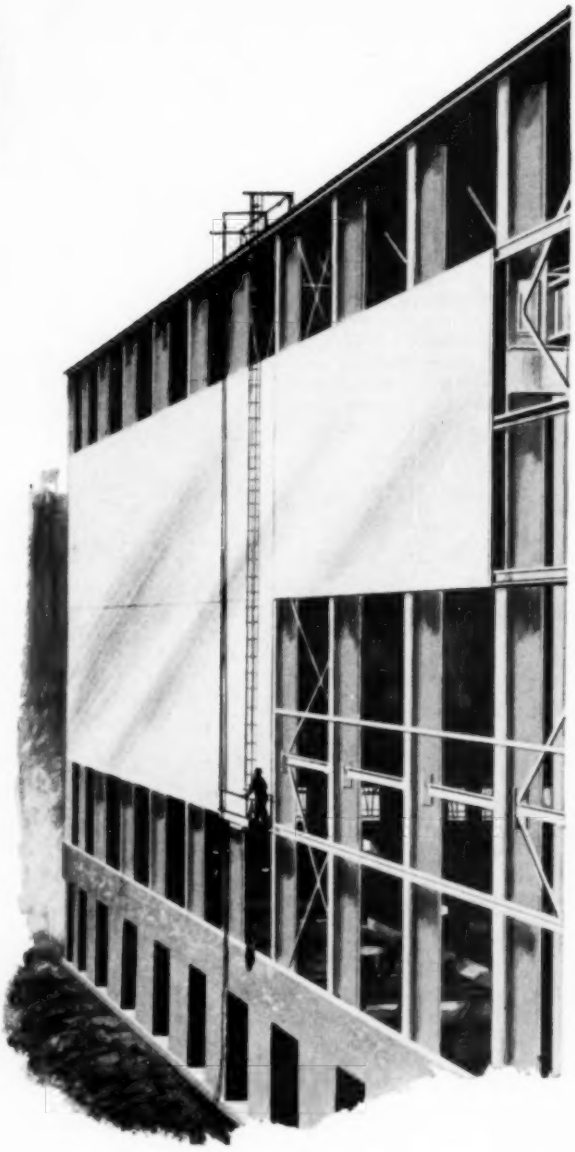

ALCOA is *How*

For the building industry—suppliers, contractors and architects—Alcoa provides materials and experience. Taking their ideas and designs, Alcoa adds the wisdom of 65 years in producing and fabricating aluminum. A large architectural division at Alcoa acts as a storeroom of building information from which anyone can draw. And for fabricators of building products, Alcoa specialists gladly help with problems of making insulated panels, corrugated sheet and modular units of aluminum. Aluminum Company of America, 879-L Alcoa Bldg., Pittsburgh 19, Pennsylvania.

Alcoa Aluminum

ALUMINUM COMPANY OF AMERICA

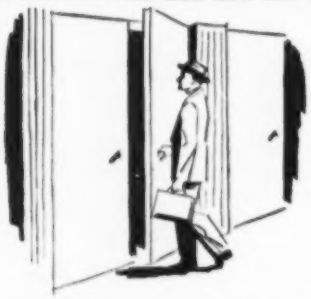

LIGHTWEIGHT DOORS and their hardware are made of aluminum by leading manufacturers. They are low in cost, durable and will remain attractive for a long time.

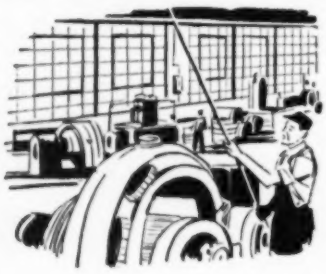

WINDOWS OF ALCOA® ALUMINUM are available from distributors everywhere. They never warp, crack or swell—are easy to operate and maintain.

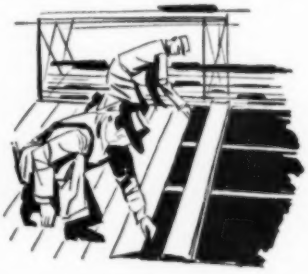

BUILDINGS OF ALCOA ALUMINUM Roofing and Siding never need painting. Low cost, lightweight and easy to install.

ALCOA ALUMINUM takes all finishes that other metals will take—plus gleaming, rust-resistant anodic coatings which are best on aluminum.

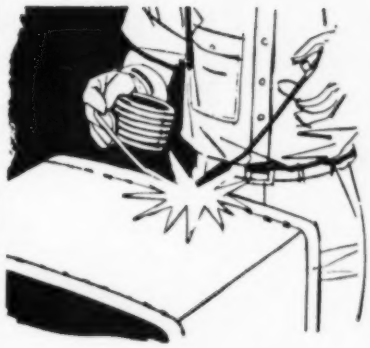

***FILLER METAL** of Alcoa Aluminum is available in many alloys for use in brazing, torch welding and arc welding. It is also packed suitably for automatic welding operations.

Products marked* are available from your local Alcoa Distributor listed here

***RIGID CONDUIT** of Alcoa Aluminum is the lowest cost corrosion-resistant, metallic conduit available. Its nonmagnetic properties improve electrical efficiency—its light weight speeds installation.

CORROSION-RESISTANT bearings of Alcoa Aluminum lower diesel maintenance. They are solid metal all through.

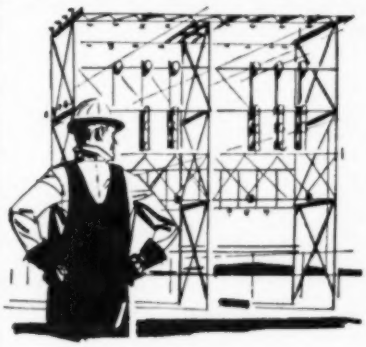

***SUBSTATIONS**—Substations built of lightweight Alcoa Aluminum Structural Rolled Shapes are quickly fabricated and erected. Aluminum's corrosion resistance eliminates current shutdowns for costly maintenance painting.

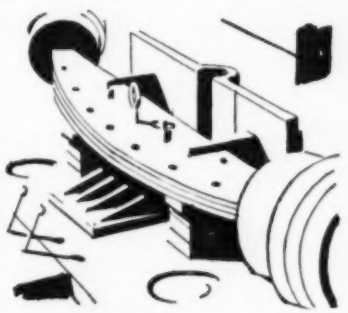

***TOOL AND JIG PLATE**—Forming and bending dies for aluminum shapes are economical when made of Alcoa Tool and Jig Plate. It is a cast product. Stress relieved, with close tolerances of flatness and surface smoothness.

ALABAMA
Birmingham
Hinkle Supply Co.

CALIFORNIA
Los Angeles
Ducommun Metals & Supply Co.
Pacific Metals Co., Ltd.
San Francisco
Pacific Metals Co., Ltd.

COLORADO
Denver
Metal Goods Corp.

CONNECTICUT
Milford
Edgcomb Steel of New England, Inc.

FLORIDA
Hialeah
Florida Metals, Inc.
Jacksonville
Florida Metals, Inc.
Tampa
Florida Metals, Inc.

GEORGIA
Atlanta
J. M. Tull Metal & Supply Co., Inc.

ILLINOIS
Chicago
Central Steel & Wire Co.
Steel Sales Corp.

LOUISIANA
New Orleans
Metal Goods Corp.

MARYLAND
Baltimore
Whitehead Metal Products Co., Inc.

MASSACHUSETTS
Boston
Edgcomb Steel of New England, Inc.
Cambridge
Whitehead Metal Products Co., Inc.

MICHIGAN
Detroit
Central Steel & Wire Co.
Steel Sales Corp.

MINNESOTA
Minneapolis
Steel Sales Co. of Minn.

MISSOURI
Kansas City
Metal Goods Corp.
St. Louis
Metal Goods Corp.

NEW JERSEY
Harrison
Whitehead Metal Products Co., Inc.

NEW YORK
Buffalo
Brace-Mueller-Huntley, Inc.
Whitehead Metal Products Co., Inc.
New York
Whitehead Metal Products Co., Inc.
Rochester
Brace-Mueller-Huntley, Inc.
Syracuse
Brace-Mueller-Huntley, Inc.
Whitehead Metal Products Co., Inc.

NORTH CAROLINA
Charlotte
Edgcomb Steel Co.

OHIO
Cincinnati
Williams & Co., Inc.
Cleveland
Williams & Co., Inc.
Columbus
Williams & Co., Inc.
Toledo
Williams & Co., Inc.

OKLAHOMA
Tulsa
Metal Goods Corp.

OREGON
Portland
Pacific Metal Co.

PENNSYLVANIA
Philadelphia
Edgcomb Steel Co.
Whitehead Metal Products Co., Inc.
Pittsburgh
Williams & Co., Inc.

TEXAS
Dallas
Metal Goods Corp.
Houston
Metal Goods Corp.

UTAH
Salt Lake City
Pacific Metals Co., Ltd.

WASHINGTON
Seattle
Pacific Metal Co.

WISCONSIN
Milwaukee
Central Steel and Wire Co.
Steel Sales Corp.

Meet The Authors

E. A. Slover (p. 1435) is assistant general manager of the Chino mines div., Kennecott Copper Corp., Hurley, N. M. Born at Newark, N. J., he holds B.S. degrees in mining and metallurgy, (Missouri School of Mines). Prior to joining Kennecott in 1939, Mr. Slover had been with the Nevada Consolidated Copper Corp., McGill, Nev. He holds membership in the Southwestern New Mexico Section, AIME.

John W. Dowding, Jr. (p. 1451), a native of Providence, R. I., is a graduate of Massachusetts Institute of Technology. Mr. Dowding had been associated with the General Electric Co. in the chemical and metallurgical training program. He is now a metallurgist with the Latrobe Steel Co., Latrobe, Pa. His main interest is photography.

Helen Towers (p. 1455), lecturer on slags and refractories, Royal Technical College, was born at Larbert, Scotland. Dr. Towers was assistant lecturer in the metallurgy dept. at the College from 1941 to 1946. She had spent the 1951-52 session at Massachusetts Institute of Technology on a research fellowship. Dr. Towers is a member of the Iron & Steel Institute, British Ceramic Society, and the West of Scotland Iron & Steel Institute.

G. A. Moore (p. 1443) has been a metallurgist with the National Bureau of Standards since 1951. Born in New York City, Dr. Moore holds degrees from Union, Harvard, and Princeton Universities. He was an instructor at Princeton from 1935 to 1940. He then joined Battelle Memorial Institute as a research engineer. Dr. Moore was assistant professor of metallurgy at the University of Pennsylvania prior to joining the National Bureau of Standards. He has had numerous papers published and holds membership in various professional societies. Dr. Moore is active in Boy Scout work in his spare time and also does color photography work.

G. A. MOORE

CYRIL WELLS

Cyril Wells (p. 1463), a graduate of Carnegie Institute of Technology (B.S., M.S., D.Sc.), was born at Lincolnshire, England. Dr. Wells has been associated with Carnegie since 1929. He is presently principal research metallurgical engineer. A Member of AIME, he is also a member of ASM and American Society for Quality Control. He has previously presented several papers before AIME.

J. H. Bechtold (p. 1469) is a research engineer with the Westinghouse Electric Co., research laboratories, East Pittsburgh. Mr. Bechtold was born at Boonville, Mo., and graduated from the University of Illinois (B.S., M.S.). For two years he was an instructor at the University in the metallurgical dept. His spare time interests are golf and bridge. He is also a Member of the Pittsburgh Local Section, AIME.

Paul E. Busby (p. 1463), a research metallurgist at the metals research laboratory of the Carnegie Institute of Technology, was born at Homestead, Pa. He holds a B.S. in metallurgical engineering (1942). His varied hobbies include photography, electronics, fishing, and woodworking.

...it takes
"KNOW-HOW"
to do an Expert Job!
FURNACE TEAR OUTS
SALAMANDER OR SLAG REMOVAL
MATERIAL HANDLING
CHICAGO CONCRETE BREAKING CO.
EDWARD GRAY, President
GENERAL OFFICES:
12233 Avenue O, Chicago 33, Ill
BAyport 1-8400
PITTSBURGH 19, PA.
Suite 704, 550 Grant St.
Atlantic 1-4674
Prepared to serve you with maximum efficiency ANYWHERE – at ANYTIME!
CONSULT US ON YOUR NEXT BLASTING PROBLEM
Serving the Steel Industry for Over 30 Years

For the story of FERROCARBO in quality steelmaking, mail the coupon today—or phone or write the FERROCARBO distributor nearest you. You'll learn why steel deoxidized with FERROCARBO is "plus steel."

KERCHNER, MARSHALL & CO.
PITTSBURGH • Cleveland • Buffalo
Philadelphia • Birmingham • Los Angeles

MILLER & COMPANY
CHICAGO • St. Louis • Cincinnati

WILLIAMS & WILSON
TORONTO • Montreal • Windsor

THE CARBORUNDUM COMPANY, Dept. JM 84-31
Niagara Falls, New York

Gentlemen:

I would like to have the FERROCARBO story—no obligation on my part.

NAME AND TITLE

COMPANY

STREET AND NUMBER CITY ZONE STATE

FERROCARBO

TRADE MARK

by CARBORUNDUM

"Carborundum" and "Ferrocarbo" are trademarks which are registered in the U. S. by The Carborundum Company, Niagara Falls, New York, and in Canada by Canadian Carborundum Company, Ltd., Niagara Falls, Ontario.

Metallurgical Engineer

Applications are invited from graduate Metallurgical Engineers, preferably in the age range 40 to 45, who have had not less than ten years broad and responsible experience in the field of nonferrous extraction metallurgy, for the position of Assistant Metallurgist to the undermentioned Corporation. The position entails duties in connection with the important group of Northern Rhodesian mining companies producing copper, cobalt, lead, zinc and other base metals, to which the Corporation acts as Consulting Engineers.

The salary to be offered will be commensurate with the successful candidate's qualifications and experience. Membership of the Corporation's Pension Fund will be a condition of employment.

Applicants must be prepared to take up residence in Kitwe, Northern Rhodesia. The cost of transportation of the successful candidate, his wife and children up to 18 years of age and reasonable personal effects will be borne by the Corporation. A modern three-bedroomed brick house, with essential furniture, will be made available at a rental which will not exceed $28.00 per month.

Excellent medical facilities are provided and recreational amenities are outstanding.

Initially the engagement will be for a period of three years, after which service may be extended indefinitely, but will be subject to six months notice of termination by either party. Repatriation privileges on the same scale as above will be granted at the end of three years service. Leave is generous and amounts at present to 60 days per annum which can be accumulated up to a maximum of 180 days.

Applications stating age, marital status, educational and professional qualifications and giving details of past experience and positions held should be addressed to:

Personnel Officer,

Anglo American Corporation of South Africa, Limited,

P.O. Box 4587,
JOHANNESBURG.

—Personnel Service—

THE following employment items are made available to AIME members on a nonprofit basis by the Engineering Societies Personnel Service, Inc., operating in cooperation with the Four Founder Societies. Local offices of the Personnel Service are at 8 W. 40th St., **New York 18;** 100 Farnsworth Ave., **Detroit;** 57 Post St., **San Francisco;** 84 E. Randolph St., **Chicago 1.** Applicants should address all mail to the proper key numbers in care of the New York office and include 6c in stamps for forwarding and returning application. The applicant agrees, if placed in a position by means of the Service, to pay the placement fee listed by the Service. AIME members may secure a weekly bulletin of positions available for $3.50 a quarter, $12 a year.

MEN AVAILABLE

Stainless Steel Metallurgist, who acquired excellent experience in production, processing and development and the practical know-how of improving overall operating methods and costs, now engaged as works manager of medium size steel plant, desires position as management assistant or director of technical development. First class references. M-113.

Metallurgical Engineer, M.S.; B.S. Chem. E., 27, three years sheet metal fabrication and processing. Vendor liaison work, trouble shooting. Good contact man. Some development work on refractory metals. Knowledge welding, brazing. Experience also includes chemical process equipment design. Desire position application, liaison or sales engineer. Veteran. Prefer vicinity of New York. M-112.

POSITIONS OPEN

Assistant Smelter Superintendent, metallurgical graduate, with a few years' experience in responsible employment in a copper smelter. Salary, $7200 a year to start plus current local cost-of-living allowance of 20£ a month. Three year contract with all expenses and full pay, plus traveling both ways. If married, house with furniture is provided. Opportunity for advancement. Location, South Africa. F9160.

Research Assistant, B.S. in science or engineering for southeastern academic X-ray diffraction laboratory. Duties include publishable fundamental research on metals; initiation of similar studies encouraged. Reply should include complete personal data and statement of professional interests. Eleven months annually. Location, North Carolina. Y9137.

Metallurgist, B.S. degree, higher degrees preferred, with experience in precision metals preferably in re-

METALLURGISTS

Would you like to work in A CHALLENGING NEW FIELD—the DEVELOPMENT of MATERIALS and PROCESSES for COMPONENTS of NUCLEAR REACTORS? We need top-flight men at the INTERMEDIATE and SENIOR LEVEL to participate in one of the most momentous programs of this century.

MODERN LABORATORIES, SUPERBLY EQUIPPED, located in suburban Pittsburgh eleven miles southeast of the New Golden Triangle. UNIQUE OPPORTUNITY FOR GRADUATE STUDY WHILE WORKING. Housing of all types readily available in attractive communities nearby.

Write today to Supervisor, Industrial Relations, P. O. Box 1468, Pittsburgh 30, Pa.

WESTINGHOUSE
ATOMIC POWER DIVISION

PHYSICAL METALLURGIST

To operate latest design X-ray Diffraction and Geiger Counter X-ray Spectrometric Equipment. Graduate degree preferred. In addition will also consider a technician with 2 years experience. Work, in the field of inorganic chemistry, will involve identification of elements, compounds, lattice parameters, phases, alloys, stresses, etc. Excellent opportunity for professional growth and chance to use initiative in development and research.

RAYTHEON MANUFACTURING COMPANY

190 Willow St., Waltham, Mass. (In Greater Boston Area)

search. Capable of directing a metallurgical laboratory of small research organization. Opportunity for advanced study. Salary, $5000 to $6500 a year. Location, Virginia. Y9118(b).

Metallurgical Engineer, graduate, for experimental work in process metallurgy; 2 to 5 years experience with open hearth or electric furnace operation; practical knowledge of melting, refining, pit practice, mechanical aptitude and resourcefulness especially desirable; permanent assignment in sales development laboratory. Y9084(b).

Metallurgist, with three to six years experience for mill processing work in the field of high temperature alloys, tool steels. Should have steel production background. Location, Pennsylvania. Y9042.

Metallurgist for basic research on materials heat treatment and investigating production manufacturing problems in machining, heat treating and grinding. Must have B.S. in metallurgy, mechanical or chemical engineering. Experience in metal and fabricating industry desirable. Must have ability to analyze and report on technical problems. Salary, $3900 to $4680 a year. Location, Connecticut. Y9079.

Metallurgist, 30 to 40, with at least five years experience covering alloy steels, nonferrous materials, plating, etc., in domestic appliance or novelty fields. Salary, $7280 to $9100 a year. Location, Brooklyn, N. Y. Y9073.

Assistant or Associate Professor of metallurgical engineering, to teach heat transfer and process metallurgy including thermodynamics. Advanced degree and experience essential. Location, Pennsylvania. Y8993.

WANTED—METALLURGIST. AN EASTERN PLANT OF A LARGE STEEL CORPORATION WITH WIDE PRODUCTION FACILITIES FOR VARIOUS TYPE PRODUCTS HAS OPENING FOR QUALIFIED PERSON TO HEAD UP METALLURGICAL DEPARTMENT. APPLICANT MUST HAVE BASIC AND PLATE MILL EXPERIENCE AND SHOULD GIVE AGE, EDUCATION, EXPERIENCE, AND DESIRED SALARY IN INITIAL LETTER.
Box J-26 JOURNAL OF METALS

EXECUTIVE ENGINEER—Graduate Metallurgist. Age 27. 5 years industrial experience, including 2 years automotive. Executive training and ability. Desires supervisory position in industry. Presently Naval Office on AEC project. Available Dec. 1, 1953.
Box J-27 JOURNAL OF METALS

PHYSICAL METALLURGISTS. Recent graduates with bachelor's and advanced degrees desired for expanding research program on copper, titanium and other metals. An opportunity for a permanent position with progressive and successful company in Southern New England. Please give details of education, experience and interests.
Box H-25 JOURNAL OF METALS

Sales Engineer, mechanical or metallurgical graduate, for sales promotion covering welding accessories. Salary, $4000 a year to start. Some traveling. Location, New York, N. Y. Y9004.

IF

You Need Supplying Promptly With Custom-Built Alloy Metal Powders To Difficult or Hard-To-Get Specifications

THEN

Write To

POWDER METALLURGY LTD.

59-62, High Holborn, London, England.

WHO

Will Undoubtedly Be Able to Satisfy You.

WANTED—For Mineral Resources Development Corporation, an agency of THE GOVERNMENT OF THE UNION OF BURMA, for positions of Departmental Head.
NON-FERROUS METALLURGIST: Qualifications: University Degree in Metallurgy or equivalent qualification. Adequate experience of methods of ore dressing, smelting and refining. Extensive plant design experience. Should be familiar with the use of electrolytic and electrothermic processes in the reduction of zinc and with oxidation and reduction of antimony. Duties: Advice on methods of beneficiation of low-grade ores and on setting up of smelting and refining industries in zinc, tin, antimony and cobalt, and extraction of sulphuric acid from smelting and industrial gases. Setting up of pilot plants. Supervision of any construction work on smelting and refining plants.
Apply to: THE DIRECTOR-GENERAL, MINERAL RESOURCES DEVELOPMENT CORPORATION, Secretariat, Rangoon, Burma, with references giving full particulars of age, education, qualifications and experience (in chronological order), stating salary and terms required.

Ready now!

PROCEDURES IN EXPERIMENTAL METALLURGY

By A. U. SEYBOLT and J. E. BURKE, both with the General Electric Company

Here is the first complete reference book to deal directly and comprehensively with the equipment, materials, and processes of laboratory metallurgy. Planned to assist all metallurgists — in addition to the trained scientist who is a novice in metallurgical techniques — the book presents, in detailed form, the unit operations that are common to all metallurgical investigations.
The equipment of laboratory metallurgy is described in the early chapters—furnaces, temperature controllers, vacuum systems, and refractories. Next, the techniques of the major unit operations—melting, heat treatment, mechanical fabrication, and powder metallurgy are discussed as they are used on a laboratory scale. Finally, two special topics of great importance are presented —the preparation of pure metals, and the preparation of metal single crystals.

1953 340 pages illus. $6.00

Introduction to SOLID STATE PHYSICS

By CHARLES KITTEL, University of California

This book emphasizes those areas of active research in solids which may be discussed in terms of simple physical models. Subjects include: Ionic crystals, thermal properties, dielectrics, ferroelectrics, paramagnetism, ferromagnetism, antiferromagnetism, superconductivity, electron theory of metals, semiconductors, transistors, imperfections in crystals, and dislocations. Advanced topics are developed in appendices.

1953 396 pages illus. $7.00

FERROUS ANALYSIS

Modern Practice and Theory

By E. C. PIGOTT, The Central Marine Engine Works, West Hartepool, England

FERROUS ANALYSIS is unique in the amount of graphical and tabular information presented. It provides a realistic, practical understanding of the metallurgical effects caused by changes in composition. By offering the rapid and reliable methods, specific to the elements concerned, this book more than meets the requirements of the practicing analyst. It provides a clear, systematic examination of each of the 31 major constituents of iron and steel.

1953 690 pages illus. $12.50

Send for your on-approval copies today

JOHN WILEY & SONS, Inc.

440 Fourth Avenue, New York 16, N. Y.

PROGRESS REPORT ON NATIONAL CARBON
TRADE-MARK
BLAST FURNACE LININGS

One out of every three blast furnaces in this country is now lined with "National" carbon. With this outstanding acceptance of carbon as a blast furnace refractory, let's take a look at its remarkable performance *over the long haul.*

Here are the facts:

- *23* "National" carbon-lined furnaces have each produced over *2* million tons.
- *5* of these have passed the *2 1/2* million ton mark.

These are all original linings — *and still going strong!*

Every year more "National" carbon goes in... more unit tonnages go up and costs come down... more operators learn what *smooth* operation really is.

The term "National" is a registered trade-mark of Union Carbide and Carbon Corporation

NATIONAL CARBON COMPANY
A Division of Union Carbide and Carbon Corporation
30 East 42nd Street, New York, 17, N. Y.

District Sales Offices: Atlanta, Chicago, Dallas, Kansas City, New York, Pittsburgh, San Francisco

IN CANADA:
National Carbon Limited—Montreal, Toronto, Winnipeg

NATIONAL CARBON PRODUCTS

CARBON LININGS FOR FERRO-ALLOY FURNACES • CARBON MOLD PLUGS • GRAPHITE THERMOCOUPLE SHEATHS • GRAPHITE STARTERS FOR HOT-TOPPING • CARBON CINDER NOTCH PLUGS • GRAPHITE AND CARBON CORES • GRAPHITE RISER RODS • CARBON BOXES AND GRAPHITE POWDERS FOR HEAT TREATING • PIPE AND FITTINGS • CARBON BRICK • PUMPS • CONDUCTOR ROLLS • SPECTROSCOPIC ELECTRODES • STEAM JETS • ANODES

New Products

New Products | New Literature | New Services

For Further Information or Literature on any Product, Fill in the Coupon and Send to JOURNAL OF METALS

Students are Requested to Apply Directly to Manufacturers for Bulletins and Information

1—PIT FURNACE: A gas fired, pit furnace for cycle annealing of small

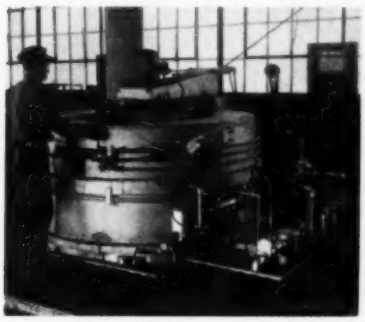

hand tools is available from *Westinghouse Electric Corp.* A removable retort makes continuous operation possible since one retort can be discharged and recharged while the other is in the furnace. Maximum operating temperature is 1600°F. The furnace can also be used for carburizing, hardening, and nitriding.

2—MICROSCOPE READER: A new Brinnell microscope reader for measurement of the diameters of indentations made by the ball indentors of all Brinnell type hardness testing machines has been announced by *Pacific Transducer Corp.* The instrument features a reticle in a flat field optical system and a self enclosed concentrated beam of light. The scale is calibrated in millimeters and tenths of millimeters. The total length of the scale is 7.0 mm. Diameter of the field of the microscope is 7.5 mm.

3—MAGNET: An Alnico magnet has been developed for use in an electronic recorder of unusual design. Less than ¼ in. square, it is made of nickel, aluminum, cobalt, and iron. Applications in industry include use in open hearth furnaces where it measures the temperature of the checker chambers. Other uses include brick and ceramic kilns, chemical retorts, etc., wherever an accurate record of more than one measurement is required. *International Nickel Co.*

4—THERMISTORS: A device no larger than an aspirin tablet that is capable of detecting high altitude guided missile temperature changes as minute as 0.0005 of one degree is announced by the Carboloy dept. of *General Electric Co.*

5—INGOT MOLD COATING: An improved ingot mold coating material is currently available in semi-works quantities. It is reported in experimental field trials and commercial runs to bring about improved surface and steel quality, as well as increased ingot yield. Runs indicate the temperature range to be from room temperature to above 700°F. *Masonite Corp.*

6—DECADE SCALER: A high speed six digit decade scaler adapted for use in telecommunication and in modern computers for frequency and nuclear measurements is available from *North American Philips Co., Inc.* Including power supply and appropriate control circuits, the instrument has a maximum cyclic rate of 30,000 events per sec, minimum resolving time of 25 microsec and a total registration of 999,999.

7—SOLDERING FURNACE: A gas fired soldering furnace, using a radiant burner as a heat source, is capable of heating, in less than 8 min, two 4-lb irons from room temperature to 900°F, or one 4-lb iron to 1200°F with a heat input of only 9100 Btu per hr. The burner is lo-

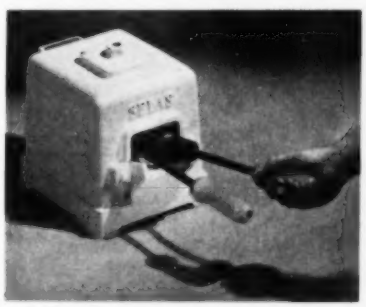

cated so that mechanical shock and flux corrosion damages are held to a minimum. *Selas Corp. of America.*

8—HOPPERTROL: Automatic positive level distribution of foundry sand from a belt to several hoppers or bins can now be accomplished. *Harry W. Dietert Co.* offers this unit to control air operated plows according to the amount of sand in the hopper.

9—MAGNET: This chip retriever removes metallic particles from places hard to reach. It removes chips from blind drill and top holes on production lines, and in electrical and mechanical assembly work. *General Scientific Equipment Co.*

10—STRAIGHTENING MACHINE: *Sutton Engineering Co.* is marketing

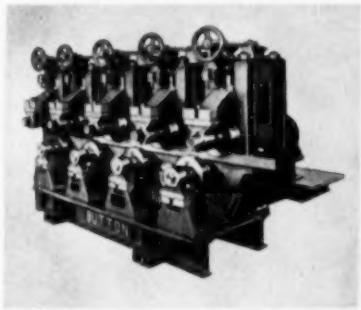

a new machine able to straighten squares from ½ to 2½ in. and flats up to 4x1 in. at speeds as high as 400 fpm. Any steel or nonferrous flats and shapes including all grades of alloy and tool steels can be used.

11—BULL BLOCK: This series 6000/30 bull block features a self contained worm drive and is capable of drawing at speeds up to 440 fpm. The *Medart Co.* bull block has a drum that is overhung which gives an advantage in that the instant the last piece of material leaves the die, the coil drops by gravity off the drum to the unloading platform where it is removed easily by the operator without using overhead cranes.

Free Literature

20—GEARS: Catalog No. 70 issued by *Grant Gear Works, Inc.*, describes the entire line of stock gears, speed reducers, sprockets and chains, and couplings and special gears. Tables and engineering information relating to power transmission are also given.

21—METAL ANALYST: A comprehensive 200-page catalog of metallurgical apparatus has been issued by *Buehler, Ltd.* The latest listing of cutters, grinders, mounting presses, cameras, furnaces, accessories, etc., and 250 recommended books for the metallurgical library are contained.

22—GRINDING CARBIDES: Illustrated 39-page booklet issued by *Carborundum Co.*, reveals new techniques and abrasive products de-

veloped to obtain efficient and economical carbide tool manufacture and maintenance. Objective appraisals concerning the advantages and limitations of the use of green grit and diamond grinding wheels are included.

23—MAGNETIC ANALYSIS: Multimethod equipment for nondestructive testing of ferromagnetic bars, wire rods, and tubing, is described in bulletin No. 10 available from *Magnetic Analysis Corp.*

24—POLYURETHANES: Latest information obtained from application research in the field of using polyurethanes as adhesives for bonding rigid materials is contained in technical bulletin published by *Monsanto Chemical Co.*

25—WASHING COMPOUND: Catalog sheet describing noncorrosive, ferrous metal cleaning concentrate designed for quick removal of quenching oils after heat treating has been released by *Ipsen Industries, Inc.* Data explain the new principle under which the compound acts and tell of what materials it is produced.

26—COMBUSTION: Bulletin graphically illustrates and explains how too much or too little air can have costly effects in combustion processes. How oxygen in flue gases will indicate almost exactly the same excess air factor for any fuel from coke to natural gas, even when the fuels are in combinations of two or more. *Arnold O. Beckman, Inc.*

27—REFRACTORY BRICK: The first complete instructional brochure on the installation of refractory brick in cement kilns, was published by *Kaiser Aluminum & Chemical Sales, Inc.*

28—TESTING TECHNIQUES: Techniques developed by *Sperry Products, Inc.*, are described in brochure. Detailed descriptions of latest ultrasonic nondestructive testing equipment are contained.

29—DATA BOOK: Catalog TC10 shows the complete line of thermocouples, radiation detectors, and resistance bulbs available from *Barber-Colman Co.* Information on protection tubes, lead wire and other accessories is also included.

30—LUBRICATOR: How to automatically lubricate entire conveyor lines without stopping the line is illustrated in a new catalog sheet distributed by *Stewart-Warner Corp.*

31—PRODUCT RESEARCH: Brochure dealing with development of a new product, improvement of an established product or the method of producing it has been issued by *Arthur D. Little, Inc.*

32—MOUNT PRESS: New bulletin describes the AB speed press. Features include use of preheated premolds, rapid closing and universal application for thermosetting or thermoplastic materials in three sizes. *Buehler Ltd.*

33—EXPLOSIVE PRODUCTS: A 48-page book offers specific aid in selection of industrial explosives. Text and pictures summarize the methods and explosive materials commonly specified. Properties of accessories are tabulated. *Atlas Powder Co.*

34—DIAL THERMOMETERS: Emphasizing the variety of ranges, bulbs, tubing, and accessories available, bulletin describes dial thermometers for long distance measurement. *Foxboro Co.*

35—PEROXYGENS: New and improved methods of treating metal surfaces with peroxygen compounds are described in bulletin No. 51 published by the *Buffalo Electro-Chemical Co., Inc.* Surface treatments such as bright dips, cleaning solutions, passivation and inhibitors are discussed.

36—FOAMGLAS: All temperature, insulation for tanks and other equipment is presented in folder published by *Pittsburgh Corning Corp.* Physical properties of the unique cellular glass insulation are given.

37—TESTING INSTRUMENTS: A buyer's guide on electric testing instruments has been announced as available from *General Electric Co.* Application data, features of each instrument, and prices are included.

38—TI DESCALING: Bulletin 25-T issued by *Hooker Electrochemical Co.*, relates their past experience with titanium descaling so that present and prospective users of Virgo descaling salt can best apply Hooker process to their problems.

39—SILICONES: Catalog issued by *Dow Corning Corp.*, describes what these silicones do. New products, ranging from adhesives to molding compounds have been added and the application index has been expanded.

40—FLOTATION: Recovery of Kyanite by flotation at *Commercialores, Inc.*, is described in bulletin. Every aspect of production beginning with the geology of the Kyanite formation and the removal of the Kyanite from the quarry to the mill is described. Crushing, grinding, etc., are also described.

41—BELTING: Rayon transmission belting is illustrated in brochure issued by *Goodyear Tire & Rubber Co.*

42—SPECTROGRAPHS: Line of grating spectrographs is illustrated and described in catalog available from *Jarrell-Ash Co.* Technical information on all standard spectrographs including the 3.4 meter, 2.5 meter and 5.5 meter adjustable types and 3.4 meter and 1.5 meter fixed position spectrographs is listed. Accessory equipment, information on production of the diffraction gratings used and other information are included.

43—TANTUNG 144: Catalog issued by *Vascoloy-Ramet Corp.* introduces this new grade of Tantung to the metal cutting tool field. Complete information on Tantung G is also given. Tantung 144 was developed as an alloy with greater hardness and for use where resistance to abrasion in cutting is of most importance, and where the absence of shock or impact will permit its use.

Journal of Metals **November**
29 West 39th St.
New York 18, N. Y.

Please send me { More Information ☐ / Free Literature ☐ / Price Data ☐ } on items indicated.

1	2	3	4	5	6	7	8	9	10
11	12	13	14	15	16	17	18	19	20
21	22	23	24	25	26	27	28	29	30
31	32	33	34	35	36	37	38	39	40
41	42	43	44	45	46	47	48	49	50

Name_____ Title_____

Company_____

Street_____

City and Zone_____ State_____

Metals for the *Electrical Industry*

GLC GRAPHITE ELECTRODES help make many of the metals essential to the production, transmission and utilization of electricity.

The performance of **GLC GRAPHITE ELECTRODES** is unsurpassed in the manufacture of electric steels, foundry metals, ferroalloys and magnesium.

ELECTRODE DIVISION

Great Lakes Carbon Corporation

Niagara Falls, N.Y. GLC® Morganton, N. C.

Graphite Electrodes, Anodes, Molds and Specialties

Sales office: Niagara Falls, N.Y. **Other offices:** New York, N.Y., Oak Park, Ill., Pittsburgh, Pa.

Sales Agents: J. B. Hayes, Birmingham, Ala., George O'Hara, Long Beach, Cal., Great Northern Carbon & Chemical Co., Ltd., Montreal, Canada.

If Your Product Requires

The Strength of a Panther

But Must be the Size of a Kitten . . .

Use **M H Chromium-Nickel Pre-alloyed Powders**

Very small amounts of Metal Hydrides' chromium-nickel pre-alloyed powders combined with iron powders, can mean volume production of small and intricate parts having high tensile strength.

Write now for complete information on properties of iron powders with alloys of varied chromium-nickel contents. Your inquiries will receive prompt, interested attention. Ask for Bulletin 800-A.

M H **METAL HYDRIDES**

INCORPORATED

24 CONGRESS ST., BEVERLY, MASS.

Industrial Notes . . .

• Bethlehem Steel Co. is making three propeller shafts weighing more than 26 tons each for the 60,000-ton aircraft carrier Saratoga. The 67-ft long shafts for the world's most powerful carrier are being forged on a 7500-ton hydraulic press, rough turned, rough bored, heat treated, tested, rough machined, and finish bored. Flange diameter is 36 in. and the main shaft is 22 in. diam, tapering to 16 in. at the propeller end. The corresponding taper in the bore is accomplished by use of a bevel bit.

• Installation of two production control Quantometers was announced by Crucible Steel Co. of America. The Quantometers reduce chemical analysis time to about 10 min and give more complete detail on metallic elements in the steel. The instruments were placed in the chemical laboratories at the Sanderson-Halcomb works, Syracuse, N. Y., and at the Midland works, Midland, Pa. Each unit consists of a high precision source unit, a spectrometer, and recording console. They are housed in an air conditioned room.

• Fall session of the semi-annual North American Philips Co., Inc., X-ray Diffraction School was held at the company's plant, 750 South Fulton Ave., Mount Vernon, N. Y., October 5 to 9. First four days of the school were devoted to classroom and laboratory work with opportunity provided for discussion of problems. Guest speakers discussed methods currently in use.

• A new midwest liaison office in Chicago is to be opened by Arthur D. Little, Inc., Cambridge, Mass. The new office, set up to serve the industrial research and engineering firm's expanding midwestern clientele, will maintain a staff capable of handling technical-economic, technical-audit, and market research surveys in that area.

• Bethlehem Steel Co.'s scrap inspection dept. has developed a quick method for the inspection of hydraulically compressed No. 2 sheet scrap. Small quantities of dynamite are inserted into a hole drilled in the scrap bundle and detonated. Six bundles are selected from each carload, taking two from the end, two from the middle, and two from the opposite end. Internal inspection of the scrap is made after the blast.

• An economic disadvantage prevents the widespread use of transistors in electrical products, according to Robert W. Galvin speaking at the National Electronics Conference, Chicago. He noted, however, that the reduction in battery drain achieved through use of transistors may speed their appearance in automobiles and portable radios.

• For the first time in Ford Motor Co. steel operations a blast furnace was drained by tapping it from the bottom. The job was done by workmen of Arthur G. McKee & Co., in preparation for relining the furnace. Pits were dug in sand that covered a street at the Rouge plant to control the flow of iron. Previous practice had been to let the iron cool and then blast it out. It will take some 45 days and 125 people to reline the 800-ton-per-day furnace.

• *A bibliography on Keysort cards issued by the New York Society of Electron Microscopists is designed to keep abreast of world literature in all fields of electron microscopy. The bibliography is already coded and punched by the bibliographer. Articles containing multiple subjects are easily located and no filing order is needed because cards are selected by needle. First issue covers 1950 to 1952 and utilizes about 700 cards. Details may be obtained from the Society at the New York Academy of Sciences' Building, 2 East 63rd St., New York 21.*

• **Ferrochrome production has started at Pacific Northwest Alloys Inc.'s plant near Spokane. One of four arc furnaces is already turning out ferrochrome. The other furnaces will go into operation when additional vacuum capacity is installed in the reduction plant. Output of ferrochrome from the one furnace is expected to be 1.5 million lb per month. Another furnace is producing ferrosilicon.**

• The Reporter item in September JOURNAL OF METALS describing Bell Telephone Laboratory's new silicon alloy diode erroneously stated that "Like transistors the diodes need a warm-up period." Actually, neither need a warm-up period. Present plans call for use of the diode in the memory organ of a computer. Bell officials also believe that it will take the place of mechanical switches used to remember telephone numbers while a call is completed. The diodes can also operate under high temperatures.

• *Scovill Mfg. Co.'s new aluminum strip mill is in production at the Waterbury, Conn., plant. The new mill uses furnaces in which all aluminum is annealed under complete atmospheric control with nitrogen substituted for oxygen. After all oxygen, carbon dioxide, and oil have been forced from the enclosure this controlled atmosphere is injected into a bell type furnace. The cold rolled aluminum strip will go on the market under the name Truspec.*

Making heat perform better is a Salem-Brosius specialty

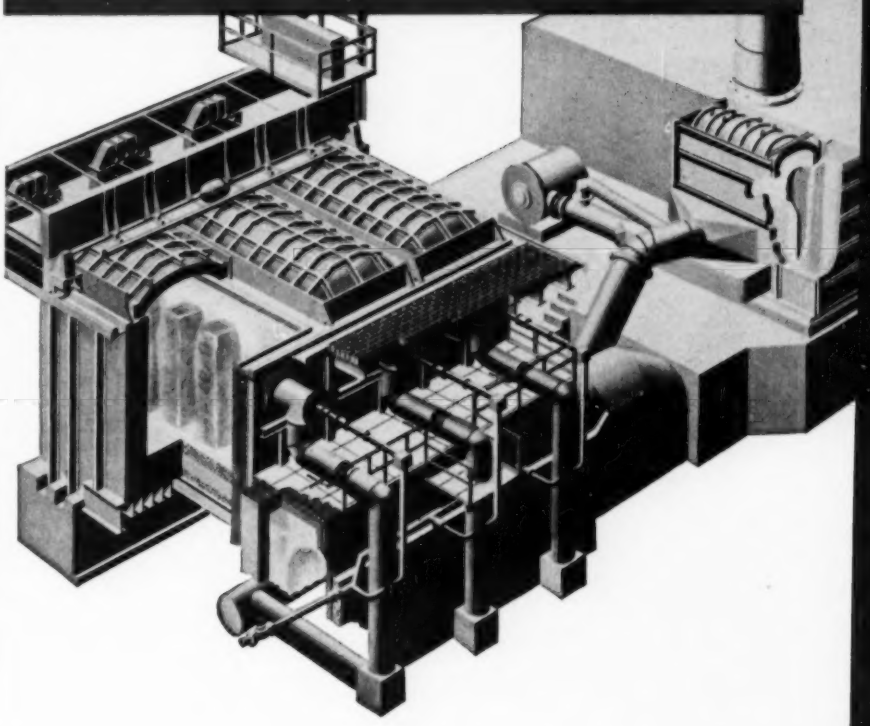

This new installation of Salem-Brosius rectangular, gas-fired soaking pit furnaces conditions steel ingots for further processing—works around the clock for one of the country's outstanding steel makers. Ingots are heated faster, more uniformly and at lower cost in these furnaces. Double-pass, metallic, needle-type recuperators that preheat combustion air and reduce fuel costs are an outstanding feature of the design. Low maintenance, easy operation and long service life are standard with Salem-Brosius designed furnaces.

Salem-Brosius engineers are specialists in performance and control of heat in manufacturing, offering furnaces custom-built to your requirements. Salem-Brosius furnaces assure you maximum high-quality output at minimum initial, operating, and service costs.

We would like to tell you more about the efficiency of these new units, and also about the well-known Salem-Brosius circular soaking pits.

If your modernization or expansion plans call for heating or heat treating furnaces of any kind, furnace or forging manipulation equipment, valves, or hot materials handling machinery; write, wire or phone Salem-Brosius!

SALEM-BROSIUS, INC.

Sales and Executive Offices: 240 Fourth Avenue, Pittsburgh 22, Pa.

A caterpillar diesel D8 tractor is being used to reclaim slag at an operation near Follansbee, W. Va. The "cat" is equipped with a No. 8S bulldozer. The slag is then run through a machine to recover residual iron.

ROY W. Drier, Michigan College of Mining and Technology professor, is scheduled to resume explorations on Isle Royale that already have disclosed a copper industry that predates King Solomon's temple and the birth of Christ.

Discoveries last spring helped clear up some of the major mysteries surrounding North America's ancient history. Modern carbon-14 dating techniques, an atomic science byproduct, established the date of some of the wood tools discovered on the island some 50 miles north of Michigan's Upper Peninsula. Mr. Drier feels that further discoveries may lead to even more ancient dating.

Isle Royale is about 50 miles long, five miles across, and reaches an elevation of 500 ft. When the first miners explored the island in the late 1840's they discovered that prehistoric people had mined all of the worthwhile lodes on the island, according to Mr. Drier. Pits as deep as 60 ft and 30 ft in diam were discovered. Because of the problem of food supply and poorness of the lodes, Mr. Drier states, the ancient miners abandoned the workings. Pits are much as they were left by these prehistoric people, except for filling in by vegetation and decay.

Mr. Drier reports that a mining engineer, studying a few square miles on the island determined that ancient workings represented the efforts of 10,000 men for 1000 years.

The most recent expedition led by Mr. Drier was sponsored jointly by Michigan Tech and J. C. Gannon, Marquette, Mich., businessman. James B. Griffin, director of museums at the University of Michigan, and Paul Beaubien, National Park Service archeologist, are among the dozen authorities who are assisting in the research.

Actual dating techniques are carried out in the Radio-Carbon laboratories of the Memorial Phoenix Project at the University of Michigan, with the cooperation of H. R. Bane. In addition to two handle-type wooden tools, the expedition found several stone mauls used by prehistoric miners for breaking copper-bearing rock. Excavation also unearthed charcoal used for heating large rocks. The rocks were doused with water to assist cracking.

Some of the old pits were only half worked, according to Mr. Drier, with excavators finding tools in the area. Indian legend makes no mention of copper mining. The legends do indicate, according to Mr. Drier, that pieces of copper were revered as Manitous or gods, and would tend to prove that the Indians did not mine copper or use it industrially. However, legend tells of a white race driven out by the Indians long before Europeans were known to have landed in North America.

Before issuing a detailed report of their findings, Mr. Drier and Mr. Griffin intend to search for a greater amount of evidence from the Isle Royale pits.

Some of the questions Mr. Drier would like to find answers for dig deep into the continent's prehistoric past. Were the men who mined the island of the same race as those who mined on the Peninsula? What happened to them, causing them to leave tools and workings as if they planned to return the next day? Were they mound builders, or does the finding of copper implements in the same formation as the

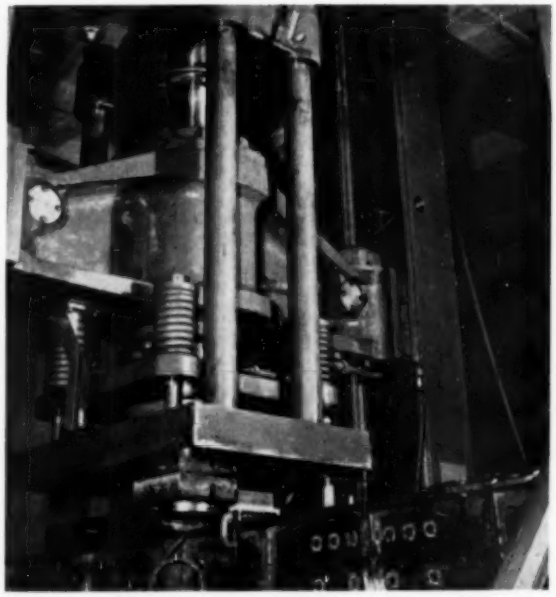

The crosshead of the new Baldwin testing machine at McGill University carries the hydraulic electric equipment which operates the machine. Hydraulic cylinder in the center applies test loads up to 400,000 lb downward. A test is being run on a welded plate girder.

skeleton of a mastodon indicate a more ancient lineage? How did they find copper even though ore was covered by thick overburden? Mr. Drier feels that the answers to these questions will unveil an age as interesting as any recorded.

◆◆◆◆◆◆

FOR some unfathomable reason, newspapers and magazines in recent weeks have been filled with *think pieces* on the automatic factory of the future. The authors envision plants where raw material is poured in at one end and a finished product, after a series of operations untouched by human hands, emerges in pristine glory. But according to many engineers, the lack of human hands appears to be the flaw in the dream. They point out that for several reasons the automatic plant is an ideal—to be striven for but never attained in a complete sense.

Instruments must be tailored to human capabilities, said one engineer. Actually, the use of automatic control and production devices can be used to reduce the manpower needed and to minimize the chance of error—but they can never shunt human brains and skill into absolute obsolescence.

One other factor is involved. If the possibility of the automatic factory is assumed, the economic chaos must be accounted for, another engineer points out. The petroleum, chemical, and several other industries could conceivably develop completely automatic operation. However, those industries face no real technological unemployment problem as do other industries.

Engineers note that many small factories are employing instrumentation on a large scale for a centralized production control picture. In one case, use of video, a literal picture is given of specific points of operation.

◆◆◆◆◆◆

AMIDST the usual torrent of Soviet propaganda, Washington experts on Russian economics discern a note of genuine progress in the nonferrous metals field. The USSR, somewhat pinched by a nonferrous metals shortage, has completed the Ust-Kamenogorsk hydroelectric development on the River Irtysh in eastern Kazakhastan. The station is one of five projected by the 1950 five year plan. Izvestia, official Communist Party newspaper, claims that the new plant will increase electric power production in the eastern Kazakhastan area by some two and a half times, which in turn will increase mining and metallurgical activity. The Soviet newspaper stated that smelter output would step up by four times and additional mining and smelting facilities are to be installed.

The five year plan calls for a total installed capacity of 4,016,000 kw. Another plant is reportedly under construction on the Irtysh River above Ust-Kamenogorsk. The two plants will serve a region wealthy in zinc, lead, silver, copper, and gold. But more important is the adjacent Chinese province, Sinkiang, an area also rich in nonferrous metals. Russia and China are joint operators of two companies in the province, one for nonferrous development and the other for petroleum. Most experts consider the companies a pretty, legal fiction, with Russia actually running the show.

◆◆◆◆◆◆

WITH all the pride of parenthood, Aluminum Co. of America unveiled its literally shiny new building on Pittsburgh's Golden Triangle. In an era in which architects are constantly experimenting with new materials to disclose never realized possibilities of beauty and function, the Alcoa building is unique. It is completely sheathed in aluminum, standing as Alcoa's proof of the maturity of the metal in the building trades. Inside and out, aluminum plays the major construction role. It is used for reversible windows, lighting fixtures, plumbing, air conditioning, ceilings, and other installations.

As Alcoa proudly notes, this super-application of aluminum to building construction is the result of many years of experiments. The Alcoa building itself went through many months of planning, model making, and engineering. Yet, when the long view is adopted, aluminum appears to be one of the infant metals. It was used in the 1880's for the cap atop the Washington Monument. However, aluminum was considered such a rarity that Tiffany's, Fifth Ave., New York jewelers, displayed the cap in its windows.

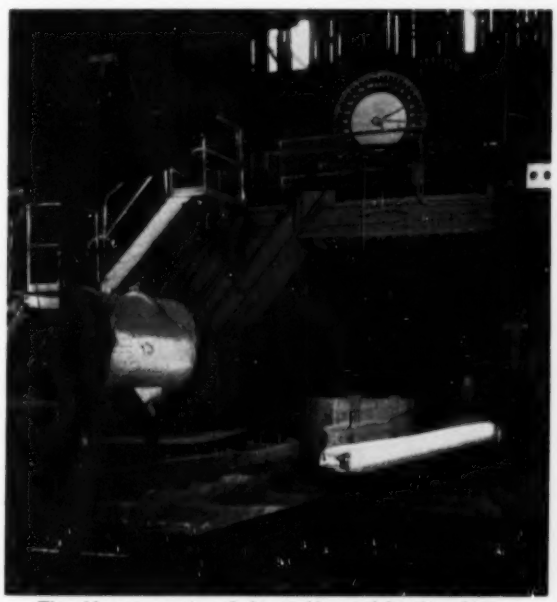

The old steam engine of this world record breaking blooming mill at Jones & Laughlin Aliquippa works was retired and replaced by an all-electric drive in a virtually new mill. The old mill set several records during World War II.

Books for Engineers

ORDER YOUR BOOKS THROUGH AIME—Address Irene K. Sharp, Book Department. Ten per cent discount given whenever possible. Order Government publications direct from the agency concerned.

Fabricated Material and Parts, by Theodore C. DuMond. *Reinhold Publishing Corp.* $6.50, 332 pp., 1953—This book is intended to serve as a reference work on methods of manufacture of small parts—casting, forging, extrusion, screw machines, and other matters—relating to design, materials, and cost factors. Details of design and manufacture are not presented, However, sufficient information is offered to afford a selection of those methods best suited to specific needs.

Pipe and Tube Bending, by Paul B. Schubert. *Industrial Press.* $5.00, 183 pp., 1953.—The book describes common methods and operating characteristics of equipment used in the bending of ferrous and nonferrous pipe and tubing. It presents formulas employed for various degrees of bend and tables for minimum radii of bends. There is also an appendix on tubing classification.

Physical Constants of Hydrocarbons, Vol. V; Paraffins, Olefins, Acetylenes, and Other Aliphatic Hydrocarbons, by Gustav Egloff. *Reinhold Publishing Corp.* $20.00, 524 pp., 1953—This is the continuation of a series of compilations of physical constants data for material not contained in Vol. I of the series. The book contains data either made available since the earlier volume or which was not previously included. Major divisions are: Alkanes or paraffins; alkenes or olefins; alkynes or acetylenes. Each section contains sources for the data.

Laboratory Instruments, by A. Elliott and J. Home Dickson. *Chemical Publishing Co., Inc.* $7.50, 414 pp., 1953—Chief aim of this book is to provide the research worker with the principles of good design necessary for the construction of instruments in the laboratory workshop. Separate chapters discuss the properties, treatment and use of various materials; methods of construction to meet special requirements; kinematic design of instruments; sensitivity and disturbing influences; optical instruments and optical glass; and the use of photography in research.

The Aluminum Industry, by Stanley V. Malcuit. *Bellman Publishing Co.* $1.00, 36 pp., 1953—This is one of a series of 75 occupational booklets used in connection with guidance activities wherever general counseling work is conducted and for individual reference purposes in the choice of a career. It lists personal qualifications required for engaging in the work; scholastic training needed; salary scale; chances for advancement; advantages and disadvantages; and possibilities for both men and women in the aluminum industry. The book also presents a history of the industry, production procedures, fabrication and mining.

Engineering Mechanics, by Linton E. Grinter. *Macmillan Co.* $5.75, 408 pp., 1953—This elementary textbook covers the normal subject matter of statics, dynamics, and kinetics, with a final chapter on virtual work. The author's aim is to present material in a logical and unified form, aiding the student in formulation of an analytical approach as well as giving him the necessary factual information.

Electric Arc Welding, by John Benjamin Austin. *American Technical Society.* $4.00, 280 pp., 1953—Here is a comprehensive treatment of the fundamentals and latest techniques of electric arc welding, equipment used, and applications in the major fields of welding.

MORE WORK IN LESS TIME!

Here at last! 4X to 3000X continuous magnification on the photographic plate . . . bayonet mounted accessories which are automatically seated and centered to allow quick, thorough object inspection under all techniques. Both are offered in the remarkable "ZC" *Galileo* Universal Microscope. Magnification of any objective setup can be instantly increased or decreased 4 times without recentering. Specimens can be viewed through monocular or binocular eyepieces, recorded on the 5" x 7" camera and the cine extension—and in transmitted light also projected—all at the same time. A built-in exposure meter insures correct results on plates, film or polaroid.

The "ZC" *Galileo* is designed to perform research or routine work in every field of metallography with maximum speed, ease and comfort. Utilizing a vertical optical path, it stands just five feet high, makes seated operation easy and comfortable. In a single compact instrument, it provides everything needed for macro- and microphotography, polarization, phase, dark field, oblique and standard microscopy in transmitted and reflected light. It will also do multiple beam interferometry. Two independent light sources are provided, and a Zircon arc 100 W bulb with condenser system is available. Switching from transmitted to reflected light is instantaneous, or both may be used together.

For the full story on the "ZC" and other optical instruments of modern design by *Galileo*, write to the address below, Dept. M.

GALILEO OPTICAL INSTRUMENTS

Imported and serviced by
OPPLEM COMPANY, INC.
Established 1890
352 Fourth Ave., New York 10, N. Y.

PROFESSIONAL SERVICES
Limited to AIME members, or to companies that have at least one AIME member on their staffs. Rates $40 per year per inch.

SCIENTISTS
CONSULTANTS
METALLURGISTS
Small Jobs Welcomed
SAM TOUR & CO., INC.
Laboratories and offices
44 Trinity Place, New York 6, N. Y.
Testing—Certifying
American Standards
Testing Bureau, Inc.

MAX STERN
Consulting Engineer
Expert for Scrap Recovery and Shipwrecking — Modernization of Plants and Yards for Ferrous and Nonferrous Metal Scrap
149 Broadway New York 6, N. Y.

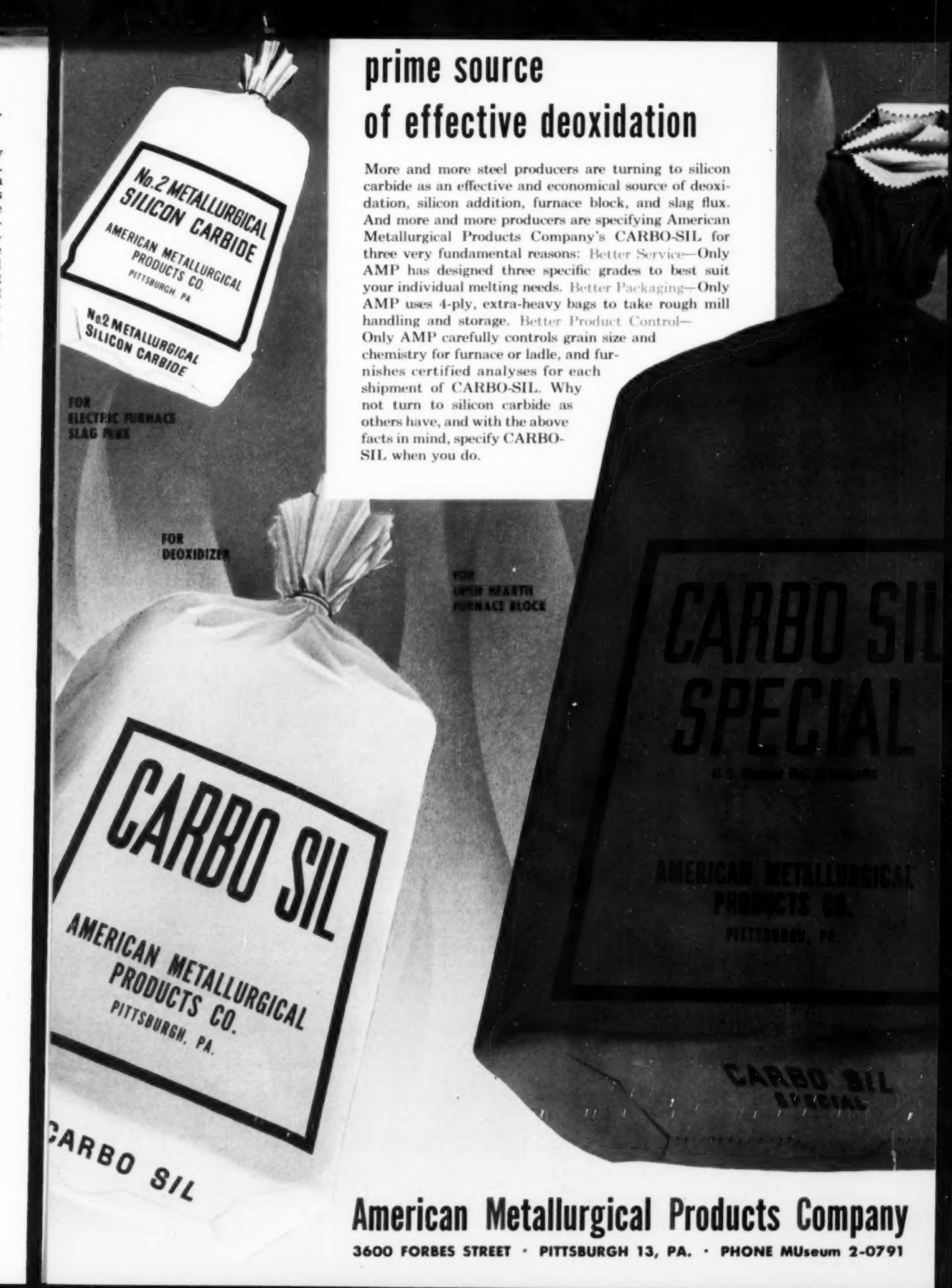

prime source of effective deoxidation

More and more steel producers are turning to silicon carbide as an effective and economical source of deoxidation, silicon addition, furnace block, and slag flux. And more and more producers are specifying American Metallurgical Products Company's CARBO-SIL for three very fundamental reasons: Better Service—Only AMP has designed three specific grades to best suit your individual melting needs. Better Packaging—Only AMP uses 4-ply, extra-heavy bags to take rough mill handling and storage. Better Product Control—Only AMP carefully controls grain size and chemistry for furnace or ladle, and furnishes certified analyses for each shipment of CARBO-SIL. Why not turn to silicon carbide as others have, and with the above facts in mind, specify CARBO-SIL when you do.

American Metallurgical Products Company

3600 FORBES STREET · PITTSBURGH 13, PA. · PHONE MUseum 2-0791

Advertisement

ELECTROMET *Data Sheet*

A Digest of the Production, Properties, and Uses of Steels and Other Metals

Published by Electro Metallurgical Company, a Division of Union Carbide and Carbon Corporation, 30 East 42nd Street, New York 17, N. Y. • In Canada: Electro Metallurgical Company of Canada, Limited, Welland, Ontario

How VANADIUM improves engineering steels and helps conserve critical alloys

In these critical times when many alloying materials are scarce, you may be able to use vanadium to good advantage. Steels alloyed with vanadium meet most of the mechanical specifications for low-alloy engineering and structural steels. In fact, vanadium can often be used in engineering steels to replace at least part, if not all, of certain alloys now in critical supply.

The metallurgy of vanadium is well known. Small additions of vanadium—0.10 to 0.30 per cent—can be used effectively to give steel extra strength, toughness, and resistance to fatigue and wear. It improves engineering steels by increasing their yield strength without sacrificing ductility. The uniformly fine grain size of vanadium-bearing steels makes them tough and resistant to abrasion, fatigue, and impact.

Better Mechanical Properties

In the following table are typical analyses for carbon-vanadium and chromium-vanadium steels that are suitable for most applications where low-alloy, high-strength steels are required. The carbon-vanadium steel is compared with plain-carbon steel; and the chromium-vanadium steel, with chromium-molybdenum steel. Note the excellent properties of the vanadium-bearing steels.

Fig. 1 — Vanadium increases the strength, toughness, and wear resistance of engineering steels for many machine parts, such as this large crankshaft.

Improves Cast Iron

A small addition of vanadium, usually from 0.10 to 0.25 per cent, refines the grain of cast iron, and materially increases its strength and hardness. Moreover, vanadium may be used in cast iron to replace at least part, if not all, of certain alloys that are now in short supply.

Vanadium in Rimmed Steel

An addition of approximately 1 lb. of vanadium per ton of steel produces non-aging characteristics in a rimmed steel. These non-aging properties, together with improved deep-drawing characteristics and the good surface inherent in rimmed steels, make these steels of particular interest at the present time.

Grades of Ferrovanadium

ELECTROMET produces ferrovanadium containing 50 to 55 per cent vanadium for the production of vanadium-bearing steels and irons. The alloy is produced in three grades with maximum 0.20, 0.50, or 3.00 per cent carbon and maximum 1.50, 2.00, and 8.00 per cent silicon, respectively. Each grade is specially adapted to fill the different requirements of iron- and steel-making.

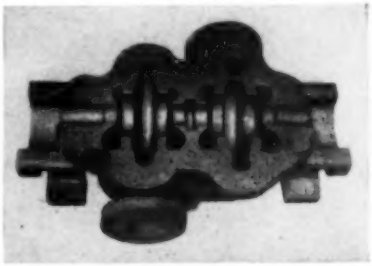

Fig. 2—Steel and iron castings treated with small additions of vanadium have high ductility and greater toughness and impact resistance.

Write for a copy of the booklet, "ELECTROMET Products and Service," which gives helpful information about the use of ferrovanadium and other alloying metals that ELECTROMET supplies. The booklet may be obtained from any ELECTROMET office: in Birmingham, Chicago, Cleveland, Detroit, Los Angeles, New York, Pittsburgh, or San Francisco. In Canada: Welland, Ontario.

Properties of Vanadium Steels Compared With Other Engineering Steels

Typical Analysis, %	Carbon Steel	Carbon-Vanadium Steel	Chromium-Molybdenum Steel	Chromium-Vanadium Steel
Vanadium	—	0.16	—	0.16
Carbon	0.50	0.49	0.50	0.50
Manganese	0.71	0.77	0.80	0.79
Silicon	0.19	0.15	0.30	0.31
Chromium	—	—	0.95	0.98
Molybdenum	—	—	0.20	—
Annealed and Furnace-Cooled				
Tensile Strength, psi	90,600	100,000	100,000	99,500
Yield Point, psi	48,900	66,000	50,000	64,100
Elongation in 2 in., %	23.3	25.0	23.0	28.4
Reduction of Area, %	37.8	49.1	45.0	59.0
Izod Impact, ft.-lb.	13.5	26.0	17.0	44.0
Quenched and Tempered				
Tensile Strength, psi	134,900	134,500	232,000	232,800
Yield Point, psi	110,800	128,000	214,500	224,200
Elongation in 2 in., %	18.3	18.3	10.0	10.4
Reduction of Area, %	54.1	56.6	39.0	43.1
Izod Impact, ft.-lb.	54.0	65.0	12.0	12.0

The term "Electromet" is a registered trademark of Union Carbide and Carbon Corporation.

Drift of Things

FOR those looking for a spot to spend a fall vacation, we can heartily recommend Colorado in October. We have just returned from Colorado Springs, using the Broadmoor Hotel as headquarters during the opening of CF&I's new seamless tube mill at Pueblo, and it will be some time before our excitement wears off. The tube mill, and the Broadmoor, have every conceivable type of equipment and facilities. CF&I's John McAllister, and Ruth Guest, girl Friday, worked at least 24 hr a day keeping things running smoothly and helping us feel at home.

We were privileged to tour the new mill at the preview held for top union officials and high ranking management. Although finishing facilities have not been completed, the mill is in operation, the first tube having been rolled on August 31. Details of the tube mill were given in the October issue of JOURNAL OF METALS, and additional operating photographs can be found in this issue.

After the mill tour, all adjourned to the Colorado State Fair Grounds where the CF&I Employees Festival had its first showing. This was truly an impressive event, as the entire cast of the Festival was composed of steelworkers, their families and friends. Groups represented were the Croatians with the Nova Kola Tamburitza Orchestra, the Negro Spiritual Chorus, the Slovenian Polka Band, the Hawaiian Islanders, Austrian Folk Dancers, the Italian Serenaders, and the Spanish Troubadors. The Minnequa Indian Dancers, an extra added attraction representing Post-Troop 22 Boy Scouts of America, did not vie for the prize for the group judged best by the audience. We had heard much about the authentic Indian dances performed by this troop during our last visit to Pueblo, but unfortunately did not have time to see them then. By coincidence, our guide at that time was Jack Lacy, editor of CF&I's *Blast*, and also scoutmaster of the troop. Jack and photographer Frank Sluder (assistant scoutmaster) were of great help in preparing material for the October CF&I issue of JOURNAL OF METALS.

Comedian Peter Donald served as master of ceremonies at the Festival, which had six performances, and used an applause meter to determine the audience's choice of winner. We were hard put to make a choice, and clapped equally loud and long for each group. Overall winner for the Festival were the Islanders, the Hawaiian group. It might just be that the gyrations of the four very attractive and suitably clad hula girls participating had something to do with the crowd's decision.

Overall reaction to the Festival was tremendous—so great in fact, that there was some talk as to the possibility of making it an annual affair. As an example of labor-management cooperation and mutual appreciation, it stood out as a major achievement. There was none of the appearance of a *show* being staged for visitors, it was more a sign of satisfied employees relaxing, and displaying their talents.

All in all, the celebration lasted four days and attracted 20,000 people to Pueblo's steelmills. Townspeople rubbed elbows with financiers as CF&I staged what has been acclaimed as the "greatest industrial open house in the west."

We stayed on for a few days, taking in more of the western air and scenery. Our cameras were not capable of reproducing the beauty of the aspens changing color, or the vastness of the area. We managed to get up a couple of mountains, visited the Royal Gorge, drove through Phantom Canyon, and spent several hours in Cripple Creek, famous mining center of half century ago. Even got down into one of the operating gold mines, but couldn't find any gold nuggets — only ore samples.

THOUGH a tentative offer from a group of industrialists in Pittsburgh is being seriously considered, and several meetings have been held, no decision had been made at the time of going to press on what is to be done about a new building for the national engineering societies.

The Pittsburgh offer results from plans to include an engineering center in the development now in progress in a triangular area at the confluence of the Allegheny and Monongahela Rivers. Land would be offered for sale to the engineering societies, and a substantial amount of money would be given for erection of a building—at least a million dollars and possibly considerably more might be forthcoming. Several other offers have been made by organizations in other parts of the country to provide land free of charge on which a building might be erected.

Opinion on whether or not the societies should leave New York is divided. The boards of the various societies are being asked to consider the matter promptly, as a decision is required well before the end of the year.—E.H.R.

NATIONAL Bureau of Standards has been given a clean bill of health by the committee of scientists appointed "to evaluate the present functions and operations of the NBS in relation to the present national needs." The committee was appointed by Secretary of Commerce Weeks as a result of the controversy that arose when Dr. Allen V. Astin, director of the bureau, was dismissed because of an adverse report on a commercial product. Dr. Astin has since been reinstated. Dr. Mervin J. Kelly, president of Bell Telephone Laboratories, was chairman of the committee, which included Clyde Williams, Battelle Memorial Institute, as AIME's representative. The committee concluded that the NBS is recognized and respected throughout the world, and its services are vital to the strength of the country. They also praised the loyalty and competence of those connected with the bureau. Recommendations of the committee that have already been acted on are that weapons research carried on by the bureau for the defense dept. be transferred to the armed services, and bureau reports on the virtues of civilian products be referred to the secretary of commerce before being publicized.

Alvin S. Cohan

For Handling Heavy or Light, viscous or non-viscous liquids, this positive displacement twin-blade impeller type nickel silver pump gives smooth even flow with minimum pulsations. Six sizes available . . . handling from 250 to 60,000 pounds per hour against a 100-lb. head. Capacity is regulated by number of r.p.m. at which pump is driven. Gear case, pump head, body, cover, rotor-retaining nut, impellers and rotary seal parts are of nickel silver. Spring is Type 316 chromium-nickel stainless steel. This new pump was developed by Waukesha Foundry Co., Waukesha, Wisc.

NEW PUMP SHOWS HOW

Nickel Silver meets exacting demands

Here's a pump used by processors of milk, canned foods, paints, cold cream, adhesives and scores of other products . . .

Its components are made of nickel silver to provide essential strength, and to assure non-pitting silvery white surfaces that resist wear and corrosion. Moreover, parts with bright, lustrous working surfaces permit quick, thorough cleaning as well as easy maintenance.

Solid white metal all the way through, nickel silvers usually provide greater strength and corrosion-resistance than do ordinary brasses and bronzes.

Wrought or cast, the impressive beauty and moderate cost of nickel silvers . . . plus their ready response to fabrication by ordinary methods . . . make these alloys particularly useful for improving both quality and quantity of output.

Gain competitive advantages by using these alloys. The several grades of nickel silvers permit selecting one with the best set of properties for any reasonable fabrication and service demands. We shall be glad to furnish you with counsel and data on these versatile alloys.

EMBLEM OF INCO SERVICE

THE INTERNATIONAL NICKEL COMPANY, INC. 67 WALL STREET NEW YORK 5, N.Y.

Allegheny Ludlum Steel Corp. is designing a commercial production continuous steel casting machine. W. B. Pierce, vice-president of the company, indicated that Allegheny Ludlum is considering equipment with 150 sq in. of mold cross-section. The firm has operated a continuous casting pilot plant for four years. The unit is patterned after a similar unit used in the brass industry.

Monsanto Chemical Co. of St. Louis and National Research Corp. of Boston are talking to Defense Materials Process Agency representatives about a loan for a titanium metal plant using a new process. The companies have engaged in a joint research program for new titanium producing method.

Aluminum Co. of America has started work on a $3.68 million modernization and expansion program expected to result in a 320 pct increase in the Cuyahoga Heights plant forging ingot making capacity. A 14 pct increase is anticipated in foundry operations.

Harvey Machine Co. claims development of an economic method for hot extrusion of alloy steel shapes at temperatures up to 2300°F and in lengths up to 30 ft. Excellent surfaces and tolerances are reported. A Harvey spokesman stated that the process involves "specially designed extrusion dies and specially developed lubricants."

Alan Wood Steel Co.'s new continuous strip pickler has been placed in operation at Ivy Rock, Pa. New building and equipment, and auxiliary facilities involved about $2.5 million. The new pickling equipment is said to be able to process about 20,000 tons of strip per month.

National Tube's Fairless works has started to produce continuous weld pipe. First operation was the rolling of 1 1/2 in. diam pipe on the first of two continuous weld mills. The skelp mill and certain finishing facilities are also operating.

Hewitt-Robins shipped the first iron ore blending and reclaiming system ever to be constructed for the Far East steel industry to the new plant of the Kawaksi Steel Corp., Chiba City, Japan. The system permits blending ores of different physical and chemical characteristics at a rate of 300 tons per hr. Variations in ore grade are virtually eliminated.

Proceeding with original plans, the Air Force announced that it will finance construction of a building for two extrusion presses to be operated by Kaiser Aluminum & Chemical Corp. at Halethrope, Md. Kaiser refused to pay for construction of the building.

Possibility of atomic power for public consumption appeared to gain strength with announcement of first steps toward building "a gigantic" atomic reactor to run the Government plutonium plant at Hanford works near Richland, Wash. General Electric will make application to the AEC to go ahead with the project, which would produce power and plutonium. Excess power would be fed to the Northwest power pool.

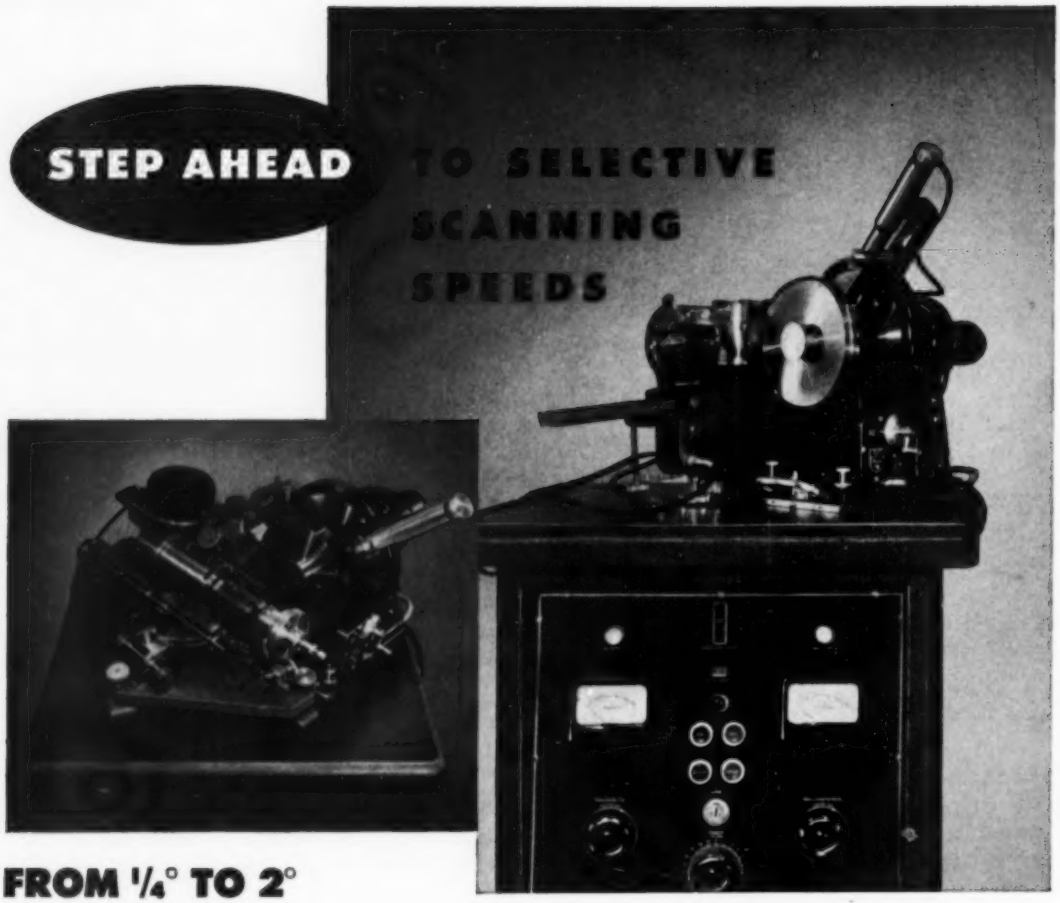

FROM ¼° TO 2°

PER MINUTE WITH UNEXCELLED RESOLUTION

★ Many users have found the facility of a wide selection of scanning speeds to be of extreme value in diffractometry. The operation of a synchronous motor drive, with change gears for speed variation, offers precise control which can be duplicated.

Scanning speeds up to 2° per minute can be obtained with exceptional resolution exceeding that attained from other apparatus under comparable operating conditions.

Work load of the NORELCO Diffractometer can actually be *doubled* by utilizing a second Wide-Range Goniometer in conjunction with the second line focus port of the NORELCO *four-window* X-ray tube.

A Norelco PRODUCT NORTH AMERICAN PHILIPS COMPANY, INC.

Serving Science and Industry

Dept. IG-11 • 750 South Fulton Avenue, Mount Vernon, N. Y.

In Canada: Rogers Majestic Electronics Ltd., 11-19 Brentcliffe Road, Leaside, Toronto 17, Ontario

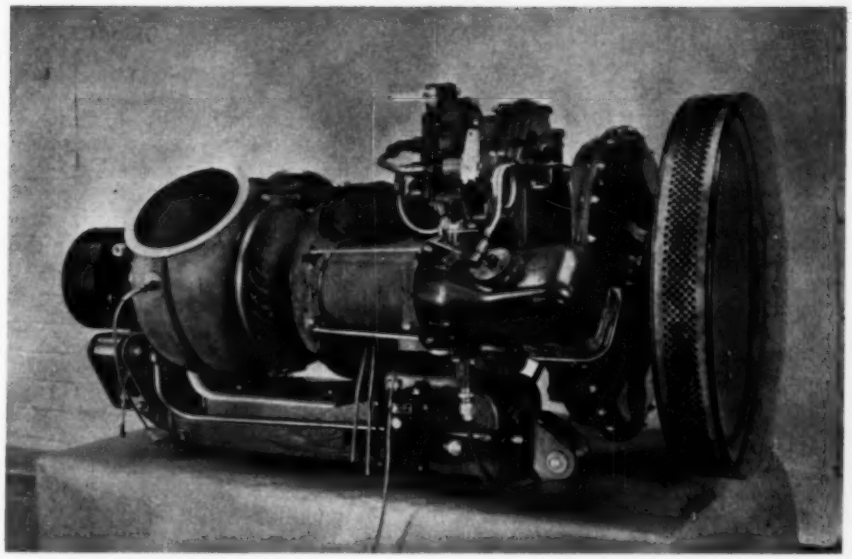

Fig. 1 — Weight of the Boeing model 502 gas turbine varies from 240 to 280 lb over the 175 to 225 hp range. The engine is basically 40 in. long, 23 in. wide and 23 in. high.

Metallurgical Aspects of The Development of Small Gas Turbines

by W. L. Slosson

OVER the past several years, the Boeing Airplane Co. has been developing and manufacturing small gas turbines for industrial and military use. As an aid towards better understanding of the metallurgical problems involved, a brief description of the construction and operation principles of the Model 502 turbine is presented. Configuration of the turbine is shown in Fig. 1, and a basic operation diagram outlining airflow, operating temperatures and component speeds is shown in Fig. 2.

The engine is composed of two stages: The first stage unit, or gas producer section; and the second stage unit, or power output section. The first stage unit consists of a single stage centrifugal type compressor, two diametrically opposed through-flow burners, a nozzle box assembly, and the first stage turbine wheel which is connected to the compressor impeller by means of the rotor shaft. The first stage unit also contains the basic accessory drive systems for fuel control, lubricating oil control and engine starting. The second stage unit consists of a nozzle ring assembly, the second stage turbine wheel, and a planetary-type reduction gear system connected to the output shaft. One of the distinctive features of this engine is the lack of a connecting shaft between the first and second stage turbine wheels.

Part of the energy in the gas stream from the burners is absorbed by the first stage turbine wheel to operate the compressor and accessory drive systems. The gas then passes through the second stage nozzle ring to the second stage turbine wheel which absorbs most of the remaining energy to drive the reduction gear system and deliver power to the output shaft.

Weight of the Model 502 turbines with accessories included varies from 240 to 280 lb over the 175 to 225 hp range. The engine is basiçally 40 in. long, 23 in. wide and 23 in. high. The diameter of the compressor impeller, first stage turbine wheel and second stage turbine wheel is 8.5 in., 7 in. and 9 in., respectively. Materials utilized in construction of the Model 502 turbine are shown in Tables I and II.

Compressor Section

Compressor materials are selected on the basis of strength and atmospheric corrosion resistance at ambient and elevated temperatures (200° to 400°F), as well as forgeability and castability to insure high quality material. Processing of the components must be closely controlled so that maximum properties and dimensional stability is gained.

To assure maintenance of proper clearance limits, warping or distortion of the compressor casing during service is of major concern. In many instances where aluminum alloy castings are subjected to elevated temperatures, the castings are stabilized at approximately 450°F (T-51 condition) or solution treated and overaged (T-7 or T-71 condition), instead of solution treated and aged to full strength (T-6 condition). These stabilizing or overaging treatments afford very good dimensional stability with some sacrifice in room temperature strength properties. Strength considerations in certain areas of the Model 502 compressor casing and burner elbow castings dictated that the T-6 condition be used and

W. L. SLOSSON is Supervisor, Materials & Metallurgy Gas Turbines, of the Seattle Div., Boeing Airplane Co.

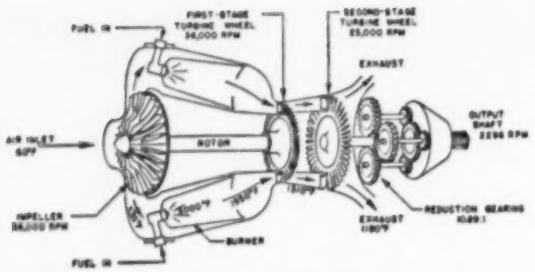

Fig. 2—Basic operational features of the model 502 gas turbine are shown diagramatically.

considerable experience with parts heat treated to this condition has revealed no serious difficulties with distortion. However, redesign of the castings and change to the T-51, T-7, or T-71 condition has constantly been held in reserve if distortion problems did occur.

The 14-S aluminum alloy impeller body is milled from a solid die forging and the blade tips bent over to the desired angle during final fabrication. The impeller is annealed prior to blade bending to provide maximum ductility for this operation. Following blade bending, the impeller body is heat treated to the T-61 condition under closely controlled procedures which assure uniform heating and quenching in order not to introduce undesirable stresses that may promote distortion of the impeller. The impeller body is then placed in a spin pit and spun at room temperature to approximately 40 pct overspeed (52,000 rpm). This spinning operation serves two purposes:

1—Prestresses the bore by plastically enlarging it under centrifugal loads, thus promoting residual compressive stresses in the bore at static conditions. The bore of the impeller is stressed in tension during engine operation, and since these residual compressive stresses must be exceeded during operation before the bore can be stressed in tension, operational tensile stresses are thereby proportionately reduced.

2—Checks quality of forging material and processing operations in the shop. Defective material or improper processing will be evidenced by bursting of the impeller, cracking, undue distortion, or other signs of stress.

Following this spin operation, the impeller body is machined to final size, Zyglo inspected for defects and anodized. Final fabrication operation on the impeller is assembly of the body to the steel bushing which serves to connect the impeller to the turbine shaft. The steel bushing is assembled in the impeller bore by means of a shrink fit, with the bushing designed to broach a spline on the inlet end of the impeller bore during this assembly operation. The spline prevents the impeller from rotating on the bushing during operation in case the shrink fit interference is accidentally exceeded by operational stresses.

Burner Section

The liner is the heart of the burner system, since it must function to produce economical combustion and at the same time uniformly dilute the extremely hot combustion gases (3000° to 4000°F) with excess air from the compressor to provide a cooler gas (1550°F) at the outlet end of the burner. The importance of maintaining a uniform outlet gas temperature of 1550°F is paramount and many indications of this point will be illustrated in discussion of subsequent components.

Burner liners are subjected to very stringent operating conditions because of the high temperatures and thermal gradients imposed on these parts during the combustion process. Such thermal conditions readily promote warping, cracking, and oxidation of the liner material unless burner design is carefully controlled so that maximum cooling of the liner wall is provided by air from the compressor. Difficulties can also be encountered with fatigue cracking of the liner as a result of high frequency alternating loads imposed by flame pulsations. Because of these factors, the metallurgist must select burner liner materials on the basis of elevated temperature strength properties, to resist warping tendencies and vibration; oxidation resistance, to assure maintenance of material section; thermal expansion and thermal conductivity properties, to provide lowest induced stresses resulting from localized hot areas; and thermal shock resistance, to resist stresses induced by rapid temperature changes.

Table I. Description of Basic Material Used in Major Components of Model 502 Gas Turbine

Component	Base Material	Remarks
Compressor impeller	14S-T61 aluminum alloy forging	
Compressor casings and elbows	356-T6 aluminum alloy castings	
Burner liner	N-155 alloy sheet	
Burner outer shell	AISI 321 alloy sheet	
First stage nozzle box assembly	AISI 310 and AISI 321 alloy sheet HS 30 alloy investment cast blades AISI 347 alloy cast flanges and wheel shroud ring.	Welded construction. AISI 310 and 19-9 WMo alloy filler metal.
First stage turbine wheel assembly	Timken 16-25-6 alloy forged hub. HS 21 alloy investment cast blades SAE 8740 steel shaft	Welded construction. Blade weld, Hastelloy-W alloy filler metal. Shaft weld, AISI 312 alloy filler metal.
Second stage nozzle ring assembly	AISI 321 alloy sheet AISI 310 alloy investment cast blades AISI 304-ELC alloy cast flanges and wheel shroud ring.	Welded construction. 19-9 WMo alloy filler metal.
Second stage turbine wheel assembly	Timken 16-25-6 alloy forged hub HS 21 alloy investment cast blades SAE 9310 steel shaft and pinion	Blades welded to hub with 19-9 WMo and Hastelloy-W alloy filler metal. Shrink-fit connection on shaft.
Exhaust system	AISI 321 alloy sheet AISI 304-ELC alloy cast flanges	Welded construction. AISI 347 alloy filler metal.
Gears	SAE 1020, 8615, 8620, 8630, and 9310 steel.	8630 gears through-hardened. Others carburized.
Accessory drive, reduction gear, and main rotor housings	356-T6 aluminum alloy castings.	
Oil sump and base	356-T6 aluminum alloy casting.	
Sleeve bearings	61S-T6 aluminum alloy. Babbitt overlay Leaded bronze. Pb-Sn or Pb-Sn-Cu overlay	

Fig. 3 shows a failure experienced with an early liner design constructed from AISI 321 sheet. Note the oxidized zones and cracking caused by hot streaks of gas impinging on the liner wall, and the general distortion of the liner as a result of the thermal stresses introduced. In this case, as with other similar liner failures experienced, ultimate failure occurred by cracking of the liner wall over the edge of the slots in the hottest zones. Analyses of these failures revealed that the cracking was of a multiple-path integranular type, indicative of stress-rupture or high-temperature tensile failure.

Numerous liner configurations and materials, including AISI 321, AISI 316, AISI 310, N-155, Inconel, HS 25, stainless-clad-copper, and ceramic coated AISI 321, have been tested by Boeing in a program aimed at developing long life liners. With current liner design, N-155 alloy shows by far the best life compatible with overall strategic material considerations. As with many turbine components, but particularly with burner liners, design is the key factor in producing a long life part with low alloy materials. If the design can assure a uniform insulating envelope of cool air around the liner at all times and thereby eliminate localized hot zones, many of the lower alloy steels can be utilized. Experience has shown that as long as warpage or cracking of the liner due to localized hot zones is a limiting factor of liner life, base material strength becomes increasingly important.

No outstanding problems or operational difficulties have been encountered with material in the outer burner shell. Temperature of this part does not exceed 500° to 700°F during operation.

First Stage Nozzle Box Assembly

Similar to burner liners, the first stage nozzle box is exposed to high temperatures and thermal gradients which promote warping, cracking and oxidation of the assembly components. Under normal operation, temperature conditions in this assembly are not as severe as those experienced with burner liners; however, if normal rated inlet temperatures are exceeded, or malfunctioning of the burner system permits extremely hot streaks of gas to pass through the box, material difficulties are accelerated. Fig. 4 shows cracking of the turbine wheel shroud ring (Arrow 1), and the diaphragm blade shroud ring (Arrow 2), in a localized area where a hot gas streak impinged on the wall of the nozzle box assembly.

Because of its excellent oxidation resistance, AISI 310 alloy is currently used on all formed sheet components of the nozzle box which are in direct contact with combustion gases. AISI 321 sheet was formerly used in this application but it was found that life of this material was limited by oxidation attack and subsequent failure due to loss of section thickness, particularly in the collector shell wall area directly opposite the burner outlet ports. Tests of ceramic coated AISI 321 sheet in this application were very favorable, and such material is considered for future production.

The nozzle diaphragm blades are investment cast and HS 30 alloy was selected for these blades because of the excellent properties of this material at 1500° to 1600°F. Under some conditions of rapid temperature changes in the gas stream, resulting from hot starts or very rapid engine accelerations, it was found that the diaphragm blades would develop thermal shock cracks over the leading edge. Tests

Table II. Nominal Composition of Corrosion and Heat Resistant Alloys Used in Model 502 Gas Turbine, Pct

Alloy	C	Cr	Ni	Co	W	Mo	Cb+Ta	Fe
AISI 302	0.14	18.0	9.0	—	—	—	—	71.0
AISI 304	0.04	19.0	9.0	—	—	—	—	71.0
E.L.C.	Max							
AISI 321*	0.06	18.0	9.5	—	—	—	—	71.0
AISI 347	0.08	18.0	9.5	—	—	—	10xC	71.0
	Max							
AISI 310	0.20	25.0	20.0	—	—	—	—	53.0
AISI 312	0.15	29.0	9.0	—	—	0.50	—	59.0
	Max					Max		
AISI 309	0.12	23.0	13.0	—	—	—	—	63.0
	Max							
HS 30	0.40	26.0	15.0	51.0	—	6.0	—	1.0
HS 21	0.20	28.0	2.5	62.0	—	5.5	—	1.0
T-16-25-6	0.15	16.0	25.0	—	—	6.0	—	51.0
N-155**	0.35	20.0	20.0	20.0	2.5	3.3	1.0	23.0
19-9 WMo	0.10	19.0	9.0	—	1.3	0.4	0.4	68.0
Hastelloy W	0.07	5.0	62.0	—	—	28.0	—	5.0
Inconel	0.05	14.0	78.0	—	—	—	—	7.0

* Also contains Ti to 6xC.
** Includes 0.15 pct N_2.

by Boeing and by other investigators revealed that HS 21 alloy is more resistant to thermal shock cracking than HS 30 alloy.

The first stage turbine wheel shroud ring on the downstream end of the nozzle box has proved to be a very important factor in life of the nozzle box assembly. The turbine wheel rotates inside this shroud ring and close blade tip clearance tolerances must be maintained around the ring to assure efficient turbine operation. Operation stresses induced by thermal gradients across the nozzle box assembly tend to distort this ring beyond wheel clearance limits, particularly under operation conditions where inlet temperatures exceed 1550°F or uneven inlet gas temperatures exist. This distortion may cause the wheel blade tips to rub the shroud or promote cracking of the shroud ring itself, as previously shown in Fig. 4. Centrifugal castings were chosen

Fig. 3—Cracking in burner linings was of a multiple-path intergranular type. Liners were constructed from AISI 321 sheet. Current design utilizes N-155 alloy.

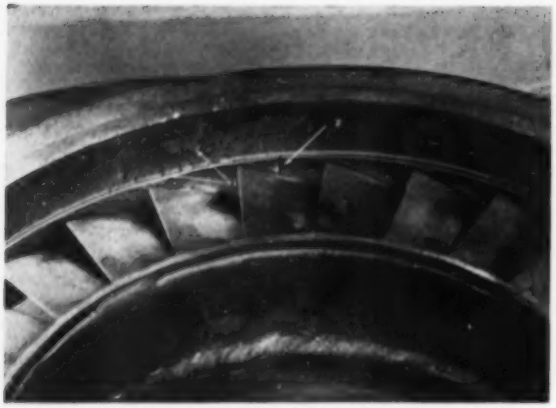

Fig. 4—Cracking of turbine wheel and diaphragm blade shrouds are shown by arrows 1 and 2 respectively.

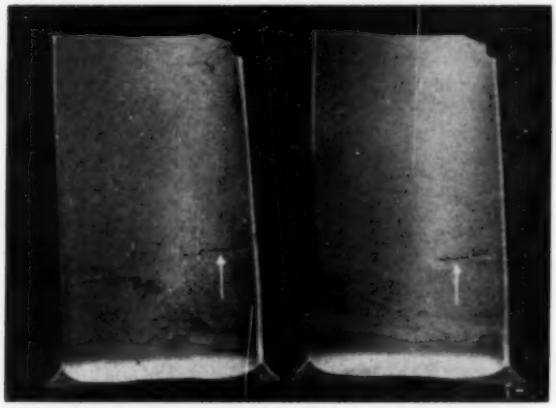

Fig. 6—Stress rupture cracks are shown by arrows near the leading edge of first stage turbine blades, 2½X.

for the wheel shroud ring because of cost and availability, as well as the thought that the balanced metal flow characteristics inherent with the centrifugal casting process would benefit maintenance of ring dimensions, both during fabrication and operation.

In efforts to save critical columbium, AISI 321 alloy and AISI 305-ELC alloy centrifugal castings were tried in this application; however, it was found that AISI 321 alloy could not be satisfactorily cast because of difficulties with titanium oxides, while AISI 305-ELC was very susceptible to cracking during welding and subsequent engine operation. No chronic cracking difficulties of this type have been experienced with current production wheel shroud rings fabricated from AISI 347 (Cb + Ta) centrifugal castings.

First Stage Turbine Wheel Assembly

The turbine wheels are designed to rotate at high speeds under activating forces imposed by the hot gas stream; therefore, not only must their components resist elevated temperature exposure, but also they must withstand complex stresses induced by rotational loads.

HS 30 alloy blades were originally used in the first stage turbine wheel, but the blades were later changed to HS 21 alloy to gain more thermal shock resistance as well as benefit over all turbine wheel welding procedures. Investment cast blades are used because of cost and availability factors in relationship to blade size and configuration. A Timken 16-25-6 alloy forged hub has been utilized throughout development and production of this wheel in view of the balanced characteristics offered by this material with respect to strength, alloy content, and weldability.

Blade cracking is a limiting factor of turbine wheel life, particularly on a small wheel of this type where the blades are welded to the hub and replacement of a cracked blade or group of defective blades does not appear economically feasible. The primary causes of blade cracking experienced through development of the first stage turbine wheel are thermal shock or stress-rupture cracking due to engine overheating, impact with foreign objects passing through the wheel, and fatigue cracking. Fatigue cracking is usually evidenced only as advancement of cracks initiated by thermal shock, stress-rupture or impact. Figs. 5, 6, and 7 show first stage turbine blade cracking caused by thermal shock, stress-rupture, and impact, respectively.

Recognition of the various modes of turbine blade cracking is an invaluable tool to the metallurgist and the designer in applying corrective measures, but positive identification of these cracks, particularly some types of thermal shock and stress-rupture cracking, is not always an easy task. Impact

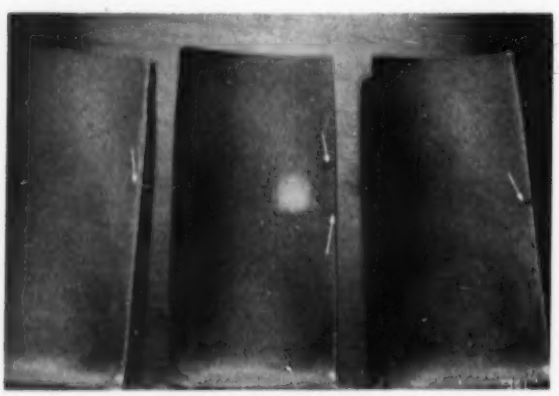

Fig. 5—Arrows point out thermal shock cracks on leading edge of first stage turbine blades, 4X.

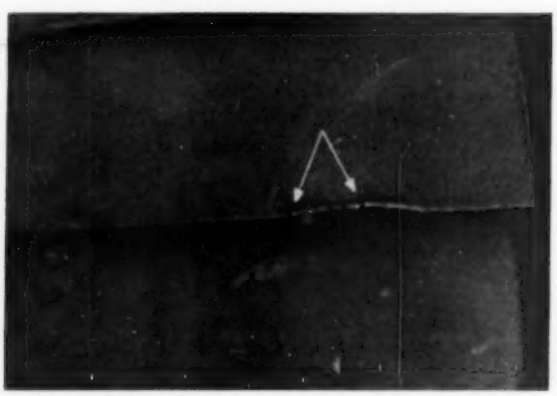

Fig. 7—Turbine blade cracking was caused by the impact with a foreign article in the gas stream, 5X.

cracks are readily recognized by bending or other physical damage in the crack area. Fatigue cracks are identified by the familiar *oyster-shell* progressive failure pattern and the fact that such cracking is normally transgranular. Differentiation between thermal shock cracks and stress-rupture cracks is difficult in many instances because both types of cracking are associated with tensile failure under conditions influenced by the combination of high temperatures, thermal stresses, and mechanical stresses.

Thermal shock cracking occurs on the edges of the blade as a result of very high instantaneous stresses induced on the blade edge by a rapid temperature change and in this respect can be termed a short-time tensile failure. Stress-rupture cracking can occur either on the edges of the blade or in areas of the blade away from the edges, and results when applied thermal and mechanical stresses overcome the strength of the blade material with respect to temperature *vs* time under load. Laboratory tests on Model 502 turbine blades have shown that thermal

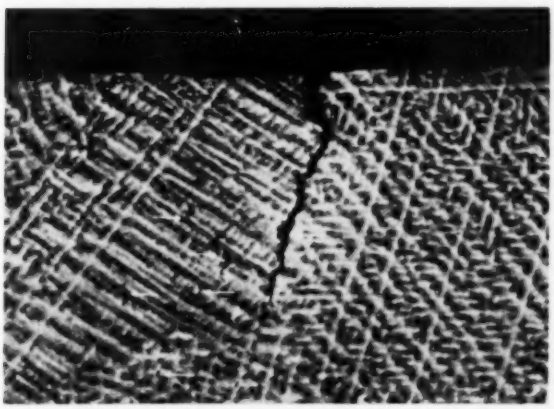

Fig. 8—Stress rupture cracks occurred along the edge of a first stage turbine blade constructed of HS 21 alloy, 100X. Electrolytic chromic acid etch.

shock cracks in these blades are more than often intergranular. Normally, stress-rupture cracking is characterized by a major intergranular crack zone surrounded by numerous small discontinuous fissures or cracks on one or both sides of the major crack area as in Fig. 8, and visible signs of strain or yielding are usually observed on the blade surface near the crack. Thermal shock cracks may occur simultaneously at several points along the blade edge, but each crack in itself tends to follow a single path and is not accompanied by the multiple short discontinuous cracks on either side of the major crack zone. These are only general rules formulated from observations made on the cobalt-base cast blades used in Model 502 turbines, and such rules may not specifically apply in other instances.

Quite early in the development of this engine, an interesting phenomenon was observed in relation to turbine blade overheating. Very often, during Zyglo inspection of wheels suspected of operating under overheating conditions, considerable porosity, similar to microshrinkage in appearance, was noted along the edges and tip of the blades. This porous

Fig. 9—After operating first stage turbine blade under severe overheating conditions, heavy porosity and cracking was found on tip of HS 30 alloy, 5X. HCl-HNO_3-$FeCl_3$ etch.

condition usually was uniform in area on each blade in a specific wheel and quite frequently cracking was found near or in the porous areas as shown in Fig. 9. Microexamination of these porous blades revealed numerous tiny voids in the affected zones, and in each instance, it was observed that these voids occurred in the same pattern as the carbide islands scattered throughout the alloy matrix shown in Fig. 10. Inspection records failed to produce any evidence that this condition existed in the blade casting as received from the manufacturer.

A series of preliminary tests were conducted in which blades were heated to successively increasing temperatures in an open oxy-acetylene flame. At blade temperatures of approximately 2300°F, tiny globules were seen sweating out on the blade surface after very short time exposure to these temperatures. Microexamination of the blades through the areas where sweating occurred revealed voids in the carbide pattern similar to those witnessed on blades removed from the questionable wheels. Another series of tests conducted in an electric furnace under more closely controlled temperatures showed that partial melting of the carbide eutectic could occur at temperatures as low as 2275°F. The cause of the porous areas on the blades was thereby established, but next remained the problem of proving

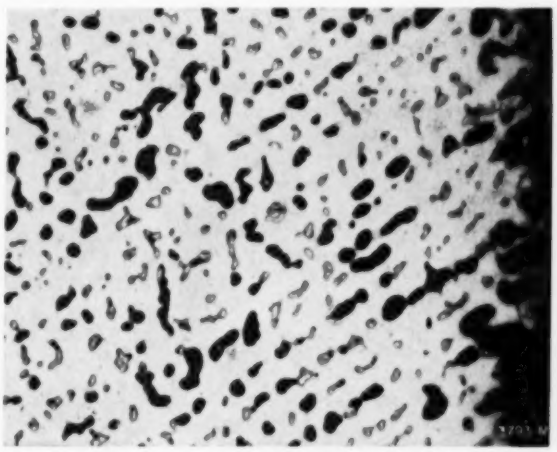

Fig. 10—A higher magnification of the porous area shown in Fig. 9, 250X. Electrolytic chromic acid etch.

Fig. 11—Arrow points out crack in balancing ring fillet immediately adjacent to weld, 5X. Electrolytic chromic acid etch.

that such high temperatures existed in the gas stream during engine operation.

It appeared probable that the thermocouple installation in the engine was not sensing transient high temperatures that could destructively overheat the thinner turbine blade airfoil. Lag of the recording instruments was also suspected as contributing to low sensitivity of the installation. To check this theory, a series of 0.016-in. diam chromel-alumel unshielded thermocouples with spot welded junctions were installed in test engines and recording of the thermocouple temperatures was performed with an oscilloscope. This test installation revealed that during engine starts, transient gas temperatures of 2500°F were encountered throughout the engine, while during very rapid engine accelerations, gas temperatures approached 2200°F. On the basis of these results, immediate corrective action was taken to provide better temperature control during starting and acceleration.

Turbine wheel material difficulties resulting from overheating are not only confined to the blades. Some test engine installations operating at relatively high nozzle box inlet temperatures have encountered first stage turbine wheel rim failures. This type of failure has been traced to stress-rupture cracking originating in the fillet of a raised balancing ring step machined in the wheel hub. The outer fillet of this balancing ring coincides with the edge of the weld area around the rim of the wheel, and cracking occurs in the hub material immediately adjacent to this weld as shown in Fig. 11.

The hub forging is hot-cold worked at 1200° to 1250°F in order to increase its strength but the effects of this working are lost in the zone adjacent to the weld because of the annealing influence of welding heat input. The rim failures experienced were therefore suspected to be a combined result of: A—Operation of the wheel at higher than normal temperatures, B—the stress-raising effect of the balance ring fillet, and C—confluence of this fillet with the weld-heat-affected area of the wheel material.

A series of spin pit tests on first stage turbine wheels under conditions where balance ring fillet radii, wheel speed, and balance ring area temperature were independently varied, definitely showed that operation temperature is the main factor in promoting balance ring fillet cracking. This conclusion is further substantiated by the fact that first stage turbine wheel rim failures have never been experienced throughout several thousand hours of accumulative engine operation where operating temperatures are closely controlled within a reasonable maximum. An added safety factor against rim failures of this type has been introduced on current production wheels through utilization of a design change in the balance ring contour, whereby the balance ring is blended to the wheel rim by means of a tapered section instead of a fillet.

Probably the most damaging and dangerous type of failure that can occur in a gas turbine engine is bursting of the turbine wheel through the hub section. The tremendous energy in the wheel fragments resulting from such a failure can literally rip an engine to pieces and seriously endanger operating personnel or surrounding equipment. Only one wheel failure of this type has been experienced in development of the Boeing turbines and this failure occurred in early 1948 in a test cell installation of one of the first developmental turbines built. Sections through the failed wheel transverse to the main fracture revealed numerous small fissures in the central portion of the hub as in Fig. 12. Examination of the main fracture and the subsidiary cracking proved that the defects causing failure developed at some point in manufacture of the wheel forging, and were not a result of turbine wheel operational loads. The hub forging concerned had not been subjected to ultrasonic inspection; however, recognizing the value of ultrasonic inspection in eliminating defective forgings of this type, immediate action was taken to have all remaining wheel forgings and finished wheels on hand inspected by this means.

Material quality control procedures which were put in effect as a direct result of the above wheel failure consist of: A—Ultrasonic inspection of each forging at the forging source, B—ultrasonic and Zyglo inspection of each forging at Boeing, C—Zyglo inspection of the machined forging prior to blade welding operations, D—Zyglo inspection of the wheel assembly after final fabrication, and E—proof spin of the finished wheel assembly (45,000 rpm at room temperature). Each forging is also checked for alloy and hardness to assure that the material will meet basic strength requirements set forth in the procurement specification.

Considerable research and development is being conducted on first stage turbine wheels with the aim of lowering wheel costs and increasing wheel life. The small size of the wheel lends well to precision casting the entire assembly, excluding the rotor shaft, and promising cast wheel types are being investigated in both spin pit test and engine oper-

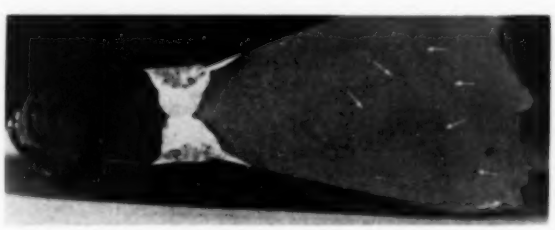

Fig. 12—Section through the hub of a first stage turbine wheel showing forging bursts, 2X. HCl-HNO_3-$FeCl_3$ etch.

ation. Results to date on these cast wheels are encouraging.

Second Stage Nozzle Ring

Because of relatively low inlet temperatures (1310°F), no serious material difficulties are encountered with this assembly as a result of engine operation.

Second Stage Turbine Wheel Assembly

The second stage turbine wheel demands the same general material property considerations as the first stage turbine wheel assembly, and as shown in Table I, blade and hub alloys are identical for both wheels. Even though operation temperatures are considerably lower for the second stage system, this relationship in material selection was maintained because of certain operating stresses induced in the second stage wheel. Since the second stage turbine wheel drives the reduction gear system and is subject to various vibratory stresses that can result from a high speed gear train, high strength and fatigue resistance at operation temperature were considered mandatory characteristics for the blade and hub alloy. Another influencing consideration

Fig. 13—Fatigue fracture surface on second stage turbine blade shown originating at trailing edge, 12X.

is the fact that since the blades on both wheels are welded to the hub in current production design, utilization of the same materials greatly benefits wheel fabrication procedures and costs.

Cracking of the blade airfoil and the blade weld during engine operation were the outstanding difficulties experienced during development of the second stage turbine wheel. The blade airfoil cracking generally occurred in the trailing edge root fillet, and in practically all instances, was due to fatigue failure originating at the edge of the blade as shown in Fig. 13. The weld cracking occurred as *hook cracks* through the weld material immediately adjacent to the blade weld fusion line as in Fig. 14. The fracture surfaces of the blade weld cracks revealed that these cracks were also generated by fatigue, with the origin point normally at one corner of the blade base-blade weld junction. Arrows "A" on Fig. 15 show the exposed fracture surfaces of the cracks seen in Fig. 14. The separate blade junctions and the fan-shaped fatigue crack fractures generating from one corner of each blade are easily observed. Arrows "B," Fig. 15, show two other partially exposed fatigue cracks generating from the opposite corners of each blade junction. Over many

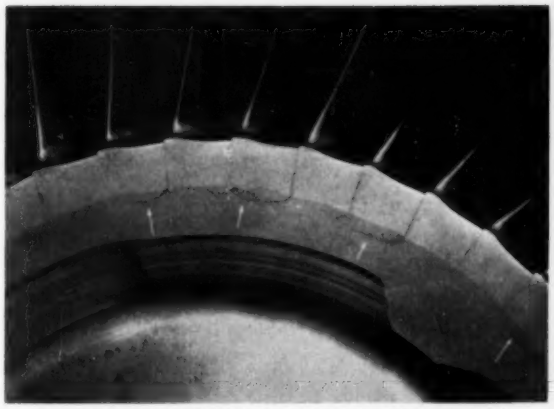

Fig. 14—Weld cracking immediately adjacent to the blade weld is shown at arrows, 3X.

wheels examined, the following significant factors were noted with respect to these weld failures:

1—Hook crack origin and progression is generally independent of preexisting weld cracks developed during welding. In other words, the existence of a weld crack in the as-fabricated wheel did not necessarily influence formation of hook cracks during engine operation of the wheel. In many instances, hook cracks occurred through sound weld material, while the adjourning blade junctions contained weld cracks that had developed during welding operations but did not progress in length or depth during engine operation.

2—Hook cracks did not consistently occur on any particular side of the wheel with relation to gas flow direction (upstream or downstream side), nor did they consistently occur on any particular corner of the blade weld junction with relation to airfoil position.

3—No significant weld hook cracks developed in the first stage turbine wheel during engine operation.

After considerable investigation, it was concluded that both the blade and blade weld cracking were primarily caused by high frequency vibrations introduced by the reduction gear system. Influence of thermal stresses in the rim of the wheel was also considered a contributing factor in the blade weld cracking problem. Corrective action taken on both problems consisted of increasing the blade airfoil

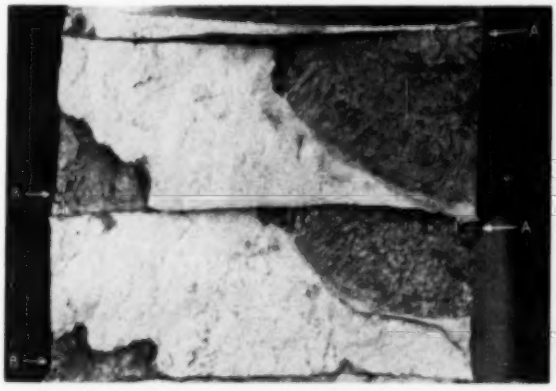

Fig. 15—Arrows *A* point out the exposed fracture surfaces of the cracks seen in Fig. 14. Arrows *B* show fatigue cracks generating from opposite corners of blade junction, 5X.

thickness and wheel hub thickness to gain a higher natural frequency in the wheel assembly, redesign of the reduction gear system to promote smoother gear action, and utilization of new blade welding procedures to provide a stronger weld with less residual welding stresses. These corrective measures have markedly reduced blade airfoil and blade weld cracking difficulties and consequently increased wheel operating life by a substantial margin.

Turbine Wheel Welding

Turbine wheel size, blade spacing, design and production considerations dictated welding as the most feasible method of blade attachment. In view of this, blade welding procedures were constantly under investigation during development of both the first and second stage turbine wheels in an endeavor to assure maximum freedom from fabricating problems and provide wheels which would guarantee satisfactory service life. Welding turbine blades to a wheel assembly is probably one of the most stringent welding operations known because of the service requirements demanded of the blade weld, the high quality weldment necessary to comply with these requirements, and the basic problem of placing a full restraint weld around a series of stress-raisers introduced by the blade base junctions.

Initial design of both welded turbine wheels specified HS 30 alloy investment cast blades and Timken 16-25-6 alloy forged hub. As a result of extensive tests, metallic arc welding with 19-9WMo electrode was selected, and a welding procedure was devised whereby the blades are first welded into a blade ring assembly, with welding performed longitudinally along the blade junction instead of across the junction. This blade ring assembly is stress relieved and then welded to the hub by means of a double U-groove circumferential weld.

During development of the blade ring assembly welding procedure for second stage turbine wheels, it was found that HS 30 alloy investment cast blades were subject to cracking in the airfoil root fillet during the welding operations. Since tests also showed that as-cast HS 21 alloy was completely free of cracking in this application, the blade alloy was changed to HS 21 on production second stage wheels.

Exhaust System

The exhaust system has presented no appreciable material problems during engine operation. Gas temperatures in the system are not over 1250°F, and the AISI 321-AISI 304 stainless steels selected for construction satisfy the requirements of the system design.

Corrosion from Fuel Residues

Normal fuels for the Model 502 turbine series are kerosene, JP-4, diesel oils, and stove oils. No difficulties with corrosion from combustion residues are encountered through use of these fuels. The turbines have been operated on leaded gasoline in several instances, but in each instance, rather severe corrosion-oxidation attack of the turbine blades and stator blades was observed after relatively short time operation as shown in Fig. 16. This attack by leaded fuel residues occurs at elevated temperatures and is attributed to a combination of at least two factors: 1—Corrosive acids generated by breakdown of lead bromide and water vapor in the combustion gases, and 2—accelerated oxidation attack due to the presence of excess oxygen and lead oxide (PbO)

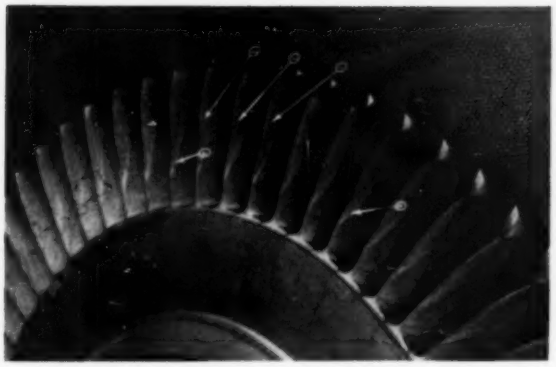

Fig. 16—Arrows 1 show corrosive acid attack and arrows 2 accelerated oxidation attack by leaded gasoline combustion residues, 2X.

in the combustion gases. Factor 2 probably exerts the most influence in gas turbine engine operation, since the turbine operates with an excess of oxygen in the gas stream. Ceramic coating the components is also a good method of preventing such attack, but maintaining an effective coating on the highly stressed rotating parts presents several difficulties which have yet to be overcome.

Influence of Type of Operation

Being a small engine with many potential uses in industry, the Model 502 turbine is exposed to some cyclic operation conditions which demand the utmost of materials and design, as well as operating control mechanisms. A specific example is the installation of the engine in a heavy duty freight-hauling truck, where the engine undergoes numerous starts and rapid accelerations during normal routine operation. Cyclic operation of this type imposes stringent loads on the engine and magnifies material problems associated with overheating, thermal shock, and fatigue. It has been proved that cyclic operation is much more severe than steady speed operation with respect to engine life, and as a result, several test engines are constantly being operated under cyclic conditions to accelerate evaluation of various components.

Critical Materials Reduction

In view of military requirements on alloy conservation and the possibility that many applications of the turbine will ultimately reach commercial fields, utilization of the lowest alloy material compatible with satisfactory operation life, design, fabrication procedures, and cost is constantly being investigated on Model 502 turbine components.

Major alloy conservation programs currently in effect include testing of parts fabricated from cermets, ceramic coated stainless steels and low alloy steels, aluminum coated low alloy steels, heat resistant cast irons, titanium alloys, and intermediate alloys containing lesser amounts of strategic elements than current production materials.

Acknowledgment

The author wishes to express thanks to the Boeing Airplane Co. for its permission to publish the data presented in this paper. The able assistance of various associates in obtaining these data is also gratefully appreciated.

CF&I Opens Streamlined Tube Mill at Pueblo, Colo.

Metallurgists inspect the first seamless tubing turned out by the new CF&I mill at Pueblo, Colo. Primary market aim for the mill is gas and oil producers in the western U. S. and Canada area.

Western U. S. and Canadian gas and oil producers are the market target for Colorado Fuel & Iron Corp.'s new seamless tube mill at Pueblo, Colo., the first such installation west of the Mississippi. October 1953 issue of JOURNAL OF METALS gave a description of technical aspects of the mill. The ultramodern mill is so situated as to be able to supply tube and casing to users in Kansas, Oklahoma, Wyoming, west Texas, the Pacific coast, and western Canada. Once full production is reached, some 150,000 net tons of seamless pipe will be turned out annually, according to A. F. Franz, CF&I president.

After heating in a 70-ft rotary furnace, billets go to one of two 340-ton piercing mills powered by 3000-hp motors. Rough tubes are further processed by a 275-ton rolling mill. A 1500-hp motor powers the rolling mill. Next step is straightening and smoothing the inside and outside of the tubing in expanding mills. Final treatment takes place when a reducing mill finishes the product to specifications. The mill will produce pipe ranging from 2⅜ to 9⅝ in. OD.

Mill construction started in February 1952; the steel framework alone required five months to build. The completed mill consists of five long, rectangular one-story buildings joined side to side and topped by a single roof. The job took 37,000 cu yd of concrete and 10,000 tons of structural steel.

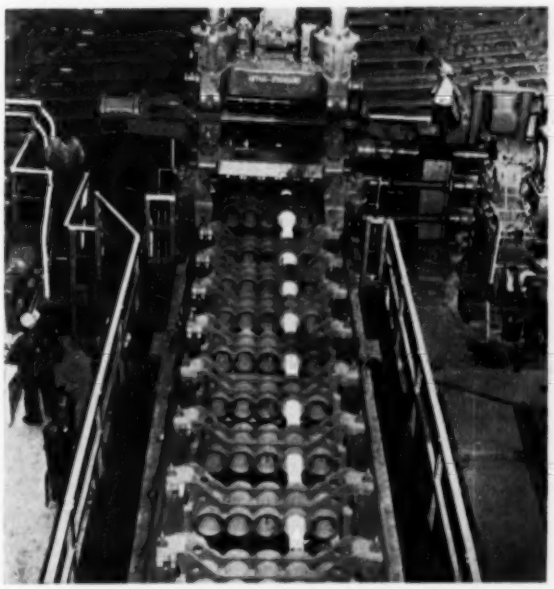

When the hollow shell comes from the piercing mill or reheat furnace to the rolling mill entry table, a mechanical ram forces the entering end of the shell over a rolling mill plug, permitting the rolls to grip the shell. When finished at the rolling mill, shell is uniform throughout.

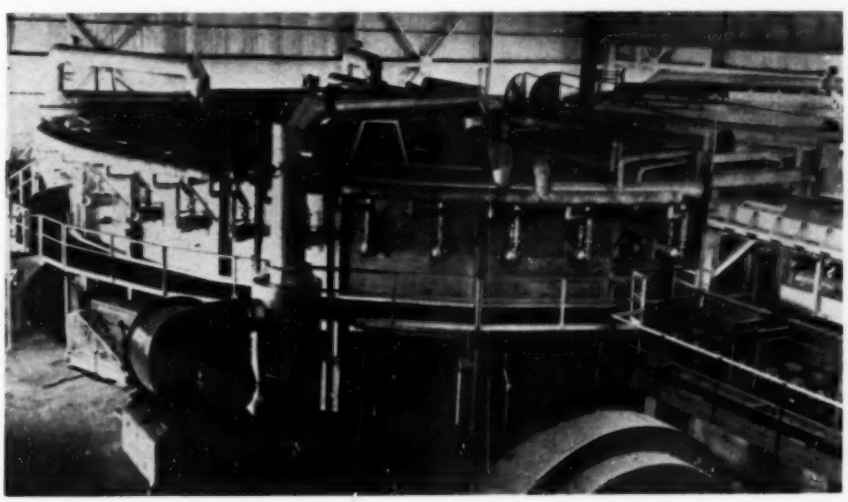

This huge 70-ft rotary furnace, one of the largest ever built for American industry, has sixty jets which heat billets from room temperature to 2300°F at the rate of 75 tons per hr. Heated billets go directly to the piercing mills.

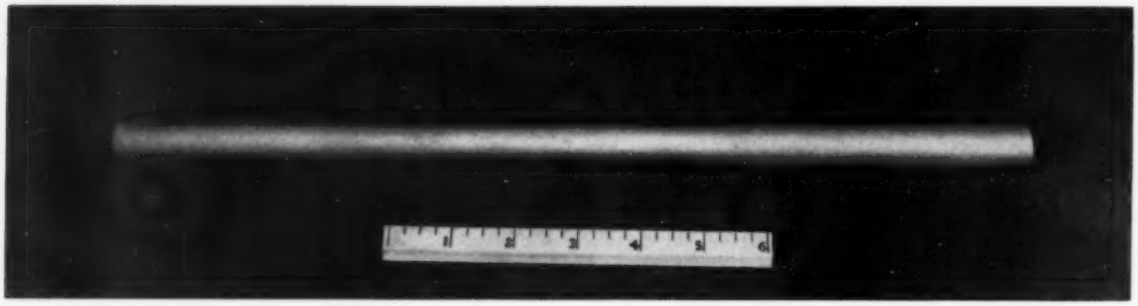

A hyper-refined single crystal of germanium prepared by zone melting. Impurities have been reduced to a concentration as low as 1 atom per 10 billion atoms of germanium.

Ultra-Pure Metals Produced By Zone-Melting Technique

by Earle E. Schumacher

IN a lecture[1] before the AIME several years ago, attention was drawn to the tremendous role played by minute quantities of impurities in controlling the properties of metals. Although great strides toward obtaining purer metals had been taken at that time, it then seemed that the ultimate goal of ultra-pure metals would not be easily reached. But it was realized that only when impurities in metals could be reduced to the vanishing point, would it be possible to realize the properties intrinsic to the completely uncontaminated material.

That was three years ago. Now, however, the goal of ultra-purity appears to be much nearer at hand for many substances. A new method for purification[2] has been developed in the metallurgical dept. at Bell Telephone Laboratories. Known as zone-melting, the method can be applied to metals, semiconductors, organic and inorganic compounds. Zone-melting was first applied to germanium with fantastic results.[3] The impurities critical to the behavior of germanium as a semiconductor, such as phosphorus, arsenic, and antimony, are being reduced to a concentration as low as 1 atom per 10 billion atoms of germanium.

The method is based on the fact that impurities are not equally soluble in the solid and liquid phases of a parent substance. Usually the impurities are more soluble in the liquid.

In the zone-melting method a series of rather narrow molten zones is moved slowly along an ingot of relatively impure material. As each molten zone advances, the liquid picks up additional impurities and leaves purer solid behind. Each successive zone causes further refining. Most of the impurities are concentrated in the last volume to freeze. This impure section may then be cut off.

The purification which may be attained depends on the number of passes, the initial impurity level, the difference in the solubility of impurities in the solid and liquid, and on how short the zone may be made. Impurities which raise the melting point can be removed by zone-melting also, although the mechanism is somewhat more complicated. In this case impurities travel in a direction opposite to that of the zone and, in general, more passes are needed.

It is not necessary to make a number of separate passes. If the induction heaters are merely aligned in series and the ingot run through them in one pass, considerable time is saved.

Fig. 1 is a schematic of the apparatus. The circular induction heaters are axially aligned. The ingot passes centrally through them from left to right. Each molten zone extracts its fraction of impurity

EARLE E. SCHUMACHER is Chief Metallurgist, Bell Telephone Laboratories, Murray Hill, N. J.

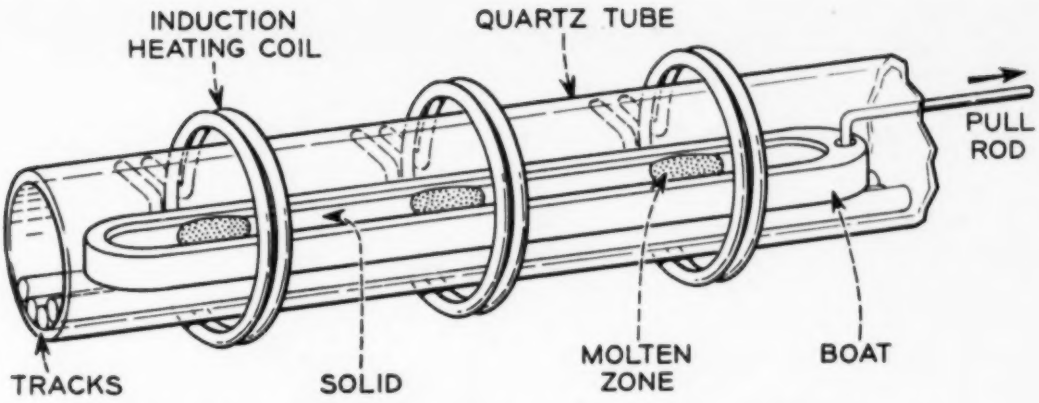

Fig. 1—Axially aligned induction heaters are shown in a diagram of the zone melting equipment.

from that left by the preceding zone. At the end of the run substantially all the impurities have been left in the final zone. This freezes, and the impurities are trapped.

Zone-melting is now operating on a production level for transistor-destined germanium. Fig. 2 is a photograph of the apparatus. It is being used as a research tool in purifying other semiconductors such as silicon and the compound indium-antimonide. Tin and antimony have been purified to new levels by zone-melting. Many other ultra-pure metallic materials should soon be available.

The method can be applied to any solute-solvent system in which there is an appreciable difference in the solubility of the impurity in the molten substance and in the solid freezing from it. The mathematical theory of the process has been thoroughly worked out and the results to be expected for a given system can be accurately predicted if these solubilities are known.

High purity plays an important role in two of the more common metals of much interest to the Bell System, copper and iron, and these are currently being investigated.

Copper from Chuquicamata, Chile, has in it something or other making it uniquely adaptable to certain copper oxide rectifier applications. Copper from nowhere else in the world can be used for these purposes. The quantity of *mystery stuff* involved is so small as to defy positive detection by all available analytical tools—including the mass spectrograph. Zone-melting offers the dual hope of concentrating the impurity to a quantity yielding unequivocal identification and of providing ultra-pure copper as a starting material to which known minor constituents can be added.

Soft magnetic materials are predicated on highly refined iron. Any solute atom, substitutional or interstitial, present in iron produces large adverse effects on magnetic properties. Present practice requires hydrogen refining at extremes of time, temperature, and expense. Zone-melting in hydrogen holds considerable promise for this application.

With this new tool metallurgists have a potent instrument for making really pure metals. Important and sometimes drastic changes in metallic properties have already been observed as the limit of purity is approached. As more materials are brought toward this limit, there will be both opportunity and challenge to exploit their properties.

References

[1] Earle E. Schumacher: Metallurgy Behind the Decimal Point. *Trans.* AIME (1950) **188**, pp. 1097-1110.

[2] W. G. Pfann: Principles of Zone-Melting. *Trans.* AIME (1952) **194**, pp. 747-753.

[3] W. G. Pfann and K. M. Olsen: Purification and Prevention of Segregation in Single Crystals of Germanium. *Phys. Rev.* (1953) **89**, No. 1, pp. 322-323.

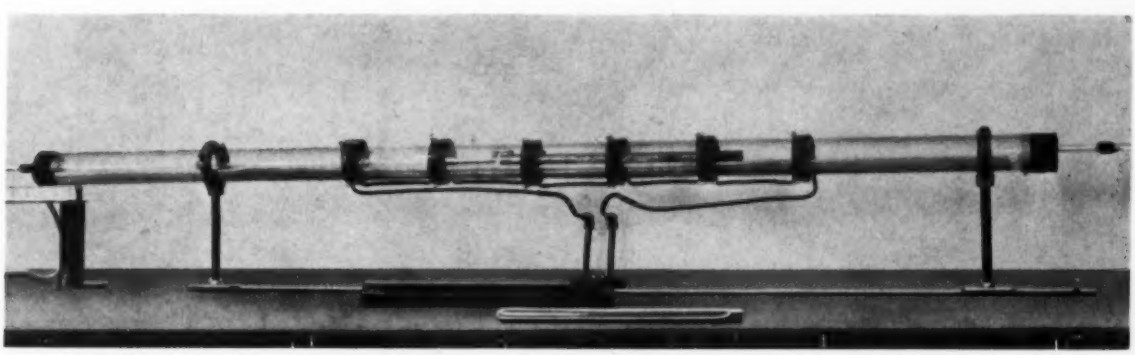

Fig. 2—Completely uncontaminated metals can be produced by the zone melting apparatus. The role played by minute quantities of impurities in controlling the properties of metals can then be determined.

Composition Control of Steel Castings Improved by New Furnace Sampling Methods

by Vincent E. Belusko

BECAUSE the single slag basic melting practice adopted for the production of steel castings displayed speed that indicated additional savings in heat time, attention was focused on the features of the practice causing delay. One of the time consuming features was the 20 to 25 min delay required for the preliminary carbon and manganese analysis. The immediate objective, therefore, became one of not only providing speedy and simple methods of sampling, but also of providing the melter with immediate and reliable information on the condition of the melt.

The sampling practice up to this time for the preliminary or rough sample analysis consisted of pouring a sample into a core sand sample mold and quenching it very slowly. The sample was then delivered to the laboratory where, if at all possible, it was drilled. On many occasions some hurried tempering treatment became necessary and at times another specimen was requested, which, after casting and quenching, received a tempering treatment on the breast of the furnace door.

The elimination, not only of sampling uncertainties, but also of the 20 to 25 min delay of preparing for and running the analysis by consistent methods to provide accurate and immediate information, became the first objective.

At a meeting of the local Technical and Operating Committee of the Steel Founders' Society, Ralph Miller, metallurgist, Sumner Iron Works of Everett, Wash., told of his successful use of the Brinell hardness test block method of rapid carbon determination. Through the courtesy of Mr. Miller, a chill block hardness test mold, as shown in Fig. 1, was made available for a preliminary study. It became apparent that this method of rapid carbon determination could be used most successfully on the greater number of the hardenable alloys produced.

VINCENT E. BELUSKO is a Metallurgist with the Electric Steel Foundry Co. (ESCO), Portland, Ore.

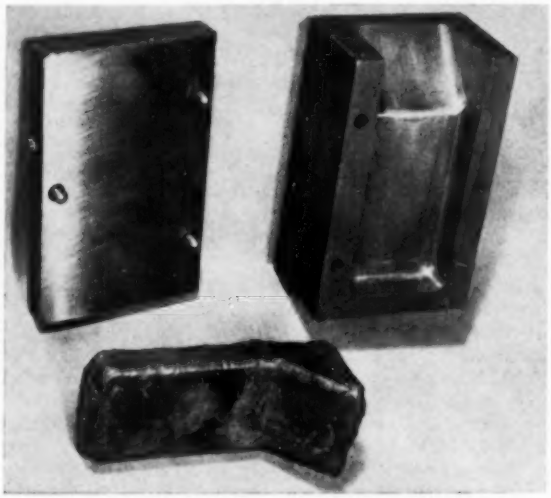

Fig. 1—The Brinell hardness test block method of rapid carbon determination utilizes the metal chill mold and the resultant steel block.

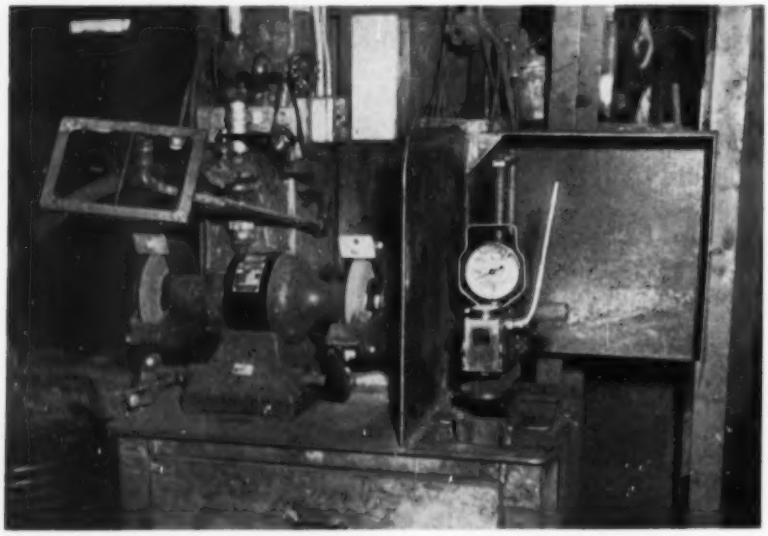

Fig. 2 — Brinell testing equipment is located beside the furnace. Carbons are run on mild, low alloy, and straight chrome steels of from 4 to 14 pct chrome.

A thorough study of this method of carbon determination was initiated on one of the low alloy manganese molybdenum heat-treatable steels on which the aim is to maintain a final 0.30 carbon. This type of steel consists of some 30 pct of production. Through the survey, information on the relationship of the diameter of the Brinell hardness impression vs carbon content as determined by routine analytical methods was obtained.

Steel Sampling

The sampling procedure consists of removing a sample of metal from the furnace in a hot, well-slagged spoon, and killing the sample held in the spoon with aluminum wire and approximately 0.5 pct manganese as low carbon manganese, and pouring into a metal chill mold as shown in Fig. 1. The resulting block is removed from the mold as soon as it is solidified and is quenched immediately and with vigorous agitation in the water pit at the furnace. When cold, the block specimen is ground lightly on one side and Brinell impressions are made under the standard 3000 kg load. The Brinell testing facilities as shown in Fig. 2 are located beside the furnace. The diameters of the impressions are read with the standard Brinell scope and reference is then made to a chart which was developed through the previously stated study, and which gives the carbon content corresponding to the diameter of the Brinell impression.

It became apparent that the measurement of the Brinell impression had to be made with extreme accuracy and, as an added precaution, two Brinell impressions on each test block were made at standards known to be completely solid locations determined by X-ray. This helped to eliminate the occasional possibilities of misinformation which sample defects such as air pockets may have in influencing test data. In addition all Brinell impression readings of the melter are checked by the control man. At present carbon determinations are made on mild, low alloy, and straight chrome steels of from 4 to 14 pct chrome.

While the carbon content survey by Brinell hardness was in progress, attention was also focused on the elimination of the preliminary manganese analysis. Chemical data indicated that an average of 92 pct of the manganese which was oxidized into the slag during the oxygen blow was recovered in the reduction phase of the process. Since the charges were standardized with the use of 40 pct foundry returns of known composition, a chance of the elimination of a chemical manganese determination was envisioned. Calculation quickly proved that such was the case even on some of the higher carbon heats which did not lend themselves to the determination of carbon by the Brinell hardness method. Of course, if the type of scrap changed, modifications must be made.

Since the higher carbon heats still required combustion carbon analysis, it became necessary to eliminate as much as possible the delay these analysis caused by their air-hardening nature. Fortunately at this time the induction furnace method of carbon analysis was coming to the fore with its time-saving advantages. A unit was soon placed into operation while a suitable sampling method was developed.

New Method

Early attempts to draw molten steel into a Pyrex glass tube were not at all heartening, although it proved to be possible, provided there was no misjudgment of metal temperature, rather complete evacuation of air from the rubber bulb, and proper timing. Because of these difficulties a new approach was made. This consisted of a transmission suction gun commonly used by the automotive trade for removal of oil from hard-to-drain sections. A specially designed air-tight adapter to receive the proper size pyrex glass tube completed the unit as shown in Fig. 3.

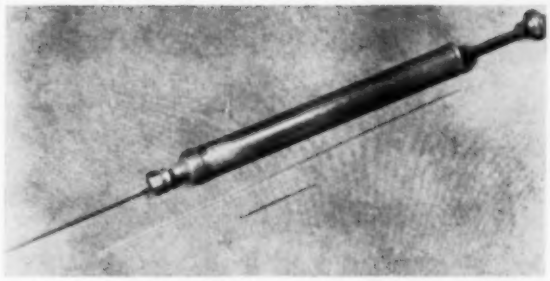

Fig. 3—A specially adapted automobile transmission suction pump is used to draw molten steel into a Pyrex glass tube.

Although it first appeared that obtaining proper samples by this method required too much effort and skill, due mainly to wide variations in the approach and positioning of the pyrex tube to the molten metal, the individual competitive spirit and pride in being able to draw molten metal into these pyrex glass tubes to the longest lengths, developed a sound and consistent sampling technique as shown in Fig. 4.

This sampling method eliminated the necessity for the melter to cast a sample, cool it and temper it by judgment on the door breast of the furnace. Now a piece of clean, unoxidized wire enclosed in a protective sheath of glass is delivered to the laboratory where it is quickly stripped of the glass sheath and cut into approximately ¼ in. lengths by means of a wire cutter. Approximately five of these quarter-inch lengths, which approach a rather consistent constant weight, are quickly weighed and placed

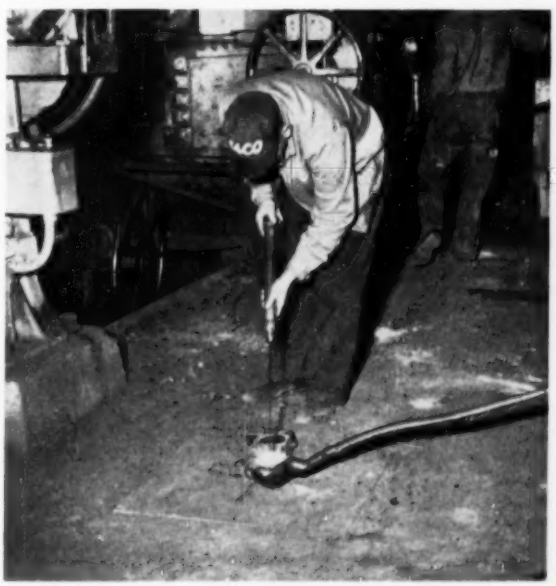

Fig. 4—A sound and consistent sampling technique was developed based upon competitive spirit and pride.

Fig. 5—Single slag basic practice has given basic steel the fluidity necessary to run light sectional castings.

into the induction furnace unit for combustion carbon analysis. The carbon analysis is completed some 3 or 4 min later.

During the time the carbon analysis is made, the reduction process of the metal oxides from the slag is given attention by the melter. Six to 8 min after drawing up the sample into the glass tube, the melter is informed by telephone what required additions are necessary. By the time the control man has arrived at the furnace, only the required temperature checks by optical pyrometer and fluidity sampling remain to be made.

The Pyrex tube sampling method provided an additional advantage since the final carbon analysis of the metal as sampled from the ladle into which it was tapped is completed some 20 min after tapping.

Slag Analysis

One of the most important samples which many operators try to eliminate are the slag pancake samples and slag viscosity tests. However, in the basic electric furnace practice for steel these tests are the main control of the quality of the material produced. The color or sheen of the pancake can give a clue to the degree of reduction of metal oxides from the slags, and from its appearance on fracture, some information of the composition of the slag can be gained.

The slag viscosimeter test of the Herty design has proven to be most valuable, especially on the Hadfield manganese steels. Control of these slags with respect to viscosity has indeed given most valuable information, and directly effected the quality of the product produced.

Fig. 6—Fluidity spiral tests confirmed that fluidity is primarily a function of temperature.

Previous to the decision of the Electric Steel Foundry Co. to change over to a single slag basic practice, the generally expressed opinion was that a basic melted steel would lack the fluidity necessary to run the light sectioned castings, shown in Fig. 5, and which are a large part of production. Studies of the fluidity of acid melted steel were made with the use of the modified fluidity spiral shown in Fig. 6 which was developed by N. K. Anderson of Alloy Steel & Metals. The results were then compared with the fluidity results of basic melted steel. These tests confirmed that fluidity is primarily a function of temperature. Although fluidity spiral lengths versus optical pyrometer readings and timing of the film on the cup sample have not been thoroughly correlated, the use of all three sampling methods for temperature control have indicated that the fluidity test provides very reliable information with respect to temperature. As a word of caution, however, it is extremely important that the tests be made under identical conditions each and every time. Variations such as pouring the metal into the cup from various heights, or sampling with a half-full spoon of metal can lead to confusion and unreliability.

The sampling methods which have been discussed were in each case first placed into use at the P. T. Lectromelt furnace. Through these improved methods an average saving of some 20 min per heat has been realized on the hardenable grades of steel produced in this furnace. The daily production of this furnace averages 14 heats per day, of which approximately eight heats are low alloy heat-treatable steels. Hence, a daily saving of some 2½ hr in furnace time has been effected and which allows the production of approximately an additional two heats per day.

These sampling methods have also been placed in use at the other furnace units in the plant to a degree dependent on the types of alloys produced. It is believed that the attention given to sampling methods at the furnace has not only resulted in better composition control, but also has realized the greatest economic and production advantages offered by the melting process.

Programs Underway To Increase U. S. Production of Strategic Beryllium

by B. H. Clemmons and James S. Browning

BERYLLIUM, obtained mainly from the beryllium-aluminum silicate, beryl, is one of our most strategic and critical metals. Strategic because suitable substitutes for many of its alloys have never been developed. Strategic because of certain uses and potential uses of a classified nature in our nuclear energy program. In this field, substitutes have been developed, but only at the expense of a reduction in efficiency.

Dependence upon foreign countries for beryllium is illustrated by the fact that in the period 1935 to 1950 the United States imported 66 pct of the entire world output of the source mineral, beryl, while contributing only 7.1 pct of the world output. Essentially all metal produced is consumed in this country.

Even though the present market value of beryl ranges from $400 to $500 per ton, known tonnages of domestic ore that can be economically mined and beneficiated are small. Large increases in these tonnages are unlikely, although a search for additional reserves is under way.

There are relatively large tonnages of low grade ores, which usually contain less than 1 pct beryl, and field work probably will develop additional reserves of this nature. Unfortunately, few of these ores can be economically beneficiated unless some accessory mineral is concurrently recovered to defray a major part of overall costs.

Various investigators have devised flotation methods for recovering beryl from feldspar-mica-quartz pegmatites. Undoubtedly, coordinated processes will be applied to certain of these ores; however, limited reserves and uncertain markets for feldspar and mica probably will preclude any large production of beryl from ores of this type.

A much more promising potential source of domestic beryl appears to lie in the spodumene-bearing pegmatites of the Lincolnton-Kings Mountain area of North Carolina.

There exists a strong and enlarging market for lithium salts, largely obtained from spodumene. Large reserves of this mineral occur in the North Carolina district, and mining and milling operations may ultimately provide for the treatment of 2000 or more tons of ore per day. These deposits contain as an accessory mineral 0.3 to 1.5 pct beryl—usually in crystals smaller than ¼-in. size. Recovery of beryl on this basis could at least triple present domestic production.

Under DMPA sponsorship the Bureau of Mines at Tuscaloosa, Ala., is studying the possibility of recovering beryl from these spodumene pegmatites. The Foote Mineral Co., which is operating a spodumene-recovery plant at Kings Mountain, N. C., is cooperating in the work.

Beryllium is a consituent of about 30 minerals, but its only commercial source at this time is beryl. Beryllium minerals occur principally in pegmatites, granites or syenites, in association with feldspar, mica, spodumene, and various other minerals. Commercial production thus far has been limited largely to pegmatites.

Beryl is not present in all pegmatites. Where it does occur, the mineral is usually present either as widely disseminated grains or as local or somewhat banded enrichments, which on occasion have yielded very large crystals—in some instances weighing as much as 50 to 60 tons. Virtually all beryl thus far produced in the United States has been obtained from enrichments of this type, where the crystals were of ¾ to 1-in. or larger diameter and would yield to hand-picking or cobbing. Much of the output has been as a byproduct operation in producing feldspar or strategic mica.

Future recovery of beryl probably will depend more on fine-grain concentration methods than in the past, because known occurrences of coarse-grained mineral have been largely exhausted.

Occurrence

Beryl-producing countries during 1950 marketed the following percentages of the total world production: Brazil 39.5 pct; Union of South Africa 22.6 pct; Southern Rhodesia 12.7 pct; United States 7.6 pct; Madagascar 7.3 pct; Mozambique 3.9 pct; miscellaneous 6.4 pct. In the United States, beryl deposits occur in South Dakota, Colorado, and in the New England, Southern Appalachian, and Rocky Mountain areas. Production to date has come principally from the Black Hills area of South Dakota, as a coproduct with columbite-tantalite, lithium minerals, feldspar, and strategic mica. Appreciable quantities have also been produced in New England, Colorado, and New Mexico.

B. H. CLEMMONS is Chief, Metallurgical Div., Region VII, U. S. Bureau of Mines and JAMES S. BROWNING is Metallurgist, U. S. Bureau of Mines, Tuscaloosa, Ala. This is an abstract of a paper that appeared in the August 1953 issue of MINING ENGINEERING.

Production and Consumption

The wide commercial application of beryllium and its alloys was largely an outgrowth of World War II. In 1936 reported world production of beryl was 480 tons, which sold for $40 per ton. In 1943 world production amounted to 6000 tons, worth approximately $120 per ton. Thereafter, production decreased for a time but rose again to 7300 tons in 1950, the price advancing to $300 per ton. Appreciable quantities of the beryl were stockpiled during the high production years, as the highest consumption figures reported for beryl have been 3058 tons in 1943 and 3007 tons in 1950.

Highest domestic production of beryl recorded was 559 tons in 1950, when a limited deposit of pure beryl was discovered and mined. In some years domestic production has been as little as 40 tons.

Uses

A preponderant part of the beryllium consumed at this time is used as a hardening agent for various alloys—especially those of copper.

Beryllium-copper alloys have commercial and strategic importance because of their resistance to fatigue, corrosion, heat, and wear. Their hardness, tensile strength, high electrical and thermal conductivity, low creep tendency, and low sparking and nonmagnetic properties are other desirable attributes. They are widely used in various aircraft parts. Other beryllium uses are for dental and surgical alloys, diamond-drill-bit matrix metal, watch balance wheels, and current carrying springs.

In the atomic energy field, beryllium has a number of important uses, most of which are classified.

Beryllium oxide is used as a high temperature refractory for aircraft sparkplugs and ultra-high-frequency insulators; in rocket combustion chambers, and in high temperature furnaces. The oxide also has application in the nuclear energy field, in ceramic glazes, and in special glasses.

Current market quotations for beryl ore are $46 to $48 per unit of contained beryllium oxide when the ore or concentrate assays 10 to 12 pct BeO. Beryllium metal is quoted at $95 to $105 per lb, depending on purity and form. Beryllium-copper master alloy is quoted at $40 per lb of contained Be plus 29.3¢ per lb of contained copper.

Processing

Beryllium has been described as the "world's No. 1 metallurgical headache" because of various difficulties encountered in recovering and working the metal. Beryllium minerals usually occur in forms that have only limited or poor response to normal concentration methods; in many instances they occur in association with minerals that can be rejected only with extreme difficulty. Pure beryl still contains only 4 to 5 pct beryllium metal, or 12 to 14 pct beryllium oxide. The most practical methods available for recovery of the metal from the source minerals are, by most standards, unusually complicated and expensive. Finally, although there are several methods of analysis for beryllium or beryllium oxide, none can be classed as simple or fully satisfactory.

There is a possibility that some heavy-media process can be applied to beryl ores to obtain a partial concentration. However, very close control will be necessary, because the 2.7-2.8 specific gravity of beryl is little different from that of feldspar, quartz, mica, and spodumene. This lack of specific gravity differential largely precludes use of jigs, tables, or similar gravity-type concentrating devices.

Gaudin and associates, in the April 1950 MINING ENGINEERING, proposed a process for treating ¾-in. to 1-g particles of beryl with a "kicker" that responded to the neutrons emitted by beryl after being irradiated in gamma rays. A device of this type may find application but appears to be too complicated and expensive for the average small producer. Under some conditions beryl can be separated by electrostatic separation.

Beryl can be recovered from ±⅛-in. to 48-mesh sizes by agglomerate tabling. But, the 48-mesh material would still require treatment by flotation. Hence, for simplicity, it is probable that flotation alone will be the most promising method of recovering beryl in sizes too small for hand-picking.

Technologists of the Bureau of Mines at College Park, Md., Salt Lake City, Utah, and Rolla, Mo., have published reports of results of flotation research on beryllium-bearing ores for their areas. Separations were of the same general type. After vigorous surface conditioning, usually followed by water washing, beryl was floated by an anionic collector of the fatty acid type.

S. M. Runke of the Rapid City, S. D., station of the Bureau of Mines recently reported a new type of separation which eliminates the expensive preflotation conditioning. Bulk flotation of feldspar and beryl is followed by retardation of feldspar and beryl flotation by petroleum sulfonate-type collectors.

In all of these flotation separations quartz and feldspar can be rejected from beryl without undue difficulty. Mica tends to report in part with the beryl and may be removed by cation active reagents at some point in the process.

Separation of beryl and spodumene is a much more difficult problem because the flotative response of the two minerals under most conditions is essentially the same.

At Tuscaloosa, in work on the Kings Mountain spodumene pegmatites, the Bureau has recently developed a reagent combination that retards beryl while permitting spodumene to float. Various details remain to be worked out, but there is reason to believe that the new procedure may permit commercial separation of beryl and spodumene by flotation. The nature of the separation cannot be revealed at this time, but a report on the work will be published at the earliest practicable date. To provide some idea of the progress, from ore containing 0.3 pct beryl products have been obtained containing 18.0 pct beryl—about 60:1 ratio of concentration.

Conclusion

Technology now places a great deal of dependence upon the beryllium alloys that have been developed for various special purpose applications, and an appreciable hardship would be suffered by the nation if these alloys were suddenly unavailable.

When all aspects of the problem are considered, it is readily apparent that present unstable world conditions dictate that the nation *must* make a concerted effort toward attainment of a greater self-sufficiency in its production of beryl. It is improbable that our requirements can be completely satisfied, but there is reason to believe that present production can be appreciably increased.

The most promising source of increased U.S. beryl production is the spodumene-bearing pegmatites of the Carolinas. Recent test work promises to solve the problem of concentrating the small percentages of beryl contained in these deposits.

Hurley Furnace and Boiler Description and Design

by E. A. Slover

THE usual reverberatory system of smelting copper concentrate or calcine has for its component parts a furnace and one or two waste heat boilers. These parts are operated on a basis of compromise, since the furnace can send gas to the boilers at too high a temperature and the boilers by plugging, due to dust or slag, can place a definite limit on the amount of fuel the furnace can burn.

Over the years the copper concentrate smelting furnace has had few advances in design. The simple rules of design such as the flame should wipe the bath and the speed of the gases should be reasonably low for dust carrying purposes seem to cover the main features.

In the construction of the individual furnaces some innovations are always being introduced. Among these are charging so that the work of smelting is a complete bath process, the use of suspended brick arches in place of sprung arches, the use of basic brick, not only in the crucible, but also in roof and sidewalls, the use of various means to feed the charge, the use of magnetite or other heavy material to construct the hearth, water cooling of bridgewall and slag skimming bay, the smelting of raw charge instead of calcine, the use of preheated air, and possibly the use of oxygen-enriched air for combustion. But the general outlines of the furnaces have not changed much except as to size.

Furnaces at Hurley

As shown on Fig. 1, the furnace at Hurley is 126 ft long between the longitudinal buckstays and 32 ft wide at the skewback plates.

The foundation is a concrete retaining wall with piers at intervals that go deeper into the earth. Purposely the wall at the burner end of the furnace is not backed-up as tightly as the other parts of the foundation so that movement due to expansion may take place here rather than into the boiler foundations. Within these foundation retaining walls of concrete, the earth has been removed to allow the placement of the crucible brick base inside of which a silica hearth is laid 4 ft 6 in. in depth. No expansion is left in the brick base and crucible where they are in contact with the hearth.

E. A. SLOVER, Member AIME, is Assistant General Manager, Chino Mines Div., Kennecott Copper Corp., Hurley, New Mexico.

Discussion on this paper, TP 3580D, may be sent, 2 copies, to AIME by Jan. 1, 1954. Manuscript, Jan. 5, 1953. Los Angeles Meeting, February 1953.

The hearth itself is of quartzite crushed to 1 in. size with fines left in the product. An 8 in. layer is laid and tamped with paving tampers to about 6 in. in thickness. Then a layer of silica flour is spread and vibrated into the hearth. This operation is repeated until a depth of 4 ft 6 in. is occupied by the silica mass onion-skinned in layers of approximately 6 in. Before firing the entire hearth is covered with broken slag to a depth of 4 in. so that a seal may be formed on the hearth.

The crucible is completely faced with magnesite chemically bonded brick while the outside, against the foundation, is made of silica brick. The sidewalls are carried up with silica brick in which expansion joints are left at intervals. Above the crucible the sidewall is corbelled to form a shelf on which the charge may build up along the sidewalls, see Fig. 2.

The arch of the furnace is sprung 20 in. silica brick, with the longitudinal centerline horizontal the length of the furnace, and some 9 ft in the center above the bath. Both straight and wedge brick are used in the construction and a thin silica mortar is troweled for joints. After the arch under heat has assumed its permanent shape, a silica slurry is spread over the arch to fill any cracks that have formed, thus giving bearing surface to the brick and preventing dust from entering the body of the arch to act as a future fluxing agent.

The uptake of the furnace slopes up to the boiler entrance where a brick pilaster divides the gas stream for the two boilers. Over this flared uptake is a suspended flat arch of firebrick. The pilaster and sidewalls are constructed of firebrick but the bottom of the uptake is lined with silica brick and fettled through holes in the roof with siliceous fettling. Close to the entrance of each boiler is a brick covered slot through which water-cooled dampers may be lowered in event of boiler trouble.

These water-cooled dampers are hung permanently in position ready to be lowered when needed. Flexible hoses to follow the dampers as they are lowered are connected at all times and individual chain blocks are used to lower the dampers. A pump supplying water is started before the dampers enter the heat.

Charging of the furnace along the sidewalls for some 80 ft from the bridgewall is accomplished by electric vibrating conveyors fed by belt from charge storage bins above the furnace. These conveyors

The Transactions papers appearing in the Journal of Metals *during 1953 will subsequently appear in* AIME Transactions *Volume 197, and may be permanently referenced to that volume.*

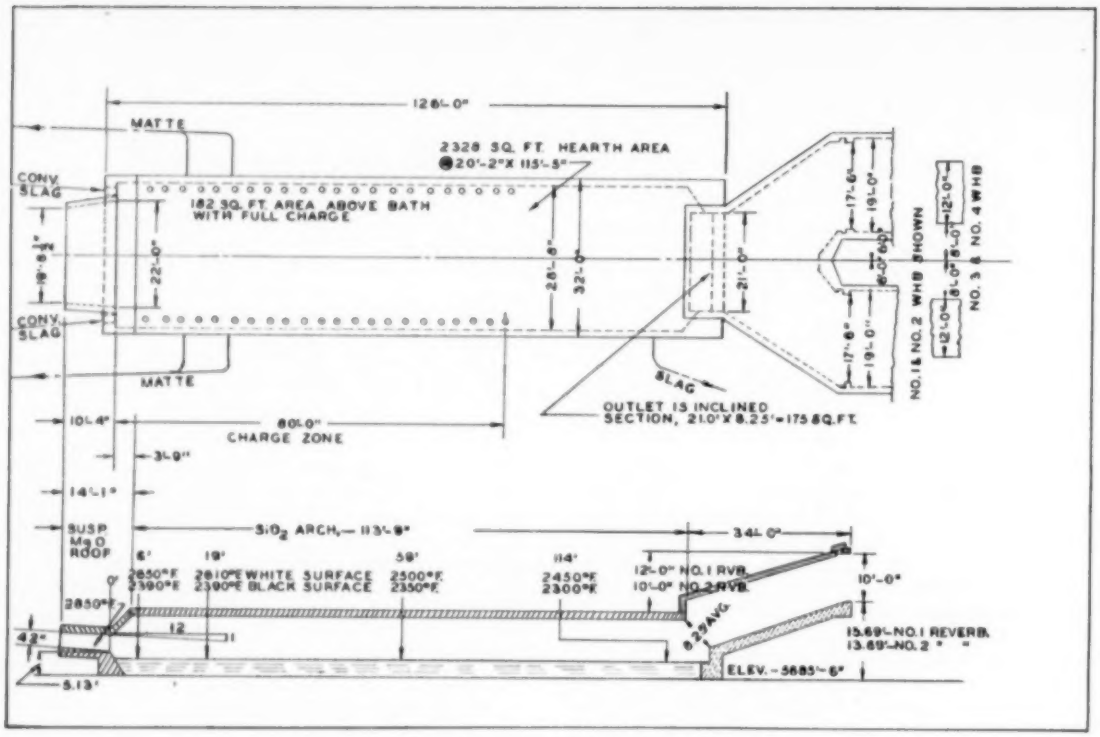

Fig. 1—General arrangement of reverberatory furnace.

are carried on steelwork separate from the building and furnace steelwork so that vibration is not transmitted. There is no trackage or flooring over the furnace except for a walkway along each vibrating conveyor. In the feeder trough are 24 door-covered slots at 40 in. centers through which charge is dropped into the furnace along the sidewalls.

The furnace was originally equipped with multi-jet air inspiration type of burners set in a panel above the bridgewall These were low pressure gas burners and the tubes through which air was inspirated to mix with the gas were rather short. Fireclay was used in the construction of these tubes.

Return converter slag is poured into the reverberatory furnace through launders on each side of the burner panel in the firing end of the furnace. Matte is tapped into ladles in the converter aisle through launders on each side of the furnace with two tap-holes available for each launder.

Once the dimensions of a furnace are fixed there has to be an overwhelming reason to change them. These reasons have their inception around the main function of the furnace, namely the transfer of heat.

The furnace as constructed never smelted much tonnage, 600 tons of concentrate being a good day's run. Magnetite soon filled the hearth so that the bath was of small proportions. With gas fuel the furnace never was hot enough to do rapid smelting. The temperature drop of the entire furnace was some 200°F from 2600°F in the combustion zone to 2400°F at the outlet.

Some minor changes were made in the multi-jet gas burners to obtain better air-gas mixing with the object of obtaining a higher temperature in the combustion zone but no pronounced success was observed.

To get this desired higher temperature in the combustion zone forced draft of pre-heated air burned with gas in a "Dutch Oven" was introduced. The thought here was to obtain as hot a flame as possible before turning the flame into the working zone of the furnace. Temperatures between 2800° and 2900°F can easily be maintained in the Dutch Oven. Two temperature gradients are given in Fig. 1. The first when the surface of the bath is covered with a white scum from the more refractory charges shows a gradual temperature drop of 400°. The other is when the bath is clean, or appears black, for less refractory charges. Here there is a very sharp drop of 460° in 6 ft, with an overall drop of 550°F. Results of this larger heat release have been a furnace without severe magnetite build-up and an increase in tonnage smelted. The furnace has not produced something for nothing but has been able to burn more gas than previously. Fuel ratio's have gone down from 6.635 to 5.627 million Btu gross and from 2.873 to 2.636 million Btu net per ton of new metal bearing material over the period 1942 to 1951.

A second reverberatory smelting furnace has been constructed at Hurley with dimensions about the same as the No. 1 furnace. This second furnace was built with the horizontal arch some 18 in. closer to the bath in order to be able to wipe the bath with the flame when burning a reduced amount of gas. A lower fuel ratio was achieved but other difficulties arose in respect to the restricted space for the charge. The furnace is being returned to an arch height similar to the original furnace.

Heat data are given in Table I. The days covered by this tabulation are not maximum smelting days but are days on which test work was done.

The changes over the years have been minor on the Hurley furnaces and when the heat transfer

was finally achieved the furnace smelted a good tonnage.

It was when an attempt was made to reach a much greater tonnage smelted that the boilers became a very definite limiting factor.

Waste Heat Boilers at Hurley

There are two sets of waste heat boilers with two boilers in each set corresponding to the two furnaces. The newer boilers will be described first. They were designed and made by Babcock & Wilcox and erected by Stearns-Roger Mfg. Co.

These boilers were designed for waste heat boiler use and incorporate ideas in regard to temperature, draft, and dust control. The smelter staff desired to obtain boilers that would allow for increased fuel burning in the furnace and at the same time would not need constant manual attention to keep them functioning.

The boilers are 12 ft in width and 35 ft in length, independently suspended from a separate structure of steel so that boiler and hopper move as a unit with expansion. They are not of great height in order to minimize the pressure in the upper parts of the boiler due to the buoyancy of the hot gases. With the setting under draft, should manual attention be necessary, the boiler can be approached by men to do the work. As the hot gases from the furnace go through the boilers the sequence of chambers is as follows: a cooling radiation chamber, a platten filled chamber where radiation in a cavity can take place, a superheater chamber, and a cross-flow two-drum boiler unit, see Fig. 3.

Table I. No. 2 Reverberatory. Averages for Tests of March 15, 16, and 17, 1951

1. Tons smelted in reverb per day	813
2. Cu ft natural gas burned in reverb per hour	153,000
3. Cu ft natural gas burned in preheater per hour	19,000
4. Cu ft natural gas charged to reverb per hour	172,000
5. Cu ft natural gas charged to reverb per day	4,128,000
6. Btu per cu ft natural gas	1,107
7. Btu per day from natural gas charged to reverb	4,570,000,000
8. Btu per ton natural gas charged to reverb No. 7 ÷ No. 1	5,620,000
9. Cu ft preheated air per min, 60°F, 24.45 in. Hg	21,000
10. Temperature, °F, preheated air	650
11. Lb preheated air per day	1,814,400
12. Btu per lb preheated air, sp ht = 0.24 Btu/lb/°F	141.6
13. Btu in preheated air per day	257,000,000
14. Btu from sulphur, per cu ft natural gas burned in the reverb	287
15. Btu from S per day No. 14 x (No. 2 x 24 hr)	1,054,000,000
16. Subtotal Btu to reverb per day, natural gas + S No. 7 + No. 15	5,624,000,000
17. Total heat into reverb per day, natural gas burned + S + preheated air (No. 2 x 24 hr) x No. 6 + No. 15 + No. 13	5,376,000,000
18. Reverb draft, H_2O	−0.04
19. Pct CO_2 + SO_2 by volume in reverb offtake gases	11.8
20. Pct O_2 by volume in reverb offtake gases	1.1
21. Pct CO by volume in reverb offtake gases	0.6
22. Pct excess air at reverb offtake	3.96
23. Highest flame temperature °F in reverb + Dutch Oven	2,890
24. Gas temperature reverb offtake, °F	2,320
25. Btu sensible heat per lb reverb offtake gas, + 60°F (No. 24 − 60°F) x sp ht 0.284	642
26. Lb reverb gases per day, at offtake	5,038,940
27. Btu sensible heat reverb gases per day	3,235,000,000
28. Btu potential heat reverb gases per day	207,000,000
29. Btu latent heat volatilization in H_2O charge + natural gas per day	512,000,000

The first cooling chamber has tubes on each side and the roof in order to reduce gas temperatures rapidly. From the boiler makers view this was desirable because the rate of steam generation of the

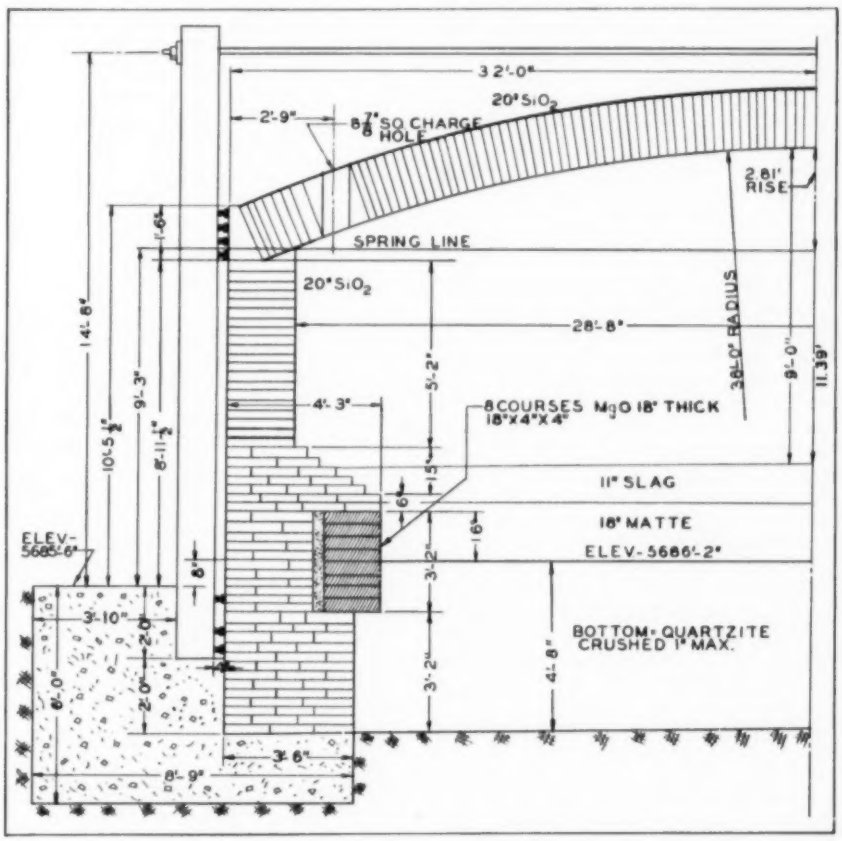

Fig. 2—Half-section of reverberatory furnace.

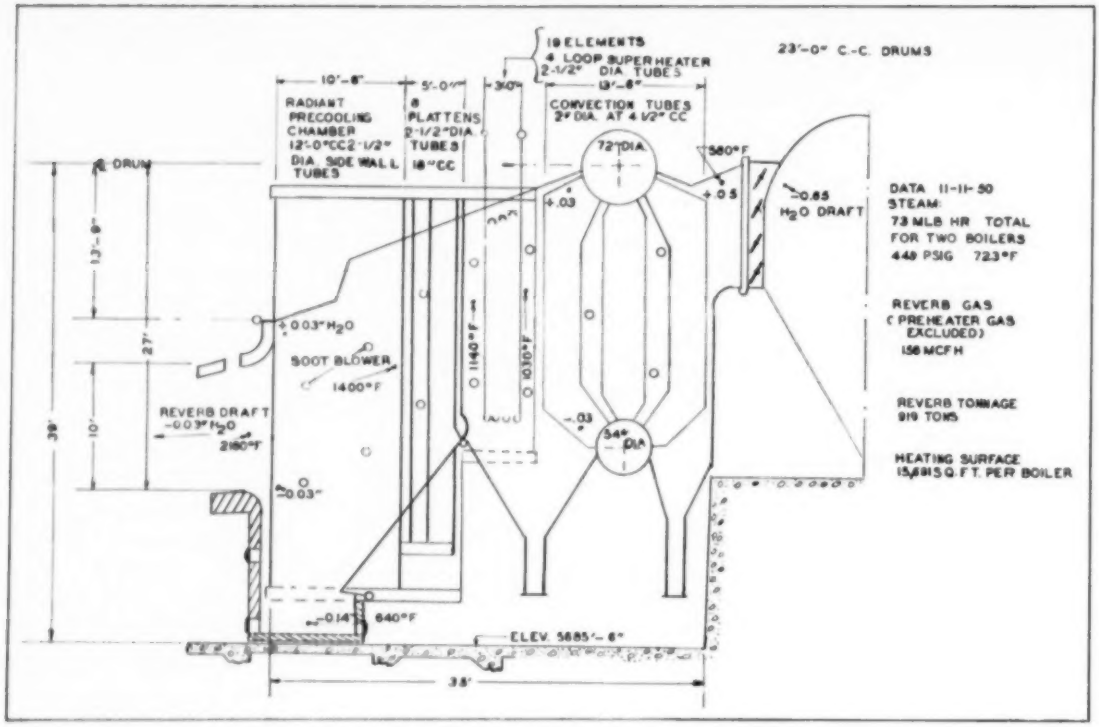

Fig. 3—No. 3 and No. 4 waste heat boilers.

first tubes of the plattens might be too high for natural circulation were the gases initially to impinge directly on these leading tubes. From the smelter point of view it was desirable to reduce the temperature of the sulphide dust before it met the leading tubes of the plattens so that sticking and corrosion would be avoided.

The platten chamber is 5 ft long, and has seven rows of plattens made up of 2½ in. tubes. There are eight passages 15½ in. wide between tubes. In this chamber the temperature of the gases is still further reduced before passing to the superheater tubes.

There are 19 superheater elements of four tubes each. Originally there were 24 superheater elements but 930°F superheater temperature was obtained. In order to reduce this temperature, five elements were removed so that now the superheat temperature follows a flat curve at 730°F.

From the superheater chamber the gases pass through a two drum special boiler. Cross flow of the tubes by the gases has been obtained.

In the entire boiler there is not a baffle to separate dust from the gas or to add draft loss to the system. The tubes are as simple in design as possible in order to make replacements easy.

In the design of these boilers it was considered necessary to have the drums at 23 ft 0 in. centers, in order to get enough height to insure proper water circulation. It was thought that the hot gas stream might go all the way through the boiler only as deep as the height of the boiler entrance (10 ft 0 in.) with the chance that about 7.5 ft of the net 17.5 ft tube height might not be touched by the hot gas. And in the calculation of the heating surface on this basis, a compromise was made between a somewhat higher offtake temperature than ordinary, and a larger amount of tubing. However, in actual operation, the bottom of the gas stream, with about 160

Table II. Waste Heat Boilers No. 3 and No. 4. Averages for Tests of March 15, 16 and 17, 1951

Heat Data		
30. Lb steam per hour, total of the two boilers		91,000
31. Lb steam per day, total of the two boilers		2,184,000
32. Temperature of feedwater at WHB, °F		325
33. Pressure of steam, psi, gage		468
34. Pressure of steam, psi, gage		480
35. Temperature of steam, °F		765
36. Btu put into steam per lb, in WHB		1,066
37. Btu put into steam per day		2,328,000,000
38. Pct CO_2 + SO_2 by volume at WHB exits		10.6
39. Pct O_2 by volume at WHB exits		2.7
40. Pct CO by volume at WHB exits		0.4
41. Pct excess air by volume at WHB exits		13.5
42. Pct air infiltration, reverb offtake to WHB exits, by volume		8.8
43. Pct H_2O draft, boiler side WHB exit dampers		+0.05
44. Pct H_2O draft, stack side WHB exit dampers		−0.52
45. Lb gases per day from WHB exits		5,501,000
46. Lb gases per hour to each boiler, reverb offtake basis		105,000
47. Lb gases per hour to each boiler, WHB exit basis		115,000
48. Temperature of gases entering WHB, °F		2,120
49. Temperature of gases leaving WHB, °F		580
50. Btu sensible heat per lb WHB exit gases, +60°F, sp ht 0.261		135.7
51. Btu sensible heat per day, leaving WHB exits		746,000,000
Input to Waste Heat Boilers		
52. Sensible heat in reverb offtake gases, Btu/day—pct	3,235,000,000—	81.9 %
53. Potential heat in reverb offtake gases	207,000,000—	5.2
54. Latent heat vol H_2O, charge + fuel, per day	512,000,000—	12.9
55. Total input to waste heat boilers	3,954,000,000—	100.0
Output from Waste Heat Boilers		
56. Btu put into steam per day	2,328,000,000—	58.9 %
57. Btu sensible heat exit gases per day	746,000,000—	18.9
58. Latent heat volume H_2O, charge + fuel, per day	512,000,000—	12.9
59. Btu unaccounted for per day	368,000,000—	9.3
60. Total output from waste heat boilers, Btu per day	3,954,000,000—	100.0
Miscellaneous		
61. Pct of heat in fuel charged to reverb recovered in steam (No. 37 ÷ No. 7) x 100		50.9
62. Pct total heat put into reverb present at WHB entrances		73.5
63. Thermal efficiency of reverb, pct 100.0 pct — No. 62		26.5
64. Efficiency of WHB, total heat basis, pct (No. 56 ÷ No. 55) x 100		58.9
65. Efficiency of WHB, sensible heat basis, pct (No. 56 ÷ No. 52) x 100		72.0

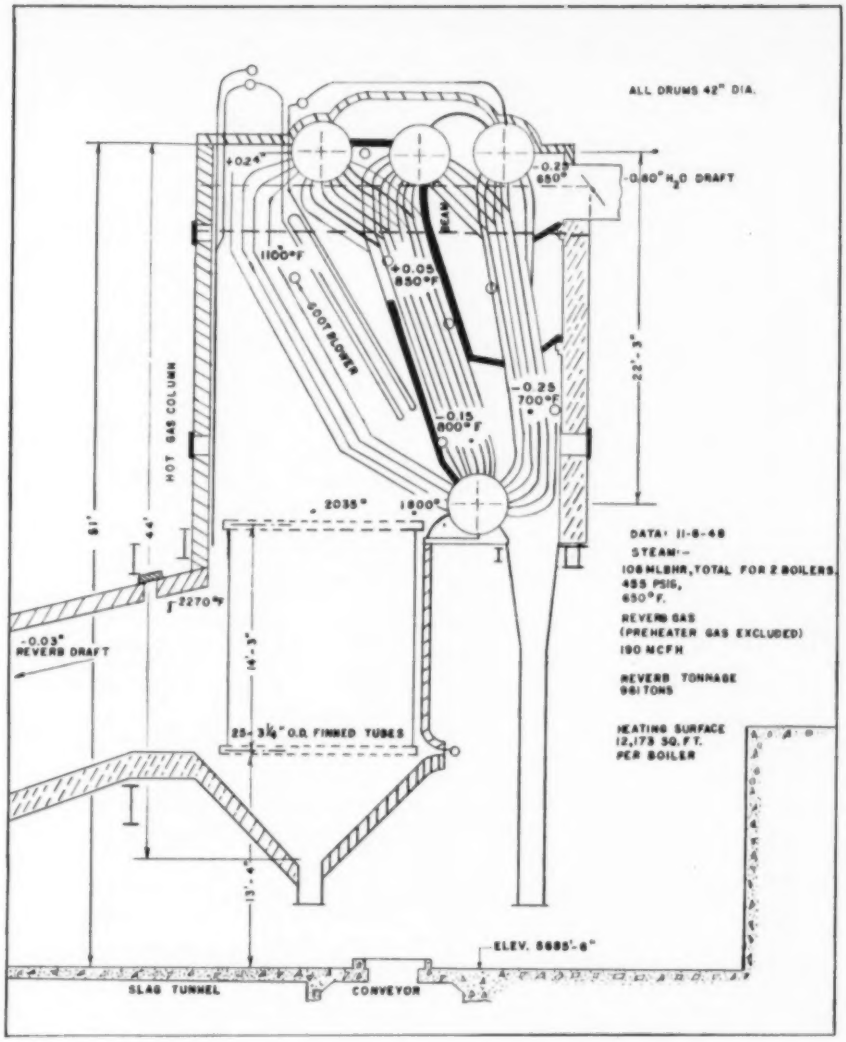

Fig. 4—No. 1 and No. 2 waste heat boilers as originally installed in 1939.

M cu ft per hr natural gas burned in the reverberatory, comes down to the top of the lower drum, with the result that the exit gas temperature is substantially lower than predicted. This dropping down of the gas stream's lower boundary may be due to the fact that there is a slight build-up of pressure in the boiler, from front to back, so the gas is forced and to some extent packed or stuffed into the boiler, causing it to spread.

The setting is attached to the tubes by Nelson studs. For the side surfaces there is a layer 1½ in. thick of B & W K2 cement, then a foam glass block of 3½ in., and finally an air-sealing layer of Air-Tight cement about ¼ in. thick. Wire attached to the studs holds the foam glass blocks in place. On the top of the boiler an additional layer of firebrick is placed between the K2 cement and the foam glass blocks and at the rear where the tubes are separated, tile is used to span the space between the tubes.

Considerable attention was given to the hopper beneath the radiation chambers of the boiler since most dust would accumulate here. Floor tubes form the steeply sloping rear wall of the hopper while the sidewalls are partly made of sidewall tubes from the radiation chamber and partly of Detrick suspended tile. The front wall is stationary and constructed of Detrick tile. Dust knocked into the hopper by the soot blowers does not slag and is removed manually by rabbles. It was thought afterward that this dust could be removed easily and continuously by a stoker arrangement working through an air seal. Since the only part of the entire boiler that does not move as a unit is the front wall of the hopper and all the vertical movement is downward it is important that the hopper bottom does not hit the floor. Both units at Hurley stop moving ½ in. from the floor.

Soot blowers are depended on to keep the boilers clean but hand lancing doors have been provided as a safety matter. To date little hand lancing has been done. In the radiation chamber, four soot blowers of the Diamond IR or surface type are used on each side of the 12 ft wide chamber. Then there are 9 IK type which travel across the entire boiler for the platten chamber and the balance of the boiler. Both types are retractive. The platten chamber has left in each platten a 15 in. vertical slot through which two soot blowers operate. The IR soot blowers use

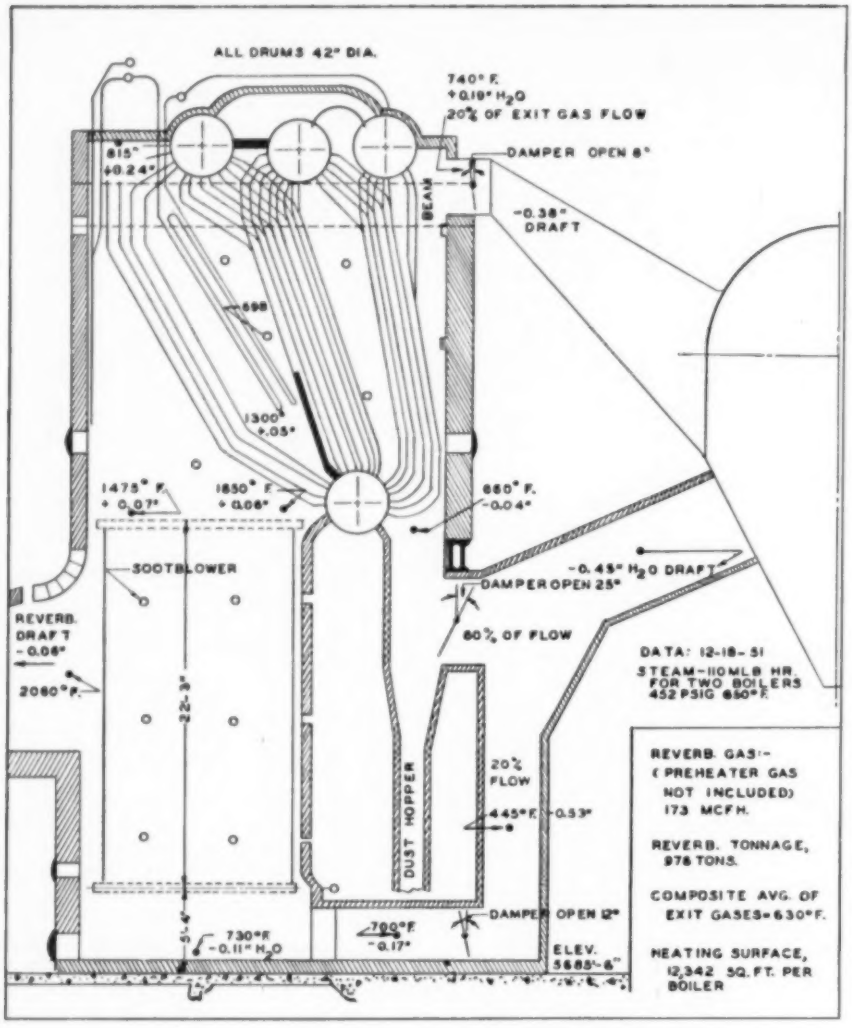

Fig. 5—No. 1 and No. 2 waste heat boilers as revised in 1951.

steam at 250 lb and IK soot blowers at 210 lb pressure. Ingersol-Rand air motors which revolve and advance the blowers and purge air at 3 lb pressure are used when the soot blowers are not in operation. The soot blowers may be operated automatically in sequence from a panel board or each may be operated individually in any sequence.

To date no tubes have been replaced or welded and there has been no trouble with this set of boilers. Also no slag has been formed in the boilers or in the hoppers. It was demonstrated that one boiler could carry the furnace with normal firing when the water-cooled dampers had the other boiler cut out for superheater tube reduction. Draft is automatically regulated using a Hagan control. Some data on this set of boilers is listed in Table II.

The two boilers of the second set which are behind the original furnace are Combustion Engineering Company's fin furnace boilers, see Fig. 4.

As far as the gas flow and baffling are concerned, these are Sterling type boilers with three passes. But the water circulation is different from a Sterling boiler. As shown in Fig. 4, the tubes are cross connected in the two back passes, with alternate rows of tubes going to different top drums. That makes what amounts to Sterling type water circulation in the front of the boiler, and an economizer in the back, with the two mixed up in the middle.

These boilers are 19 ft wide inside and have a large combustion chamber, three sides of which are composed of tubes with fins. Above this radiation chamber is the boiler with three steam drums and one mud drum suspended from I-beams below the steam drums.

There is no object in describing these boilers as originally installed other than to call attention to the troublesome features when used as waste heat boilers in a copper smelter.

First, there was a constant dust problem since the height of the boilers allowed the buoyancy of the hot gases to exert itself and the upward velocity attained drew the gases from the radiation chamber very rapidly. Except toward the bottom of the entering gas stream, the gas stream did not extend far across the chamber. The velocity of the ascending gas stream carried dust that deposited on the front bank of tubes in the boiler where, because of the lack of heat transfer in the radiation chamber, the heat baked the dust on the tubes.

Second, the pressure generated in the boilers made it impossible to lance the tubes properly to keep the dust from building up and plugging the

boiler. No increase in firing rate was possible under these conditions.

Third, the setting of both boilers had disintegrated from sulphur impregnation and finally the boilers in expanding while heating after a repair invariably sprung leaks where the tubes were rolled into the mud drum due to mud drum space restriction.

In the redesign, shown in Fig. 5, the third and fourth objections were taken care of by using foam glass, tile, and air tight cement, but no studs attached the setting to the boiler tubes. The setting is supported by steel beams and does not move with the boiler. The mud drum has been freed to move without hindrance.

The other problems were approached from the standpoint of cooling the gases in the chamber made for that purpose and removing baffles that served to hold dust.

A model of the boiler was constructed and from applied suction it was determined that one-sixth the draft of the boiler exit was needed as a vertical component applied at the bottom of the boiler to cause the hot furnace gases to penetrate well into the radiation chamber and give up a greatly increased quantity of heat. The cooler gases would not bake the dust on the lower part of the tubes in the first pass. Then, to prevent dust deposition in a narrow second pass the baffle was greatly shortened between the first and second passes and removed between the second and third passes. The reason the baffle was not completely removed before the second pass was that no short circuiting of the superheater was contemplated. In effect much additional cross flow was obtained, but to be certain of this a new central duct was constructed that forced cross flow in the boiler proper. The original outlet to the flue was also maintained. Each outlet was dampered so adjustments can be made. The water wall tubes on three sides of the radiation chamber were extended downward an additional 8 ft 0 in. into a square-shaped, flat bottomed dust collecting hopper to be certain no slag was formed from the dust knocked down.

In operation the boiler has caused no trouble but the top flue has had to be opened at times to reduce excessive pressure near the top at high firing rates on the furnace. Apparently no close approach has been made to the firing rate on the furnace that will cause the boiler to be a limiting factor.

Soot blowers have been installed on these boilers, the same in type as on the new set of boilers: the IR type, of which there are 18 on the radiation chamber, and the IK type of which there are four on each side of one boiler and four extra long ones on but one side of the other boiler. There is one G 9B blower, which is non-retractive and rotates through a whole circle. This arrangement was necessary because of the narrow space between boilers.

The boilers are well cleaned by the soot blowers but some accretion has built up at the back of the radiation chamber where dust that has been given a direction by the splitting pilaster accumulates. It is not serious.

Automatic draft control has been applied to the center flue exit, the top and bottom exit being fixed when once set.

Acknowledgment

Thanks are due by the writer to the Smelter Staff, and to H. W. Mossman and C. L. Lockart, of the Smelter Metallurgical Dept., for assistance in preparing data for this paper.

Technical Note

Change in Ingot Shape During Zone Melting

by W. G. Pfann

WHEN a molten zone traverses a long, solid ingot in a level, open boat the ingot becomes tapered. While the taper may be slight after one zone pass, it can be appreciable after repeated zone passes, even to the extent of causing an overflow of matter at the end of the boat. It will be shown here that such *matter transport* by a molten zone arises from the volume change on melting and that it corresponds in magnitude and direction to the magnitude and sign of the volume change. It will be shown also that the mechanism of matter transport is basically similar to that of solute transport by a molten zone, which has been discussed elsewhere,[1, 2] and that the two processes can be described by similar equations. Finally it will be shown that matter transport can be prevented by inclining the ingot at a critical angle.

Contraction on melting results in forward transport, that is, transport in the direction of zone travel; expansion on melting results in reverse transport. The way in which forward transport arises from the contraction on melting may be seen as follows:

At the starting end of a solid horizontal ingot of uniform rectangular cross section of height h_o, form a molten zone of length l, as shown in Fig. 1. The height h of the liquid will be αh_o where α is the ratio of density of solid to that of liquid. Advance the molten zone, at constant length, a distance dx. The volume of solid melted will be $h_o dx$; the volume of solid frozen will be $h dx$, because the height of the freezing solid will tend to be equal to that of the liquid. The resultant change, dv, in liquid volume will be the difference in these quantities multiplied by the density ratio. Hence the following equation may be used for a zone at any distance x from the origin:

$$dv = l\,dh = \alpha(h_o - h)\,dx. \qquad [1]$$

Solving Eq. 1 for h gives

$$h/h_o = 1 - (1 - \alpha)e^{-\alpha x/l} \qquad [2]$$

which is valid in all but the last zone length in the

W. G. PFANN, Member AIME, is associated with the Chemical and Metallurgical Research Dept., Bell Telephone Laboratories, Murray Hill, N. J.

TN 186E. Manuscript, July 2, 1953.

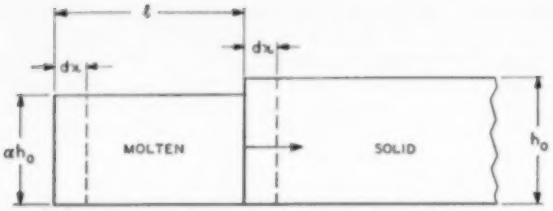

Fig. 1—Formation and advance of a molten zone in a level, uniform ingot. A transport of matter arises from the height difference between melting and freezing solids.

ingot. Eq. 2 is identical in form to Eq. 2 of ref. 1,

$$C/C_o = 1 - (1 - k)e^{-kx/l} \qquad [3]$$

for the solute concentration C after passage of a molten zone of length l through an ingot of uniform solute concentration C_o, where k is the ratio of solute concentration in the freezing solid to that in the liquid.

Eq. 2 shows that the zone accumulates height as it travels, which process continues, if the ingot is long enough, until h becomes substantially equal to h_o. No further increase in h occurs until the zone reaches the end of the ingot, whereupon it solidifies by normal freezing. This results in further increase in height and it is readily shown that

$$h/h_o = (1 - g)^{\alpha - 1} \qquad [4]$$

where h_o is the height of the liquid at the start of

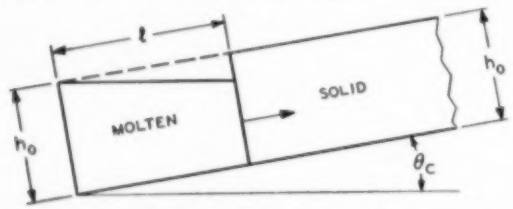

Fig. 2—Molten zone at beginning of its travel in an ingot inclined at the critical angle for zero transport.

normal freezing and g is the fraction of the zone length which has solidified. Eq. 4 is identical in form to the equation for solute concentration in normal freezing.

Likewise the ultimate distribution of height, which cannot be altered by further zone passes, is seen by analogy with solute transport to be

$$h/h_o = A'e^{\alpha x} \qquad [5]$$

where

$$\alpha = \frac{Bl}{e^{\alpha l} - 1} \text{ and } A' = \frac{Bd}{e^{\alpha d} - 1}$$

d being the ingot length. Eq. 5 shows that a large change in ingot height can be produced, even for a rather small α. For example, if $\alpha = 0.95$, $l = 1$, $d = 10$, then h/h_o is 0.58 at $x = 0$ and 1.4 at $x = 9$, which represents a variation of about 2½ to 1 in ingot height.

The transport process can be modified by inclining the ingot, which act in effect changes the value of α in Eq. 2. A case of particular interest, that of zero transport, for which $\alpha = 1$, is illustrated in Fig. 2. The critical inclination θ_c for zero transport is that for which the height of the freezing solid is h_o, where θ_c is given by

$$\theta_c = \tan^{-1} 2h_o(1-\alpha)/l \qquad [6]$$

The effect of passing 12 molten zones through a uniform germanium ingot is shown in Fig. 3 for a horizontal ingot and for an ingot inclined at the critical angle, which was 2°, determined experimentally. Germanium contracts on melting, the volume change being rather large, about 5 pct or more.* Inclination of the ingot can minimize, but cannot completely prevent, matter transport in normal freezing.

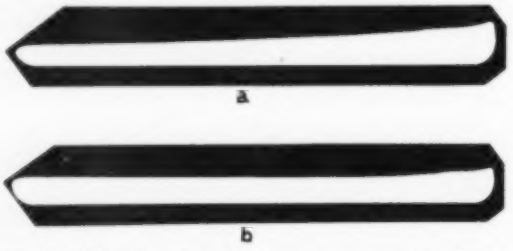

Fig. 3—Silhouettes of originally uniform germanium ingots after passage of 12 molten zones from left to right: a—ingot horizontal, b—ingot inclined at 2° from horizontal. Ingot length, 12 in.; mean zone length, 2 in.

Matter transport can also be prevented, except in the last zone, by altering the height of solid in the molten zone at the beginning of the ingot so that, on melting, the liquid height equals h_o. This method corresponds, in solute transport, to using a starting charge of concentration C_o/k in an ingot of uniform concentration C_o. It is useful for one pass only.

A consequence of matter transport is that the equations for solute distribution in ref. 1 are strictly accurate only if the ingot is inclined at the critical angle, although the error involved would be negligible in general.

Eq. 6 provides a means for estimating the volume change on freezing. However, surface tension effects have not been considered and more experimental data will be required before Eq. 6 can be used for this purpose.

The similarity of the equations which govern matter transport and solute transport suggests that these phenomena are basically the same. It appears that their common feature lies in the concept of *concentration*. In solute transport the concentration of solute freezing out of a molten zone is k times that in the zone. In matter transport the concentration of matter freezing out of a zone is α times that in the zone. The similarity of k to α lies in the fact that a density ratio is really a concentration ratio, when concentrations are expressed on a volume basis, as they have been throughout this work.

The writer is indebted to F. Monforte for performing the experiments of Fig. 3.

References

[1] W. G. Pfann: Principles of Zone-Melting: *Trans.* AIME (1952) **194**, p. 747; JOURNAL OF METALS (July 1952).

[2] W. G. Pfann and K. M. Olsen: Purification and Prevention of Segregation in Single Crystals of Germanium. *Physical Review* (1953) **89**, p. 322.

[3] B. H. Alexander: Unrecorded discussion on ref. 1 at the Philadelphia Meeting, AIME, October 20, 1952.

[4] S. E. Bradshaw: Phenomena Observed in the Melting and Solidification of Germanium. *Journal* Electrochemical Soc. To be published.

* Matter transport in the zone melting of germanium has also been observed by Alexander[3] and was attributed by him to the contraction on melting. A summary of this note was given by the writer during the same discussion. Change in ingot shape during normal freezing of germanium was discussed in a paper by Bradshaw[4] and some discussion of zone freezing was given orally. A value of 11.5 pct for the contraction on melting was given by Bradshaw.

Preparation of Metallic Iron of High Purity

by George A. Moore

A brief review is given of methods designed to produce metallic iron of high purity, and typical results are listed. A recent method, utilized at the National Bureau of Standards, consists of the extraction of ferric chloride by ether, reduction of this ferric chloride to ferrous chloride, further purification of this chloride, and the subsequent electrolytic deposition of metallic iron. Iron produced by this procedure apparently is softer than, and otherwise different in properties from, any iron previously prepared and contains appreciably smaller amounts of impurities.

THE history of attempts to produce "pure" iron reaches to antiquity and it may be presumed that each ancient armorer who succeeded in making a better steel concluded, correctly, that he had done a better job of removing the "base metals," and incorrectly, that he now at last had a "pure" metal. Early metallurgical papers mentioned use of "pure iron" in making alloys—this "pure" iron in most cases being inferior to some commercial stocks of the present time. Improvement has been continuous, and usually at a sufficient rate to convince each succeeding group of workers that they, at last, were using the really pure metal (until the analysts also improved their techniques to again discover the impurities). These adventures were reviewed in some detail by Cleaves and Thompson.[1]

Although the ores of a metal may be abundant, difficulties in extracting it may make the pure metal very rare. When impurities are restricted to a total of a few parts per million, nearly all pure metals become rarities. Lead, copper, gold, mercury, silver, zinc, aluminum, bismuth, and the six platinum metals are claimed to be available with total impurities ranging from 2 to 50 ppm. The present small and scattered world supply of so-called "pure" iron holds an unimpressive place in another group of 16 metals having approximately 100 ppm of foreign material. Of about 20 less rare metals, only the platinum metals are more costly to prepare.

While the production of such rare varieties of iron may appear insignificant in the presence of thousand-ton operations with 95 to 99 pct metal, it must be emphasized that all researches on commercially interesting irons and steels are in fact studies of the modifications of the properties of iron by additional materials. Until the properties of high purity iron are directly measured, all ferrous research must operate without known base values.

Traces of impurities may affect the properties of a metal in many ways. Infinitesimal traces of solutes, by disturbing the electronic configuration, greatly change the electrical properties of transistors and semiconductors[2-3] and slightly larger traces might alter these quantities in iron. Soluble impurities which disturb the perfection of lattice arrangement not only may alter the magnetic constants and electric properties, but by their close association with dislocation phenomena probably control the very existence of the "yield point"; determine the value of yield stress; and perhaps control the selection of slip and cleavage planes. It has been speculated that impurities might even cause the allotropic transformation in iron, but in any case their rearrangement must contribute to the unreliability of heat capacity and other thermodynamic measurements.

Impurities which do not remain in solution may cause even greater effects on the properties. Microscopically visible amounts of phases other than ferrite can be found in all high purity irons which have come to my attention. It can be calculated that from 50 to as little as 2 ppm of an insoluble material might be sufficient to completely film all grain boundaries in irons having grain sizes from ASTM Nos. 10 to 1. Should this occur, such films, even though invisible, may be very important in fracture problems, especially at extremes of temperature.[4] Studies of grain growth and diffusion normally imply consideration of a single-phase system, hence, in the presence of insoluble impurities they can be expected to give ambiguous data.[5]

High purity iron is also in demand for use as chemical and spectro-chemical standards; for work in classifying the lines of the iron spectrum; for biological work in nutrition; and for work in nuclear physics where the presence of some sensitive

G. A. MOORE, Member AIME, is Metallurgist, National Bureau of Standards, Washington, D. C.

Discussion on this paper, TP 3626D, may be sent, 2 copies, to AIME by Jan. 1, 1954. Manuscript, Feb. 18, 1953. Los Angeles Meeting, February 1953.

impurity as dilute as one part per hundred million may disrupt the experiment.

Considering the vital importance of all these factors it becomes evident that new means of producing iron of progressively higher purity must be developed.

Extensive interest in high purity iron at the National Bureau of Standards began about 1914 with the electrolytic preparation of some iron of about 99.95 pct purity, according the the analytical procedures then available. Intensive study from about 1930 until 1942, resulted in the monograph mentioned[1] and papers by Cleaves, Thompson, and Hiegel [7-10] dealing with iron of about 99.99 pct purity prepared by the nitrate crystallization process. Some larger ingots of similar iron were prepared by Cleaves and Lindberg between 1947 and 1950.

Processes Available

Numerous processes are available for purification of iron and it is frequently difficult to judge which is best. These processes can be basically classified as pyrometallurgical, electrochemical, and chemical. Some typical results obtained are listed in Table I. Basic open hearth ingot iron has represented the practical commercial limit of strictly pyrometallurgical process for at least 25 years and is represented by the various National Bureau of Standards samples No. 55 through 55B. Irons of 99.75 to 99.85 pct purity appear to represent the practical limit of this process. Some further removal of nonmetals can be accomplished by vacuum melting or hydrogen annealing.

The purity of electrolytic iron depends both on the purity of the anode metal and of the iron salt used for electrolyte. Both are normally comparable with ingot iron. Comparatively noble metals, for example copper, and active metals such as chromium, may be removed, but nickel, cobalt, manganese, and other metals similar to iron are usually unaffected. Electrolytic iron as deposited usually contains appreciable amounts of oxygen, and iron from sulphate baths usually contains considerable sulphur. The total impurities in electrolytic iron, as deposited, are comparable with ingot iron. Manganese and sulphur may be reduced by remelting in air, and oxygen by vacuum melting with a suitable slag, or by hydrogen treatment of hot sheet, or the melt. Such reworked electrolytic iron has been reported to be 99.95 to 99.97 pct Fe.

The carbonyl process is by no means a certain method of purification. Apparently nickel (and probably cobalt) is carried over with the iron, together with some copper and chromium. Carbon and oxygen are important nonmetallic impurities in the powder. Aluminum, magnesium, silicon, etc., may be introduced during remelting of the carbonyl powder.

The pyrometallurgical and electrochemical processes therefore seem to be incapable, at present, of producing iron of appreciably better than 99.95 pct

Table I. Typical Analysis of Iron by Various Processes, Expressed in Parts per Million Parts of Iron

Material	BOH Ingot Iron	Ingot, Hydrogen Purified	Carbonyl, Hydrogen Purified	Swedish, Vacuum Remelt	Electrolytic	Electrolytic, Vacuum Remelt	Electrolytic, Vacuum Remelt	Nitrate, Ingots 1-19	Nitrate, Ingots 21-26	Chloride, Electrodeposited Lot 7
Producer (Date)	Armco		C.I.T. ('35)	NPL ('51)	Various	NRC ('50)	Univ. Pa. ('50)	NBS ('39)	NBS ('49)	NBS ('52)
References	(a, b, c)	(a)	(a, d)	(e)	(a, f)	(c, f)	(g)	(f)	(f)	(f)
Impurity										
Al	20-30		20	10-40	<20-80	50-60	—	1	0.5	<0.1
B			Tr*							Nil*
Be							7-50	2	16	0.5
Ca								Nil†	8	<0.01
Co	60-80		[~50]	[~20]	80-100	90	[~5]			2.1
Cr	20-80		120	10-20	<20-100	<20-50	4	Nil†	4	Nil*
Cu	400-460		170	40-70	8-10	<20-50	[~10]	<20	4.1	4.1
Ga										Nil*
Ge										Nil†
Mg	Nil*		Tr*			Tr*		Nil†	4	1.1
Mn	160-600	280	50	40	~100	<100	5-30			<0.1
Mo	20-40				~20	<20-50	[~5]			Nil†
Ni	160-200		130	50-70	<50-220	140-400	3-8	Nil†	0.8	0.8
Pb	Tr*					Tr*				<0.05
Sb	20							<0.01		
Si	10	12	300	20-30	5-50	300	10-50	9	12	3.7
Sn	60-90				~10	<<30	[~10]	Nil†	Nil*	<0.05
Ti	Nil*					80				0.4
V	5-10				<30	<<50	[~5]			Nil*
Zr	Nil*					Tr*				Nil†
Total Metals	~1280	[~1280]	~840	~250	~500	~980	~125	<32	49	<13
As	60-120	[~20]				Tr*				Nil*
C	100-150	50	2-7	20-40	20-60	60-100	[~10]	10	19.7	
H_2	[~3]	[~5]	2	<0.05		1.7	0-2	2	0.3	
N_2	30-40	1	<10	10-20		1-10	3-16	2	6.2	
O_2	600-700	30	<20-100	10-20	~2000	26-80	3-14	27	9.0	
P	30-50	40		<10	10-50	10-20	50-60	<5	<5	
S	170-250	30	<20	40-60	0-40	20	10-40	19	7.5	
Total Nonmetals	~1180	~175	~100	~120	~2100	~175	~110	<65	<48	
Total Impurities	~2460	~1450	~940	~370	~2600	~1150	~235	<98	<97	

[~] Order estimated from value for source material or subsequent product.
* Quantitative meaning of nil and trace not given by analyst.
† Nil represents less than about 1 ppm.
* Nil represents less than about 0.1 or 0.2 ppm.

(a,b,c) Total range of composition covered by following sources:
(a) *Metals Handbook*. (1948) p. 424. Cleveland. ASM.
(b) N.B.S. certificates Nos. 55, 55A, 55B.
(c) Keeler and Davis.[14]
(d) Moore and Smith.[15]
(e) Rees et al.[4]
(f) N.B.S. files.
(g) Smith, Fostini, and Brick.[13]

purity. For greater purity, processes utilizing chemical purification of iron salts can be regarded as hopeful, and in these, major efforts should be directed to the removal of nickel, cobalt, copper, manganese, and chromium. Other elements which may be present in the starting material may usually be controlled in later processing of the metal produced. Some basic chemical processes which may be considered are as follows:

Recrystallization: Since the iron salt should not contain acid radicals yielding harmful impurities on reduction, nitrates or chlorides should be used. Recrystallization of ferric nitrate from strong nitric acid was used by Cleaves and Thompson[8] and recrystallization of ferrous chloride from dilute HCl was tried by them and earlier by investigators at the National Physical Laboratory.[11] Both procedures work efficiently provided a large part of the iron is discarded, since impurities concentrate in the mother liquids and only the primary crystals are of high purity. It is also, by the very nature of the process, difficult to maintain clean conditions when recrystallization is conducted on a large scale.

Precipitation Reactions: No reaction is known by which insoluble iron salt can be precipitated and recovered free from the impurities in the solution, giving a product which is convertible to high purity metal.[8]

The precipitation of impurities from an iron solution is possible, provided, first, that a sufficiently insoluble salt is found, and, second, that the very small volume of insoluble material can be effectively separated from solution. The precipitation of copper sulphide may meet these requirements. Many other suggested precipitation reactions have been eliminated as unsuitable either because they require the addition of undesirable reagents; or they do not operate in the acid condition necessary to prevent solution of the glass containers.

Solvent Extractions: Of all available processes, the transfer of a solute from one liquid to another probably offers the greatest number of possibilities for metal purification. These have the great advantage that they may be operated in a semi-automatic manner in closed, and therefore dust proof, systems. The number of possible liquid pairs which might be utilized is practically unlimited. It is desirable, but not necessary, that either the desired salt, or the impurities, be insoluble in one liquid, but in the absence of this requirement, it may still be found that the partition of a salt between two liquids may be almost entirely one way. For example the use of ether extraction is a familiar technique in the analysis of iron.

Proposed Method of Iron Production

At the beginning of the present campaign it was decided that the nitrate crystallization as used by Cleaves and Thompson, while a good method, was too laborious. A process giving a greater reduction of impurities might be hoped for, and a simpler method of attaining the same purity would be considered a success.

From the experience of numerous analysts, ether extraction was selected as the basic purification step. Additional purification has, however, proved necessary, and the process must also include reduction to metal, conversion of the reduced metal to solid useful form, and the elimination, as completely as possible, of oxygen and other nonmetals. The several steps considered or investigated for the proposed process, with commercially available ferric chloride of reagent grade as a starting material, are as follows:

I—*Ether Extraction* of $FeCl_3$ complex from solution in 6 N-HCl, with regeneration of aqueous solution and ether recovery.
  A—In batch operation.
  B—In countercurrent column operation.

II—*Reduction of FeCl$_3$ to FeCl$_2$* with high purity iron

$$2FeCl_3 + Fe \rightarrow 3FeCl_2$$

III—*Additional Purification of FeCl$_2$*
  A—By recrystallization
  B—By sulphide precipitation
  C—By ether extraction of impurities from solution of ether-insoluble $FeCl_2$.

IV—Electro-deposition of metal from $FeCl_2$ solution.

V—Hydrogen anneal of pellets

$$Fe(OH)_2 \rightarrow FeO + H_2O$$

$$FeO + H_2 \rightarrow Fe + H_2O$$

$$Fe_3C + 2H_2 \rightarrow 3Fe + CH_4 \text{ etc.}$$

VI—Production of massive metal
  A—Ordinary vacuum melting
  B—Drip casting
  C—Melting in magnetic field support
  D—Compacting and sintering

The apparatus used in step I for both batch and countercurrent column operations is shown diagrammatically in Figs. 1 and 2. About 25 lb of $FeCl_3$-$6H_2O$, AR grade, containing up to 150 ppm Cu and Zn (on Fe basis) and considerable arsenic, phosphate, sulphate and "insoluble matter," is dissolved in 2.5 liters of concentrated HCl plus 1.25 liters of redistilled water. The resulting saturated solution (about 9 liters) is fed to either extractor one liter at a time. About 90 pct of the iron content may be extracted by contact with 5 to 6 volumes of ether in the column extractor, but up to 30 volumes of ether may be required in the batch apparatus. The same volume of ether is used repeatedly in either case, and is recirculated at a rate of approximately 1 liter per hr.

Contrary to the implications of the standard analytical use of ether extraction in iron analysis, very appreciable amounts of cations other than Fe^{+++} appear to be carried over in the ether-HCl extract. Excepting molybdenum and tungsten, all of the metals listed in Table I have been found in the extract in at least trace amounts. In the best results so far obtained, a purification ratio as high as 30 to 1 has been observed for Cu+Zn, but the average purification efficiency is certainly much lower.

It is believed that the amount of impurity carried into the extract is closely proportional to the total amount of ether that comes in contact with the solution. Hence the column extractor, which continually treats a saturated solution, is preferred to the batch extractor on grounds of both purity and speed.

At the end of the run, most of the ether is removed from the extract by heating gradually to about 100°C. At this stage the extract contains about 2 lb of $FeCl_3$-$6H_2O$ per liter, and around 200 cc of ether per liter. Running a second extraction of this stock has not appeared feasible for a number of reasons, including the possible fire hazard associated with the further concentration of this ether-

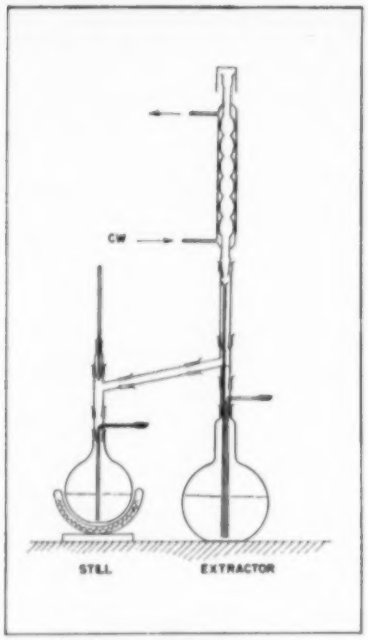

Fig. 1—Apparatus used for ether extraction of $FeCl_3$ in batch operation and for extraction of impurities from $FeCl_2$.

containing solution. The extract is instead diluted with 1 to 1½ times its volume of redistilled water, and the ether thus freed is distilled off, leaving $FeCl_3$ solution in a condition for further processing.

Step II, reduction to the ferrous state, is introduced both to bring the iron solution into convenient form for electrolysis and to prepare for additional purification reactions. A 2.5 liter batch of diluted $FeCl_3$ extract, containing about 0.5 lb of iron metal, is poured over about 0.5 lb of intermediate grade iron.

The intermediate iron used for reduction may be: Scraps of high purity iron from previous operations, or iron electrodeposited from the tailings of a batch of $FeCl_3$ solution, or directly from $FeCl_3$ solution after the first purification. The latter procedure, using about twice the current used in electrolyzing $FeCl_3$, is preferred in the absence of available scrap.

The reaction

$$2FeCl_3 + Fe \rightarrow 3FeCl_2$$

will run to completion in a few hours at room temperature, or may be hurried by warming. Some iron metal reacts with excess HCl in the extract

$$Fe + 2HCl \rightarrow FeCl_2 + H_2$$

so that the final solution contains almost as much iron from solution of the intermediate reducing metal as from the fresh extract. The $FeCl_2$ solution normally is boiled to drive off arsenic, germanium, or other metals having volatile chlorides, but no general overall reduction of impurity metals has been demonstrated.

Further purification (step III) is required since the ferric chloride extract (and therefore the $FeCl_2$ solution) contains anywhere from 5 to 20 parts of copper per million parts of iron.

Recrystallization (step IIIA) was used to produce some $FeCl_2$-$4H_2O$ which contained only 0.9 ppm total of copper, zinc, and lead, but only the first crop representing about one-fourth of the iron in solution was of this degree of purity. The process is laborious, inefficient, and it is difficult to avoid oxidation of the $FeCl_2$.

Step IIIB, sulphide precipitation, was tried in two ways. Immediately after reduction to $FeCl_2$ was completed, about 150 mg of FeS chips (chemically pure grade) were added to each liter of the acid (5 pct HCl) solution. After allowing 20 min for solution of the FeS, the solution was boiled 20 min to drive off excess H_2S. A small amount of insoluble precipitate was caught in a fine glass frit funnel. Electrolysis of solutions of this type gave irons whose copper contents varied from 1.8 to 7.8 ppm, indicating that the efficiency either of precipitation or of filtering was somewhat variable.

In a subsequent experiment, a reagent consisting of activated charcoal containing 20 pct of absorbed FeS was added at a rate of 1 to 2 grams per liter to moderately cool $FeCl_2$ solution containing about 1 pct HCl. This was intended to act as an ion exchange absorbent; very little free H_2S was released. The used reagent was filtered out cleanly on fine glass frit, and was found to have increased in copper content. Preliminary indications are that better elimination of copper is obtained by this procedure than with FeS chips, but final analytical results are not yet available.

Step IIIC was tried on the assumption that ether-soluble impurities, that accompanied $FeCl_3$ in the first ether extraction, would still be soluble in ether and could thereby be separated from ether-insoluble $FeCl_2$. To investigate this possibility about 6 volumes of redistilled ether were percolated through a $FeCl_2$ solution which contained 5 pct free HCl. No detectable amount of ferrous iron was removed, but about 0.1 pct of the total iron in the solution was extracted as $FeCl_3$. Organic wax (probably polymerized ether) and the metals, aluminum, boron, beryllium, calcium, chromium, copper, gallium, germanium, magnesium, molybdenum, nickel, silicon, tin, and zinc were identified in the concentrated extract after the ether had been boiled off. It has not been possible to date to establish the extent to which the $FeCl_2$ solution is improved by the extraction of these impurities, which were identified only in highly concentrated form. From available evidence it does not appear that this operation was in all respects as good as step IIIB, hence it is possible that some impurities are soluble in ether only when combined with $FeCl_3$ in complex ions, and that some impurities may undergo valence changes that affect their solubility in ether. At any rate the process is worth while to remove the wax, pending establishment of its other merits.

Step IV, electrodeposition of iron from acidified $FeCl_2$ solution, is an efficient and convenient method of recovering metallic iron. There is little probability of picking up impurities, and active impurities such as tin and zinc appear to be completely eliminated.

The process is operated in closed 2-liter cells, Fig. 3, using a high purity iron rod as the cathode and a high purity graphite rod as anode. Graphite powder is retained in a porous alundum cup which rests in a glass cylinder closed at the bottom by an extra coarse glass frit plate. A little colloidal graphite sometimes finds its way into the main chamber, but this normally settles between the glass beads at the bottom so that little or none migrates to the cathode. The possibility of contamination by

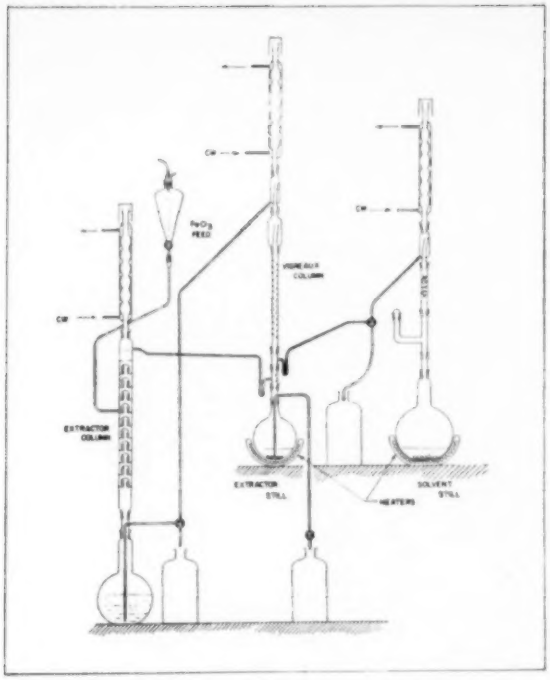

Fig. 2—Apparatus used for ether extraction of $FeCl_3$ in column operation.

graphite could be eliminated if an iridium anode were available for use. Ferric ions produced at the anode remain in the anode cylinder and do not interfere with the deposition.

The cell is normally operated at 4 amp and 16 ± 3 v, under which condition water evaporates nearly as fast as iron is deposited from solution, so that the concentration of the solution remains fairly constant. The volume is maintained by addition of fresh portions of electrolyte. Each cell can produce 1 lb of iron metal in about 300 hr of operation at the current stated. The iron cathodes contain about 0.25 pct of oxygen (as FeO or $Fe(OH)_2$), together with some other gases and possible traces of carbon.

Step V, annealing in hydrogen, has been used to remove oxygen and possible carbon. The cathode iron is slowly heated in undried hydrogen and held at 400° to 500°C for 8 to 16 hr to remove any carbon which may be present on the surface of the iron. The undried hydrogen is then replaced by dried hydrogen and the temperature raised to 1100°C and held at that point for about three days to remove oxygen.

The efficiency of the high temperature hydrogen anneal is very largely controlled by the purity and dryness of the hydrogen atmosphere. Early trials with a commercial alumina drier following a "De-Oxo" purifier allowed some tarnishing during cooling, and reduced the oxygen only to 70 ppm. Recent anneals with hydrogen from specially built driers, with cobalt indicator sight gages to observe the efficiency of drying, have given completely bright metal. It must be appreciated that no statement of oxygen analysis is pertinent except that made with respect to a finished specimen after final treatment.

Step VI, production of massive metal—Previous investigators of high purity iron and its alloys have recognized the probability of contamination of the purified metal by the refractory crucibles in which the melting was done. The extent of this contamination varies in the different reports and is influenced by the nature and purity of the refractory used and particularly by the temperature at which the refractory is fired. Small ingots of nitrate iron prepared at National Bureau of Standards (Table I, col. 8) contained traces of impurities that presumably came from the small high-fired beryllia crucibles, but larger ingots subsequently prepared in crucibles differently fabricated (Table I, col. 9) were more seriously contaminated. From this and other evidence it is doubtful that iron approaching 99.999 pct purity could survive melting in any available refractory.

Three alternative procedures offer possibilities. First, and perhaps most desirable, the possibility of melting a charge suspended in vacuum in a magnetic field[12] appears close to realization, although no practical results are yet available. Second, drip melting of a compacted bar is feasible. Both methods reduce the possibilities of contamination of the metal by refractories. The third and most convenient method of obtaining massive metal without refractory contamination is the use of powder metallurgy procedures. Encouraging possibilities of this procedure have been encountered in experiments where pellets of the iron of lot 7 (see Table I) have been compressed to bars which were subsequently squeezed, rolled, and swaged to ¼ and ⅛ in. rods, resintering as appeared to be necessary. Hardness values encountered during this series of operations remained surprisingly low. The ⅛ in. rods have been used as cell cathodes, while ¼ in. rods appear usable for property determinations when their composition has been established.

Results

To date, ten lots of iron have been prepared, ranging in size from one to a few pounds each. The majority of these runs were of an experimental nature, designed to indicate qualitatively the merits

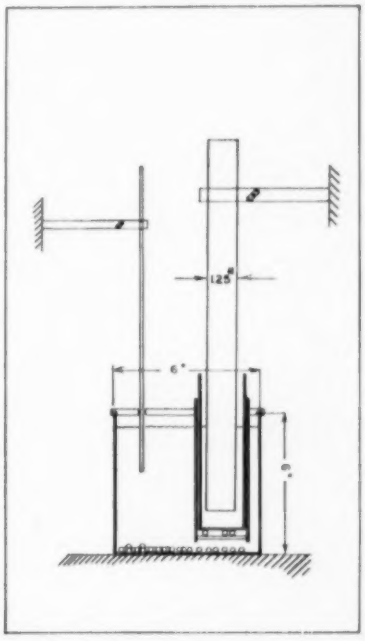

Fig. 3—Cell used for electrodeposition of iron from acidified $FeCl_2$ solution.

of variations of the steps in the purification process, and much of the metal produced has been consumed in subsequent runs, chiefly in the reduction of $FeCl_3$ to $FeCl_2$.

Procurement of verified quantitative data for all of the impurities that may be present constitutes a major research by the analytical department because the degree of precision desired is frequently far beyond that of established analytical procedures. Determination of a number of elements each of which is present in amounts of one part per million, or a small fraction of a part per million, and the determination of the absence of these or other elements with an equal degree of precision and certainty, are at best difficult and laborious processes that are not yet completely established.

Complete and verified analyses have been reported to date only for the product of the following sequence of operations:

$FeCl_3 \cdot 6H_2O$ was processed in the batch extractor and the purified ferric chloride was reduced to $FeCl_2$ with metal from previous runs. The ferrous chloride solution was treated with FeS chips and, after filtering, was electrolyzed. Pellets of the cathode iron were annealed in wet and dry hydrogen, using the commercial drier. Two batches of 25 lb each of $FeCl_3 \cdot 6H_2O$ were put through this combination of steps IA, II, IIIB, IV, and V, to produce lots 6 and 7 of iron. The analytical data for lot 7, recorded in the final column of Table I, show that very high purity iron was obtained. Practically identical results were obtained in the analysis of lot 6.

Further experimental runs indicated possible improvements in the sequence of steps used in the production of lot 7 and the final production run to date was made as follows: 75 lb of $FeCl_3 \cdot 6H_2O$ were processed in the column extractor. One-half of the processed $FeCl_3$ was electrolyzed directly to supply metallic iron for reduction of the remaining $FeCl_3$. The $FeCl_3$ solution was treated with the ion exchange sulphide reagent and, subsequently, with ether. As in other runs, iron was recovered from the purified $FeCl_3$ solution by electrodeposition. Analysis of this lot 10 is not yet complete but there are indications that the total of metallic impurities in lot 10 is less than it was in lot 7.

A few interesting observations of the behavior of iron of lot 7 have been made. The metal appears to be unusually resistant to corrosion as indicated by the resistance of pellets to tarnish in the laboratory atmosphere and by the difficulties encountered in dissolving pellets in warm HCl, for purposes of analysis. Conversion of the cathode metal to more useful forms by powder metallurgy and forming techniques, with sintering or annealing in dried hydrogen, appears to be practical. Rods ¼ and ⅛ in. in diameter have been produced and will be used for property determinations. The indentation hardness of some of these compacted specimens, after sintering at 1100°C, approximates the values usually associated with commercially pure aluminum.

Summary

The current attempt, to produce iron of higher established purity than has been attained previously, employs the following principles: purification of ferric chloride solution by ether extraction; conversion of the purified ferric chloride to ferrous chloride with subsequent purification of the ferrous chloride solution; recovery of metallic iron by electrolysis of the purified ferrous chloride with subsequent removal, from the cathode iron, of carbon and oxygen by annealing in hydrogen.

A small amount of iron containing less than 13 parts per million total of metallic impurities has been prepared and some of its properties, e.g., indentation hardness and corrosion resistance, confirm the analytical evidence that this is iron of unusually high purity. However, it is not certain that the ideal process has been achieved; subsequent modification of some of the details of the production process has produced iron which, according to incomplete analyses, contains even less metallic impurities.

One of the major difficulties encountered in this investigation has been the determination of impurities, in high purity iron, with the desired accuracy and precision.

This process for the production of high purity iron is still in the stages of experimental development, and it will be some time before enough stock can be accumulated to comply with any requests for iron of established super purity.

Acknowledgment

The writer wishes to express grateful appreciation to J. G. Thompson, Chief, Metallurgy Div., and to H. E. Cleaves, formerly Chief, Chemical Metallurgy Section, for much helpful advice, to W. S. Clabaugh and R. Gilchrist for advice on the chemistry of iron, to B. F. Scribner and Mrs. M. M. Darr for spectrographic analyses, and to the Chief of Ordnance, U.S. Army, for sponsoring the present phase of this work. The writer has been capably assisted in the laboratory by R. J. Sherman.

References

[1] H. E. Cleaves and J. G. Thompson: *The Metal-Iron* (1935) New York. McGraw-Hill Book Co.

[2] C. Wagner: The Electrochemistry of Ionic Crystals. *Journal* Electrochem. Soc. (1952) **99**, 346 C — 354 C.

[3] W. Shockley: Solid State Physics in Electronics and in Metallurgy. *Trans.* AIME (1952) **194**, pp. 829-842; JOURNAL OF METALS (August 1952).

[4] W. P. Rees, B. E. Hopkins, and H. R. Tipler: Tensile and Impact Properties of Iron and Some Iron Alloys of High Purity. *Journal* Iron and Steel Inst. (1951) **169**, pp. 157-168. (See p. 161, proposition that impurity concentration need not be sufficient to form a second phase.)

[5] W. P. Rees and B. E. Hopkins: Intergranular Brittleness in Iron-Oxygen Alloys. *Journal* Iron and Steel Inst. (1952) **174**, pp. 403-409. For production of this iron, see *Journal* Iron and Steel Inst. (1951) **168**, pp. 377-383.

[6] G. Wiener: Grain Growth in High Purity Iron. *Trans.* ASM (1952) **44**, pp. 1169-1185. See discussion by G. A. Moore, p. 1184, of Wiener's statement of a "limiting grain size."

[7] J. G. Thompson and H. E. Cleaves: A Summary of Information on the Preparation and Properties of Pure Iron. *Journal of Research*, National Bur. Standards (1936) **16**, pp. 105-130.

[8] H. E. Cleaves and J. G. Thompson: Preparation of Iron Oxide as a Source of High-Purity Iron. *Journal of Research*, National Bur. Standards (1937) **18**, pp. 595-607.

[9] J. G. Thompson and H. E. Cleaves: Preparation of High Purity Iron. *Journal of Research*, National Bur. Standards (1939) **23**, pp. 163-177.

[10] H. E. Cleaves and J. M. Hiegel: Properties of High Purity Iron. *Journal of Research*, National Bur. Standards (1942) **28**, pp. 643-667.

[11] C. H. Desch: The Work of the Alloys of Iron. Research Committee. *Proc.* Inst. Mech. Eng. (1934) **127**, pp. 277-298.

[12] R. L. Smith, R. V. Fostini, and R. M. Brick: The Low Temperature Properties of Relatively High Purity Iron-Carbon Alloys. 1st Progress Report Project SR-109 to Committee on Ship Steel (SSC-52): National Acad. of Science, N.R.C. Washington, Aug. 29, 1952.

[13] D. M. Wroughton, E. C. Okress, P. H. Brace, G. Comenetz, and J. C. R. Kelly: A Technique for Eliminating Crucibles in Heating and Melting of Metals. *Journal* Electrochem. Soc. (1952) **99**, pp. 205-211 (also *Journal of Applied Physics*, May 1952).

[14] J. H. Keeler and H. M. Davis: Density and Hydrogen Occlusion of Some Ferrous Metals. *Trans.* AIME (1953) **197**, pp. 44-48; JOURNAL OF METALS (January 1953).

[15] G. A. Moore and D. P. Smith: Occlusion and Evolution of Hydrogen by Pure Iron. *Trans.* AIME (1939) **135**, pp. 255-295.

DISCUSSION, N. C. Fick and B. W. Gonser presiding

H. B. Goodwin *(Battelle Memorial Institute, Columbus, Ohio)*—Dr. Moore's work appears to be a real advance toward the achievement of ultimate purity in iron. Having been engaged for several years in attempting to prepare large batches (300 lb) of high purity iron (although not nearly as pure as Dr. Moore's) I can appreciate how painstaking his work was.

I would like to see more details on the method of forming the pellets and of consolidating the iron into bars or rods, as apparently was done in some cases. I would also like more detail on the analytical procedures, which, in themselves, must be real advances.

In the present paper the actual sequence of steps for the various lots of iron produced is somewhat confused. This could possibly be clarified by a flowsheet-type diagram with lines showing processing of various lots.

G. A. Moore *(Author's reply)* — Charges of about ¼ lb have been compressed in a double action side pressure bar die. These have been coined by alternate use of concave and flat face plungers operating at 100,000 psi. About eight strokes are used, the compact rotated 90° and the process repeated. The bars have then been sintered in hydrogen and the process repeated. The coined bars can be rolled and swaged without difficulty. At this writing, a density of 99.5 pct of the theoretical value has been obtained on the coined compacts.

The development of the analytical methods has been under the direction of B. F. Scribner, Chief, Spectrochemistry Section, Chemistry Div., National Bureau of Standards, who has kindly supplied the following statement:

Spectrographic analyses of the iron were made by three methods which are identified and described as follows:

1—Direct Arc Method: This method involves preparation of the metal in the form of rods, approximately ¼ in. diameter, shaped by turning and filing. The rods serve as electrodes for direct-current arc excitation under optimum conditions for detecting the impurity elements. The method is useful for detecting certain elements such as molybdenum, germanium, or tin, for which the detectability by the other methods is poor. For most of the elements the method is not as sensitive as the remaining two methods and is subject to error if the impurities are segregated in the sample. The method was applied to preliminary surveys of samples, to studies of portions of samples for segregation, and to analyses in the early part of the program on pure iron.

2—Chloride Solution Method: This method involves preparation of a concentrated solution of a representative portion of the iron in hydrochloric acid. The solution is added to high purity graphite electrodes, which are dried in an oven and then subjected to arc excitation. Standard samples are prepared from ferric chloride specially purified by the ether extraction technique, and to which known amounts of the impurities are added. This method has proved to be about ten times more sensitive than the first method. It also has the advantages of simplicity in handling the sample, of ease in preparation of standard samples, and of sampling a large portion of metal.

3—Ether Concentration Method: This method involves a careful and painstaking separation of most of the impurities by extraction of the sample as iron chloride with diethyl ether. The concentrated solution containing the impurities is evaporated to dryness on a weighed portion of pure zinc oxide which serves as a carrier. The mixture is analyzed with the dc arc relative to standard samples of zinc oxide containing added amounts of impurities. Depending on the size of the iron sample used for the extraction process, this method results in a 10 to 100 fold increase in sensitivity of detection over the chloride method. However, care must be observed in the procedure; the acid is redistilled in an all-quartz apparatus, the ether is extracted with the pure acid before it is used, and extreme cleanliness is observed. The accuracy of the procedure was checked with standards of ether extracted iron to which known amounts of impurities were added.

Various sequences of steps were used on various lots and the paper makes no claim to have found the ultimate combination. We feel that a flowsheet in the paper might imply that a best process had been decided upon, and prefer to reserve this for an occasion when we can be more certain of its validity.

Technical Note

The Habit Plane of Beta in Alpha Titanium

by Paul A. Albert

THE β to α transformation has been investigated by Newkirk[1] in sponge titanium alloys which had been relatively slow-cooled so that several α grains formed in a former β grain.

P. A. ALBERT, Student Associate AIME, is Research Assistant, Engineering Research Div., New York University, New York.

TN 181E. Manuscript, June 15, 1953.

This paper is based on a thesis by P. A. Albert submitted in partial fulfillment of requirements for the degree of Master of Science in Metallurgy to the Graduate Div., College of Engineering, New York University.

For α nucleated from β, Newkirk assumed the following relationships and found them consistent with his experimental results:

$$(00.1)_\alpha \parallel (110)_\beta$$
$$[11.0]_\alpha \parallel [111]_\beta$$

Liu and Margolin,[2] in their investigation, found that the habit planes of martensitic α in β titanium consisted of planes of the families $\{334\}_\beta$ and $\{344\}_\beta$. Using Newkirk's orientation relationship, the $\{334\}_\beta$ habit plane is found to correspond to the $\{14\bar{5}0\}$ plane of α.

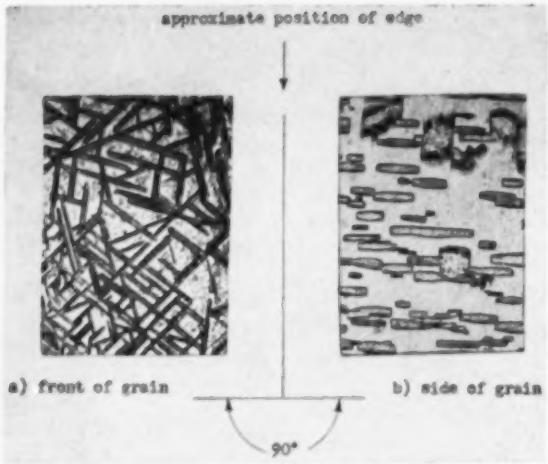

Fig. 1—Micrographs showing areas from two adjacent normal surfaces of an α grain. $\alpha+$ transformed β platelets. X75. Area reduced approximately 60 pct for reproduction.

The purpose of the present investigation was to determine the habit plane of β isothermally grown in α titanium.

Experimental Procedure

Binary alloys with alloying compositions of up to 1.25 pct N and up to 1.5 pct O were prepared using TiO_2 and TiN powders supplied by Watertown Arsenal Laboratory. The specimen preparation and melting procedures have been described.[3]

Large grains of β were obtained in the specimens by annealing at 1400°C in helium atmospheres. Suitable α grains were then obtained from the β grains by hot rolling 5 pct at 800°C, and subsequently annealing for 48 hr at temperatures slightly below the α transus.

The large-grained specimens were then annealed at temperatures in the $\alpha + \beta$ region, and subsequently water-quenched and examined.

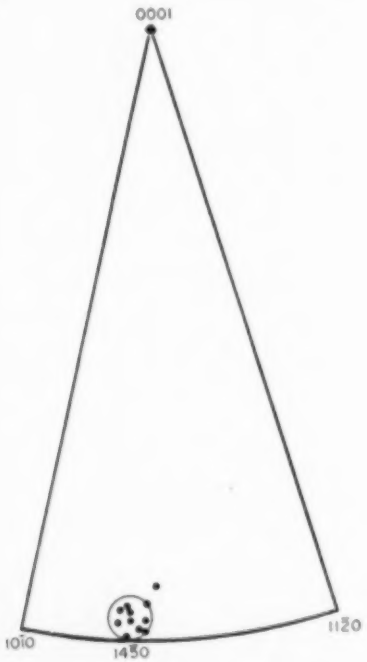

Fig. 2—Unit stereographic triangle for α titanium showing results of single-surface analysis (large circle) and points from two-surface analysis.

Analysis

The Laue back-reflection method was used to determine specimen orientations. The habit plane determinations were made by single-surface analysis and checked by two-surface analysis.[3]

The transformed β platelets were short, so that one trace did not appear on two surfaces. However, in one of the grains analyzed, a single trace direction in one surface was found to be responsible for six traces in the second surface and consequently two-surface analysis was possible.

Fig. 1a and b, micrographs of these surfaces, shows that the traces in the side surface (Fig. 1b) vary in thickness depending on the angles between the traces in the front surface (Fig. 1a) and the edge of the specimen. The habit plane determination made on this grain agreed with the results of single-surface analysis. These results were corroborated by a similar analysis of five traces in a second grain.

Results

Determination of the habit plane by single-surface analysis resulted in a group of points with a scatter of $\pm 2°$, at a position 2° from the $\{14\bar{5}0\}$ pole. The results of single-surface analysis lie within the region designated by the circle in Fig. 2. The two-surface determinations are indicated as small filled circles in Fig. 2, and it can be seen that all but one of the poles lie within the area of scatter of the single-surface points.

The habit plane of isothermal α in β has been determined in the Ti-Fe system to be $\{334\}_\beta$.[4] Since the $\{14\bar{5}0\}_\alpha$ habit of β can be converted to $\{334\}_\beta$ according to Newkirk's results,[1] it appears that whether α or martensite forms from β, or β forms from α, the same pair of planes of each lattice is involved, i.e., $\{334\}_\beta$ and $\{14\bar{5}0\}_\alpha$.

Acknowledgments

The author wishes to thank Y. C. Liu, H. Margolin, and the staff of the Metallurgy Laboratory at New York University for their assistance in this research. He also wishes to thank the U. S. Army Ordnance Corps, Watertown Arsenal, Watertown, Mass., for permission to publish this work, which was performed under Ordnance Corps Contract No. DA-30-069-ORD-935.

References

[1] J. B. Newkirk: Private communication. Also Minutes of Conference on "Crystallography of Titanium and its Alloys," New York University, June 27, 1952, under the auspices of the Ordnance Metallurgical Advisory Committee on Titanium.

[3] Y. C. Liu and H. Margolin: Martensite Habit Planes in Quenched Titanium-Manganese Alloys. *Trans.* AIME (1953) **197**, p. 667; JOURNAL OF METALS (May 1953).

[3] I. Cadoff and J. P. Nielsen: Titanium-Carbon Phase Diagram. *Trans.* AIME (1953) **197**, p. 248; JOURNAL OF METALS (February 1953).

[4] G. Hahn: The Habit Plane of Isothermal Alpha in Beta of Ti-Fe Alloys. Senior Thesis, New York University, June 1952.

Manganese as an Indicator of Blast Furnace Slag Oxidation and Desulphurizing Power

by Nicholas J. Grant, John W. Dowding, and Robert J. Murphy

A large number of blast furnace slag-metal tests were examined to determine if the manganese reduction could be used as a primary indicator of the degree of oxidation or reduction of the slag and of its desulphurizing power. Slag basicity and temperature were also evaluated. Two laboratory heats were made and sampled prior to reaching equilibrium to check blast furnace data.

IN a recent investigation of the factors affecting desulphurization in the blast furnace, is was evident that manganese reduction appeared to parallel the course of desulphurization. Grant, Kalling, and Chipman[1] pointed this out in a series of time studies utilizing closely controlled laboratory melts. Fig. 1 is a composite plot of sulphur removal and manganese reduction as a function of time under two slags of different basicity. Manganese reduction appears to approach equilibrium at approximately the same rate as does sulphur. It was also demonstrated that the addition of oxygen to the slag, as manganese oxide, caused a sharp reversal of sulphur from the slag to the metal.[1]

It has been shown that "Excess CaO" was a primary factor in measuring the degree of desulphurization under ideal reducing conditions,[1, 2] the following reaction being representative of the process:

$$CaO\,(slag) + \underline{S} + C\,(solid) = CaS\,(slag) + CO\,(gas)$$

It was also evident that a second reaction could drive the sulphur from the slag into the metal. A suggested reaction was[1]

$$CaS\,(slag) + \underline{O} = CaO\,(slag) + \underline{S}$$

Any change in the oxidizing power of the system would thus affect both the sulphur and the manganese without causing any change in the calculated basicity of the slag. "Excess CaO," "Excess Base," and other similar basicity values, under such oxidizing conditions, would therefore not be the best measure of desulphurizing power; instead, as was shown by Rocca, Grant, and Chipman[2] the oxygen content of the slag at low oxygen levels would be the controlling factor. Unfortunately, the extent to which FeO is reduced in the blast furnace makes it difficult to utilize slag FeO as an accurate indicator of the degree of oxidation. By comparison, manganese reduction in the blast furnace proceeds more slowly and is generally only about 40 to 70 pct complete. Thus manganese, which is present in significant amounts and is readily analyzed, offers an opportun-

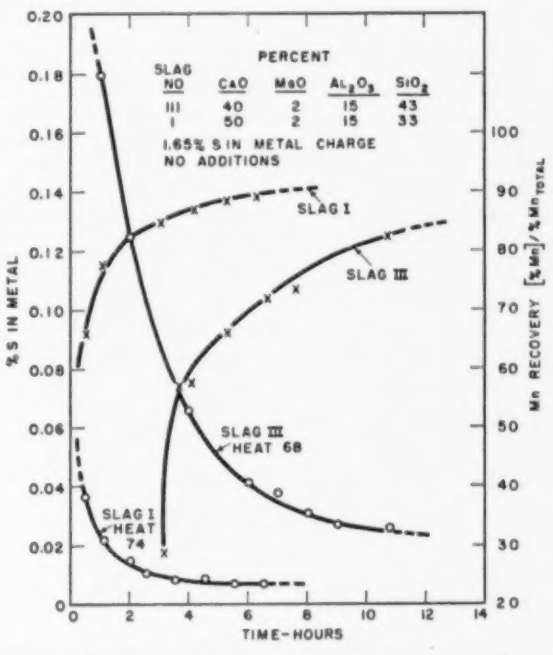

Fig. 1—Sulphur removal and manganese reduction as a function of time for two slags at 1525°C, from work of Grant, Kalling, and Chipman.[1]

N. J. GRANT, Member AIME, is Associate Professor of Metallurgy, Massachusetts Institute of Technology, Cambridge, Mass., and J. W. DOWDING and R. J. MURPHY, Junior Member AIME, formerly students of Metallurgy, MIT, are now associated with Latrobe Steel Co., Latrobe, Pa., and U. S. Steel Corp., Duquesne Works, Duquesne, Pa., respectively.

Discussion on this paper, TP 3643C, may be sent, 2 copies, to AIME by April 1, 1954. Manuscript, May 29, 1953. New York Meeting, February 1954.

This paper is based on a thesis by J. W. Dowding and R. J. Murphy submitted in partial fulfillment of the requirement for the Bachelor of Science degree to Massachusetts Institute of Technology.

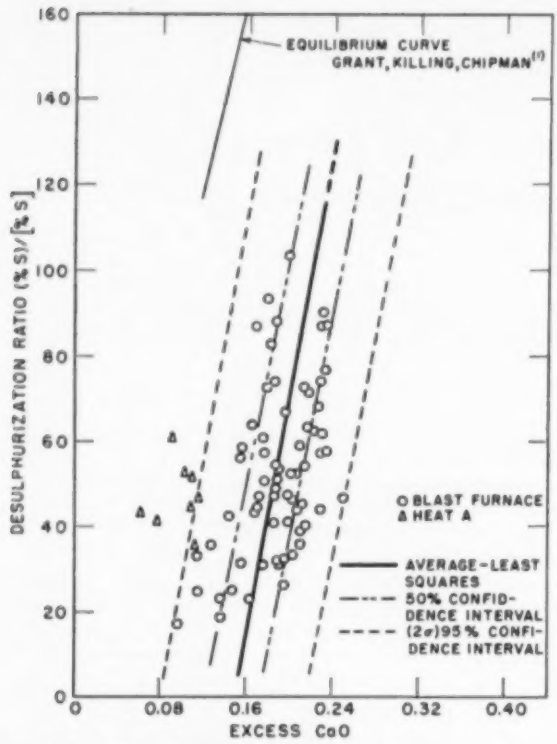

Fig. 2—Desulphurization ratio vs Excess CaO from blast furnace data, showing 50 and 95 pct (2σ) confidence intervals. Note position of experimental nonequilibrium points and equilibrium curve from Grant, Kalling, and Chipman.[1]

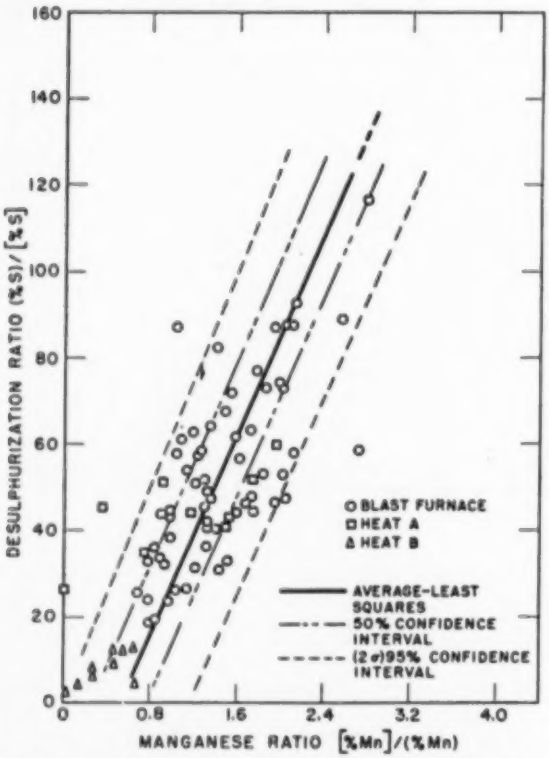

Fig. 3—Same blast furnace data as in Fig. 2 but plotting desulphurization ratio vs manganese ratio. Note position of experimental nonequilibrium points.

Table I. Desulphurizing Index of Lime and Manganese

Fig. No.	Variable	Slope of Line	Spread in Desulphurization Ratio At 50 Pct Confidence Interval	Spread in Desulphurization Ratio At 95 Pct Confidence Interval (2σ)
2	Excess CaO	1350	±32(S)/[S]	±100(S)/[S]
3	Mn reduction	59	±16(S)/[S]	± 37(S)/[S]

ity to use it as an indicator, not only of the degree of oxidation or reduction of the slag, but also of the desulphurizing power. The similar use of manganese as an indicator also was suggested recently by Oelsen and Maetz[4] and by Weilandt, Maetz, and Oelsen.[5]

Results from Blast Furnace Tests

A series of 66 acceptable tests were obtained from a blast furnace campaign (heats 5202 to 5308 furnished by Republic Steel Corp.) at a time when relatively good cast temperatures and slag-metal analyses were available. In general, three tests were taken of temperature and of the manganese, silicon, and sulphur contents of the metal. Where large variations in analysis for any of the three elements occurred, the cast was not used for this study. It is to be realized, however, that sampling cannot be perfect under operating conditions and accordingly some scatter of data was to be expected.

Fig. 2 shows the relationship between Excess CaO[2] and desulphurizing power, the latter defined in the usual manner by the ratio

$$\frac{(\%S)\ \text{slag}}{[\%S]\ \text{metal}}$$

It will be noted that whereas desulphurization improves with increasing basicity, the sulphur ratio is rather insensitive to Excess CaO between 0.16 and 0.24 Excess CaO. Without exception, the desulphurization ratios are far below those which are predicted from equilibrium studies as indicated by the upper solid curve in Fig. 2.[1] Whereas the blast furnace data show a desulphurization ratio of 30 to 100 (average of about 60) at an Excess CaO value of 0.20, the equilibrium data indicate that the ratio should be 200, or from 2 to 6 times as good.

Attempts to use Excess Base [1, 2, 6] and other basicity ratios gave even poorer relationships, as was expected, and the plots are omitted for the sake of brevity.

In Fig. 3 the same test data are shown, now plotted as desulphurizing ratio vs manganese ratio. The manganese ratio was arbitrarily chosen as "per cent manganese in the metal" over "per cent manganese in the slag." It is immediately evident that a more sensitive measure of desulphurization is attained by using manganese as the indicator.

As a comparison of the relative merits of the various plotting methods, the best curve was calculated

Table II. Initial Slag Compositions

Slag No.	Source	CaO	SiO_2	Al_2O_3	MgO
A	Present work	50	35	15	—
I	Grant, Kalling, and Chipman[1]	50	33	15	2
B	Present work	40	45	15	—
III	Grant, Kalling, and Chipman	40	43	15	2

by the method of least squares and is shown by the solid line in Figs. 2 and 3. Parallel lines were drawn to show the 50 and 95 pct (2σ limits) confidence intervals and Table I shows the spread in sulphur ratio between these two sets of curves.

Efforts to measure the effect of temperature on the distribution of points in both Figs. 2 and 3 met with complete lack of success, even though the range of temperatures noted for the casts was from about 2500° to 2750°F. It is to be recalled that equilibrium studies showed only a small beneficial result of increasing temperature on desulphurization.[1, 3, 6] These two sets of results lead to the speculation that data presented in the past on the improvements in desulphurization with increasing temperature might not be entirely due to any physical-chemical effects of higher temperatures on the sulphur distribution; instead, the higher temperatures have an indirect result on desulphurization in that the rate and degree of manganese and silicon reduction improve materially and the fluidity of the slag increases.

Laboratory Heats

To extend the results given above, the same equipment which was described previously by Grant, Kalling, and Chipman[1] was used to make two heats in which two slag compositions utilized by the former authors were selected for additional tests. One slag was considerably more acid and was selected because of its slower desulphurizing ability. The more basic slag was selected as being more typical of the blast furnace, and therefore permitting comparison with the data from blast-furnace casts shown in Figs. 2 and 3.

Table II lists the two heats A and B both made at 1525°C and compares them with slags No. 1 and III of Grant, Kalling, and Chipman. Table III lists the slag and metal analyses of the current heats A and B as a function of sampling time.

During the course of both of these heats, a number of additions of manganese oxide were made to the slag in quantities of about 3 pct (by weight) of MnO_2. Before equilibrium could be achieved, further additions were made, followed by sampling of the slag and metal. In the case of heat A, the reoxidation of the system maintained a sulphur content of the metal about comparable to that found in regular blast furnace operation, but considerably higher than the equilibrium value as indicated in Fig. 4 by reference to a slag with no additions; and it might be inferred that the degree of oxidation was also comparable to that existing in the blast furnace since the manganese recovery values ranged from about 40 to 67 pct (compared to 40 to 70 pct found in the blast furnace).

Heat B was similarly kept oxidized, with the sulphur level at a higher value than that normally

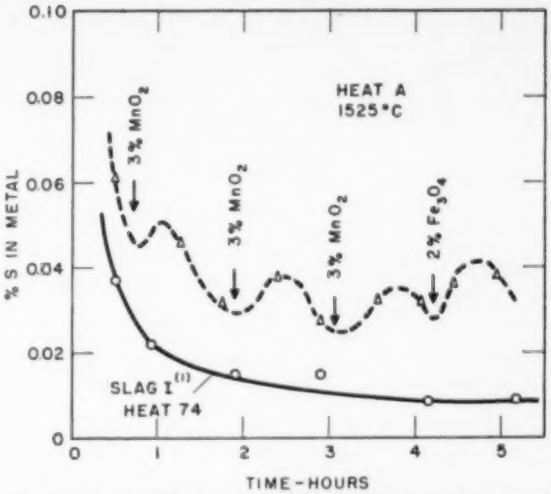

Fig. 4—Effect of additions of MnO_2 and Fe_3O_4 on sulphur removal for heat A, compared to desulphurization in a heat in the absence of oxygen additions.[1]

Table III. Composition of Slag and Metal Samples

Heat No.	Sample No.	Time, Hr	Metal, Wt Pct S	Metal, Wt Pct Mn	Metal, Wt Pct Other	Slag, Wt Pct S	Slag, Wt Pct CaO	Slag, Wt Pct SiO_2	Slag, Wt Pct Al_2O_3	Slag, Wt Pct MnO	Slag, Wt Pct FeO
A	1	0.50	0.061	0.000		1.640	49.26	34.66	15.47	0.00	0.020
		0.75			13.9 g MnO_2 added						
	2	1.25	0.045	0.581		1.585	48.56	34.12	15.29	1.03	0.014
	3	1.75	0.031	0.821		1.610	49.68	33.82	16.71	0.0	0.014
		1.92			13.0 g MnO_2 added						
	4	2.42	0.037	1.345		1.590	48.00	34.04	14.87	1.16	0.010
	5	2.92	0.027	1.466		1.640	47.94	34.04	15.95	0.95	0.015
		3.07			12.5 g MnO_2 added						
	6	3.57	0.032	1.848		1.485	48.80	32.08	16.15	6.44	0.081
	7	4.07	0.031	2.205		1.585	47.36	33.02	15.83	3.19	0.160
		4.22			6.4 g Fe_3O_4 added						
	8	4.47	0.036	2.180		1.610	48.52	32.94	16.18	2.40	0.035
	9	4.97	0.038	2.360		1.560	48.26	33.50	16.55	2.02	0.017
B	1	0.50	0.551	0.000		1.110	39.04	43.62	16.02	0.00	0.027
		0.80			14 g MnO_2 added						
	2	1.30	0.311	0.167		1.360	38.21	42.80	16.75	1.64	0.003
	3	1.80	0.212	0.276		1.435	39.32	42.98	16.01	1.30	0.043
		2.00			13.3 g MnO_2 added						
	4	2.50	0.178	0.688		1.435	38.58	41.86	15.94	3.96	0.012
	5	3.00	0.164	0.881		1.510	38.80	42.30	15.80	2.56	0.058
		3.13			12.3 g MnO_2 added						
	6	3.64	0.111	1.401		1.460	37.96	41.02	16.38	3.79	0.055
	7	4.14	0.107	1.548		1.460	38.00	41.88	15.64	3.79	0.075
		4.3			6.3 g Fe_3O_4						
	8	4.5	0.243	1.660		1.535	36.32	41.90	15.92	3.20	0.058
	9	5.05	0.115	1.500		1.560	38.32	41.74	16.42	3.25	0.054

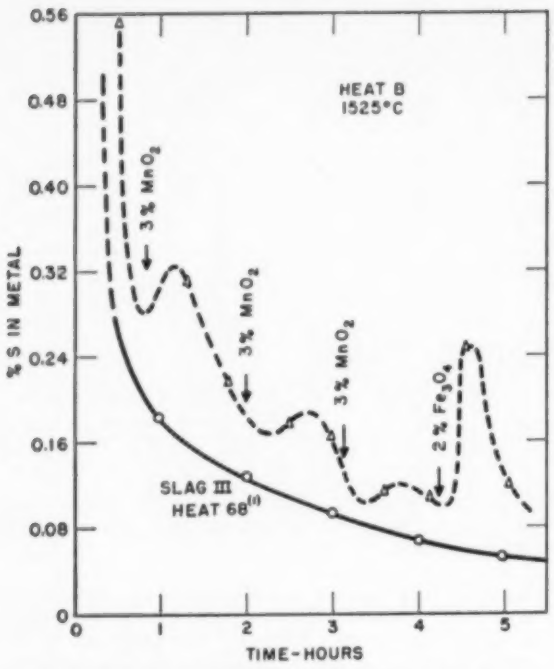

Fig. 5—Effect of additions of MnO_2 and Fe_3O_4 on sulphur removal for heat B, compared to desulphurization in a heat in the absence of oxygen additions.[1]

found in the blast furnace. The manganese recovery values were lower than in heat A, ranging from 20 to 40 pct.

At the end of each of these two heats, an addition of 2 pct (by weight) of Fe_3O_4 was added to the slag to see how it would affect desulphurization compared to additions of MnO_2. The addition of 3 pct by weight of MnO_2 results in an addition of about 1.1 pct by weight of oxygen, whereas an addition of 2 pct of Fe_3O_4 adds only about half as much oxygen or 0.55 pct. The effects of these two additives on desulphurization should be compared on the basis of their oxygen contributions and the stability of the oxides.

Fig. 4 shows the course of sulphur removal from the metal as a function of time for heat A, with the times of addition noted by arrows. While sufficient test samples were not taken to draw an exact curve in this figure, sulphur reversion is readily evident. For comparison the desulphurization curve for a similar slag from the work of Grant, Kalling, and Chipman (slag No. I, heat 74) is also shown. The sulphur reversion noted by the former authors is confirmed. Fig. 5 similarly compares the course of desulphurization for heat B, which is compared to slag III, heat 68, from the same reference.[1]

Discussion

The data presented clearly show that the blast furnace is not desulphurizing as efficiently as the slag basicity would permit. The probable reason for this is that the slag is not reduced sufficiently at any time between casts to permit higher desulphurizing power. In part this is due to the lack of time for silicon and manganese equilibrium to be approached more closely. Also, there is a continuous input of manganese oxide into the slag which provides a source of oxygen to decrease desulphurization.

The evidence of the large effect of oxygen is clearly seen in Figs. 2 and 3 where the nonequilibrium points from the experimental heats A and B are plotted along with the actual blast furnace data. These points are from tests in which manganese recoveries of 40 to 67 pct for heat A and 20 to 40 pct for heat B were recorded. These are comparable in the case of heat A with the manganese recoveries attainable in the iron blast furnace. Note that these nonequilibrium points match the grouping of Fig. 3 better than they do Fig. 2, confirming the assumptions that manganese is the better indicator of the overall blast furnace chemistry. By comparison the manganese recoveries measured for similar slags which were appreciably closer to equilibrium ranged from 80 to 94 pct[1] depending on basicity of the slag and distance from equilibrium.

The role of temperature in the blast furnace with respect to desulphurization must be an indirect one. The small effect of temperature on the equilibrium desulphurization ratio and its lack of effect in the blast furnace data which were utilized here, confirm this. The beneficial temperature effect of desulphurization must be interpreted in terms of viscosity effects on the slag and on the greater rate and extent of reduction of manganese (decreased oxygen potential).

Conclusions

1—The reversion of sulphur from slag to metal due to additions of oxygen to the system (derived from MnO_2 or Fe_3O_4) has been confirmed.

2—Manganese reduction is a better indicator of the desulphurizing power of the blast furnace than is any common measure of slag basicity.

3—The blast furnace does not desulphurize to its maximum ability because of the oxidation potential in the system. This oxidation potential is probably due primarily to the presence of considerable amounts of MnO in the slag.

4—Temperature benefits in desulphurization are probably due to indirect effects on the rest of the system.

Acknowledgments

The authors wish to express their appreciation to Charles W. Sherman and James Fulton for considerable assistance throughout this research and to John Chipman for his guidance. The work was supported by the American Iron and Steel Institute.

References

[1] N. J. Grant, U. Kalling, and J. Chipman: The Effects of Manganese and Its Oxide on Blast Furnace Desulphurization. *Trans.* AIME (1951) **191**, p. 666; JOURNAL OF METALS (August 1951).

[2] C. W. Sherman and N. J. Grant: Evaluation of pH Measurements with Regard to the Basicity of Metallurgical Slags. *Trans.* AIME (1949) **185**, p. 898; JOURNAL OF METALS (November 1949).

[3] R. Rocca, N. J. Grant, and J. Chipman: Distribution of Sulphur Between Molten Iron and Slags at Low Iron Oxide Concentrations. *Trans.* AIME (1951) **191**, p. 319; JOURNAL OF METALS (April 1951).

[4] W. Oelsen and H. Maetz: Contribution to Blast Furnace Metallurgy. *Stahl und Eisen* (1949) **69**, p. 147.

[5] B. Weilandt, H. Maetz, and W. Oelsen: Effects of Basic Oxides Upon Desulphurization in the Blast Furnace. *Arch. Eisenhuttenwesen* (1952) **23**, p. 163.

[6] G. Hatch and J. Chipman: Sulphur Equilibria Between Iron Blast Furnace Slags and Metal. *Trans.* AIME (1949) **185**, p. 274; JOURNAL OF METALS (April 1949).

Diffusion of Calcium Ion in Liquid Slag

by Helen Towers, Michel Paris, and John Chipman

A simple radioactive tracer technique is used to measure the diffusion coefficient of calcium ion in molten slags. In a slag of 40 pct CaO–40 pct SiO_2–20 pct Al_2O_3, $D_{Ca^{++}}$ at 1450°C is 1.3×10^{-6} cm^2 sec^{-1}.

THE application of the principles of thermodynamics to steel and iron making problems has proved so fruitful that the kinetic approach has tended to be neglected. It seems probable that in some reactions the rate-determining step is the diffusivity of the reactants or of the products. But knowledge of the diffusion coefficients of the constituents of liquid slag and metal is singularly lacking. The present work was undertaken as a first step toward supplying such data for slags. Furthermore, any additional information on the physical properties of liquid slags might be expected to help in elucidating their structure. It is essentially a preliminary investigation, the course of which was determined more by the necessity of establishing a method than by the immediate intrinsic interest of the results.

For example, the selection of calcium ion to be studied was dictated by the suitability of the isotope Ca^{45} in that it is a simple β emitter with a long half-life. Of the other ions commonly encountered in slags, the isotopes of iron and manganese have relatively complex radiations as well as the normal disadvantage of requiring control of the oxygen potential of the atmosphere; Mg^{27} and Al^{28} have half-lives measured only in minutes; Si^{31} has a simple decay process but its half-life of 2.8 hr is too short for preliminary studies; the only useful oxygen isotope is the stable O^{18}; and there remain only sulphur and phosphorus both of which have suitable isotopes but were rejected as being of less fundamental interest than calcium. Similarly a lime-alumina-silica slag was used in preference to calcium silicate primarily because of its low melting point and its capacity to form a glass on fairly rapid cooling.

H. TOWERS is Lecturer in Metallurgy, Royal Technical College, Glasgow, Scotland, M. PARIS, formerly Graduate Student at Massachusetts Institute of Technology, is now in Paris, France, and J. CHIPMAN, Member AIME, is Professor, Dept. of Metallurgy, Massachusetts Institute of Technology, Cambridge, Mass.

Discussion on this paper, TP 3625C, may be sent, 2 copies, to AIME by Jan. 1, 1954. Manuscript, April 16, 1953. Los Angeles Meeting, February 1953.

This paper is based on a thesis by M. Paris submitted in partial fulfillment of requirements for the degree of Master of Science to Massachusetts Institute of Technology.

Literature Review

Very few studies of diffusion in liquid silicate systems have been reported. In order to determine the origin of diopside inclusions in felspathic rocks, Bowen[1] investigated the diffusion between diopside and various mixtures of albite and anorthite. Platinum crucibles were used with diopside, the heavier of the two liquids, forming the lower half of the cell and diffusion taking place against gravity. Change in concentration along the diffusion path was found by measuring the refractive index of the quenched glass.

Nearly thirty years later McCallum and Barrett[2] used essentially the same method to determine the diffusion coefficient of lime in lime-alumina-silica slags. In this case the interest was to find the rate-determining step in the process of slag attack on refractory materials.

In an investigation of the kinetics of the sulphur reaction, Derge, Philbrook, and Goldman[3] determined the diffusion coefficient of sulphur in a typical blast furnace slag by the simple procedure of melting a slag containing 2 pct S over an identical slag sulphur-free. They make no claim to a high degree of accuracy but suggest that D_s is of the order of 10^{-6} cm^2 sec^{-1}.

Other high temperature liquid diffusion studies have been concerned with metals. Holbrook, Furnas, and Joseph[4] determined the diffusion coefficients of silicon, phosphorus, sulphur, manganese, and carbon in liquid iron by immersing a small carbon crucible containing pure iron-carbon alloy in a large vessel containing iron with a high concentration of the particular element. Their results were confirmed by Paschke and Hauttmann[5] using a similar method.

Diffusion coefficients in silicates in the glassy state have been studied by Johnson, Bristow, and Blau.[6] Both Na^{24} and Ca^{45} were used as tracers but only the

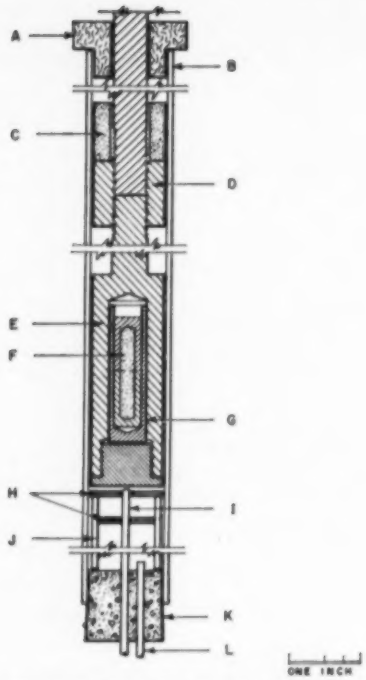

Fig. 1—Section along zirco tube containing the diffusion cell. This was heated by a globar furnace not shown in figure. A—Refractory stopper. B—Zirco tube. C—Carbocell insulating block. D—Graphite block. E—Graphite container. F—Diffusion cell. G—Graphite crucible. H—Radiation shields. I—Thermocouple sheath. J—Supporting tube. K—Rubber stopper. L—Argon inlet.

sodium results were reported. From these the authors were able to reach conclusions concerning the structure of the glass.

Experimental Method

The principle was similar to that used by Bowen.[1] Two slags of essentially the composition, 40 pct CaO-40 pct SiO_2-20 pct Al_2O_3, were brought into contact in a graphite diffusion vessel. One of the slags contained the radioactive tracer Ca^{45} but was otherwise identical in composition with the other. The assembly was held at a temperature above the melting point for a predetermined time, quenched, and sectioned longitudinally. The distribution of the tracer was determined by its action on a photographic film and from this the diffusion coefficient was calculated.

Preparation of Slags: A master slag was melted in graphite, ground to a fine powder, and analyzed. The composition was 40.32 pct CaO, 19.15 pct Al_2O_3, 40.06 pct SiO_2. A graphite crucible 3/16 in. ID and about 1 in. long was charged with this slag, held at 1400°C for 15 min, quenched, and radiographed to insure absence of bubbles. To prepare the active slag, 0.8×10^{-4} g Ca^{45} was added in the form of $Ca^{45}Cl_2$ solution to 0.6 g of the fine powder. This was equivalent to 2.7 microcuries. After evaporation to dryness the powder was thoroughly mixed and then heated in a second graphite crucible to 1400°C for 3 hr to insure homogeneity.

Diffusion Apparatus: The two crucibles were cut transversely to ½ in. lengths, then placed inside a larger graphite block as shown in Fig. 1, the two cut faces being in contact. The assembly was then inserted into the furnace in which an argon atmosphere was maintained. The temperature was measured by two Pt-10 pct Rh-Pt thermocouples, one directly below the graphite block and the other outside the zirco tube, level with the cell. An exploring standard couple was used to find the relationship between the temperatures recorded by the two permanent couples and that obtaining in the diffusion cell. The temperature variation along the length of the diffusion specimen is shown in Fig. 2. When the furnace had reached thermal equilibrium, the graphite container was lowered into position. This method did not allow the diffusion time to be known exactly but the accuracy of estimation was about ±2 pct. At the end of the experiment the container was withdrawn rapidly so that the slag solidified as a glass.

Measurement of Ca^{45} Concentration: The slag cylinder was approximately 1 in. long contained in carbon. This was ground and polished longitudinally under kerosene to give an exact semi-cylinder which was placed in contact with an Ilford G X-ray film for 1¾ hr. The film was calibrated by exposures of varying times to one of the active slags; the intensity of darkening was found to be a linear function of the logarithm of exposure time, or for a fixed time, of the logarithm of the concentration of Ca^{45}. A typical microdensitometer record of a film made from a diffusion specimen is shown in Fig. 3.

Calculation of the Diffusion Coefficient D: The particular solution of the diffusion equation for the given conditions is

$$\frac{2C}{C_o} - 1 = -\left(erf \frac{x}{2\sqrt{Dt}} \right)$$

where C_o is the initial concentration of Ca^{45} in the active slag, and C its concentration at distance x from the interface after time t. A concentration-penetration curve, (C/x) was obtained from the microdensitometer record and the interface $(x = 0)$ fixed at the point where $C/C_o = 0.5$. Values of C/C_o were then plotted against x on arithmetic probability paper and D calculated from the slope of the straight line thus obtained.

Results

Diffusion runs were made at three temperatures, 1350°, 1400°, and 1450°C; the corresponding diffusion times were of the order of 8, 6, and 4 hr respectively. Attempted measurements at 1500°C failed due to reaction involving gas evolution.

Two main difficulties were encountered during the work. The first, not unexpected, was due to convection. Fortunately, it was at least very easy to detect from the photograph when convection had

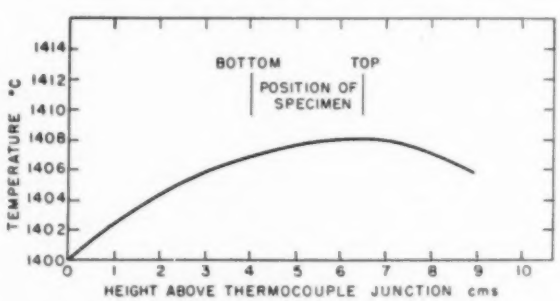

Fig. 2—Temperature variation within diffusion cell.

taken place and the results from such runs were discarded. Approximately 50 pct had to be jettisoned in this way.

The second trouble which arose was unforeseen. In almost every case the interface between the active and inactive slags was not plane but strongly curved. The effect was greater the higher the temperature. The cause of this phenomenon was not appreciated early enough for it to be avoided and indeed is as yet imperfectly understood. Apparently the interfacial tension between the active slag and graphite is less than that between the inactive slag and graphite. The curvature is simply the result of a higher energy surface being replaced by a lower. The active slag creeps along the wall and this surface layer drags with it liquid from the interior.

There were two differences in the method of preparation of the two slags which could contribute to this effect. The first lay in the length of time for which the slags were held molten. It is now known that the contact angle and therefore the interfacial tension between this slag and graphite decreases with time above a certain critical temperature. This difference in preparation was eliminated for some of the later runs but neither short nor long melting times had any effect on the shape of the interface.

The second difference was caused by the addition of $Ca^{45}Cl_2$ solution. Chloride ion is known to be surface active in glasses but the concentration in this slag was only 3.45×10^{-6} g Cl^-/g. Two runs in which the inactive slag contained the same concentration of ordinary $CaCl_2$ were unfortunately among the convection discards.

While the interfacial tension effect is obviously undesirable it is considered that the results are not thereby invalidated. If a narrow cylindrical element of liquid along the central axis were completely free to move in the direction of its length, diffusion along this cylinder should take place with but little effect from the translatory movement of the whole. After long diffusion times however there is the probability of additional Ca^{45} ions penetrating this central element from that part of the active slag which has crept along the wall.

The results are given in Fig. 4 where log D is plotted against $1/T$. Average values of D at 1350°, 1400°, and 1450°C, respectively, are 3.3×10^{-7}, 6.8×10^{-7} and 1.3×10^{-6} cm² sec⁻¹. Although these results are somewhat lacking in precision they serve to illustrate the applicability of a very simple tracer technic to diffusion studies in slags.

The slope of the line corresponds to 73 kcal for the energy of activation. This can be regarded only as an approximation which is best rounded off to 70 ± 20 kcal.

Comparison with Other Work

The diffusion coefficient of sodium in glasses at a temperature of about 1000°C was found by Johnson, Bristow, and Blau[6] to be between 10^{-6} and 10^{-7} cm² per sec. Their results for calcium are not reported. The slags used by McCallum and Barrett[5] were higher in SiO_2 and lower in Al_2O_3 than that used here. For a slag containing 37.5 pct CaO, 10 pct Al_2O_3, 52.5 pct SiO_2, D_{Ca} was found to be 9.6×10^{-6} cm² sec⁻¹ at 1450°C and 12.15×10^{-6} cm² per sec at 1500°C giving an activation energy of 29 kcal.

It is perhaps of greater interest to compare the present result for the diffusion coefficient with that obtained for electrical conductivity by Martin and Derge.[7]

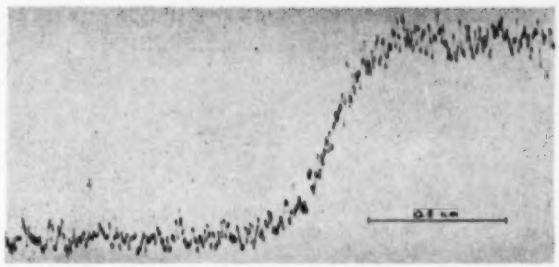

Fig. 3—Microdensitometer record along center of film exposed to slag after diffusion.

The authors are indebted to Professor C. Wagner for the following derivation of the relation between conductance and diffusion constant of an ion.

Let κ be the specific ionic conductance, C the concentration in mols cm⁻³, and z the valence of the ion. Then

$$\kappa = 96{,}500\ zCu$$

where u is the mobility in cm sec⁻¹ per volt cm⁻¹. The Nernst-Einstein relation is

$$D = BkT$$

where D is the diffusion coefficient, B the absolute mobility in cm sec⁻¹ dyne⁻¹, k is the Boltzmann constant, and T the absolute temperature. The mobility u is given by the following expression in which e is the electronic charge:

$$u = \frac{ze}{300} \quad B = \frac{ze}{300}\,\frac{D}{kT}$$

Substitution of this in the above equation for κ yields the desired relation:

$$\kappa = \frac{96{,}500}{300}\,\frac{z^2e}{kT}\,DC$$

Appropriate values of the constants are $e = 4.80 \times 10^{-10}$ *esu* and $k = 1.380 \times 10^{-16}$ ergs per degree molecule, hence

$$\kappa = 1.12 \times 10^9\ z^2\ DC/T$$

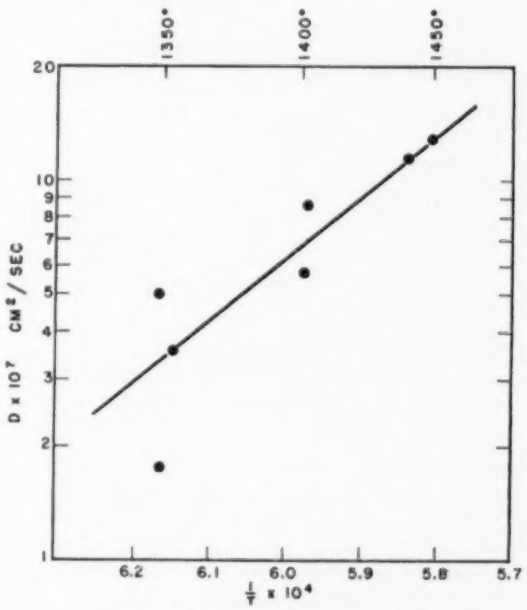

Fig. 4—Relationship between log D and $1/T$.

Taking the density of the slag as 2.8 g cm^{-3} the concentration of Ca^{++} is 0.40x2.8/56 = 0.020 mols cm^{-3}.

The diffusion coefficient found at 1450°C was 1.3x 10^{-4} cm^2 sec^{-1}. The calculated specific conductance due to Ca^{++} is therefore

$$\kappa = 0.067 \text{ ohm}^{-1} \text{ cm}^{-1}$$

For their very similar slag No. 13 at 1450° Martin and Derge found a specific conductance of 0.098 ohm^{-1} cm^{-1}.

Our results are not sufficiently accurate to warrant a conclusion that Ca^{++} is responsible for 70 pct of the conductivity. In the light of the evidence presented by Bockris and coworkers[8] that the conductance of silicate slags is wholly cationic, it seems preferable to regard the agreement between calculated and observed conductance as evidence for the validity of the method used in these diffusion experiments.

Summary

The possibilities of using radioactive isotopes to measure diffusion coefficients of the components in liquid slags have been explored and the basis of a technique established.

The diffusion of calcium ion in a slag containing 40 pct CaO, 20 pct Al_2O_3, and 40 pct SiO_2 has been measured over a temperature range of 1350° to 1450°C. The values of D are approximately $3.3x10^{-7}$ and $1.3x10^{-6}$ cm^2 sec^{-1} at these temperatures and the energy of activation is approximately 70 ± 20 kcal. The value of D is of the order of magnitude of that calculated from the electrical conductivity of similar slags.

Acknowledgments

The authors wish to record their indebtedness, for fellowships, to the International Federation of University Women and the Department of State (Smith-Mundt Fellowships); also to the French Government.

References

[1] N. L. Bowen: *Journal of Geology* (1921) **29**, p. 295.
[2] N. McCallum and L. R. Barrett: *Trans.* Brit. Ceram. Soc. (1952) **51**, p. 523.
[3] G. Derge, W. O. Philbrook, and K. M. Goldman: *Trans.* AIME (1950) **188**, p. 1111; JOURNAL OF METALS (September 1950).
[4] W. E. Holbrook, C. C. Furnas, and T. L. Joseph: *Industrial and Engineering Chemistry* (1932) **24**, p. 993.
[5] M. Paschke and A. Hautmann: *Archiv. Eisenhüttenwesen* (1935) **9**, p. 305.
[6] J. R. Johnson, R. H. Bristow, and H. H. Blau: *Journal* Amer. Ceram. Soc. (1951) **34** (6) p. 165.
[7] A. E. Martin and G. Derge: *Trans.* AIME (1943) **154**, p. 104.
[8] J. O'M Bockris, J. A. Kitchener, S. Ignatowicz, and J. W. Tomlinson: *Trans.* Faraday Soc. (1952) **48**, p. 75; Bockris, Kitchener and A. E. Davies, *ibid*, p. 536.

Technical Note

The Silver-Cadmium Beta and Zeta Phases

by L. Muldawer, M. Amsterdam, and F. Rothwarf

SILVER-cadmium near the composition AgCd shows three equilibrium phases. As with β brass, the high temperature phase is disordered body-centered cubic (β) and the low temperature phase has the ordered CsCl structure (β'). However, there is an intermediate temperature phase which is hexagonal close-packed (ζ).

In a recent paper, Speich and Mack[1] report on a study of the Ag-Cd eutectoid near the AgCd composition. Unfortunately, the phase diagram upon which they base some of their conclusions is incorrect. That diagram is taken from the Metals Handbook[2] and the error is that the β' and ζ phases have been interchanged. The Handbook gives the low temperature phase as hexagonal (designated ζ) and the intermediate temperature phase as cubic ordered (designated β'). The error may be typographical or it may be one of confusion resulting from the use of ζ, β_1, and β' for the intermediate phase in various papers.

A careful search of the literature reveals that a number of authors have indicated the correct relative positions of the β, ζ, and β' phases. The comprehensive work of Fraenkel and Wolf[3] clearly stated that the high and the low temperature phases are either identical or are very similar. Ölander,[4] on the basis of electrochemical measurements, showed that the β phase is disordered and the β' phase (designated β'' in his paper and in refs. 3 and 5) is ordered. Further work by Durrant[5] using thermal and metallographic analyses provided a more precise phase diagram. A summary of these works was given by Hansen[6] and shows the correct relative positions of the phases. Owen, Rogers, and Guthrie[7] located correctly the upper two phases by X-ray diffraction. Their failure to find the low tem-

L. MULDAWER, Junior Member AIME, is Assistant Professor of Physics, and M. AMSTERDAM and F. ROTHWARF are Graduate Students, Temple University, Philadelphia.
TN 189E. Manuscript, Aug. 12, 1953.

perature β' phase is incomprehensible. Köster[8] made measurements of the elastic modulus of AgCd as a function of temperature and again showed the true relative positions of the phases. Differences between the various workers are reported in the transformation temperatures. This is presumably because different techniques and different compositions were used. The centers of the existence regions of the three phases are found at quite different compositions.

We have investigated this region of the Ag-Cd phase diagram using X-ray diffraction on quenched samples and on samples at temperature and by measurement of electrical resistance as a function of temperature. The specimen used for X-ray diffraction contained 51.7 pct Ag by weight, while that used for resistance measurements contained 49.9 pct Ag. The relative positions of the three phases were confirmed. The transformation temperatures obtained by these three methods differed from one another. It should be noted that the β and β' phases cannot be distinguished by means of X-ray diffraction because of the almost identical scattering factors of the silver and cadmium atoms. However, in this note the low temperature phase will be indicated by β'.

High temperature diffraction patterns showed the following main phases: β at 500° and 488°C; ζ at 361°, 229°, and 204°C; and β' at 192°C. No attempt was made to determine the exact transformation temperatures since the purpose was to determine equilibrium phases. However, a lower transformation temperature around 200°C is indicated. This is subject to the error inherent in the temperature calibration of the high temperature camera.

Studies with quenched filings gave similar results except that the lower transformation temperature is indicated as being between 250° and 280°C. Durrant[5] stated that this transformation occurred between 230° and 240°C. The difficulties of quenching AgCd alloys have been observed by several workers[5, 6, 7] and the rapidity of the ζ to β' transformation may have caused the 251°C specimen to transform before quenching could be effective. The experimental technique may have played a part in this. Filings were sealed in evacuated Vycor containers, annealed at temperature for at least two days, and then quenched in ice water without, however, breaking the container. Thus, there must have been some time between the removal from the furnace and the cooling action of the ice water on the filings. A summary of these results is given in Table I. Quenching from temperatures above the upper

Table I. Phases Present in Quenched Alloys*

Annealing Temperature, °C	Strong	Medium	Weak
202	β'		α
251	β'		α
280	ζ	α	β'
303	ζ	α	β'
354	ζ	α	β'
401	ζ	α	β'
428	ζ	α	β'
446	ζ	α,β	
476	ζ,β		α
501	ζ,β		α
552	β,ζ		α

* Relative amounts indicated by the intensity of the diffraction lines.

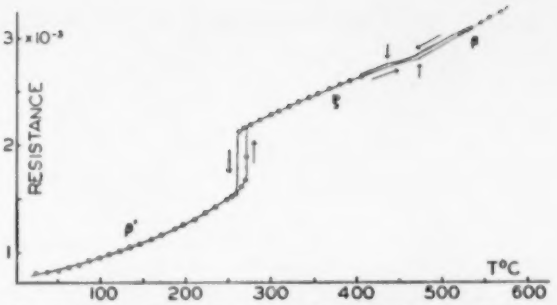

Fig. 1—AgCd resistance in ohms as a function of temperature. The ζ to β transformation points are indicated by vertical arrows. Experimental points in the neighborhood of this transformation were too close to permit inclusion in the figure.

transformation temperature invariably showed ζ as one of the predominant phases. This was due to the nature of the quench. The presence of β' phase in the intermediate region is explained similarly. The upper transformation temperature is seen to be around 450°C; this result is in accord with previous research. The presence of a good deal of α in the intermediate region is in accord with Durrant's phase diagram.

Electrical resistance measurements were made on a Ag-Cd rod about ⅛x4 in. A Kelvin bridge was used for the measurement of resistance and a thermocouple attached to the center of the rod gave the temperature. The results are shown in Fig. 1. Specific resistivity at room temperature is about 10 microhm-cm. Fraenkel and Wolf[3] measured electrical resistance but it is clear from the extremely wide hysteresis loops that their rate of change of temperature was much too fast. We investigated the hysteresis loop around 265°C very carefully; most of the points indicated were taken after the specimen had been at temperature for at least a day. The upper transformation temperature, centered around 455°C, was not obtained as carefully. The 10°C hysteresis loop observed for the lower transformation seems to be a real phenomenon and indicates a displacive transformation. The curvature in the β' region indicates the beginning of disordering. Further studies on these phenomena are being carried out.

We should like to acknowledge financial aid from the Office of Ordnance Research and a grant-in-aid from Temple University.

References

[1] G. R. Speich and D. J. Mack: Silver-Cadmium Eutectoid. *Trans.* AIME (1953) **197**, p. 549; JOURNAL OF METALS (April 1953).

[2] *Metals Handbook* (1948) Cleveland. ASM.

[3] W. Fraenkel and A. Wolf: Die Umwandlungen im festen Zustande bei Silber-Cadmiumlegierungen. *Ztsch. anorg. allgem. Chem.* (1930) **189**, p. 145.

[4] A. Ölander: Eine elektrochemische Untersuchung von Cadmium-Silber-Legierungen. *Ztsch. physikalische Chem.* (1933) **163**, p. 107.

[5] P. J. Durrant: The ϵ, γ, and β Phases of the System Cadmium-Silver. *Journal* Inst. Metals (1935) **56**, p. 155.

[6] M. Hansen: *Aufbau der Zweistofflegierungen* (1936) Berlin. J. Springer.

[7] E. A. Owen, J. Rogers and J. C. Guthrie: X-ray Study of Ag-Cd Alloys. *Journal* Inst. Metals (1939) **65**, p. 457.

[8] W. Köster: Elastizitatsmodul und Dämpfung der intermediären Phasen in den Systemen Kupfer-, Silber-, Gold-Zink und Silber-Kadmium. *Ztsch. Metallkunde* (1940) **32**, p. 151.

Neptunium-Aluminum Intermetallic Compounds

by O. J. C. Runnalls

The intermetallic compounds $NpAl_2$, $NpAl_3$, and $NpAl_4$ have been prepared, and examined by X-ray diffraction methods. The compounds are isostructural with the corresponding U-Al compounds. $NpAl_2$ is face-centered cubic with $a = 7.785$Å and has the $MgCu_2$ structure. $NpAl_3$ is simple cubic with $a = 4.262$Å and has the $AuCu_3$ structure. $NpAl_4$ is body-centered orthorhombic with $a = 4.42$Å, $b = 6.26$Å, and $c = 13.71$Å. The published description for the atomic positions in UAl_4 applies also to $NpAl_4$.

THE U-Al system has been examined by Gordon and Kaufmann.[1] They identified the following intermetallic compounds: UAl_2, UAl_3, and a third, tentatively identified as UAl_4. A structure analysis of the latter compound by Borie[2] proved that the formula UAl_4 was more consistent with the X-ray data. The crystal structures of UAl_2 and UAl_3 have been reported by Rundle and Wilson.[3] UAl_2 was found to be isostructural with $MgCu_2$. The atomic positions in the simple cubic UAl_3 cell were found similar to those in the $AuCu_3$ structure. Three analogous compounds exist in the binary system Np-Al. X-ray data for the compounds $NpAl_2$, $NpAl_3$, and $NpAl_4$ are reported below.

The neptunium used in the investigation was supplied through the courtesy of the Argonne National Laboratory as neptunium (V) nitrate. It was stated to have a radioactive content of 99.25 pct Np^{237}. The impurity limits had been established by a spectrographic analysis given in Table I. Any titanium, boron, or bismuth impurity should be effectively removed during the fluorination of NpO_2 to NpF_4, and sodium, lithium, magnesium or strontium during the alloying procedure.

The oxalate ignition technique, described by Westrum[4] for the preparation of finely-divided reactive PuO_2, was used.The neptunium (V) nitrate solution, containing 100 mg Np, was evaporated to dryness on oxalic acid crystals. The resulting oxalate was calcined to NpO_2 by heating in platinum at 650°C for 2 hr. An equimolar mixture of anhydrous hydrogen fluoride and purified hydrogen was passed over the NpO_2 for 2 hr at 500°C. According to Fried and Davidson[5] the above fluorination conditions should produce the purple-black fluoride, NpF_5. However, the light-green product showed only NpF_4 lines on an X-ray diffraction pattern and contained only an estimated 5 pct of finely dispersed black NpF_5 particles on microscopic examination.

$NpAl_3$: An intimate mixture of 50 mg of neptunium fluoride and aluminum powder (99.99 pct pure, −28 to +60 mesh) was heated to 900°C in a BeO crucible in vacuum by a tungsten coil for 2 hr, to allow the following reaction to proceed:

$$NpF_4 + 7Al \rightarrow NpAl_3 + 4AlF. \qquad [1]$$

The formation and sublimation of aluminum monofluoride in this system was verified from an X-ray diffraction analysis of the sublimate. The diffraction pattern was similar to one obtained in the aluminum reduction of UF_4 to UF_3,[6] showing both Al and AlF_3 lines.

Table I. Spectrographic Analysis

Element	Impurity, Pct	Element	Impurity, Pct
Fe	<0.1	Na	<2.0
Al	<0.2	Li	<0.0004
Ti	<1.0	Mg	<0.07
B	<0.3	Sr	<0.002
Bi	<0.5		

The resulting alloy was sintered at 1100°C for 1 hr. A powdered specimen of the crystalline product was sealed in a thin-walled quartz capillary for X-ray examination. The photograph was taken on a 14.32 cm General Electric powder diffraction camera, using filtered copper radiation. The films were calibrated in terms of a NaCl standard pattern. The wavelengths used in the calculations were 1.5418Å for Cu Kα and 1.5405Å for Cu Kα_1.

The powder diffraction pattern showed that $NpAl_3$ is simple cubic with $a = 4.262 \pm 0.005$Å, and is isostructural with UAl_3 where $a = 4.27$Å[1] or $a =$

Table II. Comparison of the $NpAl_3$ and UAl_3 X-Ray Powder Diffraction Patterns

		Observed Intensities*	
hkl	$\sin^2\theta$-$NpAl_3$	$NpAl_3$	UAl_3[1]
100	0.0329	s	s
110	0.0657	s	s
111	0.0982	s	s
200	0.1310	s−	s
210	0.1638	s	s
211	0.1965	s−	s
220	0.2618	m	m-s
221,300	0.2944	m+	m-s
310	0.3267	m−	m
311	0.3596	s	s
222	0.3925	w+	w-m
320	0.4248	m−	m
321	0.4574	m+	m-s
400	0.5231	w	w
410,322	0.5549†	m+	m-s
411,330	0.5871†	m	m
331	0.6200†	m+	m
420	0.6536†	m	m
421	0.6861†	m+	m
332	0.7187†	w+	w-m
422	0.7839†	m+	m-s
500,430	0.8170†	w+	w-m
501,431	0.8495†	s−	m-s
511,333	0.8818†	m+	w-m
520,432	0.9474†	s−	Not reported
521	0.9801†	m+	Not reported

* w, weak; m, medium; and s, strong.
† Obtained with Cu $K_{\alpha 1}$ radiation.

O. J. C. RUNNALLS is associated with the Chemistry Branch, Atomic Energy of Canada Limited, Chalk River, Ont., Canada.

Discussion on this paper, TP 3654E, may be sent, 2 copies, to AIME by April 1, 1954. Manuscript, July 3, 1953. New York Meeting, February 1954.

Table III. Unit Cell Dimensions for $NpAl_4$ and UAl_4

	$NpAl_4$	UAl_4[2]
a	4.42±0.01Å	4.41±0.02Å
b	6.26±0.01Å	6.27±0.02Å
c	13.71±0.03Å	13.71±0.03Å

4.287Å[3] (see Table II). The calculated density is 6.82 gram cm^{-3}, assuming one $NpAl_3$ formula weight per unit cell. The atomic positions in the structure are:

1 Np at 0,0,0.
3 Al at 0,½,½; ½,0,½; ½,½,0.

The unit cell is illustrated in Fig. 1.

$NpAl_4$: A 50 mg sample of $NpAl_3$ was diluted with aluminum to form a mixture containing 30 wt pct Np. The mixture was heated to 1100°C in the vacuum furnace, and the resulting alloy was cooled at 100°C per hr to 600°C, then cooled to room temperature. The small ingot was reacted with 3N NaOH to dissolve the free aluminum present. Several single crystals were obtained from the crystalline residue, Fig. 2. An X-ray diffraction pattern on a powdered crystal showed a close similarity to the UAl_4 pattern, suggesting that the compound was $NpAl_4$.

Small single crystals, mounted in thin-walled quartz capillaries, were used as X-ray specimens. A series of three rotation photographs about each crystallographic axis was made using filtered copper radiation in a 5 cm radius General Electric rotation camera. An orthorhombic cell with dimensions similar to UAl_4 was revealed, Table III.

The calculated density of $NpAl_4$ is 6.04 gram cm^{-3}, assuming four formula weights per unit cell. The spectra found missing by Borie[2] in the UAl_4 analysis also were missing in the $NpAl_4$ pattern, i.e., the reflections present were:

(a) hkl — only for $h + k + l = 2n$
(b) $hk0$ — only for $h = 2n$ and $k = 2n$
(c) $h0l$ — only for $h + l = 2n$
(d) $0kl$ — only for $k + l = 2n$.

These data indicate that the cell is body-centered with an $00l$ glide plane and may be described by either the space group *Ima* or *Imma*.

A visual comparison of the intensities of $NpAl_4$ and UAl_4 showed the two to be identical. Hence, Borie's description[2] for UAl_4 has been applied here for the atomic positions in space group *Imma*.

$(0,0,0;\ ½,½,½)+$
4 Np in (*e*) $0,¼,z;\ 0,¾,\bar{z};\ z = 0.111$
4 Al in (*e*) $0,¼,z;\ 0,¾,\bar{z};\ z = -0.111$
4 Al in (*b*) $0,0,½;\ 0,½,½$
8 Al in (*h*) $0,y,z;\ 0,\bar{y},\bar{z};\ 0,½+y,\bar{z};\ 0,½-y,z;\ y = -0.033;\ z = 0.314.$

Table IV. Interatomic Distances in $NpAl_4$

Atom	No. of Neighbors	Kind of Neighbors	Distance, Å
Np(4e)	3	Al(4e)	3.13
	4	Al(4b)	3.11
	4	Al(8h)	3.01
	2	Al(8h)	3.30
Al(4e)	3	Np(4e)	3.13
	4	Al(4b)	3.11
	4	Al(8h)	2.79
	2	Al(8h)	3.10
Al(4b)	4	Np(4e)	3.11
	4	Al(4e)	3.11
	2	Al(4b)	3.13
	2	Al(8h)	2.56
Al(8h)	2	Np(4e)	3.01
	1	Np(4e)	3.30
	2	Al(4e)	2.79
	1	Al(4e)	3.10
	1	Al(4b)	2.56
	2	Al(8h)	2.82
	1	Al(8h)	3.54
	1	Al(8h)	2.72

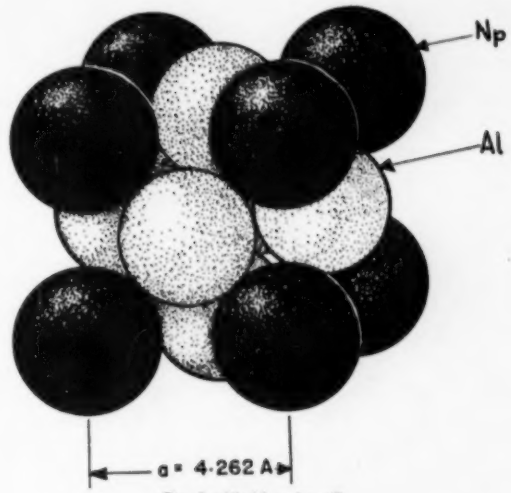

Fig. 1—$NpAl_4$ unit cell.

Fig. 2—Single crystals of $NpAl_4$.

The interatomic distances are tabulated in Table IV and the unit cell is illustrated in Fig. 3.

$NpAl_4$: A 16 mg powdered sample of $NpAl_4$ was heated in a BeO crucible for 1 hr at 1150°C in a high vacuum furnace. The product was identified as $NpAl_3$ from its powder diffraction pattern. A further treatment for 15 min at 1375°C produced a crystalline residue with an X-ray diffraction pattern similar to UAl_4. Several weak lines not due to $NpAl_3$ were present also. The latter fitted the published description for NpO.[7]

The powder diffraction pattern showed that $NpAl_4$ is face-centered cubic with $a = 7.785 \pm 0.005$Å. The

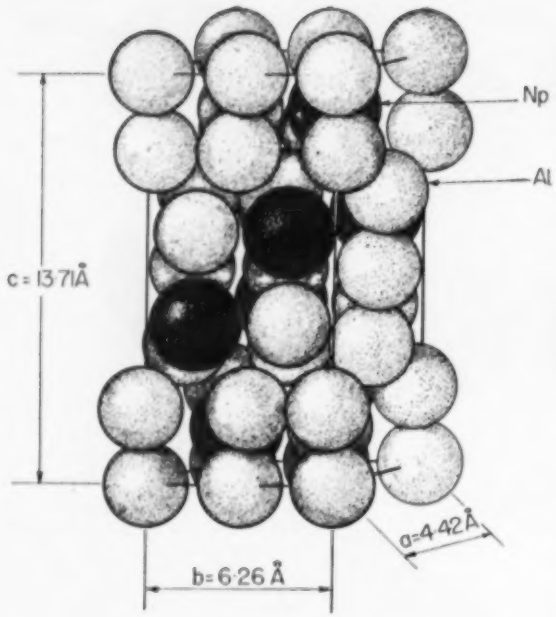

Fig. 3—$NpAl_4$ unit cell.

compound is isostructural with UAl_3 where a = 7.74Å[1] or a = 7.811Å[2] (see Table V).

The calculated density is 8.19 gram cm^{-3}, assuming eight $NpAl_3$ formula weights per unit cell. The atomic positions in the structure are:

(0,0,0; 0,½,½; ½,0,½; ½,½,0) +
8 Np in 0,0,0; ¼,¼,¼
16 Al in ⅝,⅝,⅝; ⅝,⅞,⅞; ⅞,⅝,⅞; ⅞,⅞,⅝.

The interatomic distances are tabulated in Table VI and the unit cell is illustrated in Fig. 4.

Discussion

The presence of NpO lines in the $NpAl_3$ powder diffraction pattern suggests that no other compound

Table V. Comparison of the $NpAl_3$ and UAl_3 Powder Diffraction Patterns

hkl	$\sin^2\theta$ $NpAl_3$	Observed Intensities*	
		$NpAl_3$	UAl_3[3]
111	0.0301	m−	w-m
220	0.0801	s	s
311	0.1094	s	s
400	0.1584	w	w
331	0.1882	m	m
422	0.2374	s	s
333,511	0.2671	s−	s
440	0.3158	m	m
531	0.3452	m	m
620	0.3941	m+	m
533	0.4233	m−	m-w
622	0.4331	vw	Not reported
444	0.4722	w	w
551,711	0.5019	w+	w-m
642	0.5509	s	s
553,731	0.5804	s	s
800	0.6290	w	vw
733	0.6585	w	vw
660,822	0.7061†	m+	m-s
555,751	0.7356†	m+	m-s
840	0.7840†	m−	m
753,911	0.8133†	m	m
664	0.8614†	m	m
931	0.8908†	m+	m
844	0.9398†	m+	Not reported
933	0.9694†	m	Not reported

* vw, very weak; w, weak; m, medium; and s, strong.
† Obtained with Cu $K_{\alpha 1}$ radiation.

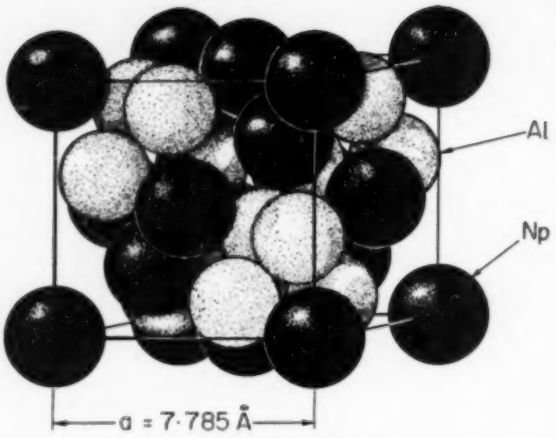

Fig. 4—$NpAl_3$ unit cell.

exists between the composition range $NpAl_2$ and Np. The Np in a mechanical mixture of Np and $NpAl_3$ would oxidize in air to NpO during the preparation of a powdered X-ray sample. On the Al-rich side, no compound exists between Al and $NpAl_4$, according to X-ray evidence, i.e., a powder diffraction pattern of a 30 pct Np in Al alloy showed only Al and $NpAl_4$ lines. Further, the observed decomposition of $NpAl_4$ on heating parallels that for UAl_4. The Np-Al system is, therefore, closely analogous to the U-Al binary system, with three intermetallic compounds characterized as follows:

1—$NpAl_2$ face-centered cubic with a = 7.785Å and the $MgCu_2$ structure.

2—$NpAl_3$ simple cubic with a = 4.262Å and the $AuCu_3$ structure.

Table VI. Interatomic Distances in $NpAl_2$

About each Np	4 Np at 3.37Å	12 Al at 3.23Å
About each Al	6 Al at 2.75Å	6 Np at 3.23Å

3—$NpAl_4$ body-centered orthorhombic with a = 4.42Å, b = 6.26Å, and c = 13.71Å and the UAl_4 structure.

Acknowledgment

The author is grateful to R. R. Boucher for technical assistance in the preparation of the compounds. The unit cell models were drawn by W. A. Cobbett. The neptunium was kindly supplied by the Argonne National Laboratory, Lemont, Ill.

References

[1] P. Gordon and A. R. Kaufmann: *Trans.* AIME (1950) **188**, p. 182; JOURNAL OF METALS (January 1950).

[2] B. S. Borie: *Trans.* AIME (1951) **191**, p. 800; JOURNAL OF METALS (September 1951).

[3] R. E. Rundle and A. S. Wilson: *Acta Crystallographica* (1949) **2**, p. 148.

[4] E. F. Westrum: Paper in "The Transuranium Elements." Edited by G. T. Seaborg, J. J. Katz, and W. M. Manning. (1949) p. 938. New York. McGraw-Hill Book Co.

[5] S. Fried and N. Davidson: *Journal* ACS (1948) **70**, p. 3539.

[6] O. J. C. Runnalls: *Canadian Journal of Chemistry* (1953) **31**, p. 694.

[7] W. H. Zachariasen: Paper in "The Transuranium Elements." Edited by G. T. Seaborg, J. J. Katz, and W. M. Manning. (1949) p. 1490. New York. McGraw-Hill Book Co.

Diffusion and Solubility of Boron in Iron and Steel

by Paul E. Busby, Mary E. Warga, and Cyril Wells

Fundamental data on the rate of diffusion of boron in austenite and solubility of boron in the α and γ phases of iron and steel have been obtained from deboronizing experiments and provide partial explanations for some of the phenomena observed in boron steels. The rate of diffusion of boron is about the same as carbon in austenite. The solubility of boron in austenite at normal heat-treating temperatures is less than 0.001 pct. A partial tentative Fe-B phase diagram in the important low boron concentration ranges and an equation representing the diffusion of boron in austenite are presented.

ALTHOUGH a search of the literature revealed that boron diffusion had not been studied quantitatively and systematically prior to 1948, a few qualitative observations which were made by following the diffusion of boron into iron packed in ferro-boron[1-6] suggest that boron obeys normal diffusion laws and that the rate of diffusion increases with increasing temperature. The claim of Cornelius and Bollenrath[1] that boron does not appear to influence the rate of carbon diffusion has recently been substantiated by Wells, Batz, and Mehl.[4] Calculations based on data from the paper by Campbell and Fay[2] indicated that the diffusion coefficient (D) for boron in iron at 900°C is approximately 3×10^{-7} sq cm per sec; a value of 2×10^{-7} sq cm per sec at 1038°C has been reported by Digges et al[5] in connection with decarburizing experiments on a commercial boron steel containing 0.43 pct C.

During the period 1948 to 1950 several diffusivity constant (D) values for the diffusion of boron in the γ phase of iron and steel and a number of solubility values for boron in both α and γ phases were reported. It was concluded tentatively as a result of Metals Research Laboratory studies that D values for boron in γ and α phases are about the same as for carbon in the comparable phases[6] and that carbon up to 0.4 pct did not affect the rate of diffusion of boron in γ iron above 1000°C within the limits of experimental error. Whether saturation of the γ or α phases with carbon would significantly affect rates of diffusion of boron through them was then and still remains in doubt. The best estimate of Q (activation energy) was reported to be about 25,000 cal, somewhat lower than that for carbon in γ iron. The solubility of boron in γ iron at 1000°C was thought to be higher than 0.004 pct B but not as high as a more recent analysis of available data shows it to be. The solubility of boron in α iron at 700°C was reported to be 0.0004 pct B, but it would not have surprised the authors if the true solubility value is actually lower than this. Breaks in diffusion curves which were not understood when first obtained prior to 1950 have now been recognized as indicating solubility limits, and these are included in the present paper.

P. E. BUSBY is Research Metallurgical Engineer, C. WELLS, Member AIME, is Principal Research Metallurgical Engineer, Metals Research Laboratory, Carnegie Institute of Technology, Pittsburgh, and M. E. WARGA is Director, Spectroscopy Laboratory, University of Pittsburgh, Pittsburgh.

Discussion on this paper, TP 3633E, may be sent, 2 copies, to AIME by April 1, 1954. Manuscript, April 15, 1953; revision, July 10, 1953. New York Meeting, February 1954.

Experimental Procedure

Two methods were employed in an effort to determine diffusion coefficients (D) for boron in austenite. Early experiments involved the use of welded couples prepared in accordance with the procedure of Wells and Mehl,[7] but when the results of these experiments proved to be unsatisfactory for calculating D values, studies were continued by means of deboronizing experiments. In both cases, boron analyses following the diffusion anneal were carried out spectrographically and all D values were computed using the Grube solution of Fick's law. The precision of the spectrographic method used proved to be about equal to that reported by Corliss and Scribner[8] —average deviation from the mean about 5 pct of the amount present when the boron content is 0.003 pct.

Concentration-penetration curves obtained from spectrographic analyses of welded couples generally indicated that practically no boron was transported across the weld interface during the diffusion anneal. Furthermore the concentration-penetration

Table I. Chemical Composition of Materials

Material No.	Element, Pct								
	C	Mn	P	S	Si	Ni	Cr	Mo	B
1	0.43	1.64	0.020	0.019	0.37	0.01	0.04	0.01	0.0038
2*	<0.005	0.001	<0.001	<0.001	<0.001	<0.00015	<0.00005	<0.0001	0.015
3*	0.28	0.001	<0.001	<0.001	<0.001	<0.00015	<0.00005	<0.0001	0.0014
4	0.025	0.26	0.006	0.031	0.008	0.03	0.02	0.01	0.040
5	0.41	0.45	0.010	0.023	0.16	0.12	0.19	0.06	0.030
6	0.032	0.30	0.010	0.024	0.19	0.06	0.03	0.03	0.025
7	0.036	0.25	0.007	0.025	0.12	0.05	0.03	0.02	0.03

* Spectrographic traces of other elements, except for aluminum which is about 0.05 pct.

curves for duplicate experiments (same steels and heat treatment) and the D values calculated therefrom were not reproducible. Diffusion coefficients determined from couple experiments were as much as 100 times lower than those obtained from later deboronizing experiments. Since results of welded couple experiments are not included in this paper, subsequent sections will be limited to data pertaining to deboronizing experiments.

Composition of Materials: The compositions of the materials used for deboronizing experiments are given in Table I. Steel 1 was obtained from the Bureau of Standards and is one of the commercial steels (C-18) described by Digges and Reinhart.[9] Materials 2 and 3 are high purity heats produced from electrolytic iron and excess aluminum together with ferro-boron (material 2) and ferro-boron plus graphite (material 3); the charge was heated to near the melting point under vacuum after which purified argon was admitted as an atmosphere and the crucible was lowered slowly from the heating zone. Materials 4 through 7 consist of laboratory heats of plain C-B steels similar in purity to high quality commercial steels. Aluminum was added to all materials prior to the addition of boron.

Boron additions were made with bortam (steel 1), ferro-boron (2 and 3), and Grainal No. 79 (all others). The wide variations in the boron contents among the various alloys were necessitated by the lack of available information on the solubility of boron in the α and γ phases of iron.[10] Materials 2 and 3 were heat-treated in the as-solidified form (1 in. rounds) and all other materials were forged to 1 or 1¼ in. diameter rounds prior to the diffusion anneal.

Diffusion Anneal: Samples for deboronizing experiments consisted of cylinders 1 to 1¼ in. in diameter and about 2 in. long; both ends of the specimens were faced perpendicular to the axis of the cylinder prior to the deboronizing (and decarburizing) heat treatment in an atmosphere of wet hydrogen. Times and temperatures of the various treatments which yielded diffusion and solubility data are recorded in Tables II and III. Temperatures are probably correct within 5°C and errors in the reported times are negligible.

Specimens were heat-treated in a wire-wound resistance tube furnace using a McDanel tube as an atmosphere chamber. Temperatures were measured by means of a calibrated Pt-Pt-10 pct Rh thermocouple wired to the diffusion specimen. The hydrogen atmosphere was obtained by passing tank hydrogen through water at room temperature prior to admission to the furnace; the flow of wet hydrogen was maintained for the duration of the diffusion anneal. When the heat treatment was completed, specimens were removed from the furnace and cooled rapidly in air or water-quenched.

Determination of Boron: Following the diffusion anneal, specimens were machined to ½ in. diameter cylinders to avoid radial diffusion effects. Boron determinations were made on surfaces prepared by removing successive layers of the sample perpendicular to the cylindrical axis with a boron free wheel on a surface grinder. Depending on the location with respect to the original surface, the layers varied from 0.003 to 0.020 in. in thickness. The distance measurements which are subsequently utilized in plotting concentration-penetration curves are believed to be accurate to about 0.0005 in. (0.001 cm).

Calculation of D: In order to calculate diffusion coefficients from concentration-penetration data, the Grube solution of Fick's law was applied. The procedure used has already been described[11] and involves the use of the equation

$$1 - \frac{2C}{Co} = \phi\left(\frac{x}{2\sqrt{Dt}}\right)$$

where: Co is twice the maximum boron content of the deboronized specimen, pct; C, $Co/2$ plus the boron content at a discrete value of x, pct; x, the distance from the surface, cm; D, the diffusion coefficient, sq cm per sec; t, the diffusion time, sec; and ϕ, the Gauss error function or probability integral.

After boron analyses were obtained, values of C/Co were plotted on probability paper as a function of x and the line of best fit was determined by the method of least squares. Data obtained from this line, together with the time of diffusion, permit the equation above to be solved for D.

In order to obtain the proper gradient for the calculation of D, values of C and $Co/2$ were corrected for the surface concentration (Cs) of boron in solution. This concentration was calculated for each experiment by substituting the value of the

Table II. Summary of Experiments Which Provided Diffusion Coefficients in Austenite

Test No.	Material	Time, Hr	Temperature, °C	$Dx10^{-7}$ Sq Cm per Sec
1	1	29.0	950	2.6
2	3	11.5	992	3.6
3	1	11.0	998	4.1
4	1	11.1	1000	4.5
5	1	11.1	1000	5.8
6	1	6.0	1072	8.3
7	1	6.0	1072	9.0
8	1	5.0	1203	10.9
9	1	4.0	1299	23.3

intercept, C/Co, obtained from the probability plot, in the equation $C = Co/2 - Cs$ and solving for Cs. The proper values for substitution in the Grube expression then become $Co/2 - Cs$ and $C - Cs$.

Although D values cannot be calculated from results of experiments in which the initial boron content is above the solubility at the temperature of diffusion, such data are useful for estimating the solubility of boron since the gradient of boron in solution must vary from near zero at the surface to the limit of solid solubility at the deboronizing temperature. Stanley[13] has already demonstrated that the values for the solubility of carbon in ferrite determined by this method are in agreement with those obtained by the Van Ostrand-Dewey method.

Results

Diffusion in Austenite: The results of deboronizing (and decarburizing) experiments which were conducted on steel 1 at temperatures ranging from 950° to 1300°C are summarized in Table II. In addition, data obtained on a pure Fe-C-B alloy (steel 3) are included for comparison. A typical concentration-penetration curve for boron, and the associated curve for carbon are presented in Fig. 1.* The boron curve is similar to the carbon curve wherein the concentration of carbon follows a Gaussian curve from the original composition to zero at the surface except that boron diffuses to the surface where it forms an insoluble oxide and accumulates to the high concentration shown. However if the high concentration of insoluble boron at the surface is disregarded, diffusion coefficients may be calculated. The obvious objection to these deboronizing experiments is the fact that both carbon and boron atoms are diffusing to the surface simultaneously.

Results of deboronizing experiments carried out on steel 1 are plotted in Fig. 2 as log D vs the reciprocal of temperature. The line of best fit shown was computed using the method of least squares. The activation energy, Q, determined from the slope of this line is about 21,000 cal per mol or roughly half that reported for the diffusion of carbon in austenite.[4] The data may be represented approximately by the equation: $D = 2\text{x}10^{-6}\ e^{-21,000/RT}$. Based on a standard statistical analysis† it appears that within the range 8.2 to 6.2 (abscissa, Fig. 2) the odds are about 20 to 1 in favor of true values of D falling between limits represented by the upper and lower (dashed) curves. The odds are also estimated to be 20 to 1 that the true value of Q falls between limits of 21,000 + 7000 cal and 21,000 − 7000 cal.

Solubility: Data on the solubility of boron in austenite were obtained from the results of deboronizing experiments in the range 800° to 1100°C. Estimates of solubility limits from diffusion experiments are based on the knowledge that a change of phase in a system is accompanied by a sudden change in the concentration of the solute element. In order to determine the solubility of boron in austenite above 1000°C, materials containing more than 0.003 pct B were selected because the smooth curves obtained from deboronizing experiments, Fig. 1, indicated that at least 0.003 pct B is in solid solution at these temperatures. Experiments on these high boron materials at temperatures between 1000° and 1100°C produced curves of the type shown in Fig. 3. From this curve, the solubility of boron in austenite at 1002°C is estimated to be about 0.009 pct B, i.e., the concentration of boron about 0.07 cm from the surface where the "break" in the penetration curve indicates that austenite was in equilibrium with austenite plus boride.

The curves of Fig. 4 were obtained from results of spectrographic analyses of two individual specimens which were annealed at approximately 800°C. The intercepts indicated by the horizontal arrows are considered to represent the solubility of boron in austenite, and the similarities in the curves demonstrate the reproducibility of the method. From

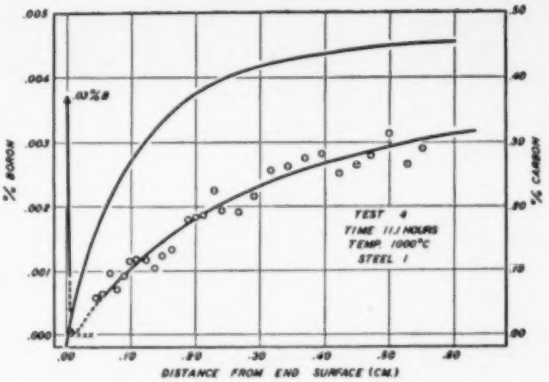

Fig. 1—Concentration-penetration curves for boron and carbon from test 4 after deboronization and decarburization in wet hydrogen. The symbol "x" denotes that no boron line was observed on the spectrographic plate.

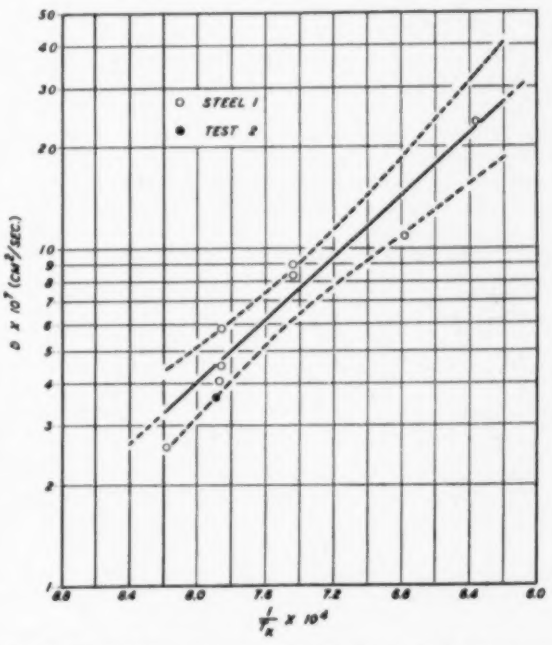

Fig. 2—Effect of temperature on the diffusion coefficient for boron in austenite. All tests made on steel 1, except test 2 which was a high purity Fe-C-B alloy.

* Chips for carbon analyses were obtained from successive circumferential layers taken from portions of the cylinder not used for spectrographic analysis. It may be noted that the boron curve apparently approaches a maximum concentration of approximately 0.003 pct B whereas Table I indicates that this steel should contain 0.0038 pct B. This result is believed to be due to segregation of boron from specimen to specimen rather than a consequence of radial diffusion, since the maximum boron concentration obtained in various specimens appears to be unrelated to the time and temperature of heat treatment.

† Procedures for estimating the limits of accuracy of a set of data are given in many standard texts[12,14,15] and technical papers.[16]

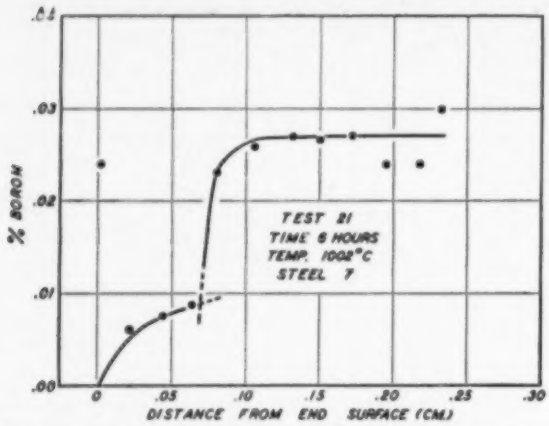

Fig. 3—Concentration-penetration curve for test 21, indicating the solubility limit of boron in austenite to be about 0.009 pct B at the diffusion temperature.

these curves, the solubility of boron in austenite at 800°C is estimated to be about 0.0006 pct B.

The curve of Fig. 4A is associated with the microstructure of Fig. 5a which reveals that carbon was removed preferentially from the surface of the specimen during the diffusion run, so that the banding which existed in this commercial steel prior to heat treatment is accentuated. As a result of segregation, the α and γ phases coexisted at the temperature of diffusion, and because of the differences in the rate of diffusion of carbon in the separate phases, carbon was removed more rapidly from the α regions; subsequent cooling produced the structure of conspicuous ferrite and pearlite bands.

The distance from the surface represented by the right side of the micrograph, Fig. 5a, is about 0.10 cm so that the "break" in the boron penetration curve occurs at a position where the structure has evidently not been affected by the circumstances just described, i.e., a position where the steel was essentially all austenite at temperature.‡ Chemical analyses indicate that the carbon content at the boron interface is about 0.25 pct and the D value based on carbon penetration data for this specimen shows that diffusion in austenite controlled the rate of removal of carbon. The microstructure of this steel after diffusion at 930°C shows, as expected, much less evidence of banding as indicated in Fig. 5b.

‡ As a result of the high manganese content, the A_3 in this steel at a position where decarburization has not been extensive is considerably less than 910°C.

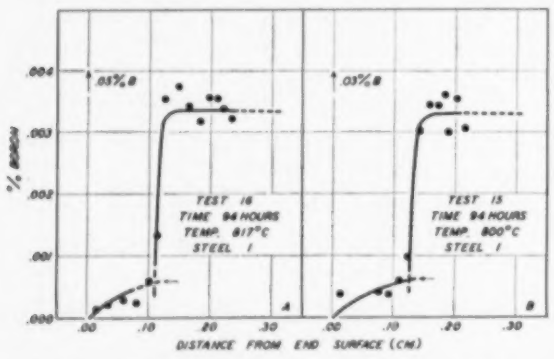

Fig. 4—Concentration-penetration curves for tests 16 and 15 showing the reproducibility of the deboronizing method for estimating solubility limits.

Information on the solubility of boron in the α phase was obtained from the results of deboronizing experiments conducted on alloys containing Fe+B and Fe+C+B at temperatures between 700° and 850°C. Curves similar to those just described were obtained, and the solubility limits were similarly estimated.

Results of tests which provided data on the solubility of boron in α and γ are listed in Table III. In some cases, the solubility values are given as less than or greater than a given amount when the numerical values are known to be in error. For example, the table includes results of a deboronizing experiment (test 1) which yielded a smooth concentration penetration curve from which a D value was calculated; such data indicate that all boron in the sample was in solid solution at the diffusion temperature and it may be concluded that the solubility is greater than this amount. In test 14 the interface movement resulting from the diffusion treatment was only about 0.035 cm as determined by metallographic examination of the specimen and the "break" in the concentration-penetration curve. The only boron determination available between the surface and the interface gave a value less than 0.0002 pct B after which the boron content rose sharply from 0.0035 to 0.031 pct. Thus, these data suggest that the solubility of boron in α at 850°C is somewhat less than 0.0035 pct B. In the case of tests 16 and 17 a small amount of α existed in the samples at the position of the interface so that the determined value is an average of the solubilities in both α and γ. Since other data demonstrate that the solubility of boron in α at 800°C is higher than that in γ, the solubility value for γ is believed to be slightly less than the determined value; by similar reasoning, the value obtained for the solubility of boron in ferrite at 751°C (test 12) is probably too low. However, it must be emphasized that in the last three mentioned experiments, the magnitude of error introduced by accepting the determined values is probably less than the limit of analysis.

Table III. Summary of Experiments Which Provided Solubility Data

Test No.	Material	Time, Hr	Temperature, °C	Solubility, Pct B in α	Solubility, Pct B in γ
11	1	94	700	0.0003	
12	1	97.8	751	0.0006	
13	2	17	835	0.0018	
14	4	17.1	830	<0.0035	
15	1	94	800		0.0006
16	1	94	817		0.0006
17	1	94	817		0.0006
18	1	35.5	900		0.0012
19	1	29	930		0.0010
1	1	29	950		>0.003
20	7	6	1002		0.008
21	7	6	1002		0.009
22	5	6	1072		0.016
23	6	6	1086		0.016

Data listed in Table III are plotted in Fig. 6 together with previously published information[10] on the Fe-B system and suggest a peritectoid reaction at about 915°C.

Although D values calculated from welded couple experiments show considerable lack of reproducibility, solubility values do not. Results from three couples gave solubility limits (based on the Van Ostrand-Dewey method) of 0.0035 pct B in austenite at 982°C, 0.002 pct B in α at 842°C, and 0.002 pct B in α at 825°C, which are in fair agreement with

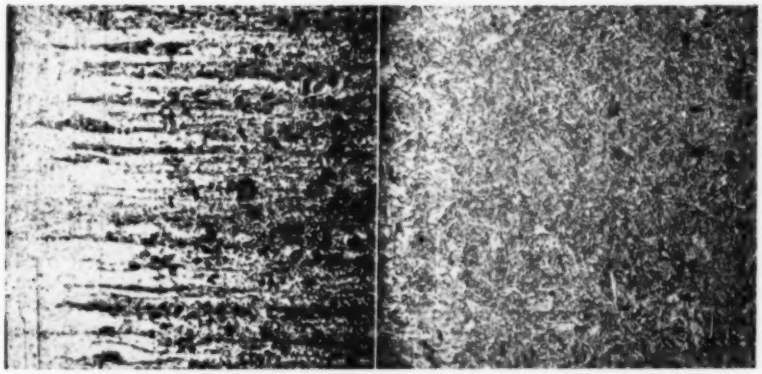

a—Etched in nital. X75. Area reduced approximately 40 pct for reproduction.

b—Etched in nital. X50. Area reduced approximately 40 pct for reproduction.

Fig. 5—Micrographs of steel 1 after decarburization at (a) 817°C, test 16, showing the preferential removal of carbon and (b) 930°C, test 19.

the data plotted in Fig. 6. The value for austenite was obtained from a couple consisting of two commercial steels containing 1.7 pct C and 0.04 and 0 pct B, respectively; the values for α were obtained from specimens of material 6 (Table I) welded to a boron-free steel of otherwise similar composition.

Discussion

Much of the information included in this paper has already been discussed in the foregoing sections. However, a few additional comments regarding some of the solubility and diffusion data, as well as their relation to hardenability, appear to be justified.

It has already been shown[4] that boron up to 0.009 pct does not significantly affect the rate of diffusion of carbon; the authors stated that "while it is suspected that boron . . . lowers D slightly, the evidence is not conclusive." In the present study, the observation that the boron concentration data from deboronizing experiments fit a straight line on the probability plot of C/Co vs x within the wide limits of experimental error, is accepted as evidence that the rate of diffusion of boron in austenite does not vary with, 1—boron concentration, at least, up to about 0.003 pct B or 2—carbon concentration up to 0.43 pct. The latter conclusion is substantiated by the similarity of results obtained from decarburized 0.43 and 0.28 pct C steels; in connection with the former conclusion it may be stated that some of the concentration-penetration curves suggest a slight departure from linearity on the probability plot. At some future time more and better data may show this curvature to be real, thus indicating an increase of D with concentration.

The solubility of boron in the α phase and in the γ phase up to 0.43 pct C is apparently independent of carbon content although the result of one welded couple experiment suggests that the solubility of boron in austenite may be lowered when the austenite is saturated with carbon. It appears reasonable therefore, to accept the Fe-B diagram of Fig.6 as a first approximation despite the fact that many of the solubility values on which the diagram is based were obtained from commercial materials containing up to 0.43 pct C as well as alloying elements.

The present investigation was initiated on the basis that a knowledge of diffusion rate and solubility of boron in the α and γ phases of iron and steel might provide needed basic data for understanding the mechanism by which boron improves the hardenability of steels. It is generally accepted that boron increases hardenability of hypoeutectoid steels by suppressing the rate of nucleation of proeutectoid ferrite. Among the intriguing aspects of the influence of boron however is the fact that published data[9, 17] with one exception[22] indicate that the relative increase in hardenability resulting from the addition of boron appears to be practically independent of the amount of boron present as determined by chemical or spectrographic analysis. The hardenability effect is known to be a function of carbon content.[17-20] There is also evidence that the effect of boron may be affected by heat-treating temperature[9, 18] and, in some steels the hardenability effect can be completely destroyed by high temperature homogenization and cannot be recovered by subsequent heat treatments.[18]

Data presented in Table III show that the solubility of boron in austenite is about 0.0006 pct at normal heat-treating temperatures. This may account in part for the often observed fact[9, 17, 18] that the effect of boron on hardenability appears to be independent of the amount of boron present. Since boron in quantities over the solubility limit would probably not affect hardenability, the relationship between boron content and improved hardenability could be expected only when the former lies between 0 and 0.0006 pct; the amount of boron added

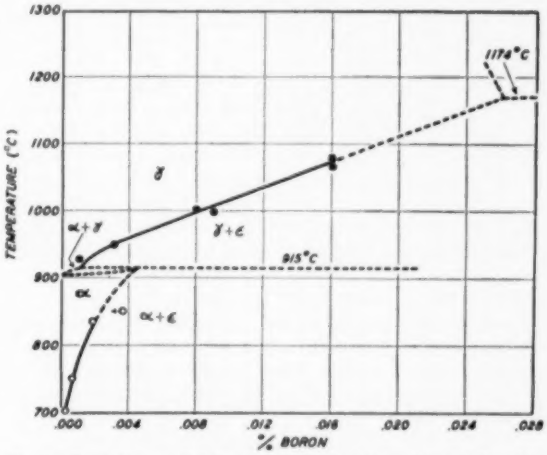

Fig. 6—Tentative partial Fe-B diagram based on deboronizing (decarburizing) experiments. Isotherms from Metals Handbook.[20]

to steels is usually greater than this amount. Another condition which has led to difficulty in this connection is the high affinity of boron for oxygen[8] and nitrogen[2, 5, 9] which leads to the ready formation of compounds and renders the boron ineffective; in some steels, improved hardenability is not obtained even when analysis indicates the presence of relatively large amounts of boron. It is therefore not surprising that the anticipated relationship between boron content and improved hardenability has not yet been determined experimentally with adequate precision.

Before other observations concerning the influence of boron on the hardenability of steels can be understood, the new data provided in this paper must be substantially augmented. The increase in solubility with increasing temperature is probably an important part of the required explanation of the effect of austenitizing temperature. In fact, solubility theory alone might reasonably be used to explain this effect if it were not for the disturbing observations which have been reported regarding the so called "boron constituent."[10, 18] Spretnak and Speiser[21] have explained some of the characteristics of the boron constituent on the basis of positive adsorption theory which should not be overlooked in the search for the full understanding of the effect of boron additions on the hardenability of hypoeutectoid steels. Before this objective can be attained however, further studies appear to be required to determine the causes for the lack of consistent behavior among boron-treated steels.

Summary

1—A spectrographic method was developed for determining boron in the range 0.0006 to 0.02 pct. The precision of the method is about the same as that developed by the Bureau of Standards[8] and the sensitivity is of the order of 0.0002 pct.

2—Diffusion coefficients for boron in austenite were determined by the Grube method from the results of welded couple and deboronizing experiments. Reasonable D values were obtained from the latter experiments carried out on a commercial 0.43 pct C steel in the range 950° to 1300°C, but results from the welded couples are not in good agreement nor reproducible.

3—The diffusion of boron in austenite is comparable with that of carbon and may be represented by the equation

$$D_\gamma = 2\text{x}10^{-5}\, e^{-81{,}000/RT}$$

Within the limits of experimental error, D_γ appears to be independent of carbon and boron up to 0.43 and 0.003 pct, respectively.

4—The solubility of boron in austenite at normal heat-treating temperatures is less than 0.001 pct B, but increases rapidly with temperature above 925°C. The solubility of boron in α at 835°C is about 0.002 pct, i.e., considerably higher than that in austenite at the same temperature, suggesting a peritectoid reaction. Solubility in both α and γ phases appears to be unaffected by carbon content, unless the austenite is saturated with carbon, in which case the solubility limit may be somewhat lowered.

5—The low solubility of boron in austenite explains some of the unusual effects of boron on the hardenability of steel but additional experimental data are required before the mechanism can be fully understood.

Acknowledgment

Part of this work was carried out under contracts with the Ordnance Department, Department of the Army and the Office of Naval Research, Department of the Navy. The authors are indebted to T. G. Digges, H. A. Bright, and C. H. Corliss of the National Bureau of Standards for providing some of the steels and spectrographic determinations, to the Metallurgical Department of the Central Alloy District of the Republic Steel Corp. for supplying many of the alloys, and to G. Cressman, D. P. Hart, A. M. Hanna, L. R. Redmerski, M. Conrad, M. A. Redmerski, and J. Vojtecky of the Metals Research Laboratory for conducting the heat treatments and spectrographic analyses.

References

[1] H. Cornelius and F. Bollenrath: Einflusz von Kohlenstoff auf die Diffusion einiger Elements in Stahl. *Archiv. Eisenhüttenwesen* (September 1941) **15**, p. 145.

[2] T. D. Campbell and H. Fay: The Case Hardening of Steel by Boron and Nitrogen. *Industrial and Engineering Chemistry* (1924) **16**, p. 719.

[3] T. Kase: Cementation of Boron on Some Metals. Abstracted in *Metals and Alloys* (1938) **9**, p. M.A. 661.

[4] Cyril Wells, Walter Batz, and Robert F. Mehl: Diffusion Coefficient of Carbon in Austenite. *Trans.* AIME (1950) **188**, p. 553; JOURNAL OF METALS (March 1950).

[5] T. G. Digges, Carolyn R. Irish, and Nesbit L. Carwile: Effect of Boron on the Hardenability of High Purity Alloys and Commercial Steels. *Journal of Research.* National Bur. Standards (1948) **41**, R.P. 1938, p. 545.

[6] C. E. Birchenall: Volume Diffusion—An Empirical Survey. *Atom Movements.* (1951) p. 112. Cleveland. ASM.

[7] C. Wells and R. F. Mehl: Rate of Diffusion of Carbon in Austenite. *Trans.* AIME (1940) **140**, p. 279.

[8] C. H. Corliss and B. F. Scribner: Spectrographic Determination of Boron in Steel. *Journal of Research.* National Bur. Standards (1946) **36**, R.P. 1705, p. 351.

[9] T. G. Digges and F. M. Reinhart: Influence of Boron on Some Properties of Experimental and Commercial Steels. *Journal of Research.* National Bur. Standards. (1947) **39**, R.P. 1815, p. 67.

[10] R. M. Parke: Boron-Iron Constitution Diagram. *Metals Handbook* (1948) p. 1175. Cleveland. ASM.

[11] C. Wells: Chemical Techniques and Analysis of Diffusion Data. *Atom Movements* (1951) p. 26. Cleveland. ASM.

[12] J. K. Stanley: The Diffusion and Solubility of Carbon in Alpha Iron. *Trans.* AIME (1949) **185**, p. 752; JOURNAL OF METALS (October 1949).

[13] M. Ezekial: *Methods of Correlation Analysis* (1941) Second Edition. New York. John Wiley and Sons.

[14] G. W. Snedecor: *Statistical Methods* (1946) Fourth Edition. Ames, Iowa. The Iowa State College Press.

[15] H. Arkin and R. R. Colton: *An Outline of Statistical Methods* (1939) Fourth Edition. New York. Barnes and Noble.

[16] E. G. Olds and C. Wells: Statistical Methods for Evaluating the Quality of Certain Wrought Steel Products. *Trans.* ASM (1950) **42**, p. 845.

[17] M. C. Udy and P. C. Rosenthal: Boron in Certain Alloy Steels. *Trans.* AIME (1947) **172**, p. 273; METALS TECHNOLOGY (October 1946).

[18] R. A. Grange and T. M. Garvey: Factors Affecting the Hardenability of Boron-Treated Steels. *Trans.* ASM (1946) **37**, p. 136.

[19] G. D. Rahrer and C. D. Armstrong: The Effect of Carbon Content on the Hardenability of Boron Steels. *Trans.* ASM (1948) **40**, p. 1099.

[20] W. Crafts and J. L. Lamont: Effect of Some Elements on Hardenability. *Trans.* AIME (1944) **158**, p. 157.

[21] J. W. Spretnak and Rudolph Speiser: Grain and Grain-Boundary Compositions: Mechanism of Temper Brittleness. *Trans.* ASM (1951) **43**, p. 734.

[22] Yûnoshin Imai and Hikotarô Imai: The Research Inst. for Iron, Steel and Other Metals. *Sci. Repts.* Research Inst. Tôhoku Univ. (April 1950) Series A, Vol. 2, No. 2 (in English). Sendai, Japan.

Effects of Temperature on the Flow and Fracture Characteristics of Molybdenum

by J. H. Bechtold

Tensile properties of annealed molybdenum were investigated from 1000° to −200°C. In the vicinity of room temperature a well-defined transition in tensile properties occurs. Reduction in area decreases from over 80 pct to 0 pct and, simultaneously, the yield strength increases about 60,000 psi.

MOLYBDENUM, tungsten, iron, and many other metals and alloys with the body-centered cubic and hexagonal close-packed crystal structures change from ductile to brittle behavior over some relatively narrow temperature range. The temperature at which this transition in ductility occurs depends on chemical composition, microstructure, and method of testing. When fine grained, completely recrystallized molybdenum of commercial purity is tested in uniaxial tension at a slow strain rate, the transition occurs at slightly below room temperature.[1] Iron[2] and tungsten[3] tested under similar conditions become brittle at temperatures close to the boiling point of nitrogen, −195°C and at about 200°C, respectively. A sharp change in ductility is uncommon in metals with the face-centered cubic crystal structure, however, a relatively sharp transition in notched bar impact properties has been observed below room temperature in a face-centered cubic copper-antimony alloy.[4]

A transition from ductile to brittle behavior is usually explained by the concepts originally developed by Ludwik,[5] and discussed and elaborated on by others including Orowan,[6] Hollomon and Jaffe,[7] and Gensamer.[8] In brief, there are two aspects to strength, first the resistance to flow and second the resistance to fracture. Both are functions of temperature, strain, strain rate, stress system, composition, and microstructure. With decreased test temperature the flow stress required to initiate plastic deformation increases more rapidly than the fracture strength and brittle fracture occurs at that temperature where the yield strength equals or exceeds a brittle fracture strength.

This investigation was conducted to determine the effects of temperature, strain, and rate of straining on the flow and fracture strengths of molybdenum above, through, and below the ductile-to-brittle transition. Other variables were held constant during testing. This information is believed to show

J. H. BECHTOLD, Junior Member AIME, is associated with the Research Laboratories, Westinghouse Electric Corp., East Pittsburgh, Pa.

Discussion on this paper, TP 3644E, may be sent, 2 copies, to AIME by April 1, 1954. Manuscript, March 10, 1953; revision, July 1, 1953. New York Meeting, February 1954.

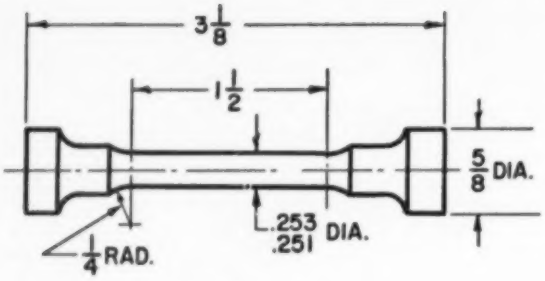

Fig. 1—Tensile specimen.

clearly the characteristics that lead to the brittleness in molybdenum at low temperatures and probably in other metals with a body-centered cubic crystal structure as well.

Material and Test Procedures

High purity molybdenum powder reduced from ammonium molybdate was hydrostatically pressed into a compact about 3x3x24 in. and sintered by a modification of the Hall-Ramage[9] process to a density equivalent to 97 to 98 pct of the theoretical density of molybdenum. It was rolled to 5/8 in. diameter by a process designed to give a uniform, fine grain structure after a final recrystallization anneal.[10] The chemical composition of this molybdenum sample, WNS-5000S, was as follows: 0.014 pct C, 0.0017 pct O_2, 0.0056 pct N_2, 0.001 to 0.10 pct Fe,* 0.0005 to 0.05 pct Si,* trace of Cu,* and trace of Mg.*

* Probable concentration range estimated from spectrographic analysis.

Tensile specimens with the dimensions shown in Fig. 1 were machined from the as-rolled bars and annealed after machining for 1 hr at 1150°C. This annealing treatment produced a uniform recrystallized grain structure of approximately 900 grains per sq mm (ASTM grain size No. 6 to 7). The tensile testing machine combined the features of a constant rate of extension and an autographically recorded load-elongation curve. For the low temperature tests the specimens were cooled in gaseous nitrogen by the method of Wessel and Olleman.[11] Above 400°C the specimens were protected from oxidation by a nitrogen atmosphere.

Room Temperature Tensile Properties of Annealed Molybdenum

The relation between stress and plastic strain for a number of metals is expressed by the following empirical equation:

$$\sigma = K\delta^n \qquad [1]$$

where σ is the true stress, i.e., load divided by instantaneous area; δ, the natural strain, ln A_o/A; K, a constant, the true stress at unit natural strain; and n, a second constant usually referred to as the work-hardening exponent. Preliminary tensile tests revealed that, with certain limitations, plastic flow in molybdenum follows this relation. The form of Eq. 1 indicates that a straight line of slope n should be obtained when true stress is plotted as a function of natural strain on logarithmic coordinates. The curve obtained by plotting true stress vs natural strain on logarithmic coordinates is referred to here as the flow curve and Eq. 1 as the flow equation.

The room temperature (18°C) flow curve of molybdenum extended at a constant rate of 2.8×10^{-4} sec^{-1} is shown in Fig. 2. At room temperature, annealed molybdenum has an upper and lower yield point and is in the low temperature portion of the ductile-to-brittle transition zone, but it still has considerable ductility and necks locally prior to fracture. All deviations from the flow equation observed over the entire temperature range studied are present at this temperature.

The initial, approximately horizontal, portion of the flow curve is due to the yield point phenomenon. At most temperatures the flow curve is a single straight line from the limit of the yield point elongation to the strain at which necking occurs. However, at room temperature and at other temperatures in the low temperature portion of the ductile-to-brittle transition zone the slope of the flow curve changes after about 0.04 strain. The reason for this

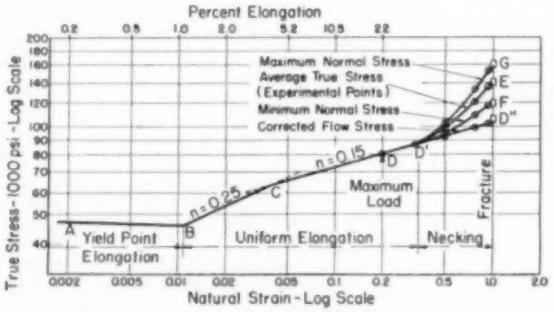

Fig. 2—Flow curve of annealed molybdenum at 17° to 18°C. Grain size, 900 grains per sq mm. Rate of extension, 2.8×10^{-4} sec^{-1}.

change in slope is unknown, but it has been observed for a large number of samples with different compositions and microstructures.

Once necking occurs, the flow curve diverges upward sharply as shown by the average stress in Fig 2. To ascertain if this divergence in the flow curve is due to radial constraint from necking or to the basic flow characteristics of molybdenum, the distribution of stress over the cross section under the root of the neck of several specimens strained beyond the maximum load point was analyzed. The distribution of stress calculated by the equations of Davidenkov[12] for one specimen which was strained almost to fracture ($\delta = 1.0$) is shown in Fig. 3. The minimum normal stress is the real flow stress because the metal would deform at this stress and not the average normal stress in the absence of the neck. However, when the minimum normal stress is plotted as a function of strain, Fig. 2, it still diverges upward from the flow curve extrapolated from lower strains.

When a tensile specimen necks down, plastic deformation is restricted to the necked region, and the effective gage length decreases. Consequently, the strain rate increases if the rate of extension is held constant, as it was in these tests. If the radius of curvature of the contour of the neck is taken as the approximate gage length of the necked specimens, the actual rate of strain at the root of the neck can be estimated. Using data reported later in this

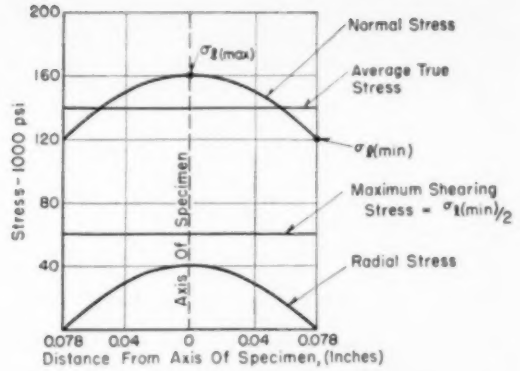

Fig. 3—Distribution of stress over the cross section under the root of the neck of a specimen strained to about $\delta = 1.0$ at 17° to 18°C. Distribution of stress calculated by equations of Davidenkov.[13]

paper on the effects of strain rate on the yield strength of molybdenum, the minimum normal stresses were corrected to a strain rate of 2.8×10^{-4} sec^{-1}. The corrected flow stresses fall quite well on an extrapolation of the flow curve before necking, indicating that molybdenum obeys the flow equation after necking and the divergence of the experimental points after necking is due to radial constraint and increased strain rate resulting from the formation of the neck.

As a result of these observations the flow curves at higher and lower temperatures were determined experimentally only to the strain at which necking occurred. The flow stresses at higher strains or at fracture were estimated by extrapolating the experimentally determined portion of the flow curve to the desired strain.

Effects of Temperature on Tensile Properties

Tensile specimens were pulled to fracture at several temperatures between −195°C and +970°C at a constant rate of extension of 2.8×10^{-4} sec^{-1}. Test results are plotted as a function of test temperature in Fig. 4. To facilitate discussion, Fig. 4 is divided into four zones based in part on yield strength,† ductility‡ and fracture characteristics. The first, or "brittle zone," extends from the lowest test temperature to about −75°C and is characterized by the absence of measurable ductility and bright transgranular fractures. The second, or "transition zone," extends from −75°C to about +150°C and is characterized by a rapid increase in ductility and a correspondingly rapid decrease in the yield strength with increased test temperature. In this zone there is a change from bright, brittle, transgranular fractures at the lower temperatures to dull fibrous fractures at the higher temperatures. The third or "ductile zone" extends from about 150° to about 900°C and is characterized by excellent ductility, a yield strength essentially independent of temperature, except when affected by yield point phenomena, and a dull fibrous fracture. The fourth, or "unstable zone" occurs above about 900°C and is due to thermal instability, probably recovery, or partial recrystallization during testing.[10]

† The yield strength is defined herein as the stress at which the engineering load-elongation curve deviates from linearity, i.e., the proportional limit.
‡ The reduction in area at fracture is taken as the measure of ductility.

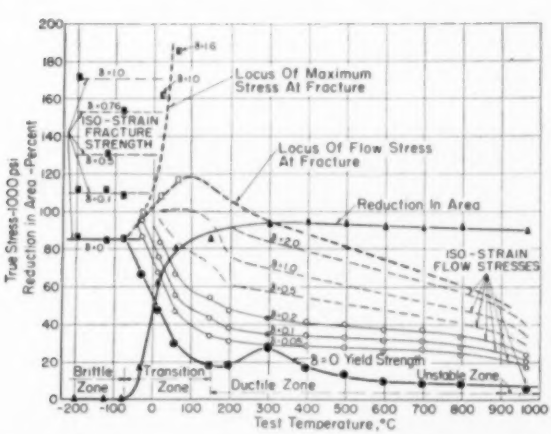

Fig. 4—Effects of temperature on the flow and fracture characteristics of annealed molybdenum. Grain size, 900 grains per sq mm. Rate of extension, 2.8×10^{-4} sec^{-1}. Flow stresses above $\delta = 0.20$ and flow stress at fracture above 60°C estimated from flow curves in Fig. 5.

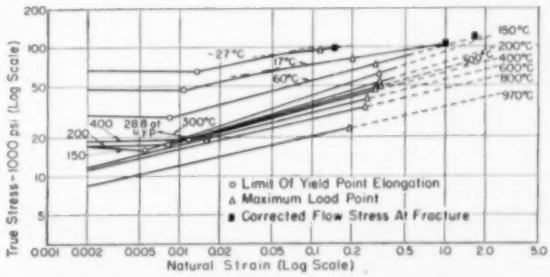

Fig. 5—Flow curves of annealed molybdenum at several test temperatures. Grain size, 900 grains per sq mm. Rate of extension, 2.8×10^{-4} sec^{-1}.

Yielding; The most pronounced effect of temperature on yield strength occurs in the transition zone. The increase of about 65,000 psi between +150°C and −75°C is exceedingly large for a metal with a melting point of 2620°C. Presumably the yield strength would continue to increase at lower temperatures but fracture precedes yielding. The intersection of the yield strength curve with the brittle fracture strength curve divides the transition and brittle zones. In the ductile zone, the yield strength decreases gradually with increasing test temperature, except between 200° and 400°C where a maximum associated with a very pronounced upper and lower yield point occurs.

Flow curves for several test temperatures are shown in Fig. 5. These curves show that the yield point phenomenon occurs at temperatures below about 600°C and is most prominent at about 300°C. The curves are linear from the limit of the yield point elongation to the maximum load point except at the two lowest test temperatures where the slope changes after a strain of about 0.04.

Flow stresses at several strains are replotted as a function of temperature as iso-strain flow curves in Fig. 4. At small strains the iso-strain flow curves roughly parallel the yield strength curve. However, the maximum in the yield stress curve at about 300°C is not observed once the yield point strain is exceeded. The slope of the iso-strain flow curves

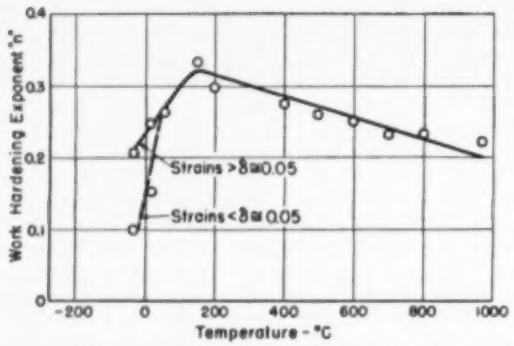

Fig. 6—Effect of temperature on the work hardening exponent of molybdenum.

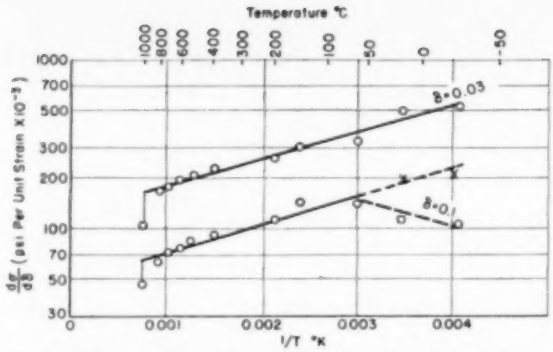

Fig. 7—Effect of temperature on the rate of work hardening of molybdenum at strains of $\delta = 0.03$ and $\delta = 0.10$.

is greater at higher strains due to an increase in the rate of work hardening with decreased test temperature. The iso-strain flow curves for large strains decrease quite rapidly above 800° to 900°C due to thermal softening or partial recrystallization during test.

Strain Hardening: The slopes of the flow curves in Fig. 5, which are the work hardening exponent n in Eq. 1 are plotted as a function of test temperature in Fig. 6 and are a maximum at 150°C. The rate of work hardening, i.e., the rate of change of stress with strain, obtained by differentiating the flow equation is as follows:

$$d\sigma/d\delta = n\sigma/\delta. \qquad [2]$$

When the logarithm of the rate of work hardening is plotted as a function of the reciprocal of the absolute temperature, Fig. 7, straight lines are obtained at a strain of 0.03 and above 60°C at a strain of 0.1, indicating that there probably is a unique relation between temperature and rate of work hardening. Below 60°C the experimental points for 0.1 strain do not fall on the 0.1 strain curve because of the change in slope in the flow curves at low temperatures as discussed previously. These results are interpreted to mean that there is no significant difference in the mechanism of strain hardening in the ductile and transition zones at small strains.

Fracture: In the brittle zone and in the lower temperature portion of the transition zone, the frac-

Fig. 8—Microstructure normal to the fracture in specimen tested at −196°C. No measurable ductility. Electrolytic polish. Etched in alkaline $K_3Fe(CN)_6$ solution. X100. Area reduced approximately 75 pct for reproduction.

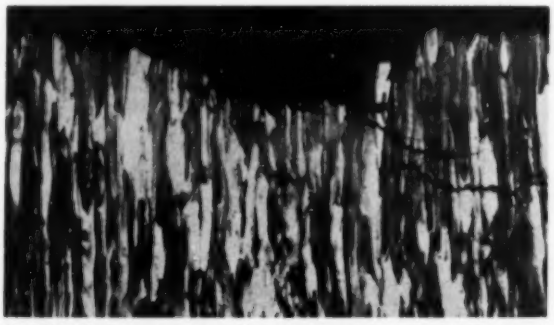

Fig. 9—Microstructure normal to the fracture in specimen tested at 17°C. 62 pct reduction in area at fracture. Electrolytic polish. Etched in alkaline $K_3Fe(CN)_6$ solution. X100. Area reduced approximately 75 pct for reproduction.

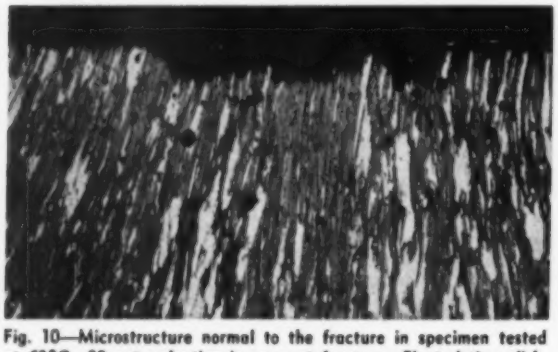

Fig. 10—Microstructure normal to the fracture in specimen tested at 60°C. 80 pct reduction in area at fracture. Electrolytic polish. Etched in alkaline $K_3Fe(CN)_6$ solution. X100. Area reduced approximately 75 pct for reproduction.

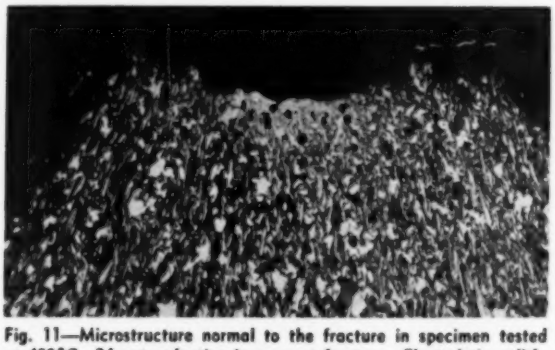

Fig. 11—Microstructure normal to the fracture in specimen tested at 400°C. 94 pct reduction in area at fracture. Electrolytic polish. Etched in alkaline $K_3Fe(CN)_6$ solution. X100. Area reduced approximately 75 pct for reproduction.

tures have a bright crystalline appearance, although fracture in the transition zone may be preceded by considerable plastic deformation. In the high temperature portion of the transition zone and in the ductile zone the fracture surfaces are dull and fibrous. Photographs of the microstructure normal to the fracture in specimens tested at −195°C (brittle zone), at 17° and 60°C (transition zone), and at 400°C (ductile zone), are shown in Figs. 8, 9, 10, and 11, respectively. At −195°C and +17°C the fractures are entirely of the bright brittle type. The fracture occurs suddenly and the actual break is surrounded by numerous cracks. The fracture at 60°C is intermediate between the brittle and ductile types, the fracture at the center being of the dull fibrous type and nearer the surface the bright brittle type. Above 60°C the fracture is entirely of the dull fibrous type. The dull fibrous type of fracture appears to proceed slowly, starting at the center of the specimen, and it was impossible to determine when fracture first started. Both the bright brittle and dull fibrous types of fracture are transgranular; however, the bright brittle type can be better classified as a cleavage type of fracture whereas the dull fibrous fracture is probably more adequately described as a shearing type of fracture.

The stress at fracture in the brittle zone was about 85,000 psi and essentially independent of test temperature as shown in Fig. 4. The effect of strain on the fracture strength in the brittle zone cannot be determined directly, since fracture precedes plastic strain. However, an estimate was obtained by prestraining specimens at room temperature and then fracturing in the brittle zone. The brittle fracture strength after various amounts of prestrain is shown by the iso-strain brittle fracture curves in Fig. 4. The curves indicate that the brittle fracture strength of molybdenum increases with strain. Only the 0 and the 0.1 strain brittle fracture curves were determined by more than one test and the curves at higher strain levels may be inaccurate. Also necking occurred during prestraining to the higher strain levels and the distribution of stress at the fracture was probably not uniform. It has been shown previously[1] that notched tensile specimens tested in the brittle zone fracture when the maximum normal stress calculated from elasticity theory equals the brittle fracture strength of unnotched specimens. It was assumed that the necks act as notches and the maximum normal stress was calculated by the method of Neuber,[13] and taken as the correct brittle fracture strength. The correction is quite small and the qualitative picture of the effect of strain on the brittle fracture strength is the same whether the correction is used or not.

The brittle fracture strength in the brittle zone and the maximum normal stress at fracture in the lower portion of the transition zone are about the same when compared after equivalent amounts of strain. Apparently, the Ludwik hypothesis, that fracture occurs when the maximum normal stress exceeds a brittle fracture strength, holds in these regions. However, at higher temperatures where the fracture is of the dull fibrous instead of the bright crystalline type, it is unlikely that fracture is governed by a normal stress fracture strength. At least it is not the same fracture strength as that measured in the brittle zone.

In the brittle zone strain markings are always found in a few grains in the vicinity of the fracture although fracture occurs before measurable elongation. An example of these strain markings in a specimen tested at −195°C is shown in Fig. 12. The markings are different from slip markings observed at higher temperatures and are quite reminiscent of the mechanical twins (Neumann bands) found in ingot iron deformed at low temperatures. Bruckner[11] has postulated that brittle fracture in ingot iron may be nucleated by mechanical twinning. However, it was impossible to ascertain if the strain markings in molybdenum are mechanical twins and, if they are, whether they are the cause or the result of fracture. It is possible that twinning provides the microstress concentrations (Griffith cracks) necessary for brittle fracture at a stress well below the theoretical cleavage strength of molybdenum.

Fig. 12—Deformation markings resembling "Neumann bands" in the vicinity of the fracture in specimen fractured at −196°C. Electrolytic polish. Etched in alkaline $K_3Fe(CN)_6$ solution. X500. Area reduced approximately 50 pct for reproduction.

Effects of Strain Rate: The temperature of the ductile-to-brittle transition is not a characteristic temperature but depends on the method of testing, e.g., the strain rate and the contour of the specimen. The effect of strain rate was studied to illustrate how this variable affects the ductile to brittle transi-

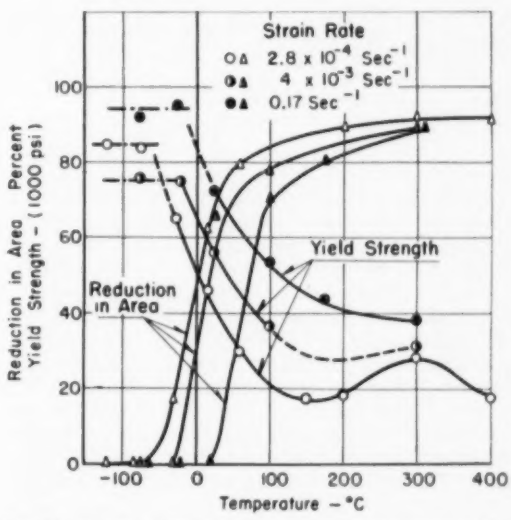

Fig. 13—Effects of temperature and strain rate on the ductility, yield strength, and brittle fracture strength of annealed molybdenum. Grain size, 900 grains per sq mm.

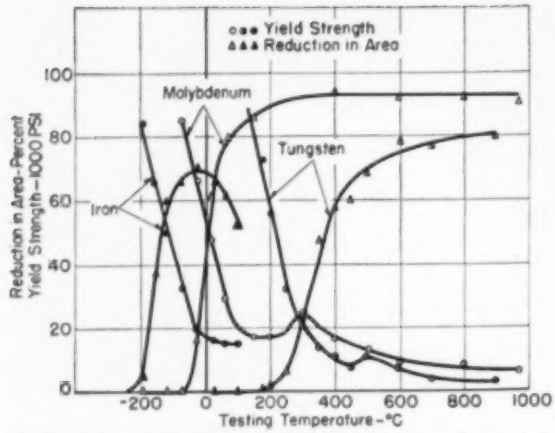

Fig. 14—Effect of temperature on tensile properties of annealed ingot iron,[9] molybdenum, and tungsten.[8]

tion temperature and the flow characteristics in the transition zone. Reduction in area at fracture, yield strength, and brittle fracture strength are plotted as a function of temperature for three different strain rates in Fig. 13. An increase in the strain rate raises the transition temperature zone primarily through an increase in the yield strength.

Discussion

The usefulness of molybdenum for applications where mechanical properties are important is fairly well restricted to the ductile zone since at lower temperatures the metal is brittle, or approaching brittle behavior, and at higher temperatures it is structurally unstable. The exact temperature limits of the ductile zone are not completely defined by any one type of test but depend on the conditions under which the metal is loaded. To increase the utility of molybdenum as a structural material, it is desirable to extend the ductile zone to higher and lower temperatures. It is not too difficult to raise the high temperature limit of the ductile zone since this merely requires raising the recrystallization temperature, which can be done quite readily by solid solution alloying.[10] To shift the low temperature limit of the ductile zone to a lower temperature, presents a more formidable problem.

The conditions which lead to brittle behavior in molybdenum are believed to be exactly the same as those which cause low temperature brittleness in iron, steel, and other metals with the body-centered cubic crystal structure. The striking similarity in the effect of temperature on the tensile properties of iron, molybdenum, and tungsten is shown in Fig. 14. Not only does each of these metals exhibit a sharp transition in ductility but each exhibits a rapid increase in yield strength in the transition zone. The fracture strength below the transition zone and the yield strength above the transition zone are about the same when the impurities and microstructures are similar. It should be possible to apply, qualitatively at least, the extensive knowledge of the effects of composition, microstructure, and testing method on the ductile-to-brittle transition of iron and ferritic iron alloys to predict the effects of these variables on the behavior of molybdenum.

From the literature on the low temperature brittleness of iron and ferritic alloys two things are evident. First, although numerous theories have been advanced to explain the ductile-to-brittle transition, the basic reason for the phenomenon has not been determined. Second, although it is possible to lower the temperature of the transition temperature somewhat by removal of impurities and by alloying, low temperature brittleness has never been overcome except by the addition of enough alloying element to change the crystal structure from body-centered cubic to face-centered cubic. Since molybdenum, unlike iron, is body-centered cubic at all temperatures, it is very unlikely that this method of lowering the ductile-to-brittle transition temperature is possible.

Basically, the problem is not one of ductility but of resistance to deformation, specifically the rapid increase in the yield strength with decreasing testing temperature and brittle fracture at a low stress relative to the theoretical strength of the crystal lattice. Particularly important is whether this increase in yield strength is caused by traces of interstitial solute atoms or is a basic characteristic of crystallographic slip in molybdenum. If the increase in yield strength in the transition zone is related to impurities, it is reasonable to expect that the activation energy associated with yielding would be related to the activation energy for diffusion of the element causing the increase in yield strength.

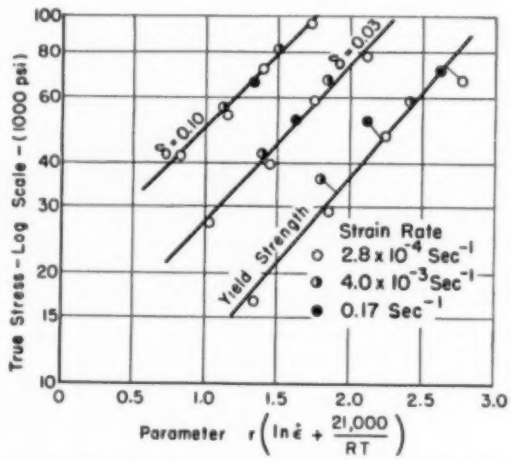

Fig. 15—Demonstration of equivalence of temperature and strain rate for molybdenum tested in the transition range.

Zener and Hollomon[10] have shown for steel tested at low temperatures that stress is related to temperature T and strain rate δ as follows:

$$\sigma = \sigma_o [(\dot{\epsilon} e^{Q/RT})^r, \delta'] \quad [3]$$

where δ' is a function representing the condition of the metal, i.e., the amount of strain hardening, grain size, etc.; Q, a heat of activation; σ_o, a constant; and r another constant. At a constant strain rate and condition of the metal, Eq. 3 implies the following relation between stress and temperature:

$$\sigma = \sigma_o' e^{q/RT} \quad [4]$$

where

$$q = Qr. \quad [5]$$

Table I. Activation Energy for Flow in Ductile-to-Brittle Transition Zone

Condition of Metal, Natural Strain	q, Cal per Gram Mol	r	Heat of Activation Q, Cal per Gram Mol
0.0	1700	0.08	21,000
0.03	1300	0.06	21,000
0.10	1100	0.05	22,000

At constant temperature and condition of the metal, Eq. 3 implies the following relation between stress and strain rate:

$$\sigma = \sigma_o'' \dot{\epsilon}^r. \qquad [6]$$

These equations apply for molybdenum in the transition zone, −75° to +150°C, and values of q associated with the yield strength and the 0.03 and 0.10 strain flow stresses are recorded in Table I. The exponent r was determined from strain rate data at 24°C and also recorded in Table I. The heat of activation Q determined by Eq. 5 is about 21,000 cal per mol.

Originally it was hoped that the activation energy calculated in this manner could be correlated with the activation energy for the diffusion of some interstitial impurity such as carbon, nitrogen, or hydrogen, and thereby predict if the rapid increase in strength in the transition zone might be related to one of these impurity elements. Unfortunately, there are no data available in the literature on the activation energy for the diffusion of these impurities in molybdenum. However, the activation energy is of the magnitude of that expected for diffusion of interstitial impurities in molybdenum. The activation energy associated with flow in molybdenum is somewhat higher than the value of 10,000 to 14,000 cal per gram mol obtained by Zener and Hollomon for steel.[16] However, it is considerably lower than the 37,800 cal per gram mol obtained by Sherby and Dorn[17] for slip in aluminum in the temperature range 150° to 250°C.

The equivalence of temperature and strain rate on the flow strength of molybdenum is demonstrated in Fig. 15 where the logarithm of the yield strength and the flow stresses at 0.03 and 0.10 strain are plotted vs the parameter, $r[\ln \dot{\epsilon} + 21{,}000/RT]$ for all tests made in the transition zone.

Summary

The flow and fracture characteristics of a sample of annealed molybdenum were studied between −195°C and +970°C by tension tests at a constant rate of extension of 2.8×10^{-4} sec^{-1}. This temperature range can be divided into four zones; a brittle zone, a transition zone, a ductile zone, and an unstable zone.

The "brittle zone" occurs below −75°C and is characterized by the lack of measurable ductility and bright transgranular cleavage type fractures.

The "transition zone" extends from about −75°C to +150°C and is characterized by a rapid increase in yield strength and a simultaneous decrease in ductility with decreased test temperature and a change from bright transgranular fracture to a dull fibrous fracture.

The "ductile zone" extends from about 150°C to about 900°C and is characterized by low yield strength, excellent ductility and a dull, fibrous fracture.

The "unstable zone" extends above 900°C and is due to thermal instability of the microstructure developed during test.

The ductile-to-brittle transition in molybdenum is caused by a rapid increase of the yield strength with decreased test temperature through the transition zone and a brittle fracture at a stress well below the theoretical strength of the crystal lattice. The activation energy associated with the increase in yield strength is about 21,000 cal per gram mol.

Strain markings resembling mechanical twins were observed in the brittle zone and they may be related to the brittle fracture strength.

The equivalence of temperature and strain rate in the transition zone through the Zener-Hollomon parameter, $(\ln \dot{\epsilon} + Q/RT)$, is demonstrated.

Acknowledgments

The author wishes to acknowledge his indebtedness to the members of the Metallurgical and Ceramic Dept. of the Westinghouse Research Laboratories and particularly to Howard Scott for many helpful comments and criticisms. Special appreciation is due J. W. Marden, retired, formerly manager, Molybdenum Development Div., Bloomfield Plant, Westinghouse Electric Corp.

References

[1] J. H. Bechtold and Howard Scott: Some Mechanical Properties of Arc-Cast and Powder Metallurgy Molybdenum. *Journal* Electrochemical Soc. (1951) **98**, No. 12, p. 495.

[2] G. W. Geil and N. L. Carwile: Tensile Properties of Ingot Iron at Low Temperatures. *Journal of Research*, National Bur. of Standards (1950) **45**, pp. 129-137.

[3] P. Shewmon and J. H. Bechtold: Effects of Temperature on the Flow and Fracture Characteristics of Tungsten. To be published in *Trans.* ASM (1954).

[4] D. McLean: The Embrittlement of Copper-Antimony Alloys at Low Temperatures. *Journal* Inst. Metals (1952) **81**, pp. 121-123.

[5] P. Ludwik: *Elements der Technologischen Mechanik*. (1909) Berlin. J. Springer.

[6] E. Orowan: Fracture and Strength of Solids. *Reports on Progress in Physics* (1948-1949) **12**, pp. 185-230.

[7] J. H. Hollomon and L. D. Jaffe: *Ferrous Metallurgical Design*. (1947) pp. 76-121. New York. John Wiley and Sons.

[8] M. Gensamer: Strength and Ductility. *Trans.* ASM (1946) **36**, pp. 36-60.

[9] R. D. Hall and J. H. Ramage: Metal Powder Consolidation. U. S. Patent 2,431,690, December 2, 1947.

[10] J. H. Bechtold: Recrystallization Data Applied to Control of the Mechanical Properties of Molybdenum. To be published in *Trans.* ASM (1954).

[11] E. T. Wessel and R. D. Olleman: Apparatus for Tensile Testing at Sub-Atmospheric Temperature. ASTM *Bull. No. 187* (January 1953) pp. 56-60.

[12] N. N. Davidenkov and N. I. Spiridonova: Mechanical Methods of Testing. ASTM (1946) **49**, pp. 1147-1156.

[13] H. Neuber: Theory of Notch Stresses. (1946) Ann Arbor, Mich. J. W. Edwards.

[14] W. H. Brucker: Micromechanism of Fracture in the Tension Impact Test. *Welding Journal* (1950) **29**, pp. 467-S—476-S.

[15] J. L. Ham, F. P. Bens, and G. A. Timmons: Arc-Cast Molybdenum Base Alloys. Quarterly Report to ONR covering period May 1 to July 31, 1951, Contract N8onr-787000, Climax Molybdenum Co.

[16] C. Zener and J. H. Hollomon: Effect of Strain Rate on the Plastic Flow of Steels. *Journal of Applied Physics* (1944) **15**, pp. 22-32.

[17] O. D. Sherby and J. E. Dorn: Creep Correlations in Alpha-Solid Solutions of Aluminum. *Trans.* AIME (1952) **194**, p. 959; JOURNAL OF METALS (September 1952).

Technical Note

Formation of Sigma Phase in the Mn-Mo System

by B. F. Decker, R. M. Waterstrat, and J. S. Kasper

THE existence of σ phase in the Mn-Mo system was discovered in this laboratory several years ago,[1] but neither the conditions of its formation nor its composition were known, and preliminary attempts to reproduce the phase were unsuccessful. We wish now to specify the information appropriate to σ phase formation on the basis of experiments performed since that time.

The starting materials were in every case electrolytic manganese and high purity molybdenum. Two methods of preparation were employed: 1—arc-melting varying combinations of the elements in an inert atmosphere and subsequent heat treating, and 2—sintering compressed mixtures of finely divided powders of the elements. In the latter method, the powders were first passed through 200 mesh screen and then compressed into cylinders of ⅜ in. diameter and ½ in. length, which were sintered at elevated temperatures in an atmosphere of dry hydrogen. For some samples, the sintering temperature was 1200°C (for 1 hr), and these were then heat-treated at lower temperatures for times up to 24 hr. Eventually it was found, for the proper composition, that essentially pure σ phase could be produced by sintering at 1125°C for 3 hr. Quenching to room temperature was effected by means of a stream of cold, dry hydrogen in a water-cooled chamber.

Table I. Results Obtained from Samples Produced by Sintering Compressed Mixtures

Sample	Treatment	Wt Pct Mn	Wt Pct Mo	At. Pct Mn	X-Ray Pattern
1	Sintered 1125°C 3 hr	53.0	46.7	66.5	σ + some α-Mn
2	Sintered 1125°C 3 hr	49.8	49.6	63.7	σ + trace α-Mn†
3	Sintered 1125°C 3 hr	43.4	56.5	57.3	σ + some Mo
4	Sintered 1125°C 3 hr	33.1	66.8	46.4	σ + some Mo
5	Sintered 1200°C 1 hr + 1125°C 24 hr	80*	20*	87.5*	α-Mn + trace σ
6	Sintered 1200°C 1 hr + 1125°C 24 hr	90*	10*	94.0*	α-Mn

* Nominal starting composition.
† Only evidence for α-Mn is one very weak line.

The arc-melting procedure was found to be unsatisfactory after an investigation of many samples at different compositions and temperatures. Large quantities of manganese were vaporized during melting and none of the products were homogeneous or contained extended regions of pure σ phase. Nonetheless, these experiments established that no σ formation occurs in the Mn-Mo system below 1115°C, and indicated, at least roughly, the composition range of interest for further exploration.

The more definite results obtained from samples produced by the second method are given in Table I.

B. F. DECKER, R. M. WATERSTRAT, and J. S. KASPER are associated with the Metallurgy Research Dept., Research Laboratory, General Electric Co., Schenectady.

TN 196E. Manuscript, Aug. 24, 1953.

Table II. X-ray Powder Pattern for Mn-Mo Sigma (64 Atomic Pct Mn). Crystal system, tetragonal $a_o = 9.10$, $c_o = 4.74$A. Cr Kα radiation.

Mn-Mo σ			Fe-Mo σ*	
hkl	*d*	*I**	*d*	*I**
311	2.463	m	2.46	w
002	2.368	m	2.35	mw
410	2.205	s	2.21	s
330	2.144	ms	2.13	m
202	2.097	ms	2.08	m
212	2.045	s	2.04	ms
411	2.000	vs	1.99	s
331	1.952	s	1.93	m
222	1.907	mw	1.90	w
312	1.829	mw+	1.82	w
431, 501	1.697	vvw		
511	1.672	vvw		
432	1.444	mw	1.44	vw
611, 512	1.426	mw	1.43	mw
313	1.385	vw		
621, 522	1.377	ms	1.37	m
541	1.362	vvw		
532, 631	1.304	s	1.30	ms
413, 550, 710	1.286	vs		
602	1.279	m		
333	1.272	ms	1.28	s
612	1.267	m		
701, 720	1.253	s		
551, 711	1.244	m	1.246	mw
622	1.232	mw		
542, 641	1.221	mw	1.220	m
721	1.211	ms		
433, 503	1.195	vvw	1.205	w
004	1.187	s	1.177	m

* w, weak; mw, medium weak; vw, very weak; vvw, very, very weak; m, medium; ms, medium strong; s, strong; vs, very strong.

A portion of sample 2 heated for 16 hr at 1000°C in a Vycor tube transformed to molybdenum plus unidentified phases of complex X-ray pattern.

From these few results it appears that the region of σ phase is quite narrow in composition. It is of interest that the composition is such as to make for difficulties in correlating this structure on an electron atom basis with other σ structures of iron, cobalt, and nickel. In that respect Mn-Mo shows the same anomaly as Mn-Cr and Mn-V systems.[2] A second feature is that in common with the two other known molybdenum σ's (Fe-Mo and Co-Mo), Mn-Mo σ exists only at elevated temperatures.

The X-ray powder pattern of the pure σ phase of Mn-Mo is given in Table II. It agrees well with the patterns established for other σ structures, especially with that for Fe-Mo σ as given by Goldschmidt.[3] An attempt is being made to establish whether an ordering of the respective atoms occurs and such information will be reported in a future publication.

Acknowledgment

The authors acknowledge gratefully the assistance of Mrs. J. R. Belanger in some portions of this work.

References

[1] J. S. Kasper, B. F. Decker, and J. R. Belanger: *Journal of Applied Physics* (1951) **22**, p. 361.
[2] A. H. Sully: *Journal* Inst. Metals (1951) **80**, p. 173.
[3] H. J. Goldschmidt: *Research* (1949) **2**, p. 343.

Bending of Molybdenum Single Crystals

by K. T. Aust, R. Maddin, and N. K. Chen

Lattice rotations occurring on the tension and compression sides during the bending of molybdenum single crystals at room temperature were followed in detail. Observations were also made concerning crystallite rotations and slip traces. The results indicated the participation of {110} as slip planes and the <111> as slip directions. Crystallite fragmentation during bending was also noted.

SEVERAL investigations have been conducted on pure bending of face-centered cubic metals.[1-3] Structural changes as a result of "bend-gliding," and the importance of bending and constraints during conditions of axial stressing, have been noted.[4,5] It was evident that the mechanism by which the bending deformation occurs is more complex than the case of simple shear. Studies of the bending of body-centered cubic metals from the aspect of the crystallographic mechanism appear to be lacking. Molybdenum single crystals therefore were subjected to deformation by bending in order to determine the reaction of the body-centered cubic lattice to bending stresses.

It might be expected for the bending of single crystals that lattice rotation as represented by the axis of compression would proceed toward the pole of the active slip plane and that rotation of the tensile stress axis should indicate the slip direction.[1] It was believed therefore that a study of the tension and compression sides of bent molybdenum single crystals should give data concerning the operative slip system. Specific problems which are pertinent to the overall picture of plastic deformation were also investigated, e.g., whether the constraints offered by pure bending give rise to the deformation band, and also the nature of the asterism occurring on the tension and compression sides during the stages of deformation.

Experimental Procedure

Eight single crystal specimens were grown from sintered molybdenum rods ⅛ in. diameter using the method described previously.[6] The purity of this material was reported as 99.9 pct as described elsewhere.[7] The specimens were ⅛ to 1/10 in. in diameter x 7 in. long, with single crystals approximately 1 to 2 in. in length occupying the entire center sections of each specimen. The specimens were electrolytically polished using an electrolyte of 300 cc methyl alcohol, 60 cc H_2SO_4, 130 cc HCl, and a current density of 4 amp per sq in.

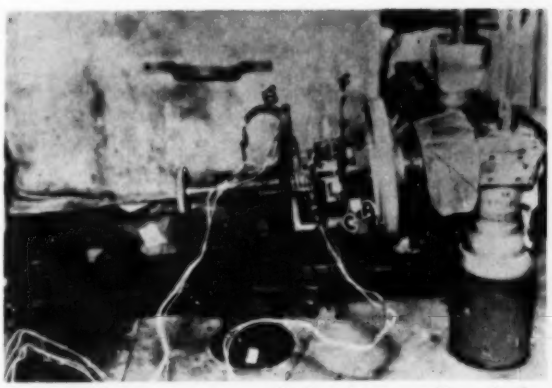

Fig. 1—Bending apparatus assembled at X-ray machine. A, B—Stationary bearings. C—Single crystal specimen. D—Movable steel plate. E—Load cell. F—Deflection cell.

Each specimen was then loaded in a bending apparatus similar to that used by Yen and Hibbard,[1] as shown in Fig. 1. The load was applied by means of a spring and screw arrangement through four ball-bearing surfaces set 1.5 in. apart. Either the inner two bearings or the outer two (*A*, *B*, Fig. 1) were attached to a movable steel plate (*D*) through which the load was transmitted. Since the apparatus was mounted on a track of the X-ray apparatus, the tension or compression side of the specimen could

K. T. AUST, Junior Member AIME, is Research Associate, Metallurgy Section, R. MADDIN, Member AIME, is Associate Professor, and N. K. CHEN, Junior Member AIME, is Assistant Professor, Dept. of Metallurgy, The Johns Hopkins University, Baltimore.

Discussion on this paper, TP 3623E, may be sent, 2 copies, to AIME by April 1, 1954. Manuscript, May 13, 1953. New York Meeting, February 1954.

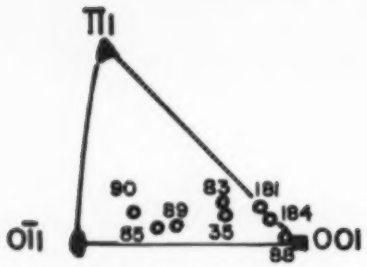

Fig. 2—Orientations of crystals investigated.

be set up for exposure by interchanging the bearings. For example, when the inner two bearings were attached to the movable plate, the specimen was set up for exposure on the tension side, and when the outer two bearings were attached to the movable plate the specimen was exposed to the X-rays on the compression side.

The load was measured by a calibrated clip gage (*E* in Fig. 1), using SR-4 type A-1 strain gages; the deflection was measured similarly using a calibrated clip gage (*F*). Load and deflection were measured by employing strain indicators. The load could be measured to a minimum of 0.0005 lb and the deflection to 0.0001 in.

X-ray back-reflection Laue photograms of the same position on each specimen were taken before bending, and at successive stages during the bending with the load applied but not increasing. The lattice rotations were then plotted in a standard stereographic projection from the photograms. The entire course of deformation was followed in detail on the compression side for specimens M-35, M-83, M-88, M-90, and M-181, and on the tension side for specimens M-85, M-89, and M-184. Considerable accuracy could be attained in the determination of these lattice rotations with the present experimental arrangement, since it was only necessary to keep the film to specimen distance constant without any realignment of the specimen. However, determination of the lattice rotations in the opposite sides of the specimens could not be obtained with the same accuracy, particularly where the total rotation was small, since only the initial and final orientations were determined and realignment of the specimen was required after unloading. The nature of the asterism occurring on the tension and compression sides of the bent specimens was noted from the X-ray photograms.

The eight specimens, M-35, M-83, M-85, M-88, M-89, M-90, M-181, and M-184 were bent through

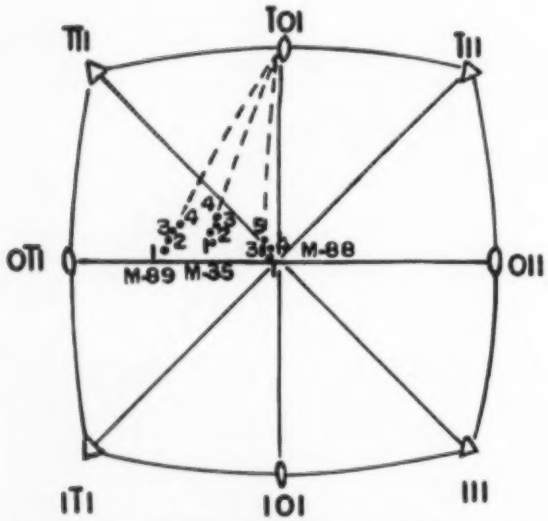

Fig. 3—Projection of M-35, M-88, and M-89 showing specimen axis rotations on the compression side.

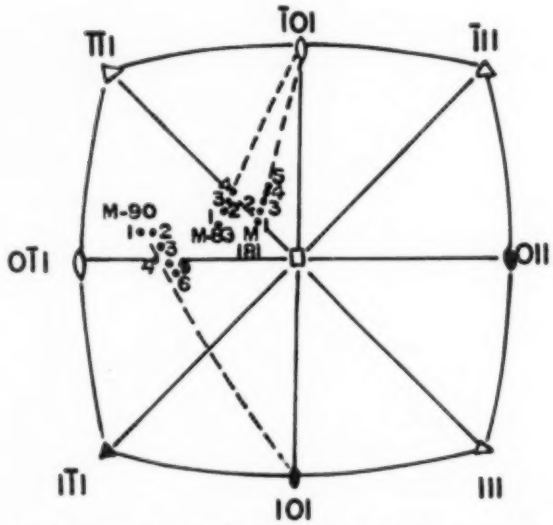

Fig. 4—Projection of M-83, M-90, and M-181 showing specimen axis rotations on the compression side.

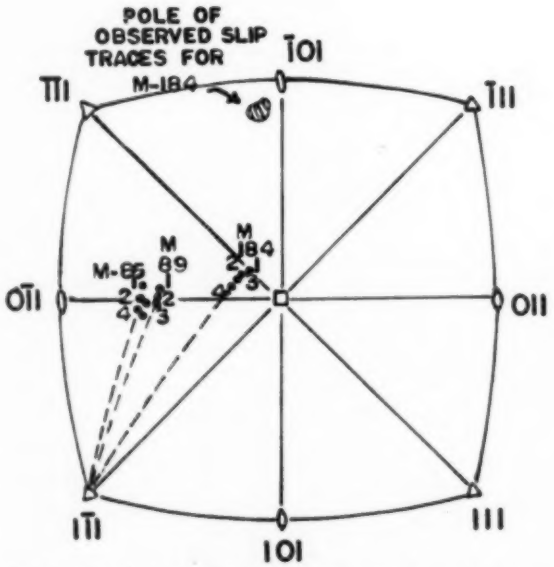

Fig. 5—Projection of M-85, M-89, and M-184 showing specimen axis rotation on the tension side and pole of observed slip traces for M-184.

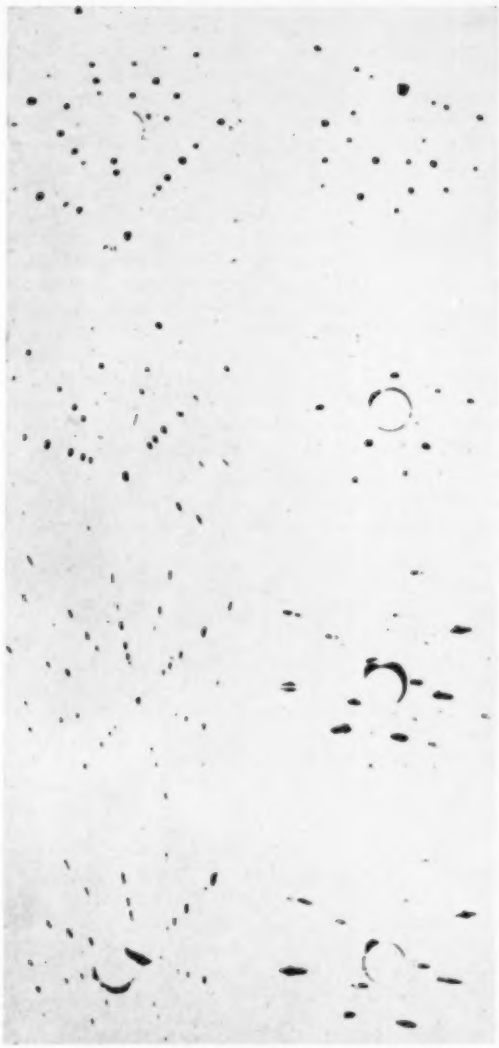

Fig. 6—Laue photograms of compression side of M-181 (left) and tension side of M-85 (right) after increasing amounts of deflection from 0° to 12° and 16°, respectively.

the following final angles: 13°, 10°, 16°, 10°, 16°, 11°, 12°, and 15°, respectively. Micrographic examination was carried out to determine the characteristics of the deformation markings appearing on the surface of the electropolished specimens after bending, and also to determine the pole of the slip plane. Measurements on those specimens where the slip lines could be observed satisfactorily were made at each 15° for several positions around the specimen axis on the metallograph. An indicator was attached to the specimen along a reference mark that was also used for the X-ray determination of the orientation. The angle of rotation was measured on a protractor attached to the metallograph stage as noted by the indicator. The angle between the specimen axis and the slip marking was then determined at a magnification of X400. The orientation of the specimens after deformation was always used in correlating slip traces measured on the metallograph with the orientation determined from X-ray.

Results and Discussion

Lattice Rotation: The specimen axis orientations for the initially unstrained crystals are shown in Fig. 2 in a standard cubic stereographic projection. The specimen axis or lattice rotations which occurred on the compression side during the bending tests are shown in Figs. 3 and 4. It is evident from Fig. 3 that specimens M-35 and M-89 showed a definite rotation toward the $(\bar{1}01)$ pole although the evidence for specimen M-88 is only slight. In Fig. 4 the specimen axis rotation for specimens M-83 and M-181 was again clearly toward the $(\bar{1}01)$ pole. However, some scatter in the rotations was obtained for specimen M-90, although there is an apparent rotation toward the (101) pole.

The specimen axis shift for the tension side of specimens M-85, M-89, and M-184 after increased amounts of bending are shown in Fig. 5. The rotations were clearly toward the $[1\bar{1}1]$ direction for each of these three specimens. It should be noted that the $[1\bar{1}1]$ direction is contained in the $(\bar{1}01)$ plane.

The results presented in Figs. 3 and 4 have shown that the lattice rotations on the compression side of bent single crystals of molybdenum were always toward a {110} pole. Also, rotations on the tension side, as illustrated in Fig. 5, were toward the $[1\bar{1}1]$ direction. It is well established that for a single crystal loaded in compression, the lattice rotation takes place in such a manner that the slip plane approaches the compression plane; for tensile loading the slip direction approaches the stress or tension axis.[8] It would also be expected from the bending work of Yen and Hibbard[1] that rotation of the lattice on the compression side would proceed toward the pole of the active slip plane and that rotation on the tension side should indicate the direction of glide. The present results, therefore, appear to indicate that the slip planes are of the type {110} and the slip direction <111> for molybdenum single

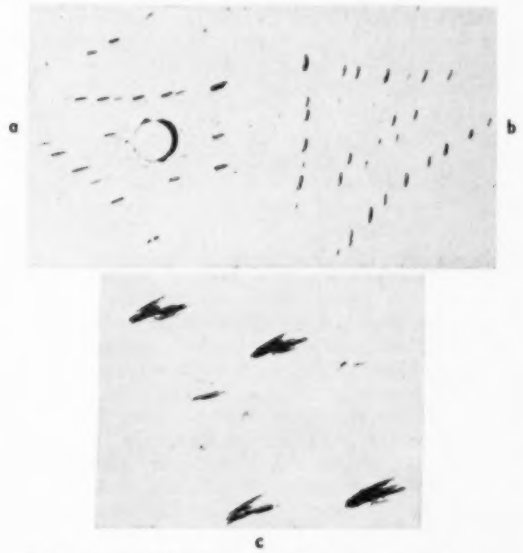

Fig. 7—Laue photograms of M-35 after bending through 13°. a (upper left)—Tension side. b (upper right)—Compression side. Note change in direction of asterism. Film to specimen distance 3 cm. c (lower center)—Same Laue reflections as in Fig. 7a, but with film to specimen distance equal to 12 cm.

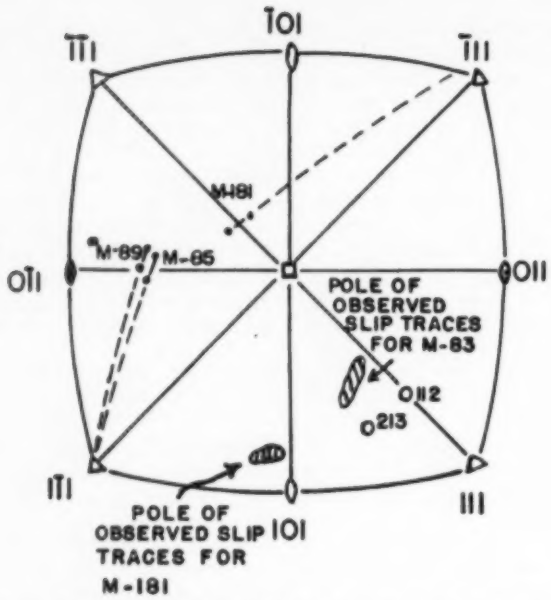

Fig. 8—Projection of M-181, M-85, and another grain in specimen M-89 showing crystallite rotations obtained from asterism on the tension side and pole of observed slip traces for M-83 and M-181.

crystals deformed at room temperature. These results for lattice rotation in bending also support earlier findings of Chen and Maddin[7] on the plastic behavior of molybdenum single crystals. It is also worthy of note that the change of orientation on the compression and tension sides of a molybdenum single crystal (e.g., M-89) appears to resemble that of two separate crystals deforming under compression and tension loading, respectively. Yen and Hibbard[4] also reached a similar conclusion for the transverse bending of single crystals of aluminum.

Asterism: X-ray back-reflection patterns, in conjunction with the load-deflection tests, revealed that the distortion of the Laue spots appeared when the specimen was subjected to loading beyond the yield. A progressive increase in the amount of asterism on the tension or compression sides was also noted with increasing plastic deformation due to bending, Fig. 6. The extent of asterism was usually somewhat larger on the tension side than on the compression side, although about equal amounts of asterism were obtained on the tension and compression sides of M-35. X-ray photograms of the neutral region, i.e., 90° from the tension or compression sides where the stress, theoretically, should be zero, indicated very little asterism even after considerable bending.

It was observed that the Laue spots from the tension side appeared to be elongated in the direction approximately parallel to the specimen axis, whereas those on the compression side were elongated in the direction 90° to the former one, Fig. 7a and b. However, the asterism characteristic of the compression side was slightly curved, thus indicating that crystallite rotation may have occurred about two or more axes. The asterism from the tension side was generally a line-type streak for the usual film to specimen distance of 3 cm. However, when the Laue reflection from the tension side is enlarged by increasing the film to specimen distance to 12 cm, a very complex type of asterism is revealed, Fig. 7c.

It is evident, however, that the present observations concerning the type and extent of asterism suggest that the tension and compression sides of a bent molybdenum single crystal may be deforming as two different crystals.

Evidence was presented by Chen and Maddin[7] for molybdenum single crystals deformed in tension that asterism is crystallographic in nature and represents a true account of plasticity in the specimen. It appears possible, therefore, to obtain information on the slip elements by plotting stereographically the crystallite rotations from the end points of Laue spots showing asterism. This was done in Fig. 8 for the tension side of those specimens which showed considerable asterism of the line-type streak. The crystallite rotations on the compression side were not determined due to the curvature of the Laue spots. Two of the specimens, M-85 and M-89, indicated a possible rotation toward the [$1\bar{1}1$] direction, while specimen M-181 gave slight evidence for rotation toward [$\bar{1}11$]. It is interesting to note that the crystallite rotations as determined from the

Fig. 9—Laue photograms of tension side of M-184 after increasing amounts of deflection from 0° to 15° showing a break-up of the Laue reflections into high intensity regions connected by diffuse areas.

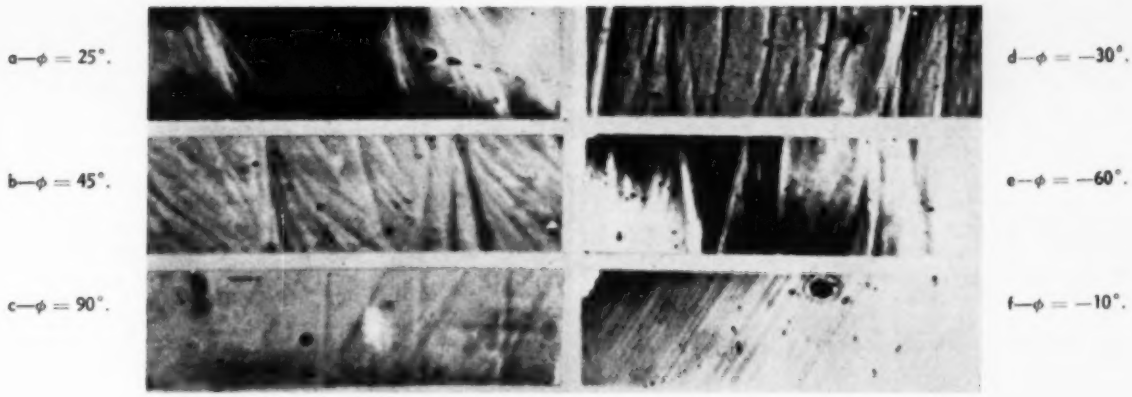

Fig. 10—Deformation bands and slip lines of tension side, a, b, and c, and compression side, d, e, and f, of specimen M-89. Specimen axis is horizontal. Bend axis is rotated in a plane perpendicular to the plane of the paper an amount shown by ϕ. $\phi = 0$ refers to position where bend axis is vertical and in the plane of the paper. X200.

extent of asterism were the same as the lattice or specimen axis rotations for specimens M-85 and M-89. The lattice rotation on the tension side of M-181 gave a slight indication of movement toward $[\bar{1}11]$ and the crystallite rotation was toward $[\bar{1}11]$. The pole of the observed slip traces on the tension side of M-181 (Fig. 8) appeared to indicate the operation of the slip plane (101), which contains both of these directions. The present results of stereographic analysis of asterism indicate that in the determination of slip elements, it appears of value to consider the alterations in the structure as shown by the formation of asterism.

Yen and Hibbard[1] have observed a splitting of the Laue reflections into discrete spots after bending in two of their ten single-crystal specimens of aluminum. They attributed this split-up of Laue spots to crystallite fragmentation. A break-up of Laue spots into individual areas was also observed in a single crystal of molybdenum bent through an angle of 15° at 2400°C° which was attributed to polygonization. In the present studies, division of the Laue reflections into high intensity areas was observed in all of the crystals bent, Fig. 9. However, these high intensity regions were always connected by diffuse areas. Consequently, it seems reasonable to interpret this phenomenon in terms of crystallite fragmentation where the individual crystallites are connected by high strain regions which may account for the diffuseness existing between the fragments producing the high intensity reflections.

Metallographic Observations: Microscopic examination of both the tension and compression sides of M-89 were made at low and high magnifications. Fig. 10 shows representative micrographs of the markings at different positions around the periphery on the tension and compression sides. No marked difference was observable in the microscopic appearance of the markings on the tension and compression sides. Two distinct types of markings can be noted — deformation bands and slip lines. Whenever the slip lines could be clearly observed in the specimens examined, they were always straight. The deformation band, however, became wavy as it was followed around the specimen. At the position represented by Fig. 10c, the deformation band can be seen to split into two bands. The appearance of the bands illustrated in Fig. 10a, b, d, and e, is somewhat similar to the "slip lines" observed in extended sodium, potassium,[10] and mercury single crystals[11] at low magnifications. Stereographic analyses of the lines on more than one surface of M-89 appeared to indicate that the lines correspond to the (101) plane. This result is in agreement with the X-ray data for the rotation on the compression side of M-89 (Fig. 3), i.e., toward the $(\bar{1}01)$ pole.

Stereographic analyses of the slip lines on the tension side of specimens M-184, M-181, and M-83 gave the following results: The pole of the observed slip traces for M-184 was in the vicinity of $(\bar{1}01)$, i.e., within 5° to 10°, as illustrated in Fig. 5. The lattice rotation on the tension side of this same crystal, M-184, gave a definite movement toward the $[1\bar{1}1]$ direction which is contained in the $(\bar{1}01)$ plane. The slip plane on the tension side of M-181, as determined from slip traces, was near the (101) pole, Fig. 8. The (101) plane might account for the lattice or crystallite rotations on the tension side of M-181. Although the pole of the slip traces for the tension side of M-83 was not located at any plane of low indices, it was closer to the (112) or (213) planes than to any of the {110} planes, Fig. 8. This is in agreement with previous observations of the extension of molybdenum single crystals with this initial orientation.[7]

It can be concluded from the present data that in three of the four cases where slip lines could be clearly observed, the pole of the slip traces was located near the {110} planes.

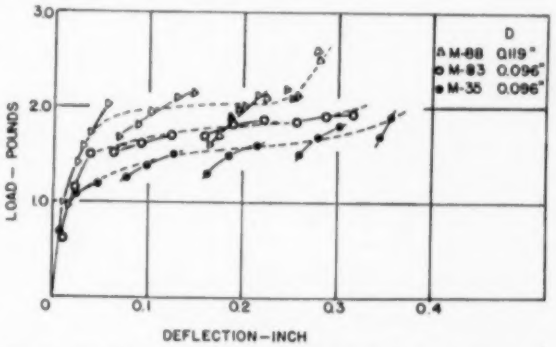

Fig. 11—Load-deflection curves of specimens M-35, M-83, and M-88.

Load-Deflection Data: Typical load-deflection curves for molybdenum crystals under bending are shown in Fig. 11. These curves indicate a normal type of stress-strain behavior with relaxation during loading. This relaxation occurred during the time when the X-ray patterns were obtained, with the load applied but not increased for intervals of approximately 1 hr. It is believed that the load-relaxation shown here may be characteristic of the specimen rather than due to relaxation of the spring, since the spring was rated at 50 lb and the loads were never above 3 lb when these relaxations were observed.[9] The various load-deflection curves did not appear to vary greatly for different orientations if the cross-sectional areas of the crystals are considered.

[9] This belief is also supported by bending tests on ⅛ in. diam steel rods in which no relaxation effect was observed using the same bending apparatus with loads up to 5 lb and times up to 15 hr.

The maximum normal stress S_n for round specimens is given by the simple beam formula

$$S_n = \frac{2PL}{3\pi r^3} \qquad [1]$$

where P is the load in grams, L is the lever arm in mm (115 mm in the present work), and r is the radius of the specimen. The maximum normal stress for the onset of plastic deformation was of the order of 7½ kg per sq mm for the various crystals tested. Since no definite yield points were observed, the value of P was arbitrarily taken as the intersection of the best straight lines through the curve where the load-deflection initially showed a steep rise and the curve where the load-deflection is gradually flattened. If it is assumed that slip takes place under the same conditions as uniaxial loading, the resolved shear stress, S_s, along the operative slip plane may be calculated by multiplying Eq. 1 by $\sin \chi \cos \lambda$, where χ is the angle between the specimen axis and the major axis of the glide ellipse and λ is the angle between the specimen axis and the slip direction. For those specimens where the results appeared to indicate that the plane acting was $(\bar{1}01)$ $[1\bar{1}1]$, the resolved shear stress in bending is calculated to be approximately 3½ kg per sq mm (5000 psi). Kochendorfer[5] has reported that the critical shear stress observed in bending may be 1.7 times greater than that in uniaxial loading for round specimens. This might indicate a resolved shear stress of the order of 2 kg per sq mm for molybdenum single crystals subjected to uniaxial loading. However, the values of resolved shear stress reported here can only be regarded as approximate because of the arbitrary value of P in Eq. 1 and because of the assumptions made in the calculations.

Table I. Summary of Slip Elements

Specimen No.	Slip Elements	
	Compression Side	Tension Side
M-35	$(\bar{1}01)^1$	—*
M-83	$(\bar{1}01)^1$	~(112) or (213)[2]
M-85	—*	$[1\bar{1}1]^{1,3}$
M-88	$(\bar{1}01)^{1 \text{ and } 3}$	$(\bar{1}01)^3$
M-89	$(\bar{1}01)^1$	$[1\bar{1}1]^{1,3}$
M-90	~(101)[1]	—*
M-181	$(\bar{1}01)^1$	$[\bar{1}11]$,[2] $[\bar{1}11]$,[3] (101)[3]
M-184	—*	$[11\bar{1}]^3$ $(\bar{1}01)^3$

1—Lattice rotation.
2—Asterism analysis.
3—Slip traces.
* Insufficient rotation for positive indication.

Summary

A summary of the slip elements determined in this investigation is shown in Table I.

1—Lattice rotation during bending of molybdenum single crystals was found to occur toward the {110} pole on the compression side and toward the <111> direction on the tension side.

2—Crystallite rotation determined from asterism and observations of slip traces appeared to indicate the participation of the {110} planes and the <111> directions.

3—The results in 1 and 2 above support the suggestions of Chen and Maddin that the slip planes are of the type {110} and the slip direction <111> for molybdenum single crystals deformed at room temperature.

4—The orientation change on the compression and tension sides of a molybdenum single crystal during bending are similar to that of two separate crystals deforming under compression and tension loading, respectively.

5—A relaxation in load up to 0.5 lb was obtained in the bending of molybdenum single crystals.

6—Laue reflections generally revealed a break-up which is interpreted as crystallite fragmentation.

Acknowledgments

The authors would like to thank Professor R. B. Pond for his help in the construction of the apparatus and the Office of Naval Research for support of their work under Project NR034-403. The assistance of Mrs. Dorothy Schaeffer in the growth of the molybdenum single crystals is gratefully acknowledged.

References

[1] M. K. Yen and W. R. Hibbard, Jr.: The Transverse Bending of Single Crystals of Aluminum. *Trans.* AIME (1949) **185**, p. 710; JOURNAL OF METALS (October 1949).

[2] R. W. Cahn: Recrystallization of Single Crystals After Plastic Bending. *Journal* Inst. Metals (1949) **76**, p. 121.

[5] A. Kochendorfer: *Plastishe Eigenshaften von Kristallen und Metallischen Werkstoffen* (1941) J. Springer.

[6] R. Maddin, C. H. Mathewson, and W. R. Hibbard, Jr.: The Active Slip Systems in the Simple Axial Extension of Single Crystalline Alpha Brass. *Trans.* AIME (1949) **185**, p. 527; JOURNAL OF METALS (August 1949).

[7] N. K. Chen and C. H. Mathewson: Structural Studies of Plastic Deformation in Aluminum Single Crystals. *Trans.* AIME (1951) **191**, p. 653; JOURNAL OF METALS (August 1951).

[8] N. K. Chen, R. Maddin, and R. B. Pond: The Growth of Molybdenum Single Crystals. *Trans.* AIME (1951) **191**, p. 461; JOURNAL OF METALS (June 1951).

[9] N. K. Chen and R. Maddin: Plasticity of Molybdenum Single Crystals. *Trans.* AIME (1951) **191**, p. 937; JOURNAL OF METALS (October 1951).

[10] C. S. Barrett: *Structure of Metals* (1952) New York. McGraw Hill Book Co.

[11] N. K. Chen and R. Maddin: Observations on Cleavage and Polygonization of Molybdenum Single Crystals. *Trans.* AIME (1951) **191**, p. 531; JOURNAL OF METALS (July 1951).

[12] E. N. DaC Andrade and L. C. Tsien: Glide of Single Crystals of Sodium and Potassium. *Proc.* Royal Soc. (1937) **163**, p. 1.

[13] K. M. Greenland: Slip Bands on Mercury Single Crystals. *Proc.* Royal Soc. (1937) **163**, p. 28.

AIME OFFICERS:
President—Andrew Fletcher
Vice-Presidents—T. B. Counselman, L. E. Elkins, O. B. J. Fraser, J. L. Gillson, A. B. Kinzel, J. B. Morrow
President-Elect—L. F. Reinartz
Treasurer and Controller—G. I. Brigden
AIME STAFF:
Secretary—E. H. Robie
Ass't. Secretaries—J. B. Alford, H. N. Appleton, E. J. Kennedy, Jr., Ernest Kirkendall, R. E. O'Brien
Ass't. Treasurer—P. J. Apol

Electric Furnace Steel Men to Meet in Cincinnati

THE Electric Furnace Steel Committee of the AIME will hold its Eleventh Annual Conference at the Netherland Plaza Hotel in Cincinnati from Dec. 2 to 4, 1953.

This year a plant trip has been scheduled for the afternoon of the day preceding the technical sessions instead of an Educational Session on the Saturday morning following.

All operating men, repair and maintenance men, metallurgists, ceramic and refractory engineers, observers, and any others interested in the production of more steel, better steel, and cheaper steel are invited to attend. The complete program will be mailed in November.

Hotel reservations should be made directly with the headquarters hotel or other Cincinnati hotels.

The $7 registration fee includes a copy of the bound Proceedings when published. There is no registration fee for students at any of the sessions unless they desire a copy of the Proceedings. AIME Members are entitled to a $2 reduction in the registration fee upon presentation of membership cards.

For those who did not attend the 1952 Conference, bound copies of the Proceedings are available from Institute headquarters. Price $10 to the public ($10.50 foreign), less 30 pct to AIME Members.

Preliminary Program of Electric Furnace Steel Conference

WEDNESDAY, DECEMBER 2

9 am to 9 pm
Registration

1 to 5 pm
Plant Trip:

Leave and return by chartered buses from Netherland Plaza Hotel. One hr plant trip through Armco Steel Corp., Middletown, Ohio.

THURSDAY, DECEMBER 3

8:30 am
Registration

9:30 am
Opening Session:

Welcoming remarks; announcements and reports.

9:45 am
Induction Stirring in Arc Furnaces:

Development of induction stirring; manufacture of the Timken stirrer; arc furnace rotating type magnetic stirrer.

2:00 pm
General Session:

Application and manufacture of high strength and high alloy steels for the jet engine program; conservation of chromium; rapid bath analysis; measurement of electric furnace bottom shell temperature.

6:30 pm
Reception and Cocktail Party

7:00 pm
Annual Fellowship Dinner

FRIDAY, DECEMBER 4

8:30 am
Registration

9:30 am
Ingot Session on Modern High Powered Arc Furnace:

Furnace design, maintenance and operation; round vs oval furnace; electric vs open hearth furnace; solidification of steel in ingot molds.

9:30 am
Castings Session on Inclusions in Steel:

Deoxidation and its effects on the properties of steel; effects of steelmaking practice on inclusions; bull session on furnace operations.

2:00 pm
Ingot Session on Metallurgy:

Nitrogen in stainless steels; sources of inclusions from pouring refractories; sulphur control in electric steelmaking; McQuaid-Ehn grain size by spectrochemical analysis of ladle samples.

2:00 pm
Castings Session on Mechanical Aspects of Furnace Operation:

Fume control; new developments in furnace design and operation; continuation of bull session on furnace operations.

1954 Officers Will Be Declared Elected

No opposing candidates for nominations for AIME officers in 1954 had been received on Sept. 1, so the ticket as published in the July issues of the JOURNAL OF METALS and MINING ENGINEERING will be formally declared elected at the November meeting of the Board of Directors, as provided in the AIME bylaws. The ticket is as follows: President-Elect, H. DeWitt Smith; Vice-Presidents, T. B. Counselman and Harold Decker; Directors, the above with E. C. Babson, George D. Dub, Ralph E. Kirk, Carleton C. Long, Earl R. Marble, and Philip J. Shenon. All of these men will serve three-year terms as Director beginning next February. Another Director will be elected by the incoming Board at the February meeting, for a one-year term, to fill the unexpired term of T. B. Counselman.

AIME Board Votes On Bylaw Changes

Local Sections

At the meeting of the Board of Directors in Seattle on Sept. 22, it was voted to delete the following words from Art. XI, Sec. 3 of the AIME bylaws: ". . . only one Section shall be authorized in any one locality or district and . . ." This will permit organization of two or more Local Sections in one geographical area provided, in the opinion of the Board, they will serve a useful purpose and increase service to members.

Technical Papers

At its meeting on Sept. 22 in Seattle, the AIME Board voted approval of the proposed change in the bylaws relating to the release of technical papers. Heretofore there has been nothing in the bylaws asserting the right of the Institute to have sole publication privileges for papers presented at other than Local Section meetings. Article X of the AIME bylaws has now been amended by adding Sec. 2, which reads as follows: "All papers presented before meetings of the Institute—Annual, Regional, Branch, Divisional, and Local Section—are the property of the Institute, except those previously published elsewhere, those withheld from publication by the author, or those released by the Secretary of the Institute."

Art. XI, Sec. 3, 6th paragraph, is amended to read as follows: "Papers presented at Local Section meetings, and discussions thereon if reported, shall be the property of the Institute, except those previously published elsewhere, those withheld from publication by the author, or those released by the Secretary of the Institute."

E. M. Weiss Joins Journal of Metals Staff

In September, Edwin M. Weiss was added to the staff of the JOURNAL OF METALS in New York as Assistant Editor. Mr. Weiss comes to the Institute from a short term with the U. S. Steel Corp. in Chicago. Before that he spent the better part of two years in the foreign minerals region of the U. S. Bureau of Mines. He was born in Fort Wayne, Ind., and educated at Ohio State and the University of Wisconsin. He holds a B.A. in English and chemistry, and an M.S. in economic geology.

Connecticut Section's First Technical Session

The first technical session of the Connecticut Section AIME for the 1953 to 1954 season was held on September 16 at the Connecticut Light & Power Co. Auditorium in Waterbury. Introductory remarks were made by L. W. Thelin, Chairman of the Connecticut Section and R. J. Christine, Vice-Chairman of the Section, was in charge of the technical session.

Walter E. Allan, production engineer, Waterbury brass goods branch of the American Brass Co. discussed the material considerations and tool design for the press working of metals. A film, *The Science of Making Brass*, produced in technicolor by the Kennecott Copper Corp. and the Chase Brass & Copper Co. was also included in the program.

Eastern Section, NOHC Meets in Philadelphia

The Eastern Section of the National Open Hearth Committee, AIME, under the Chairmanship of Rex M. Baker held its annual fall meeting at the Warwick Hotel, Philadelphia, Pa., on October 9. The technical session under J. E. Mateer and J. T. Clisham included a prize winning paper by Julius Boullosa. At the annual dinner Don Mathews was presented with a silver plate honoring him as one of the four men who started the Eastern Section.

Spokane Hosts Meeting

Spokane Members of AIME were host to Mr. and Mrs. Andrew Fletcher and Mr. and Mrs. Roy O'Brien on Sept. 28 at the Ridpath Hotel. After dinner, Mr. Fletcher addressed the 112 persons who attended, and spoke about the future outlook for the Institute and the lead and zinc mining industries. The success of the party was due to the efforts of the Spokane Section of the Women's Auxiliary, Mrs. D. W. Smith and the efforts of the Vice-Chairman of the Subsection, D. Myers and the Program Chairman, M. E. Volin.

Young engineers' night was the designation of the Chicago section's October 7 meeting. From left to right are: Otto Zmeskal, Illinois Institute of Technology; James Lommel, winner of undergraduate paper contest; L. F. Mondolfo, Illinois Tech student advisor; W. John King, Section Student Relations; Dillon Evers, Purdue University; and John F. Radavich, co-author of winning graduate paper. Not shown are Louis Horvath co-author of the graduate paper and Donald C. Simpson winner of the second prize in the undergraduate paper contest. Presentation of checks and certificates was made by Clayton G. Ball, Section Chairman. William G. Caples, vice-president in charge of human relations of Inland Steel Co., spoke on the nontechnical problems confronting engineers in industry.

Personals

R. W. Cahn, dept. of metallurgy, University of Birmingham, England, will spend the calendar year of 1954 as a visiting lecturer in the dept. of mechanical engineering at Johns Hopkins University, Baltimore.

Stuart Solomon is now employed by the U. S. Steel Co., Duquesne works, as a member of their management candidate program.

Walter W. Walker has joined the Hughes Aircraft Co., Tucson, Ariz. He had been associated with the California Research & Development Co.

J. I. Dodson is products metallurgist for the Kaiser Steel Corp., Fontana, Calif. He had formerly been with Pacific Northwest Alloys, Spokane, Wash.

James B. Macelwane, dean of the Institute of Technology, St. Louis University, was recently honored at a reception in celebration of his golden jubilee as a member of the Society of Jesus.

Everett G. Fahlman, president of the Permold Co., Medina, Ohio, was appointed deputy director of the aluminum div., National Production Authority, Dept. of Commerce.

Arthur B. Van Tine has joined the staff of the dept. of geology at Rensselaer Polytechnic Institute. Professor Van Tine had been with the Colorado School of Mines and consultant to Shell Oil Co. and Pure Oil Co.

Harold Meese, metallurgist and professor at Michigan College of Mining and Technology, has been released from active duty with the Office of Naval Material.

W. P. Ruemmler has joined the National Lead Co. as production superintendent at the cobalt plant, Fredericktown, Mo. He had formerly been plant manager of the East Chicago plant of Eagle-Picher Co.

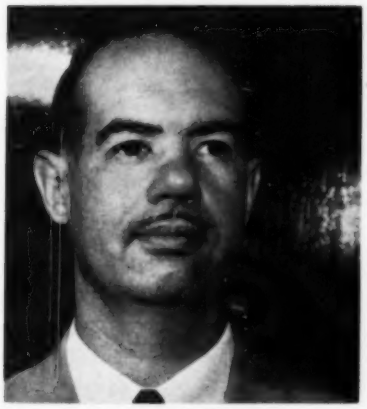

W. P. RUEMMLER

B. L. JOHNSON

Birger L. Johnson has joined the Latrobe Steel Co., Latrobe, Pa., where he is in charge of the metallurgical laboratory and will direct the company's research activities in physical metallurgy. Mr. Johnson was formerly with Mack Truck Co. as head of the metallurgy section, research div., Plainfield, N. J.

A. C. RICHARDSON

A. C. Richardson has been named technical director, Battelle Memorial Institute, Columbus. Mr. Richardson has had supervisory charge of research in mineral processing at Battelle for the past 20 years. Mr. Richardson was one of the co-authors of the Blast Furnace, Coke Oven and Raw Materials Committee, JOURNAL OF METALS Award Paper that was presented at the Conference held during April 1953.

E. R. Rowley has been named president of Titanium Metal Corp. of America. He also becomes a director and member of the executive committee. He had been production manager of National Lead Co. **Philip C. Muccilli** has been appointed to succeed Mr. Rowley.

E. C. Handwerk has resigned from the New Jersey Zinc Co., research and development dept. He is now associated with the Wyandotte Chemicals Corp. as director of production research.

Barney Foust has accepted a position as chief metallurgist with Marsman & Co., Inc., Manila, Philippines. He had been mill superintendent for San Mauricio Mining Co., Philippines.

Roy A. Hunt, chairman of the executive committee, Aluminum Co. of America, recently received the Alcoa 50-year service club award.

Hans W. Wawrousek has been awarded an Allegheny Ludlum graduate fellowship in the dept. of metallurgical engineering, Rensselaer Polytechnic Institute, Troy, N. Y.

Eric L. Anderson, superintendent of electrical dept., Bethlehem Steel Co., Johnstown, Pa., was elected president of the Assn. of Iron and Steel Engineers. **John H. Vohr,** general superintendent of U. S. Steel Corp., Gary, Ind., was elected first vice-president; **W. H. Collison,** assistant general superintendent, blast furnace div., Great Lakes Steel Corp., Ecorse, Mich., was named second vice-president.

William M. Staples was named to the post of manager of construction by Chemical Construction Corp.

Ross B. Hopkins has been appointed plant metallurgist for Rodney Metals, Inc., New Bedford, Mass. Mr. Hopkins has been associated with the American Steel & Wire Co. for the past 13 years.

Herbert E. Treichler, vice-president of the Texas Gulf Sulphur Co., has retired after more than 35 years of association with the company. Mr. Treichler came to Texas Gulf Sulphur from International Nickel Co., Ontario.

H. E. TREICHLER

Coming Events

Nov. 4-6, Time and Motion Study and Management Clinic, Sheraton Hotel, Chicago.

Nov. 5-6, Pittsburgh Diffraction Conference, Mellon Institute, Pittsburgh.

Nov. 5-7, Electron Microscope Society of America, annual meeting, Pocono Manor Inn, Pocono Manor, Pa.

Nov. 6, AIME, Pittsburgh Section, NOHC, Pittsburgh Section, off-the-record meeting, William Penn Hotel, Pittsburgh.

Nov. 10, Society for Applied Spectroscopy, Hotel New Yorker, New York.

Nov. 11, AIME, Connecticut Section, Hammond Metallurgical Laboratory, Yale University, New Haven.

Nov. 11, AIME, National Open Hearth Steel Committee, Western Section, Rodger Young Auditorium, Los Angeles.

Nov. 11-14, Society of Naval Architects and Marine Engineers, annual meeting, Waldorf-Astoria, New York.

Nov. 13, AIME, St. Louis Section, coal meeting, York Hotel, St. Louis.

Nov. 17, American Fair Trade Council, open forum, Hotel Roosevelt, New York.

Nov. 23-24, Operations Research Society of America, Statler Hotel, Boston.

Nov. 29-Dec. 4, ASME, annual meeting, Statler Hotel, New York.

Nov. 30-Dec. 5, Exposition of Chemical Industries, Commercial Museum and Convention Hall Philadelphia.

Dec. 1-4, National Assn. of Corrosion Engineers, conference, University of Oklahoma.

Dec. 2, AIME, Chicago Local Section, Chicago.

Dec. 2-4, AIME, Electric Furnace Steel Conference, Netherland-Plaza Hotel, Cincinnati.

Dec. 11, AIME, St. Louis Section, York Hotel, St. Louis.

Dec. 13-16, American Institute of Chemical Engineers, annual meeting, Hotel Jefferson, St. Louis.

Dec. 27, Conference on Scientific Editorial Problems, AAAS, Boston.

Dec. 28-29, Annual Chemical Engineering Symposium, University of Michigan, Ann Arbor.

Jan. 6, 1954, AIME, Chicago Section, Chicago.

Jan. 8, AIME, St. Louis Local Section, York Hotel, St. Louis.

Jan. 13, AIME, Connecticut Section, Bridgeport Brass Co., Bridgeport.

Jan. 20, AIME, National Open Hearth Steel Committee, Western Section, Rodger Young Auditorium, Los Angeles.

Feb. 2, AIME, Chicago Local Section, Chicago.

Feb. 15-18, AIME, annual meeting, Metals Branch, Hotel McAlpin; Mining and Petroleum Branches, Hotel Statler, New York.

Mar. 8-10, American Institute of Chemical Engineers, Statler Hotel, Washington, D. C.

Mar. 10, AIME, Connecticut Section, American Brass Co., Torrington, Conn.

Mar. 17, AIME, National Open Hearth Steel Committee, Western Section, Rodger Young Auditorium, Los Angeles.

Apr. 5-7, AIME, Blast Furnace, Coke Oven, Raw Materials and National Open Hearth Conference, Palmer House, Chicago.

Obituaries

Frederick E. Wright (Member 1904) former petrologist at Carnegie Institution, died on Aug. 25. He was secretary of the National Academy of Sciences and staff petrologist from 1906 until his retirement in 1944, of the geophysical laboratory of the Carnegie Institution of Washington. Dr. Wright was born in Marquette, Mich. He received a Ph.D. from Heidelberg University. He was then an instructor at the Michigan College of Mines. From 1906 to 1917 he was a geologist for the U. S. Geological Survey. Dr. Wright received an honorary doctorate in science from the University of Michigan in 1940. During World War I he was a major in Army Ordnance and later served in a civilian capacity with the Office of Science Research and Development.

Harlan S. Emlaw (Member 1898) died on Feb. 5, 1953. He was a retired mining engineer, formerly president of American Potash & Chemical Corp. Born in Grand Haven, Mich., Mr. Emlaw received his E.M. from Michigan College of Mining and Technology in 1895. He first worked as a surveyor in Cripple Creek, Colo.; then as an engineer with Basin & Bay State Mining Co. in Montana and with the Washoe plant of Anaconda Copper Mining Co. For several years Mr. Emlaw was general superintendent of mines for Cerro de Pasco Corp. in Peru. At various times he was vice-president of the Fresnello Co. and president of Golden Queen Mining Co., Tri-State Zinc Inc., and Buell Engineering Co. Mr. Emlaw was a Legion of Honor Member of AIME.

Kleber Bordez (Member 1949) died. Mr. Bordez was born in France and studied at the Ecole Nationale Superieure des Mines de St. Etienne. Seven years he was director of a flotation plant in Turkey and for ten years director of the Mines d'Aouli in French Morocco. Since 1945 he had been director general of the Cie Francaise des Mines du Laurium in Greece.

NECROLOGY

Date Elected	Name	Date of Death
1903	Galen H. Clevenger	Aug. 2, 1953
1916	John Davenport	Apr. 4, 1953
1944	Harry J. Evans	June 1, 1953
1920	C. S. T. Farish	Aug. 29, 1953
1904	H. P. Henderson	Sept. 19, 1953
1925	John M. Jennings	Mar. 5, 1953
1946	A. R. Llewellyn	May 14, 1953
1940	Ralph B. Lloyd	Sept. 9, 1953
1919	A. E. MacArthur	Aug. 16, 1953
1888	T. A. Rickard	Aug. 15, 1953
1936	S. C. Sandusky	July 24, 1953
1916	Louis A. Scholl, Jr.	Sept. 22, 1953
1917	William Huff Wagner	Aug. 31, 1953
1902	L. Webster Wickes	Sept. 16, 1953

Proposed for Membership

Metals Branch AIME

Total AIME membership on Sept. 30, 1953 was 19,401; in addition 1748 Student Associates were enrolled.

ADMISSIONS COMMITTEE

O. B. J. Fraser, Chairman; Philip D. Wilson, Vice-Chairman; F. A. Ayer, A. C. Brinker, R. H. Dickson, Max Gensamer, Ivan A. Given, Fred W. Hanson, T. D. Jones, G. W. Lutjen, E. A. Prentis, Sidney Rolle, J. T. Sherman, F. T. Sisco, R. L. Ziegfeld.

The Institute desires to extend its privileges to every person to whom it can be of service, but does not desire as members persons who are unqualified. Institute members are urged to review this list as soon as possible and immediately to inform the Secretary's office if names of people are found who are known to be unqualified for AIME membership.

In the following list C/S means change of status; R, reinstatement; M, Member; J, Junior Member; A, Associate Member; S, Student Associate.

California
Los Angeles—Olson, Harold C. (M)
Mar Vista—Balkins, Cleon V. (A)

Colorado
Grand Junction—Lundquist, Adolph Q. (M)
Grand Junction—Thompson, Craig D. (J)

Connecticut
Hamden—Pond, Marvin H. (M)

Florida
Lakeland—Creasy, M. Richard (A)

Illinois
Park Forest—Nachtman, Elliot S. (M) (R. C/S—S-M)
So. Holland—Mooney, Ernest J. (M)

Indiana
Indianapolis—Kurtz, Fred E. (A)

Maryland
Silver Spring—Siegel, Harold A. (J)

Massachusetts
Ipswich—Wang, Chih C. (A) (R. C/S—S-A)
Somerville—Schiff, Norman N. (J)

Minnesota
Hibbing—Linden, John F. (M) (R. C/S—J-M)

Missouri
St. Louis—Streett, James D. (A)

New Jersey
Fords—Opie, William R. (M) (C/S—J-M)
Maplewood—Banks, Robert R. (J)

New Mexico
Carlsbad—Wadia, Dorab R. (J) (R. C/S—S-J)

New York
Cohoes—Cremisio, Richard S. (J)
Lewiston—Wamstad, Marvin L. (A)
Mt. Vernon—Medoff, Jack I. (A)
Schenectady—Bishop, Shields M. (J)
Schenectady—Blake, Alfred E. (A)

Ohio
Canton—Wyandt, John J. (A)
Columbus—Holden, Frank C. (M)
Euclid—Ferryman, Roger M. (J)
Hudson—Davis, Dwight E. (J)
Lakewood—Staako, Joseph G. (J)
Middletown—Bussert, Charles E. (M)

Pennsylvania
Bala-Cynwyd—Brown, Norman (M) (R. C/S—S-M)
Beaver—Boal, George Y. (M)
Ellwood City—Pawol, Joseph J. (A)
Export—Bassett, James G. (M)
Philadelphia—Pijawka, Walter C. (A)
Pittsburgh—Troutman, Ward M. (A)

Texas
El Paso—Lindeman, Carl A. (A)

Utah
American Fork—Aime, Jack (M)

Argentina
Buenos Aires—Michaux, Andre B. (M)

Canada
Hamilton, Ont.—Hindson, Ralph D. (A)

New Zealand
Ardmore—Titchener, Alan L. (M)

Peru
La Oroya—Koeppel, Walter E. (A)

An important CHROME-MAGNESITE Refractory for metallurgical furnaces

- HIGH TEMPERATURE STABILITY IN STRENGTH AND VOLUME
- GOOD SPALLING RESISTANCE
- HIGHLY RESISTANT TO SLAGGING AND EROSION

CHROMEX B is an extremely hard burned, dense, basic refractory especially suited for use under severe service conditions in vulnerable parts of smelting, refining and melting furnaces.

Important Uses of CHROMEX B include—

Copper and nickel converter linings
Copper refining furnace walls
Aluminum melting furnace bottoms
Lead dross reverberatory furnace walls and roofs
Copper blast furnace hearths and setters
Non-ferrous secondary metal furnace parts

Harbison-Walker Products comprise all types and classes of commercial basic, silica, alumina-silica, and alumina refractories.

TRADE MARK
REG. U.S. PAT. OFF.

Harbison-Walker Refractories Company

AND SUBSIDIARIES

WORLD'S LARGEST PRODUCER OF REFRACTORIES

General Offices . . . . . Pittsburgh 22, Pennsylvania

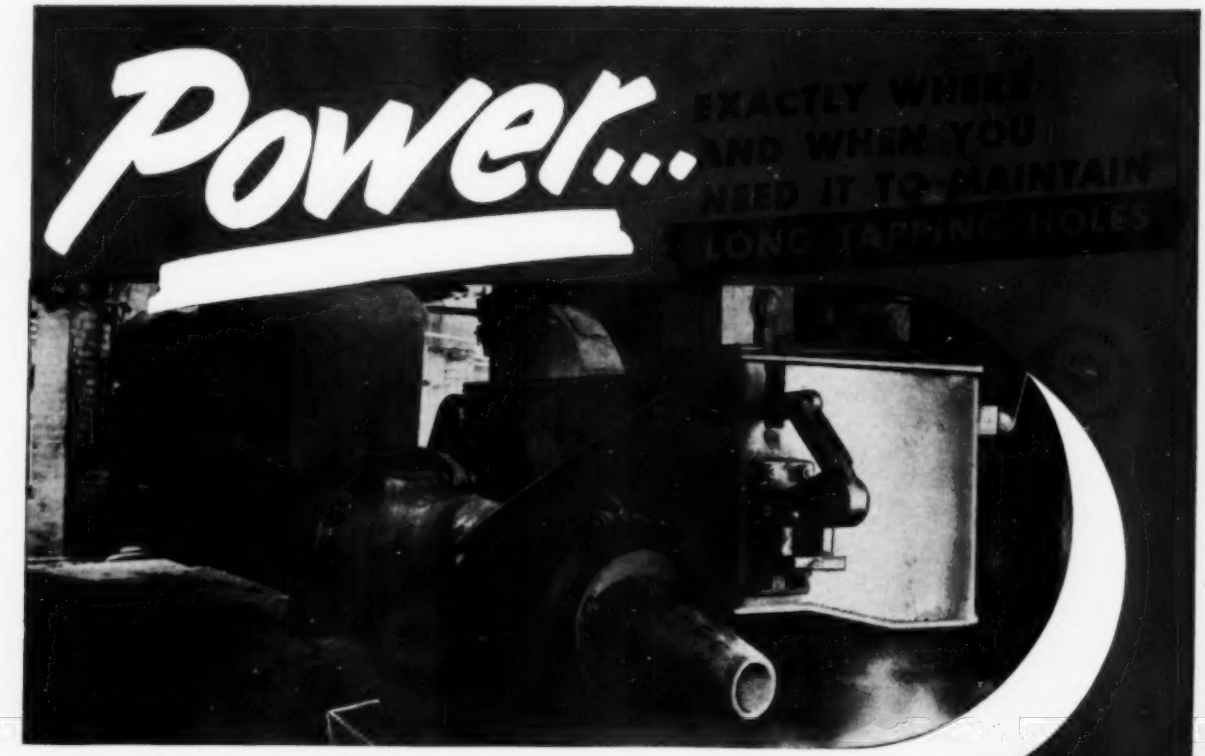

Bailey CLAY GUN

Here is the means to best results and safety in plugging blast furnace tapping holes. Positive closing every time the gun is used is assured by the exclusive Bailey pedestal support and lever mechanism. Operated by two separate motor drives, the gun is quickly, accurately and solidly positioned when the tap-hole is to be closed. Ample power to maintain long tapping holes is provided by an electrically-driven piston which develops a clay pressure of 600 pounds per square inch.

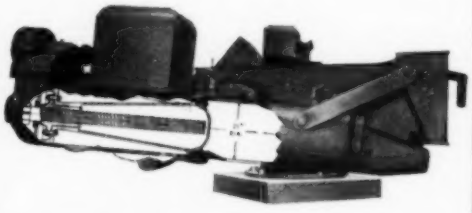

The Bailey Clay Gun is of the plunger type, in which the plunger is driven by a highly efficient power screw and double reduction gear drive.

1221 BANKSVILLE ROAD PITTSBURGH 16, PA